

# Foundations of Antenna Theory and Techniques



PEARSON  
Prentice  
Hall

Vincent F. Fusco

# Foundations of Antenna Theory and Techniques



We work with leading authors to develop the strongest educational materials in Engineering bringing cutting-edge thinking and best learning practice to a global market.

Under a range of well-known imprints, including Prentice Hall, we craft high-quality print and electronic publications which help readers to understand and apply their content, whether studying or at work.

To find out more about the complete range of our publishing, please visit us on the World Wide Web at: [www.pearsoned.co.uk](http://www.pearsoned.co.uk)

---

# Foundations of Antenna Theory and Techniques

---

**Vincent F. Fusco**  
The Queens University of Belfast



Harlow, England • London • New York • Boston • San Francisco • Toronto • Sydney • Singapore • Hong Kong  
Tokyo • Seoul • Taipei • New Delhi • Cape Town • Madrid • Mexico City • Amsterdam • Munich • Paris • Milan

**Pearson Education Limited**

Edinburgh Gate  
Harlow  
Essex CM20 2JE  
England

and Associated Companies throughout the world

*Visit us on the World Wide Web at:*  
[www.pearsoned.co.uk](http://www.pearsoned.co.uk)

**First published 2005**

© Pearson Education Limited 2005

The right of Vincent F. Fusco to be identified as author of this work has been asserted by him in accordance with the Copyright, Designs and Patents Act 1988.

All rights reserved. No part of this publication may be reproduced, stored in a retrieval system, or transmitted in any form or by any means, electronic, mechanical, photocopying, recording or otherwise, without either the prior written permission of the publisher or a licence permitting restricted copying in the United Kingdom issued by the Copyright Licensing Agency Ltd, 90 Tottenham Court Road, London W1T 4LP.

All trademarks used herein are the property of their respective owners. The use of any trademark in this text does not vest in the author or publisher any trademark ownership rights in such trademarks, nor does the use of such trademarks imply any affiliation with or endorsement of this book by such owners.

ISBN 0 130 26267 6

**British Library Cataloguing-in-Publication Data**

A catalogue record for this book is available from the British Library

**Library of Congress Cataloguing-in-Publication Data**

A catalog record for this book is available from the Library of Congress

10 9 8 7 6 5 4 3 2 1  
08 07 06 05

Typeset in 10/12pt Times by 35  
Printed and bound in Malaysia

*The publisher's policy is to use paper manufactured from sustainable forests.*

# Contents

---

<b>Preface</b>	<b>ix</b>
<b>List of principle symbols</b>	<b>xii</b>
<b>Acknowledgements</b>	<b>xv</b>
<b>1 Basic concepts</b>	<b>1</b>
1.1 Radiation	1
1.2 The Hertzian dipole	5
1.3 Hertzian dipole polar pattern	8
1.4 The Hertzian dipole reconsidered	9
References	18
Problems	18
<b>2 Electromagnetic wave propagation and power flow</b>	<b>20</b>
2.1 Maxwell's equations basics	20
2.2 Plane wave propagation in space	24
2.3 Power flow	28
2.4 Antenna directivity, power gain and efficiency	31
References	38
Problems	39
<b>3 Linear dipole antennas</b>	<b>40</b>
3.1 Dipole antenna of finite length	40
3.2 Current distribution on a finite-length dipole (far-field effect of a sinusoidal current)	42
3.3 Dipole antenna radiation resistance	46
3.4 Short dipole antenna	47
3.5 Gain of a half-wave dipole relative to a Hertzian dipole and power transfer	49

References	54
Problems	55
<b>4 Antenna array techniques</b>	<b>56</b>
4.1 Radiation patterns for two antennas	56
4.2 One-dimensional linear arrays and far-field transformation	60
4.3 Two-dimensional stacked arrays	70
4.4 Non-uniform current excitation array	72
4.5 Antenna input impedance	76
4.6 Induced-emf method and mutual coupling	79
4.7 End-fire array example with mutual coupling	85
4.8 Dipole antennas in relation to a ground plane	89
References	92
Problems	93
<b>5 Systems and characterisation considerations</b>	<b>94</b>
5.1 Effective length of an antenna and reciprocity	95
5.2 Antenna aperture and the free-space link equation	95
5.3 Effective temperature of an antenna and noise effects	101
5.4 Polarisation of plane electromagnetic waves	108
5.5 Distance to antenna far field	112
5.6 Clearance	114
5.7 Antenna characterisation principles	117
References	126
Problems	126
<b>6 Antenna-matching techniques</b>	<b>128</b>
6.1 Transmission line principles	129
6.2 Lumped matching circuits	136
6.3 Reactive matching circuits	142
6.4 Balun matching	148
6.5 Power splitting/combining networks	151
6.6 Impedance matching and the Smith chart	153
References	161
Problems	162
<b>7 Basic antenna types</b>	<b>164</b>
7.1 Small rectangular loop antennas	165
7.2 Slot antennas	167
7.3 Yagi antennas	170
7.4 Rectangular microstrip patch antennas	172
7.5 Reflector antennas	177
7.6 Helical antennas	182
7.7 Horn antennas	186
7.8 Straight-wire travelling-wave antennas	187

7.9	Planar inverted-F antennas	190
7.10	Dielectric resonator antennas	192
7.11	Reflectarray antennas	193
7.12	Equi-angular spiral antennas	195
7.13	Fractal antennas	197
	References	198
	Problems	200
<b>8</b>	<b>Appendices</b>	<b>201</b>
8.1	Linear array factor program	201
8.2	Reciprocity in a two-port network	211
8.3	Noise equivalent bandwidth, minimum discernible level and noise temperature measurement	212
8.4	Scattering parameter matrix	214
	<b>Bibliography</b>	<b>217</b>
	<b>Glossary of terms</b>	<b>221</b>
	<b>Index</b>	<b>225</b>



# Preface

---

This book is designed as a set of topics that interlock in order to give the reader a reasonably paced introduction to the theory that underpins antenna design techniques.

The earliest recorded pioneer of studies related to the creation and detection of electromagnetic radiation through free space was Heinrich Rudolf Hertz (1857–1894). Hertz demonstrated by a series of experiments around 1886 that electromagnetic waves transmitted through the air had wave-like characteristics. By good fortune, the spark gap means by which he created his electromagnetic energy generated centimetre wavelengths. This involved creating a discharge of a Leyden jar (a capacitor) through one coil while causing a spark to pass across a short air gap between the ends of the other coil. Oliver Heaviside had pointed out in 1877 that such a discharge of a capacitor in association with an inductor, the coil, would lead to oscillatory current. In effect, Hertz created a broadband signal generator producing energy over a very wide range of frequencies. Working at centimetre wavelengths meant that he could conveniently reflect these waves by dielectric prisms and metal parabolic mirrors in much the same way as light can be manipulated.

Hertz went on to show, using the principle of resonance, that with identical transmit and receive circuits he could considerably increase the free-space transmission distance between transmitter and receiver. In addition, he realised that the relationship between electromagnetic wave propagation amplitude and distance obeyed the inverse distance relationship. It is this property that makes wireless communication attractive as a virtual wire communication means.

Among Hertz's many key discoveries was the linear oscillator, comprising two metal rods terminating in metal spheres. In fact, he had created a dipole antenna similar in many respects to that much used in today's communication systems. Using this dipole, he showed that the electromagnetic waves he was producing had their electric field component parallel to his rod antennas, i.e. they were linearly polarised. This principle is used today to reduce interference between radio communication systems that

share the same frequency response. Hertz's seminal work ultimately led to the creation of wireless communication across all the frequency ranges in use today.

The work of Hertz went a long way towards validating the set of mathematical relationships postulated by James Clerk Maxwell (1831–1879). Maxwell's equations give the coherent framework within which it is possible to establish the relationships between electricity, magnetism and electromagnetic wave propagation. Maxwell proved that radio waves were an electromagnetic phenomenon and that their maximum speed of propagation in a vacuum was the same as that of light,  $3 \times 10^8$  m/s. His work showed theoretically that, like light, electromagnetic waves could be focused using a parabolic reflector. Maxwell's equations are the starting point for RF and microwave designers in their attempts to quantify and control electromagnetic wave phenomena in order to produce useful engineering artefacts such as antennas.

Samuel Morse had invented the printing telegraph in 1835, while Alexander Graham Bell had patented his telephone transmitter and receiver in 1876 and distant communication over wires was established. The theoretical work of Maxwell, underpinned by the supporting experimental evidence provided by Hertz, had by the 1890s led to the idea that Hertzian waves as they were by that time known might be used as an alternative to wire in order to transmit telegraphic or telephone signals over large distances. The major thrust to providing realisation of these assertions came about as a consequence of the work of Guglielmo Marconi (1874–1937), who from 1894 onwards began to demonstrate wireless communication over useful distances.

A key breakthrough came when Marconi used transmit and receive antennas, which were elevated above the ground. This dramatically improved free-space operating distance from a few hundred metres to several kilometres. Encouraged by these results and realising that one of the most commercially attractive uses for wireless communications at that time was in facilitating ships in distress to summon assistance, Marconi was granted the world's first patent for a wireless telegraph in 1897.

Marconi then formed 'The Wireless Telegraph and Signal Company Ltd' later to become 'The Marconi Company'. A further significant technical breakthrough for Marconi came in 1900, when he obtained a patent for a resonant tuner with a variable capacitor, which could bring the transmitter and receiver into resonance. An extension to this work meant that multiple antennas could be connected to a single transmitter and receiver. With these improvements, Marconi's company had a number of commercial successes with shipboard coastal radio. His major success came in December 1901, when he managed to receive a signal in Newfoundland that had been sent from Cornwall in England. With this, the monopoly control by the British Post Office of transatlantic submarine cable telephony was broken. In the period 1902 to the 1920s, many key developments related to long-wave wireless telephony occurred; for example, valves were invented, which improved transmitter power and receiver sensitivity. Short-wave transatlantic radio communications were pioneered in the 1930s at AT&T, Western Electric and Bell Laboratories in the United States. Engineers such as H.T. Friis and E. Bruce developed theories and antenna types that are still widely used today.

The seminal work of these and other pioneers is constantly evolving, through developments in radar in the 1950s to satellite communications in the 1960s and 1970s and with the aid of miniaturisation in electronics to modern developments in adaptive

antennas for base station and multiband antennas for personal mobile communication wireless handsets that are currently taking place.

The motivation for this book is the recent huge expansion in mobile telecommunications, with the resultant scarcity of qualified RF specialists. One of the key areas of these systems and perhaps the least understood is the point of entry or exit of a wireless signal to and from the system, i.e. the antenna. Engineers with a working knowledge of the basic fundamentals of these structures are increasingly in demand. Their scarcity is compounded by the fact that many university undergraduate programmes have dropped electromagnetic field courses in favour of more digital signal-processing type of activities. Consequently, this book is intended to act as an interpretational guide to the many volumes of excellent (but for the beginner sometimes hard to digest) material that exist in classical textbooks on the subject of electromagnetic waves. Thus it is hoped that this book will facilitate the basis for a study of the concepts that underpin antenna theory and techniques.

The structure of the material is broadly as follows:

- basic concept of radiation and the elementary building block for linear antenna modelling;
- plane wave propagation and power flow;
- basic antenna definitions and the concept of the linear dipole antenna;
- single and multiple dipole antenna radiation pattern formation;
- antenna systems and related characterisation methods;
- basic antenna-matching techniques;
- some popular antenna types.

The text is not meant to be a replacement for the many excellent textbooks on antenna theory that currently exist. It is meant to act as a detailed first reference or as the core of a training tool for those undergraduates, postgraduates or engineers wishing to receive the fundamental theoretical underpinning required for a fruitful appreciation of this rewarding subject.

V.F. Fusco  
November 2004

# List of principle symbols

---

$\alpha$	attenuation coefficient, phase lead or lag used to steer an antenna pattern
$\beta, k$	wave number
$\Delta$	power splitter coupling coefficient
$\epsilon_r$	relative dielectric constant
$\epsilon_0$	permittivity of free space $8.85 \times 10^{-12}$ F/m
$\mu_0$	permeability of free space $4\pi \times 10^{-7}$ H/m
$\phi$	azimuth angle
$\Gamma$	reflection coefficient
$\lambda$	free-space wavelength
$\theta$	elevation angle
$\sigma$	conductivity
$\tau$	tilt angle for polarisation ellipse
$\eta$	wave impedance of free space, white noise power, antenna radiation efficiency
$\omega$	angular frequency in rads/sec
$\psi$	phase delay due to spatially displayed elements, transmission line propagation constant
	wavelength
*	complex conjugate
$A_e$	effective antenna aperture
$ AR $	axial ratio of an ellipse
$B$	bandwidth in Hertz, shunt admittance
$B', B_N$	noise equivalent bandwidth
$c$	velocity of electromagnetic wave propagation, $3 \times 10^8$ m/s
$C$	capacitance
$D$	antenna directivity
$d$	array element separation
$\text{dBi}$	decibels relative to an isotropic source

$\text{dBm}$	decibels relative to 1 mW
EIRP	effective isotropic radiated power
$E_{\text{max}}$	maximum radiated electric field
$E_r$	radial component of electric field
$E_{x,y}$	x,y directed component of electric field
$E_\theta$	elevation component of electric field
$E_\phi$	azimuth component of electric field
$F$	noise factor
$F(\theta)$	pattern multiplication factor
$G$	antenna gain, shunt conductance
$G_R$	gain of receive antenna
$G_T$	gain of transmit antenna
$G/T$	gain to equivalent noise temperature ratio
$G^v(f)$	Noise power at filter input
$h$	height of microstrip substrate
$h_e$	effective length of antenna
$H(f)$	filter impulse response
Hz	Hertz
$H_\phi$	azimuthal component of magnetic field
$I_0, I(o)$	antenna terminal current excitation
$I(z)$	wire antenna current distribution
$k$	Boltzmann's constant, $1.38 \times 10^{-23}$ J/K
$l_{\text{eff}}$	effective length of antenna
$L$	attenuator loss, inductance
$L_i$	insertion loss
MDS	minimum discernible signal level
$n_a$	added noise power
$n_o$	output noise power
$N_f$	noise figure
$P_{\text{inc}}$	incident power
$P_n$	available noise power
$P_R$	power received by antenna
$P_T$	power transmitted by antenna
$q$	charge on electron
$Q$	quality factor
$r$	distance to observation point
$r_n$	$n$ th clearance radius in Fresnel region
$R$	conductor resistance, series resistance
$R_L$	antenna ohmic loss
$R_{\text{rad}}$	radiation resistance
$S_{ij}$	s- parameter for port ij
S/N	signal-to-noise ratio
$T$	absolute temperature in Kelvin
$T_e$	effective noise temperature
$T_N$	Tchebyscheff polynomial
$T_{\text{sys}}$	system noise temperature

xiv List of principle symbols

$v_p$	phase velocity
$V_{ij}$	open circuit voltage induced on antenna $i$ by a signal from antenna $j$
$V_{oc}$	antenna open-circuit terminal voltage
VSWR	voltage standing wave ratio
$x_n$	$n$ th antenna array element separation
$Y$	noise power ratio
$Z$	antenna input impedance
$Z_{ij}$	mutual impedance between two antennas
$Z_0$	characteristic impedance
$Z_s$	sending end impedance
$Z_T$	terminating impedance
<b><math>B</math></b>	magnetic flux density
<b><math>E</math></b>	electric field vector
<b><math>H</math></b>	magnetic field vector
<b><math>J</math></b>	current density

# Acknowledgements

---

I would like to take this opportunity to thank all of those who have contributed directly and indirectly to the creation of this book. Thanks are due to Lorraine Irvine and Joanne Banford for their typing of the manuscript. To my wife Cathy, my son Adam and daughter Kathryn for the support and patience they have shown me.

We are grateful to the following for permission to reproduce copyright material:

Figure 4.15 based on *Applied Electromagnetism*, 1st edition, p. 195 and Fig. 7.26, by L. Shen and J. Kong, © 1983, Figures 5.9 and 5.10 and Equations (5.116)–(5.130) from *Engineering Applications of Electromagnetic Theory*, 1st edition, pp. 406–11, by S. Liao, © 1988, reprinted with permission of Brooks/Cole, an imprint of the Wadsworth Group, a division of Thomson Learning, [www.thomsonrights.com](http://www.thomsonrights.com), fax 800 730 2215; Figure 4.16 and text pp. 118, inclusive of Equations (4.33)–(4.39), and Equations (5.69)–(5.79) and (5.80)–(5.82) based on *Antenna Engineering Handbook*, 1st edition, Fig. 2.15 and pp. 2.20–2.22, 34.29–34.30 and 34.14–34.15, © 1961 by the McGraw-Hill Book Company, Inc., reproduced with permission of The McGraw-Hill Companies (Jasik, H. 1961); Equations (1.20)–(1.34) based on ‘Basic sources of electric and magnetic fields newly examined,’ *IEEE Antennas and Propagation Magazine*, Vol. 43, No. 1, February 2001, pp. 31–5, © 2001 IEEE (Bennett, W. S. 2001); Equations (4.41)–(4.56) and Section 4.6 based on *Electromagnetic Waves and Radiating Systems*, 2nd edition, pp. 382, 387–8 and 536–8, Prentice-Hall, Inc., reproduced with permission of Professor Keith Balmain (Jordan, E. C. and Balmain, K. G. 1968); Equation (5.33) and Section 5.2 based on *Field and Waves in Communication Electronics*, pp. 716–19, copyright © 1965 by John Wiley & Sons, Inc., reprinted by permission of John Wiley & Sons, Inc. (Ramo, S., Winnery, J. R. and Van Duzer, T. 1965).

Section 5.6 based on *Analog Line-of-Sight Radio Links: A Test Manual*, Section 8.3.2, Prentice-Hall International, © 1987 Prentice-Hall International (UK) Ltd (Townsend, A. A. R. 1987); Section 7.4 based on and reprinted with permission from *Microstrip Antennas [7.6]*, pp. 43, 46, 49–51, 57, 64–6, by I. J. Bahl and P. B. Bhartia, © 1980, Artech House, Inc., Norwood, MA, USA, [www.artechhouse.com](http://www.artechhouse.com).

In some instances we have been unable to trace the owners of the copyright material, and we would appreciate any information that would enable us to do so.

# Basic concepts

---

In order to understand the basic principles upon which the operation of antennas rely, it is essential to have an appreciation of how radiation occurs. A simple explanation that shows how an accelerated charge gives rise to radiation is therefore presented first.

This concept is then extended to demonstrate how in the presence of a conductor of short but finite length the radiation from the conductor will be distributed preferentially in space. Examination of this apparently simple structure will yield considerable insight into the behaviour of more complex antennas and arrays of antennas. This basic study also aids the comprehension of the field behaviour close to and far from the basic radiation element, the Hertzian dipole, named after Henrich Hertz (1857–94), who demonstrated the propagation of electromagnetic waves through space [1] and who is credited with the invention of the first antennas.

### 1.1 Radiation

When a time-varying voltage or current is applied to a conductor, free electrons are accelerated. These electrons are able to travel in the spaces between atoms under the influence of the exciting voltage, or current, applied to the conductor. If the current or voltage is alternating, then electrons at a given location on the conductor move back and forward in sympathy with the disturbing force. The acceleration (or deceleration) of these electrons causes radiation to occur [2]. To see why this happens, consider the effect of a single electron with charge  $-q$  C moving along a straight piece of wire. As the charge is accelerated a current will be formed, since by definition current is the rate of change of charge.

As this current flows then a magnetic field,  $H$ , will be set up whose sense is defined by the right-hand screw rule (Figure 1.1). Here the magnetic field lines,  $H$ , form closed loops. Electric field lines,  $E$ , come from infinity to the charge,  $-q$ , as lines of flux,

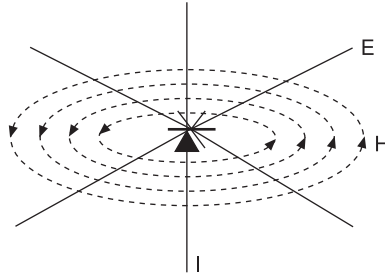


Figure 1.1 Instantaneous magnetic flux lines

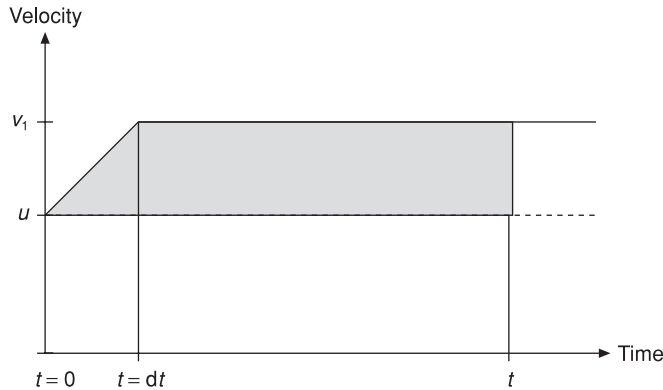


Figure 1.2 Charge velocity profile

thus forming the Coulomb field. The Coulomb field is always present, even if the charge is not in motion. Consider now what happens if the electron is subjected to a period of acceleration, assumed to be linear and applied between  $t = 0$  and  $t = dt$ , after which time the electron travels at constant velocity until time  $t$  (Figure 1.2). Thus the charge is subjected to an acceleration,  $a$ , given by:

$$v_1 = u + a dt \tag{1.1}$$

This means that the charge now reaches a point, say B, on the wire that is a little further on from where it would have been if no acceleration had occurred (point A, Figure 1.3a).

Consider Figure 1.3a in a little more detail, Figure 1.3b, oriented in the Cartesian  $(x, y, z)$  or spherical coordinate system,  $r(\theta, \phi)$ , defined in Figure 1.3c. At time  $t = t_0$ , a single electron is accelerated, such that at time  $t = t_1$  it is at the position shown. An observer positioned at some distant location P will still think that the elementary charge particle is at position  $t = t_0$ , since, as we will show in Section 2.2, its new position will not be registered at position P until a finite time delay later. In addition, a single electric field line coming from some far located point, P, must now reach the charge at position,  $t = t_1$ , rather than at the original position,  $t = t_0$ . To facilitate this, a kink must form in the flux line. Hence the acceleration of the charge particle

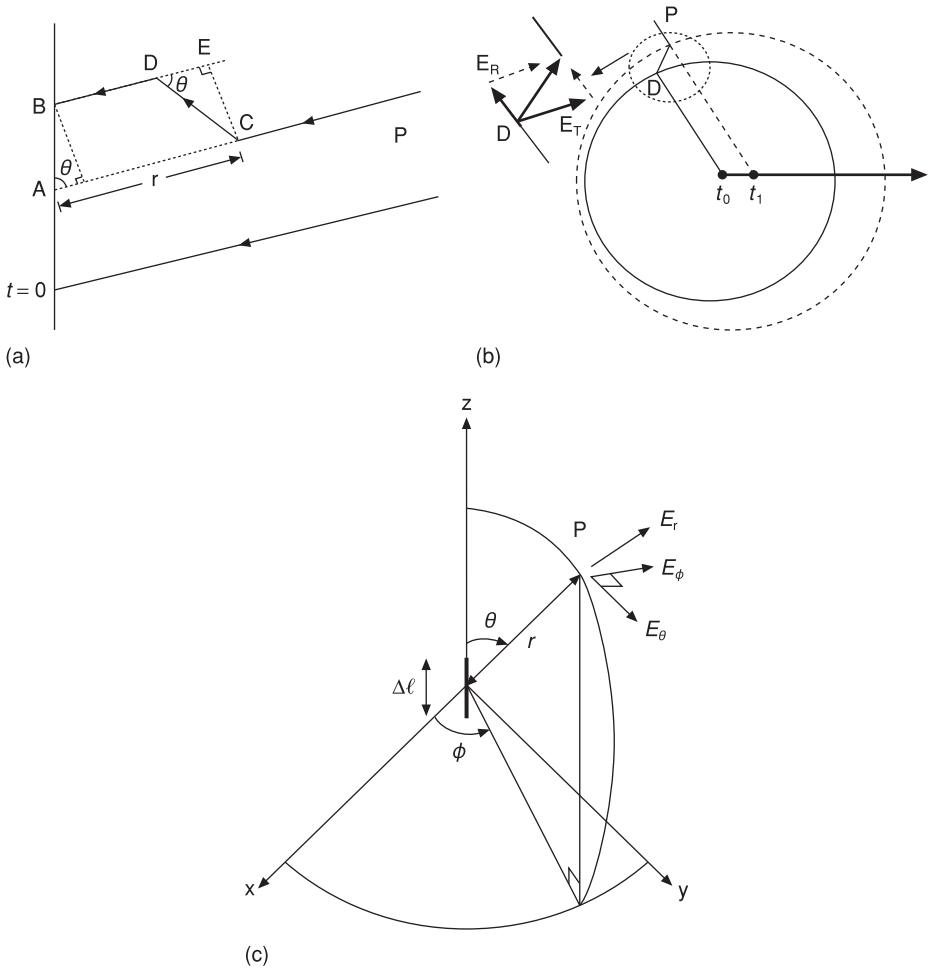


**Figure 1.3** Radiation production

has caused an electromagnetic disturbance. Consideration of the region of the kink in Figure 1.3b shows that there are two field components, a radial component  $E_R$ , which lines up with the Coulomb field, and a transverse component,  $E_T$ . Now since the  $E_R$  component is indistinguishable from the Coulomb field that existed prior to the electron being accelerated no intelligence about the disturbing force is conveyed by that component. On the other hand, the transverse component  $E_T$  is directly attributable to the accelerating charge, and it therefore represents the radiation field component caused by the acceleration of the electron.

To an observer positioned at P, the kink in this line does not appear instantaneously but requires a finite amount of time,  $t$ , defined by the speed of propagation of the electromagnetic energy,  $c$ , to reach the observer (see Section 2.2). The circles in Figure 1.3b, solid circle centred at  $t = t_0$ , dashed circle at  $t = t_1$ , propagate at the speed of light, and the separation between these circles represents the distance an electromagnetic

wave would propagate over the duration of the acceleration. This delay between the electron being accelerated and the effect being detected at P is given as

$$t = \frac{r}{c} \quad (1.2)$$

where  $c$  is the velocity of propagation of electromagnetic waves, and  $r$  is the distance to the point of observation. The overall effect of the acceleration applied to the electron is to generate an outward-propagating wavefront that expands with time.

Considering Figure 1.3c (which defines the spherical coordinate system normally associated with antenna work), the single electron in our radiation model can be considered as a point charge. Hence the radial electric field,  $E_r$ , at distance,  $r$ , can be written as

$$E_r = \frac{-q}{4\pi\epsilon_0 r^2} \quad (1.3)$$

Notice how this term does not contain any acceleration information, hence no intelligence about the source that caused the acceleration to occur. The term  $E_\phi$  will exhibit no variation with  $\phi$ , since the wire is axially symmetrical and hence the very short wire has no field variation associated with this parameter.

On the other hand, the tangential electric field,  $E_\theta$ , at the same distance is given by Figure 1.3a as

$$E_\theta = E_r \tan\theta = \frac{-q}{4\pi\epsilon_0 r^2} \frac{CE}{DE} \quad (1.4)$$

but

$$CE = CD \sin\theta$$

and by the rule of similar triangles

$$CD = AB$$

thus

$$CE = AB \sin\theta$$

Here distance AB is the additional distance travelled by the accelerated electron when compared with the case where no acceleration occurs; thus distance AB is equal to the shaded area under the velocity time graph shown in Figure 1.2. Therefore, since

$$AB = \frac{1}{2} dt(v_1 - u) + (t - dt)(v_1 - u)$$

and

$$v_1 = u + a dt$$

then

$$\begin{aligned} AB &= \frac{1}{2} a dt^2 + (t - dt) a dt \\ &= \frac{1}{2} a dt^2 + at dt - a dt^2 \end{aligned}$$

assuming  $dt$  is small, then

$$AB \approx at \, dt$$

By similar reasoning,

$$DE = c \, dt$$

Hence

$$E_\theta = \frac{-q}{\epsilon_0 r^2} \frac{at}{c} \sin\theta \quad (1.5)$$

using  $t = r/c$

$$E_\theta = \frac{-q}{4\pi\epsilon_0 r^2} \frac{ar}{c^2} \sin\theta \quad (1.6)$$

Finally,

$$E_\theta = \frac{-qa}{4\pi\epsilon_0 c^2 r} \sin\theta \quad (1.7)$$

This term varies according to  $\sin\theta$  and has its greatest value when  $\theta = 90^\circ$ , i.e. in the equatorial ( $x$ - $y$ ) plane of the spherical coordinate system shown in Figure 1.3c. The term illustrates that the strength of the tangential electric field  $E_\theta$  is directly proportional to the acceleration producing it, thus radiation will be greater at higher frequencies. In essence to an observer at some point P (Figure 1.3a) the tangential component of the induced kink is recorded as a consequence of the change of velocity of the charge producing it.

Note that from equation (1.3)  $E_r$  varies according to  $1/r^2$ , while from equation (1.7)  $E_\theta$  varies according to  $1/r$ . Therefore at large distances,  $r$ , from the radiator the radial field will have decayed, leaving only the  $E_\theta$  and associated symmetrical  $E_\phi$  fields. Hence the resultant field far from the radiator is transverse (i.e. no component in the propagation direction,  $r$ ; see Section 2.2). It is the  $1/r$  decay feature of the tangential field component of the electric field strength of a radiating electromagnetic wave that makes long-distance wireless communication feasible. If the  $E_\theta$  component of electric field strength was to decay at  $1/r^2$ , as it does for the radial field component, then the signal at long distances would very quickly diminish to almost zero, thereby severely limiting the range of all wireless systems.

## 1.2 The Hertzian dipole

The Hertzian dipole is an antenna consisting of an extremely short piece of straight conductor that carries an alternating current, which as a consequence of its short length is uniform over that length. In order to ensure that the current distribution is uniform, the antenna is assumed to be electrically short. This concept is very useful in the study of many real antennas of finite length, since these may be regarded as having equivalent

properties to a summation of a number of short dipoles connected together with their radiation patterns deduced from a knowledge of their geometric disposition and superposition of the basic Hertzian dipole radiation pattern.

Assume that the Hertzian dipole is excited with a sinusoidal current,  $i$ , which is uniform along its length,  $\Delta\ell$ , oriented along the  $z$ -axis of Figure 1.3c

$$i = I_0 \sin\omega t \quad (1.8)$$

The current flowing in the antenna consists of  $N$  electrons, each of charge  $q$  C moving with velocity  $v$  m/s. In time,  $\Delta\ell/v$ ,  $Nq$  C would flow through the length of the antenna; hence, since current is defined as

$$i = \frac{dq}{dt} = \frac{Nqv}{\Delta\ell} = I_0 \sin\omega t \quad (1.9)$$

then we can write

$$v = \frac{\Delta\ell I_0 \sin\omega t}{Nq} \quad (1.10)$$

Now, since by definition acceleration  $a = dv/dt$ , then

$$a = \frac{\Delta\ell \omega I_0 \cos\omega t}{Nq} \quad (1.11)$$

We can now deduce from equation (1.7) that the tangential electric field,  $E_\theta$ , due to  $N$  electrons is

$$E_\theta = Nq \frac{a \sin\theta}{4\pi\epsilon_0 c^2 r} \quad (1.12)$$

Thus for the Hertzian dipole, length  $\Delta\ell$ , the radiated electric field  $E_\theta$  at a fixed distance  $r$  at angle  $\theta$  to the dipole is

$$E_\theta(t) = \frac{\Delta\ell \omega I_0 \sin\theta}{4\pi\epsilon_0 c^2 r} \cos\omega \left( t - \frac{r}{c} \right) \quad (1.13)$$

Here the term  $t - (r/c)$  has been introduced to represent the delay that the acceleration effect at the antenna experiences before it is received at some distance  $r$  at angle  $\theta$  from the antenna. That is to say, the radiated field at distance  $r$  lags the acceleration, causing it to occur.

The expression for radiated electric field can be rewritten in revised antenna notation by noting that the wavenumber,  $k = 2\pi/\lambda_0$  and that, from Section 2.2,  $\eta = 1/\epsilon_0 c = E_\theta/H_\phi$ , is the wave impedance and is equal to  $377 \Omega$ , or  $120\pi \Omega$ ; also,  $\lambda_0$  is the free-space wavelength.

Hence  $E_\theta$  in equation (1.13) becomes

$$E_\theta(t) = \eta \frac{I_0 \Delta\ell k \sin\theta}{4\pi r} \cos\omega \left( t - \frac{r}{c} \right) \quad (1.14)$$

from which the antenna  $H_\phi$  field component can be written as

$$H_\phi(t) = \frac{E_\theta}{\eta} = I_0 \frac{\Delta\ell k \sin\theta}{4\pi r} \cos\omega\left(t - \frac{r}{c}\right) \quad (1.15)$$

Notice how the magnetic component does not vary with  $\phi$ ; hence it exhibits circular symmetry. Equations (1.14) and (1.15) suggest that the waves propagating from the Hertzian dipole antenna can be visualised as an expanding wavefront centred at the antenna. Examination in the next section of the governing equations shows that this energy is not radiated uniformly in all directions.

In an even more compact notational form  $I_0 \cos\omega(t - (r/c))$  is written in many antenna textbooks as  $\text{Re} \{I_0 \exp(j\omega(t - r/c))\}$  or  $I_0 e^{j(\omega t - \beta r)}$  or  $I_0 e^{j(\omega t - kr)}$ . Hence with appropriate substitutions we can write

$$E_\theta(t) = \frac{60\pi I \Delta\ell \sin\theta}{\lambda_0 r} e^{-jkr} \quad (1.16)$$

where  $k = 2\pi/\lambda_0 = \omega r/c$  and  $I = I_0 e^{j\omega t}$ .

This equation is the fundamental building block for much of the work to follow.

### Exercise 1.1

Calculate the radial component of electric field associated with a point charge when it is placed in free space at a distance of 1 m from the charge.

#### Solution

From equation (1.3), the radial electric field is

$$\frac{-1.6 \times 10^{-9}}{4\pi \times 8.85 \times 10^{-12} \times 1 \times 1} = -0.16 \text{ V/m}$$

### Exercise 1.2

How does  $E_\theta(t)$  vary as a function of  $\Delta\ell/\lambda_0$ . Comment on the engineering significance of this result.

#### Solution

Using equation (1.16), we can see that  $E_\theta(t)$  is directly proportional to  $\Delta\ell/\lambda_0$ , therefore if  $\Delta\ell$  is small relative to  $\lambda_0$ ,  $E_\theta(t)$  will also be small. Hence for effective radiation along boresight  $\theta = 90^\circ$  the length of the element must be comparable with the wavelength of the radiating element.

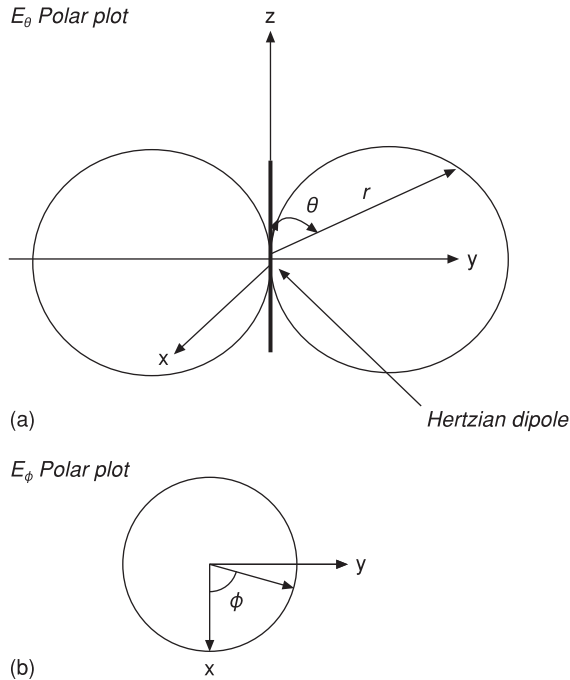


Figure 1.4 Polar plot of electric field amplitude

### 1.3 Hertzian dipole polar pattern

When equation (1.16) is plotted in polar coordinates, the curve formed is a representative plot of the  $E_\theta$  radiation characteristic; for example, Figure 1.4 shows the  $E_\theta$  plot in the plane in which the dipole lies. Due to the axial symmetry of the cylindrical Hertzian dipole element, the resulting radiation pattern must be uniform in a plane perpendicular to the axis of the z-axis oriented Hertzian dipole, the x–y ( $\phi$ ) plane, and as a consequence the polar pattern in that plane is a circle, i.e. there is no variation of field intensity in the  $\phi$  direction (Figure 1.4). When equation (1.16) is plotted in polar format, the radiation pattern as a function of  $\theta$  is a figure-of-eight shape. When compared with the polar pattern that would be obtained for an isotropic source (i.e. a sphere), the Hertzian dipole polar pattern exhibits a power reduction along the axis of the antenna. Thus even a very short antenna such as the Hertzian dipole exhibits preferential radiation in some directions. It should be noted that in order to draw polar patterns in terms of power, the length of the electric field component defined by equation (1.16) should be squared.

Normalised far-field polar (radiation) patterns are usually presented in terms of

$$\frac{\text{magnitude in direction } \theta}{\text{magnitude in the equatorial plane } (\theta = 90^\circ)}$$

which for the Hertzian dipole from equation (1.16) gives  $\sin\theta$ .

From the polar pattern it is possible to determine its half-power beamwidth, which for an antenna is defined as being the angular separation between the directions on each side of the direction of maximum radiation to those points where the radiated field has fallen to  $1/\sqrt{2}$  of its maximum value, i.e. radiated power has fallen to half of its maximum value.

### Exercise 1.3

Show that for a Hertzian dipole the radiated field strength at some distance  $r$  has a half-power beamwidth of  $90^\circ$ .

#### Solution

For a Hertzian dipole equation (1.16) its normalised far field pattern equation is written as

$$\sin\theta = \pm \frac{1}{\sqrt{2}}$$

since half power is proportional to  $1/\sqrt{2}$  electric field strength.

$$\text{Hence } \theta = \sin^{-1}\left(\pm \frac{1}{\sqrt{2}}\right) = 45^\circ \text{ or } 135^\circ$$

giving the Hertzian dipole a half-power beamwidth of  $(135^\circ - 45^\circ) = 90^\circ$ . This means that power is spread over a wide angle, and Chapter 4 shows methods to focus radiation from antennas by using them in an array configuration.

## 1.4 The Hertzian dipole reconsidered

We previously defined the Hertzian dipole as a fictitious antenna that supported a uniform current distribution over its very short length. The accumulation of charge at the ends of this short wire could be represented by allowing the dipole to be modelled as two charges,  $+q$  and  $-q$ , placed at the end points of the dipole. These charges of opposite polarity will oscillate as a complementary charge pair, called an oscillating charge doublet.

We can use this model to determine how the radiated electric field from the Hertzian dipole behaves close into the radiator, i.e. in the near field or Fresnel region (see Section 5.5). Unlike the far-field region, in this region the antenna radiation pattern is a function of the exact position of where it is measured. The electric field potential at the observation point P in Figure 1.5 for a Hertzian dipole of length  $\Delta\ell$  is, according to Coulombs law,

$$v = \frac{+q}{4\pi\epsilon_0 r_1} + \frac{-q}{4\pi\epsilon_0 r_2} \quad (1.17)$$

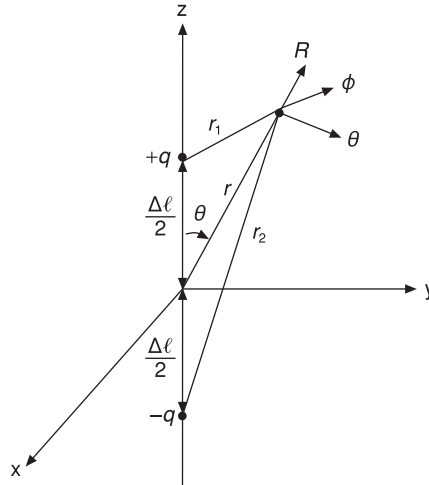


Figure 1.5 Oscillating dipole representation of a Hertzian dipole

#### Exercise 1.4

Point charges  $4 \times 10^{-9}$  C and  $-2 \times 10^{-9}$  C are located at Cartesian  $(x, y, z)$  space at  $(2, 0, 0)$  and  $(6, 0, 0)$ . Find the electric field potential at position  $(4, 2, 0)$ .

#### Solution

Since the field point to be estimated lies in the  $(x, y)$  plane, we can use simple geometry to establish distances  $r_1, r_2$ , required by equation (1.17) as being equal to  $\sqrt{8}$ , thus

$$\begin{aligned} v &= \frac{4 \times 10^{-9}}{4\pi\epsilon_0\sqrt{8}} - \frac{2 \times 10^{-9}}{4\pi\epsilon_0\sqrt{8}} \\ &= \frac{1 \times 10^{-9}}{2\pi\epsilon_0\sqrt{8}} = 6.4 \text{ V/m} \end{aligned}$$

Now from geometrical considerations

$$\begin{aligned} r_1 &= \sqrt{\left(r - \frac{\Delta\ell}{2} \cos\theta\right)^2 + \left(\frac{\Delta\ell}{2} \sin\theta\right)^2} \\ &\approx r - \frac{\Delta\ell}{2} \cos\theta \end{aligned} \tag{1.18}$$

and

$$r_2 \approx r + \frac{\Delta\ell}{2} \cos\theta$$

thus

$$r_2 - r_1 \approx \Delta \ell \cos \theta$$

For a sinusoidal excitation controlling the oscillating charge doublet

$$i = I_0 \sin \omega t$$

we can find an expression for charge, since by definition

$$q = \int i \, dt = \frac{-I_0}{\omega} \cos \omega t \quad (1.19)$$

Remembering that this charge will be observed at point P some time,  $r/c$ , later, after it has occurred at the dipole, we can write

$$q = \frac{-I_0}{\omega} \cos \omega \left( t - \frac{r}{c} \right) \quad (1.20)$$

Thus from equation (1.17)

$$v = \frac{-I_0}{4\pi\omega\epsilon_0} \left( \frac{1}{r_1} - \frac{1}{r_2} \right) \cos \omega \left( t - \frac{r}{c} \right)$$

By noting that  $r_1 r_2 \approx r^2$  and  $r^2 \gg \Delta \ell^2 / 4 \cos^2 \theta$ , then since  $r_2 - r_1 = \Delta \ell \cos \theta$

$$v = \frac{-I_0 \Delta \ell}{4\pi\omega\epsilon_0} \frac{1}{r^2} \cos \theta \cos \omega \left( t - \frac{r}{c} \right) \quad (1.21)$$

Now that we know the potential occurring at some point P in space due to an oscillating current at the dipole, we can find the resultant electric field at this observation point. When this is converted to the spherical coordinate system as defined below, it will yield the three components of electric field at the observation point. Thus

$$E_r = \frac{-\partial v}{\partial r} = \frac{I_0 \Delta \ell}{4\pi\epsilon_0} \cos \theta \left[ \frac{1}{cr^2} \sin \omega \left( t - \frac{r}{c} \right) - \frac{1}{\omega r^3} \cos \omega \left( t - \frac{r}{c} \right) \right] \quad (1.22)$$

$$E_\theta = -\frac{1}{r} \frac{\partial v}{\partial \theta} = -\frac{I_0 \Delta \ell}{4\pi\omega\epsilon_0} \sin \theta \left[ \frac{1}{r^3} \cos \omega \left( t - \frac{r}{c} \right) \right] \quad (1.23)$$

$$E_\phi = -\frac{1}{r \sin \theta} \frac{\partial v}{\partial \phi} = 0$$

The zero result for  $E_\phi$  is due to the symmetry of the electric field in the  $\phi$  plane. Hence from equations (1.22) and (1.23) we see that an oscillating current moving in an infinitely small length of wire will induce electromagnetic radiation.

In the derivation of equations (1.22) and (1.23), we have used the transformation from a Cartesian coordinate system to a spherical coordinate system, i.e.

$$\mathbf{E} = \frac{\partial v}{\partial x} \mathbf{i} + \frac{\partial v}{\partial y} \mathbf{j} + \frac{\partial v}{\partial z} \mathbf{k}$$

is equivalent to

$$\mathbf{E} = \frac{\partial v}{\partial r} \ell_r + \frac{1}{r} \left( \frac{\partial v}{\partial \theta} \ell_\theta + \frac{1}{\sin \theta} \frac{\partial v}{\partial \phi} \ell_\phi \right) \quad (1.24)$$

where  $i, j, k, \ell_r, \ell_\theta, \ell_\phi$  are orthogonal unit vectors in each coordinate system.

Comparing these results with the results obtained in equation (1.16), where it was assumed that  $r$  was a large distance from the antenna, we see here that close to the antenna the  $1/r^3$  term determines the rate of decrease of the  $E_\theta$  field with distance. Here the electric field created by the dipole dominates, and in this area the energy stored represents a capacitive region, which since it is reactive does not contribute to radiated power.

Alternatively, if the short dipole is considered as a conductor carrying current, then the associated magnetic field can be found by direct application of the Biot–Savart law [3] as

$$H_\phi = \frac{I_0 \Delta \ell \sin \theta}{4\pi \epsilon_0 r^2} \sin \omega \left( t - \frac{r}{c} \right) \quad (1.25)$$

which when added to the previously derived expression, the  $H_\phi$  component for large distances  $r$ , equation (1.15), gives

$$H_\phi = \frac{I_0 \Delta \ell}{4\pi} \sin \theta \left[ \frac{\omega}{cr} \cos \omega \left( t - \frac{r}{c} \right) + \frac{1}{r^2} \sin \omega \left( t - \frac{r}{c} \right) \right] \quad (1.26)$$

The second term in this expression will dominate when  $r$  is small, and it is said to represent the induction component of the field close to the antenna.

### Exercise 1.5

Show that according to the definition in [4] the boundary point between the induction field and the radiation field occurs when from equation (1.26)  $r \approx \lambda/6$ .

### Solution

According to [4], the boundary point between the near- and far-field regions can be defined as the distance when both induction and radiation fields have equal magnitude. This position can be established from equation (1.26) such that

$$\left| \frac{1}{r^2} \sin \omega \left( t - \frac{r}{c} \right) \right| = \left| \frac{\omega}{cr} \cos \omega \left( t - \frac{r}{c} \right) \right|$$

or

$$\frac{\omega}{cr} = \frac{1}{r^2}$$

$$\text{hence } r = \frac{c}{\omega} = \frac{f\lambda}{2\pi f} = \frac{\lambda}{2\pi} \approx \frac{\lambda}{6}$$

Inside this region, each of the field components is in phase quadrature, with energy absorbed each quarter of a cycle being returned to the field during the next quarter of a cycle. Thus inside this region energy is collapsed back to the radiating element and then returned to the region, giving rise to the antenna reactance.

Thus in the near field of the antenna, i.e. close to the radiator,  $r < \lambda/6$ , we have a capacitive field and an inductive field, given in terms of their electrical and magnetic field quantities  $E_\theta$  and  $H_\phi$ , respectively. Outside the region, the energy leaves in the form of a propagating electromagnetic wave travelling at the speed of light. The interaction of these two fields results in a reactive quantity normally referred to as the induction or near field of the antenna.

By applying Poynting's theorem (Section 2.3), we get the instantaneous value of radiated power per unit area as  $P = E_\theta H_\phi$ . In the antenna near field

$$P = \frac{I_0^2 \Delta \ell^2}{16\pi^2 \omega \epsilon_0} \sin^2 \theta \frac{1}{r^5} \sin \omega \left( t - \frac{r}{c} \right) \cos \omega \left( t - \frac{r}{c} \right) \quad (1.27)$$

### Exercise 1.6

Use Poynting's theorem to gauge how the instantaneous value of radiated power decreases with distance in the near field of an electrically short antenna.

#### Solution

From equation (1.27), we see that in the near field power falls off rapidly as  $1/r^5$ . Thus at short distances from the antenna the near-field power level has decreased almost to zero; for example, a doubling of range leads to a 1/32 or -15 dB reduction in field strength.

### Exercise 1.7

Use the result in equation (1.27) to determine the frequency of the near-field reactive power.

#### Solution

From equation (1.27), we can write

$$\sin \omega \left( t - \frac{r}{c} \right) \cos \omega \left( t - \frac{r}{c} \right) = \frac{1}{2} \sin 2\omega \left( t - \frac{r}{c} \right)$$

Thus in the near field reactive power fluctuates at twice the generator frequency.

Consider now the Biot-Savart law [3] [5] under time-varying current excitation operating over a short length of wire embedded in a longer piece of wire (Figure 1.6).

$$H_\phi(t) = \frac{\Delta \ell \sin \theta}{4\pi r^2} i(t) \quad (1.28)$$

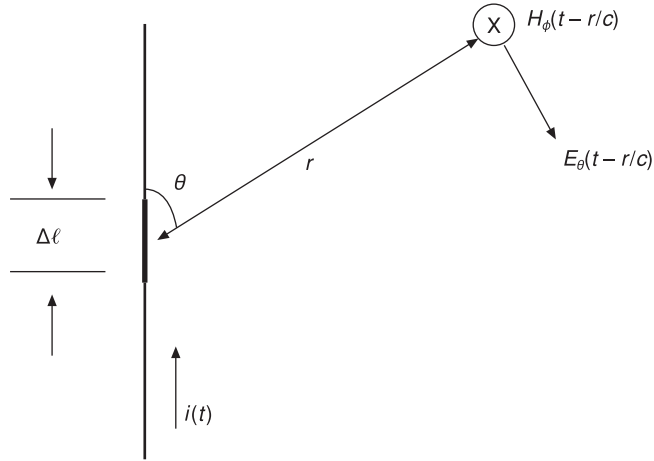


**Figure 1.6** Field from short section of wire

At a distant observation point,

$$H_{\phi}(t) = \frac{\Delta\ell \sin\theta}{4\pi r^2} i\left(t - \frac{r}{c}\right) \quad (1.29)$$

In Section 1.1, we showed how the electromagnetic radiation effect occurs when a charge is accelerated and consequently how the far-field component is proportional to the rate of change of time-delayed current. From the basic definition of differentiation, we can write

$$\frac{di(t)}{dt} = \lim_{\Delta t \rightarrow 0} \left[ \frac{i(t + \Delta t) - i(t)}{\Delta t} \right] \quad (1.30)$$

If we let  $\Delta t = r/c$  and  $t = t - r/c$ , then we can rearrange equation (1.30) as

$$i(t) = \lim_{r/c \rightarrow 0} \left[ i\left(t - \frac{r}{c}\right) + \frac{r}{c} \frac{di\left(t - \frac{r}{c}\right)}{dt} \right]$$

Hence equation (1.29) can be written [6] as

$$H_{\phi}(t) = \frac{\Delta\ell \sin\theta}{4\pi r^2} \left[ i\left(t - \frac{r}{c}\right) + \frac{r}{c} \frac{di\left(t - \frac{r}{c}\right)}{dt} \right] \quad (1.31)$$

and from Section 2.2 we know that  $E_{\theta}/H_{\phi} = \eta$ , the free-space impedance. Thus we can write

$$E_{\theta}(t) = \eta \frac{\Delta\ell \sin\theta}{4\pi r^2} \left[ i\left(t - \frac{r}{c}\right) + \frac{r}{c} \frac{di\left(t - \frac{r}{c}\right)}{dt} \right] \quad (1.32)$$

Equation (1.32) represents the radiated electric field due to the time-varying current impressed on a wire segment embedded in a long wire. If the wire segment were to be removed from the long wire, then charge would accumulate at the ends of the wire and a charge doublet would be created. This will provide an additional contribution to the radiation field described by equation (1.23) that will supplement that given by equation (1.32).

For compatibility with equation (1.32), we now rearrange equation (1.23) as

$$E_{\theta} = \frac{\eta \Delta \ell}{4\pi\omega r^2} \left[ \frac{c}{r} q \left( t - \frac{r}{c} \right) \right]$$

where we have used  $1/\epsilon_0 = \eta c$  (see Section 2.2). Thus the total radiated electric field becomes the superposition of both radiation fields.

$$E_{\theta}(t) = \frac{\eta \Delta \ell \sin\theta}{4\pi r^2} \left[ \frac{c}{r} q \left( t - \frac{r}{c} \right) + i \left( t - \frac{r}{c} \right) + \frac{r}{c} \frac{di \left( t - \frac{r}{c} \right)}{dt} \right] \quad (1.33)$$

Using the form given in equation (1.31) and (1.33), it is possible to establish the radiation characteristics of a wire dipole under arbitrary excitation conditions.

Upon substitution of  $i(t - r/c) = I_0 \sin\omega(t - r/c)$  and using complex notation

$$E_{\theta}(t) = \frac{\eta I_0 \Delta \ell k \sin\theta}{4\pi r^2} \left( 1 + \frac{1}{jkr} + jkr \right) e^{-jkr} \quad (1.34)$$

Using the same approach, equation (1.31) becomes

Note: The treatment leading to equations (1.20) through (1.34) is based on equations (2) through (7) in W.S. Bennett, Basic sources of electric and magnetic fields newly examined, *IEEE Antennas and Propagation Magazine*, Vol. 43, No. 1, 2001, pp. 31–5. © 2001 IEEE.

$$H_{\phi} = \frac{I_0 \Delta \ell \sin\theta}{4\pi r^2} (1 + jkr) e^{-jkr} \quad (1.35)$$

### Exercise 1.8

Show that as the distance from the antenna to the field sampling point is reduced, the ratio  $E_{\theta}/H_{\phi}$ , equal to  $377 \Omega$  for free space, is no longer applicable.

#### Solution

For small values of  $r$ , the first and second terms in the parenthesis of equation (1.34) dominate. Thus

$$\frac{E_{\theta}}{H_{\phi}} = \eta \frac{\left( \frac{1}{r^2} + \frac{1}{jkr^3} \right)}{\frac{1}{r^2}} = \eta \left( 1 + \frac{1}{jkr} \right) = \eta \left( \frac{1 - j\Delta r}{2\pi r} \right)$$

hence in the near field the  $377 \Omega$  wave impedance applicable to far-field calculations becomes a function of distance and exhibits a large capacitive reactance as  $r$  tends to zero.

and

$$E_r = \frac{\eta I_0 \Delta \ell \cos \theta}{2\pi r^2} \left( 1 + \frac{1}{jkr} \right) e^{-jkr} \quad (1.36)$$

$$\text{here } \eta = \sqrt{\frac{\mu_0}{\epsilon_0}}$$

### Exercise 1.9

Show that in the far field of a linear wire antenna, everywhere, except near the antenna axis, the  $E_\theta$  component dominates the radial  $E_r$  field component.

#### Solution

By taking the ratio of equation (1.34) and (1.36) at large  $r$ , we see that

$$\left| \frac{E_R}{E_\theta} \right| \propto \frac{1}{r \tan \theta}$$

so that when  $\theta$  tends to zero, i.e. in a spherical coordinate system along the z-axis,  $E_R \gg E_\theta$ , otherwise as  $\theta$  tends to  $90^\circ$   $E_\theta \gg E_R$ .

From the expression for  $E_\theta$ , we can identify the induction and far-field radiation components.

### Exercise 1.10

Consider a short antenna of length 1 cm excited with a 100 mA current at 1 GHz and calculate the magnitude of the tangential electric field along the antenna boresight at a distance of  $100\lambda$ .

#### Solution

Antenna length,  $\ell$ , is 1 cm, operating frequency is 1 GHz and  $\lambda_0 = 30$  cm; therefore  $\Delta \ell / \lambda_0 = 1/30$  so we can reasonably approximate the antenna as a Hertzian dipole. Thus we can apply equation (1.34) for  $E_\theta$ , which at a distance of  $100\lambda$  the first two terms in the parenthesis can be ignored since we are in the far field of the antenna. Hence equation (1.34) becomes

$$E_\theta = j\eta \frac{I_0 \Delta \ell \sin \theta}{4\pi} \frac{k}{r}$$

Thus

$$E_\theta = j \frac{377 \times 0.1}{200 \times 30 \times 30}$$

$$|E_\theta| = 0.21 \text{ V/cm}$$

Equation (1.34) may be viewed by consideration of the action of the free electrons in the wire segment under excitation. Here, since each free electron carries a charge and since this charge is affected by the field created by the dynamic displacement of other free electrons due to the applied oscillating current, the fields thus created exert forces on the free electrons that were responsible for creating the fields in the first place. Thus the forces created act to resist electron motion. Furthermore, the second field term in equation (1.34) is  $90^\circ$  out of phase with the third term in equation (1.34). Thus we say that the dynamic fields produced by this field term act to oppose the rate of change of the applied current.

Energy in the near field produced by this process is delivered to the magnetic field created around the moving electrons and is returned to the electrons as the magnetic fields collapse when the electrons decelerate. Hence we have a reactive near-field component that is inductive and does not contribute to the radiated power.

A cross-section through the field close to the dipole at an instant in time would show that as time passes the field will continually expand outwards at the velocity of light. The radiation process is one in which closed loops of electric field form continuously as the field oscillates. As a loop is formed it propagates outwards (Section 2.2), maintaining a steady flow of energy (Section 2.3) into free space.

Figure 1.7 shows the radiation field from a Hertzian dipole in terms of its electric and magnetic flux lines plotted in a polar coordinate system. The instantaneous amplitude of the  $E_\theta$  component is given by equation (1.34). More details on how the radiation field can be plotted as it evolves with time is given in [4].

We can see heuristically how the radiation process evolves in time if we consider what happens when a short dipole is excited by a voltage pulse. If the pulse length is short compared with the length of the dipole, then when the charge induced by the pulse is decelerated, radiation will occur at the ends of the dipole and a closed electric field line set up (Figure 1.8a). The charges are then reflected from the open ends of the dipole back towards the centre of the dipole (Figure 1.8b). At this position, as the field lines join a closed flux loop is formed (Figure 1.8c). During these charge movements, the flux loop is expanding into space. As the process repeats this closed loop breaks off into space (Figure 1.8d) and a new loop forms in the opposite sense.

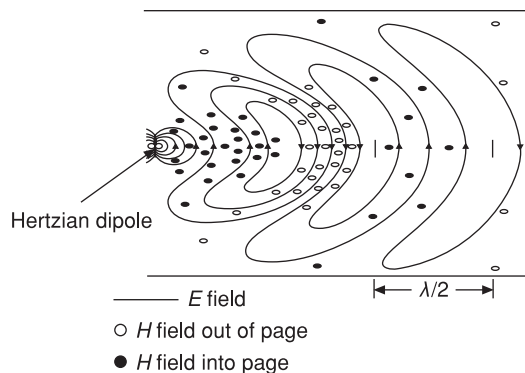
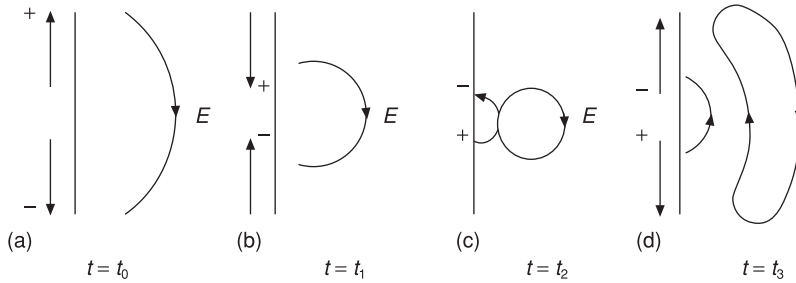


Figure 1.7 Radiation field of a Hertzian dipole



**Figure 1.8** Short dipole carrying an oscillating charge packet moving under the influence of a sinusoidal oscillation period  $T$

Once the process settles down, i.e. after many loops are formed and several closed loops have been formed, the distance between field maxima along the boresight normal to the antenna axis is one-half of a free-space wavelength as determined by the frequency of the source used to excite the system (Figure 1.7). Although not discussed here, an explanation of this effect based on time-domain pulse tracking along the arms of a dipole antenna can be obtained directly from equation (1.33). This way of conceptualising the problem can be useful [7].

## References

- [1] Bray, J., *The Communications Miracle, The Telecommunication Pioneers from Morse to the Information Superhighway*, Plenum Press, 1995.
- [2] Feynman, R.P., Leighton, R.B. and Sands, M., *The Feynman Lectures on Physics, Mainly Mechanics Radiation and Heat*, Addison-Wesley, 1963, Chapter 28.
- [3] Paul, C.R. and Nasar, S.A., *Introduction to Electromagnetic Fields*, McGraw-Hill, 1982, Chapter 4.
- [4] Jordan, E.C. and Balmain, K.G., *Electromagnetic Waves and Radiating Systems* (2nd edition), Prentice Hall, 1968, Chapter 14.
- [5] Karmel, P.L., Colef, G.D. and Camisa, R.L., *Introduction to Electromagnetic and Microwave Engineering*, Wiley Series in Microwave and Optical Engineering, John Wiley & Sons, 1998, pp. 253–4 and 628–30.
- [6] Bennett, W.S., Basic sources of electric and magnetic fields newly examined, *IEEE Antennas and Propagation Magazine*, Vol. 43, No. 1, 2001, pp. 31–5.
- [7] Cloude, S., *An Introduction to Electromagnetic Wave Propagation and Antennas*, UCL Press, 1995, pp. 43–5.

## Problems

- 1.1 Show that radiation occurs only from contributions of acceleration that are transverse to the line that joins the observation point P and the charge source that is being accelerated.

- 1.2** Describe why the electromagnetic radiation associated with a change of current at the source is not sensed immediately at a distantly located observation point P.
- 1.3** Calculate the half-power beamwidth for a straight wire antenna of length 1.5 cm, operating at 1 GHz. You may assume that the antenna is centre-fed.  
Would you expect the reactance of the antenna seen at its excitation terminals to be capacitive or inductive?
- 1.4** Why is the electromagnetic field close into the antenna, i.e. at distances less than  $\lambda/2\pi$ , called the induction field? What are the essential properties of this electromagnetic component of the total radiated field, and how do they influence the reactive impedance presented by the antenna at its excitation terminals? How rapidly do these components decay with distance from the antenna?

# Electromagnetic wave propagation and power flow

---

Maxwell's equations, named after James Clerk Maxwell (1831–79), govern the propagation behaviour of electromagnetic waves. An understanding of how these waves propagate in free space is an essential first step in developing an appreciation of antenna techniques. With this in mind, we first introduce Ampere's law and Faraday's law and show how these underpin the construction of Maxwell's equations, from which the wave equations that model the propagation of plane waves in free space are developed. These equations yield various insights into the definition of wave impedance and the speed at which electromagnetic energy propagates. In addition, the concept of transverse waves is developed further. From these ideas it is shown how the power flow associated with plane propagating waves can be determined. Using these concepts as underpinning, fundamental antenna-related figures of merit, such as power gain and directivity, are developed by considering that propagating plane waves are observed in the far-field region of antennas or antenna arrays.

### 2.1 Maxwell's equations basics

The equations that characterise the macroscopic propagation properties of electromagnetic waves are known as Maxwell's equations [8]. These equations are derived from Ampere's law and Faraday's law, the fundamental experimental laws of electricity.

Ampere's law states that the integral of the magnetic field around a closed path,  $c$ , forming the boundary to an area,  $a$ , through which a current  $I$  flows, is equal to that current.

$$\oint_c H_s ds = \int_s J_n da \quad (2.1)$$

where  $J_n$  is the normal component of current flowing through an elemental area,  $da$ , of a surface,  $s$ , bounded by a closed contour,  $c$ , around which the magnetic field,  $H_s$ , (i.e. the component of the magnetic field along the closed contour  $c$ ) is integrated (see Figure 1.6). The circle on the integral sign in equation (2.1) means that integration is being carried out over a closed contour.

Faraday's law states that when the magnetic flux through a circuit is changing, an induced voltage is set up whose magnitude is proportional to the rate of change of that flux.

$$\oint_c E_s ds = -\frac{\partial}{\partial t} \int_s B_n da \quad (2.2)$$

where  $B_n$  is the normal component of magnetic flux density crossing an elemental area,  $da$ , of a surface,  $s$ , bounded by a closed contour,  $c$ , around which the electric field,  $E_s$ , is integrated.

If two new equations are introduced, then equations (2.1) and (2.2) can be further simplified. The first of these equations connects flux density,  $\mathbf{B}$ , and magnetic field,  $\mathbf{H}$ , as

$$\mathbf{B} = \mu\mathbf{H} \quad (2.3)$$

here  $\mathbf{B}$  and  $\mathbf{H}$  are vectors oriented in the same direction, and  $\mu$  is the permeability of the medium.

The next equation forms the connection between electric field  $\mathbf{E}$  and current density  $\mathbf{J}$  in a conducting medium of conductivity,  $\sigma$ . Again the vectors are oriented in the same direction:

$$\mathbf{J} = \sigma\mathbf{E} \quad (2.4)$$

For low-frequency work these equations are sufficient. However, at very high frequencies another term has to be added to the current density; Maxwell called this term displacement current. For example, in Figure 2.1 a high-frequency AC source drives a closed loop containing a parallel-plate capacitor.

According to Ampere's law, given by equation (2.1), the integral of the magnetic contour A should give the current through any surface '1' of which contour A forms the boundary and that cuts the wire. If the surface '2' is now arranged to pass between

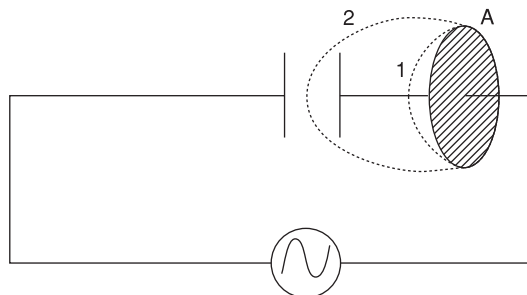


Figure 2.1 Displacement current contours

the plates of the capacitor, then no current would be observed to be moving through this surface and the resulting current would be zero, *contradicting the first result*. To reconcile the difference an additional term, the displacement current term, was added by Maxwell. To find how this was done, consider the following.

Let the parallel-plate capacitor in Figure 2.1 have capacitance value  $C$ , plate area  $A$  and plate separation  $d$ . Let the excitation voltage  $V = v \sin \omega t$ . Under these conditions, the charging current through the capacitor value  $C$  is

$$I_c = C \frac{dV}{dt} = \omega C v \cos \omega t \quad (2.5)$$

where for an ideal parallel-plate capacitor  $C = \epsilon A/d$ . Between the capacitor plates the magnitude of the electric field  $E$  is  $v/d$ , so that if a total displacement current is defined as

$$I_d = C \frac{dV}{dt} = \omega \frac{\epsilon A}{d} v \cos \omega t = \epsilon \frac{d(v/d)}{dt} = \epsilon \frac{dE}{dt} \quad (2.6)$$

the consequence of this is that the result for displacement current is now exactly that for the charging current. Thus the introduction of the concept of displacement current resolves the discrepancy, albeit in a fairly arbitrary way.

### Exercise 2.1

A 1 V AC signal at 1 GHz is applied to an air-spaced parallel-plate capacitor of area  $1 \text{ cm}^2$  and with plate separation of 1 mm. Calculate the magnitude of the displacement current associated with this arrangement.

### Solution

From equation (2.6), the magnitude of the displacement current  $I_d$  is

$$\begin{aligned} \frac{\omega E A V}{d} &= \frac{2\pi \times 1 \times 10^9 \times 8.85 \times 10^{-12} \times 1 \times 0.01 \times 0.01 \times 1}{1 \times 10^{-3}} \\ &= 5.6 \text{ mA.} \end{aligned}$$

With this in mind, the current density vector equation (2.4) becomes

$$\mathbf{J} = \sigma \mathbf{E} + \epsilon \frac{\partial \mathbf{E}}{\partial t} \quad (2.7)$$

Hence in a non-conducting medium such as air,  $\sigma$  becomes zero and the displacement current is the only remaining current term.

Substituting equation (2.7) into (2.1) and (2.3) into (2.2) yields

$$\oint_c \mathbf{H}_s \cdot d\mathbf{s} = \epsilon \frac{\partial}{\partial t} \oint_s \mathbf{E}_n \cdot d\mathbf{a} \quad (2.8)$$

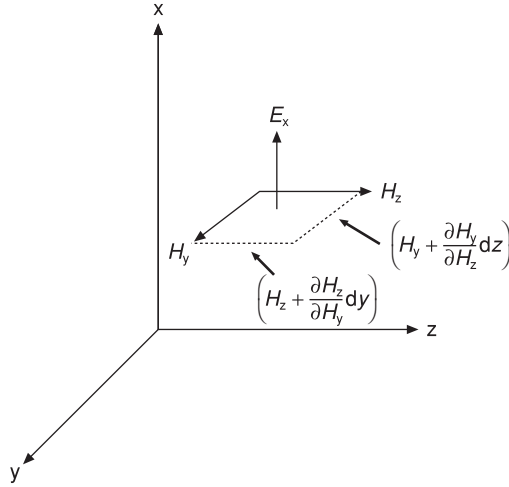


**Figure 2.2** Maxwell's equations

and

$$\oint_c E_s d\ell = -\mu \frac{\partial}{\partial t} \int_s H_n da \quad (2.9)$$

these equations are the integral form of Maxwell's equations for free space or non-conducting dielectric media [8].

Consider equation (2.8) in graphical form for a very small element of area,  $dydz$ , and normal  $E$  field component  $E_x$  (Figure 2.2). We can now write

$$\begin{aligned} \epsilon \frac{\partial}{\partial t} E_x dy dz &= H_y dy + \left( \left( H_z + \frac{\partial H_y}{\partial z} dy \right) \right) dz - \left( H_y + \frac{\partial H_y}{\partial z} dz \right) dy - H_z dz \\ &= \left( \frac{\partial H_z}{\partial y} - \frac{\partial H_y}{\partial z} \right) dy dz \end{aligned}$$

Hence

$$\epsilon \frac{\partial E_x}{\partial t} = \left( \frac{\partial H_z}{\partial y} - \frac{\partial H_y}{\partial z} \right) \quad (2.10)$$

Applying the same procedure to the  $E_y, E_z$  field components, the other components of the  $E$  vector can be found as

$$\epsilon \frac{\partial E_y}{\partial t} = \left( \frac{\partial H_x}{\partial z} - \frac{\partial H_z}{\partial x} \right) \quad (2.11)$$

$$\epsilon \frac{\partial E_z}{\partial t} = \left( \frac{\partial H_y}{\partial x} - \frac{\partial H_x}{\partial y} \right) \quad (2.12)$$

By a similar process, equation (2.9) can be expressed as

$$-\mu \frac{\partial H_x}{\partial t} = \left( \frac{\partial E_z}{\partial y} - \frac{\partial E_y}{\partial z} \right) \quad (2.13)$$

$$-\mu \frac{\partial H_y}{\partial t} = \left( \frac{\partial E_x}{\partial z} - \frac{\partial E_z}{\partial x} \right) \quad (2.14)$$

$$-\mu \frac{\partial H_z}{\partial t} = \left( \frac{\partial E_y}{\partial x} - \frac{\partial E_x}{\partial y} \right) \quad (2.15)$$

These equations can now be used to construct the wave equation used to determine the characteristics of plane wave propagation, i.e. the sort of wave we would expect to see in the far field of an antenna. It should be noted that in Figure 2.2 we have oriented the  $z$ -axis to point in the right-hand direction, since this direction is normally associated with the direction of propagation.

## 2.2 Plane wave propagation in space

An electromagnetic wave initiated from a point source in free space will propagate uniformly in all directions, and the radiation will take the form of a spherical wavefront (Figure 2.3). At large distances from the source (a large distance is defined in Section 5.5), the waves will appear to have plane wave properties, as defined below. The velocity of the wave when propagating in free space is  $c$ , given by

$$c = \frac{1}{\sqrt{\mu_0 \epsilon_0}} \text{ m/s}$$

where  $\mu_0$  is the permeability of free space ( $4\pi \times 10^{-7}$  H/m<sup>2</sup>), and  $\epsilon_0$  is the permeability of free space ( $1/36\pi \times 10^{-9}$  V/m)

Hence

$$c = 3 \times 10^8 \text{ m/s}$$

With a plane wave  $\mathbf{E}$  and  $\mathbf{H}$  always oscillate in phase and in space quadrature (Figure 2.3). The ratio  $\eta = \sqrt{\epsilon_0/\mu_0}$ , 377  $\Omega$ , defines the free-space wave impedance.

A plane wave is said to be a transverse wave, since its field vectors  $\mathbf{E}$  and  $\mathbf{H}$  are orthogonal and lie in a plane that is transverse, i.e. in a cross-sectional plane, normal to the direction of wave propagation. Consequently, no component of field lies along the propagation direction. At any given time, if we instantaneously sample the magnitude and direction of  $\mathbf{E}$  and  $\mathbf{H}$  at any transverse plane the surface in which  $\mathbf{E}$  and  $\mathbf{H}$  have maximum values defines the wave front of the propagating signal. More generally, the wavefront is defined such that  $\mathbf{E}$  and  $\mathbf{H}$  have constant phase across it. To see why these concepts for plane-wave propagation are valid, we must consider a model for an electromagnetic field that is varying both in time and with distance.

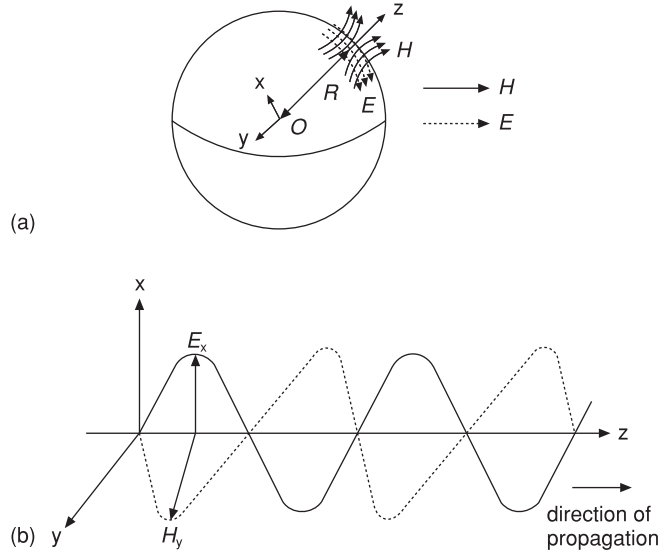


**Figure 2.3** Electromagnetic wave propagation in the  $z$ -direction

For a sinusoidal variation, a wave propagating in the positive  $z$ -direction can be written as

$$A \sin(\omega t - \beta z) \quad (2.16)$$

### Exercise 2.2

For the linearly polarised signal  $E_x = \sin(\omega t - \beta z)$  propagating in free space at a frequency of 1 GHz, calculate the phase constant of the signal.

**Solution**

$$\text{Phase constant } \beta = \frac{2\pi}{\lambda}$$

and

$$c = f\lambda$$

$$\text{therefore } \lambda = \frac{3 \times 10^8}{1 \times 10^9} = 0.3 \text{ m}$$

$$\text{thus } \beta = 21 \text{ rads/m}$$

Here  $A$  is a constant that defines magnitude, and  $\beta$  is the phase change in radians and is equal to  $2\pi/\lambda_0$ . This simple equation allows us to model a wave propagating in the positive  $z$ -direction such that the phase of the wave at position  $z$  lags that at the origin.

Exercise 2.3

Show that  $\beta z = \omega z/c$ , where  $z$  is the distance travelled by the signal in the propagation direction, and  $c$  is the speed of light.

**Solution**

By definition,  $\beta = \frac{2\pi}{\lambda}$  and  $\lambda = \frac{c}{f}$

$$\text{Thus } \beta = \frac{2\pi f}{c} = \frac{\omega}{c}$$

$$\text{Hence } \beta z = \frac{\omega z}{c}$$


---

Since the wave is propagating in free space,

$$c = \frac{\omega}{\beta} = f\lambda_0 \quad (2.17)$$

where  $\lambda_0$  is the free-space wavelength, from which we can rewrite equation (2.16) as

$$A \sin\omega\left(t - \frac{z}{c}\right) \quad (2.18)$$

Here the term  $z/c$  represents the time delay for the wave travelling from the origin to point  $z$ . Thus we can write the field components in the transverse plane to the  $z$ -direction as

$$E_x = A \sin\omega\left(t - \frac{z}{c}\right) \quad (2.19)$$

and

$$H_y = A \left(\frac{\epsilon_0}{\mu_0}\right)^{1/2} \sin\omega\left(t - \frac{z}{c}\right) \quad (2.20)$$

Using these equations as solutions to Maxwell's equations (Section 2.1), we can deduce the principal properties that plane waves propagating in space exhibit.

Consider the situation where we have an electric field directed in the  $x$ -axis,  $E_x$ , in which case  $E_y$  and  $E_z$  are set to zero. Now, substituting into Maxwell's equations (Section 2.1), we get a simplified set of equations:

$$\epsilon_0 \frac{\partial E_x}{\partial t} = \frac{\partial H_z}{\partial y} - \frac{\partial H_y}{\partial z} \quad (2.21)$$

$$-\mu_0 \frac{\partial H_x}{\partial t} = 0 \quad (2.22)$$

$$-\mu_0 \frac{\partial H_y}{\partial t} = \frac{\partial E_x}{\partial z} \quad (2.23)$$

$$-\mu_0 \frac{\partial H_z}{\partial t} = -\frac{\partial E_x}{\partial y} \quad (2.24)$$

From equation (2.22), we can see that  $H_x$  must equal zero. If we also enforce the condition that there is no field component along the  $z$ -axis, i.e.  $H_z = 0$ , the equation set above reduces to

$$\epsilon_0 \frac{\partial E_x}{\partial t} = -\frac{\partial H_y}{\partial z} \quad (2.25)$$

$$\mu_0 \frac{\partial H_y}{\partial t} = -\frac{\partial E_x}{\partial z} \quad (2.26)$$

Differentiating these equations with respect to  $t$  and  $z$ , respectively, yields

$$\epsilon_0 \frac{\partial^2 E_x}{\partial t^2} = -\frac{\partial^2 H_y}{\partial t \partial z} \quad (2.27)$$

$$\mu_0 \frac{\partial^2 H_y}{\partial z \partial t} = -\frac{\partial^2 E_x}{\partial z^2} \quad (2.28)$$

Now since

$$\frac{\partial^2 H_y}{\partial t \partial z} = \frac{\partial^2 H_y}{\partial z \partial t} \quad (2.29)$$

then

$$\frac{\partial^2 E_x}{\partial z^2} - \epsilon_0 \mu_0 \frac{\partial^2 E_x}{\partial t^2} = 0 \quad (2.30)$$

or

$$\frac{\partial^2 H_y}{\partial z^2} - \epsilon_0 \mu_0 \frac{\partial^2 H_y}{\partial t^2} = 0 \quad (2.31)$$

These are the equations that describe the propagation of a plane wave in space. Equations (2.19) and (2.20) will now be used to solve equations (2.30) and (2.31) for  $E_x$  and  $H_y$ , respectively.

### Exercise 2.4

Show that a transverse plane wave propagates at the speed of light when propagating in free space.

#### Solution

Consider the properties of equation (2.19), rewritten here as

$$E_x = A \sin \omega [t - (\epsilon_0 \mu_0)^{1/2} z] \quad (2.32)$$

At some time  $t_1$ , the propagating wave will be at position  $z_1$  and the wave will have the same magnitude at some other time  $t_2$  position  $z_2$  that it had at  $t_1$ ,  $z_1$ , provided that

$$t_1 - (\epsilon_0 \mu_0)^{1/2} z_1 = t_2 - (\epsilon_0 \mu_0)^{1/2} z_2 \quad (2.33)$$

Now since

$$\text{velocity} = \frac{\text{distance travelled}}{\text{time difference}} = \frac{z_2 - z_1}{t_1 - t_2} \quad (2.34)$$

$$\text{then velocity} = \frac{1}{(\epsilon_0 \mu_0)^{1/2}} = 3 \times 10^8 \text{ m/s}$$

as previously stated at the outset of this section.

Inspection of equations (2.30) and (2.31) shows that the magnetic and electric field components lie at right angles to each other and are in phase.

Another form for the solution can also be used, since a cosine function will also satisfy equations (2.30) and (2.31), as will any linear combination of sines and cosines. This leads to the exponential form for representing the solution, which sometimes helps in the analysis of more complex problems.

$$E_x = A \left[ \cos \omega \left( t - \frac{z}{c} \right) + j \sin \omega \left( t - \frac{z}{c} \right) \right] \quad (2.35)$$

$$\therefore E_x = A \exp \left[ j \left( \omega \left( t - \frac{z}{c} \right) \right) \right] \quad (2.36)$$

$$\text{and } H_y = A \left( \frac{\epsilon_0}{\mu_0} \right)^{1/2} \exp \left[ j \left( \omega \left( t - \frac{z}{c} \right) \right) \right] \quad (2.37)$$

Here only the real part of the exponent has physical significance. The form of the equations given in (2.36) and (2.37) is normally assumed to be implicit, meaning the real part only, and as a consequence the full form given in equations (2.36) and (2.37) is used in most textbooks with the understanding that it represents only the real part of the field component it is used to describe.

### 2.3 Power flow

As a wave from an antenna propagates through space, its electric and magnetic constituent field parts carry energy. The power associated with the rate of change of this energy can be found in a way that is analogous to the technique used in conventional circuit analysis, where power is written as the product of voltage and current. Consider now an example important for antenna theory.

If a plane wave propagating in space is allowed to pass through a surface that is perpendicular to the direction of travel of the wave,  $\Delta S$  (Figure 2.4a), then there will be a flow of power through the surface. The power level in units of  $\text{W/m}^2$  and the direction

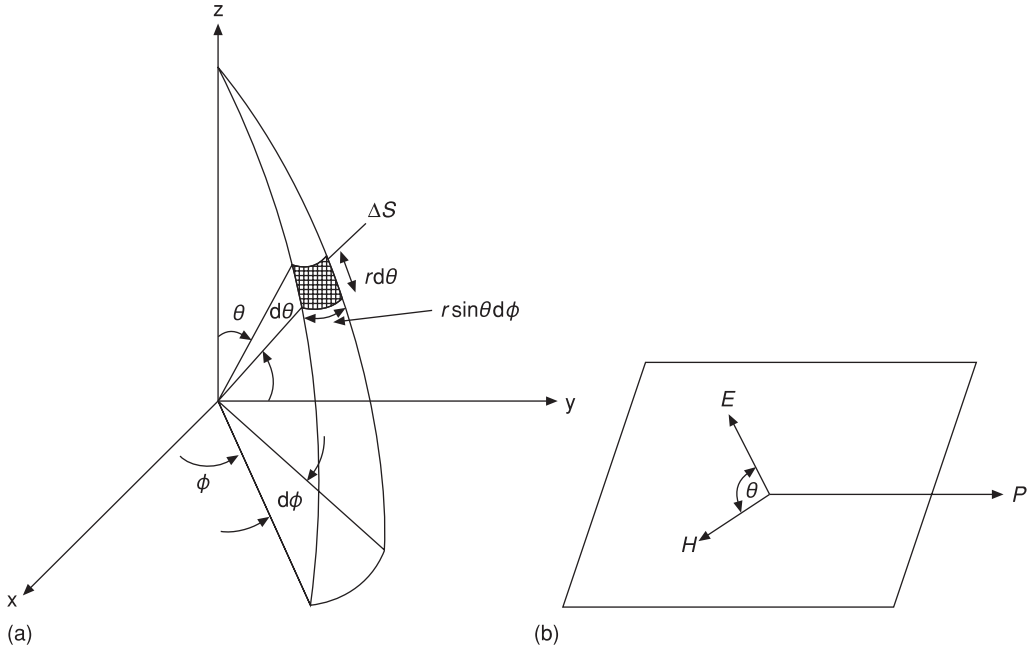


**Figure 2.4** Spherical coordinate system used for power flow calculations

of power flow across the defined surface are given by Poynting's theorem, which allows the instantaneous power per unit area at a point flowing through a surface to be defined in terms of the instantaneous values for electric and magnetic fields  $E$  and  $H$  as

$$P_{\text{inst}} = EH \sin\theta \quad (2.38)$$

### Exercise 2.5

Compute the instantaneous and average power flows associated with the linearly polarised electric field component propagating in free space, defined here as

$$E_x = 20 \sin\left(\omega t - \frac{z}{c}\right)$$

**Solution**

$$E_x = 20 \sin\left(\omega t - \frac{z}{c}\right)$$

therefore

$$H_y = \frac{20}{377} \cos\left(\omega t - \frac{z}{c}\right)$$

From these we see that  $E_x$  and  $H_y$  are orthogonal, thus  $\sin 90^\circ = 1$ .

Therefore, on applying equation (2.38)

$$P_{\text{inst}} = \frac{20 \times 20}{377} = 1.06 \text{ V/m}$$

$$\text{and } P_{\text{avg}} = \frac{1}{2} P_{\text{inst}} = 0.53 \text{ V/m}$$

The direction of the power flow is given by the right-hand corkscrew rule (Figure 2.4b), and  $\theta$  is the angle between the  $E$  and  $H$  fields and is  $90^\circ$  for a ‘transverse’ plane wave.

Consider now the flow of power  $\Delta P$  through an elemental surface of the sphere,  $\Delta S$ , as defined in Figure 2.4a:

$$\Delta P = E_\theta H_\phi r \sin\theta d\phi r d\theta \quad (2.39)$$

From this the instantaneous power over the complete sphere can be found as

$$P_{\text{inst}} = \int_0^\pi \int_0^{2\pi} E_\theta H_\phi r^2 \sin\theta d\theta d\phi \quad (2.40)$$

Most textbooks use a more general form in which  $E_\theta H_\phi$  is written as  $\text{Re} [E_\theta H_\phi^*]$ , where \* denotes complex conjugation.

Applying equation (2.40) to a Hertzian dipole, for which from Section 1.2 we already have expressions for  $E_\theta$  and  $H_\phi$ , namely after equation (1.16):

$$E_\theta = \frac{60\pi I \Delta\ell \sin\theta}{\lambda r}$$

and

$$H_\phi = \frac{E_\theta}{120\pi}$$

from which we can write

$$P_{\text{inst}} = 60\pi^2 I \left( \frac{\Delta\ell}{\lambda} \right)^2 \int_0^\pi \sin^3\theta d\theta \quad (2.41)$$

Now

$$\begin{aligned} \int_0^\pi \sin^3\theta d\theta &= - \int_{-1}^1 (1 - \cos^2\theta) d \cos\theta \\ &= \int_{-1}^1 (\cos^2\theta - 1) d \cos\theta \\ &= \left[ \frac{\cos^3\theta}{3} - \cos\theta \right]_{-1}^1 \\ &= \frac{4}{3} \end{aligned}$$

Hence

$$P_{\text{inst}} = 80\pi^2 I^2 \left( \frac{\Delta\ell}{\lambda} \right)^2 \quad (2.42)$$

or as average power radiated for sinusoidal current excitation:

$$P_{\text{av}} = \frac{1}{2} P_{\text{inst}}$$

$$P_{\text{av}} = 40\pi^2 I^2 \left( \frac{\Delta\ell}{\lambda} \right)^2 \quad (2.43)$$

From equation (2.43), it can be seen that radiated power is proportional to the square of the ratio of the antenna length divided by its operating wavelength. Thus for efficient radiation this quantity should exceed 1. *This is a very important finding, since it tells us that for an antenna to be an efficient radiator its length must be at least comparable with a wavelength at its desired frequency of operation.*

If we have an isotropic source radiating uniformly in all directions, we can find an expression for the power radiated by using the same process as we described for the Hertzian dipole above. Once again the power radiated by an isotropic source radiating  $P_{\text{inst}}$  W of power is given as

$$P_{\text{inst}} = \int_0^\pi \int_0^{2\pi} E_\theta H_\phi r^2 \sin\theta \, d\theta \, d\phi \quad (2.44)$$

and using  $E_\theta = \text{constant}$  and  $H_\phi = E_\theta/120\pi$ , then

$$P_{\text{inst}} = \int_0^\pi \int_0^{2\pi} \frac{E_\theta^2}{120\pi} r^2 \sin\theta \, d\theta \, d\phi \quad (2.45)$$

$$= \frac{E_\theta^2 r^2}{60} [-\cos\theta]_0^\pi$$

$$= \frac{E_\theta^2 r^2}{30} \text{ W} \quad (2.46)$$

This expression can now be used to establish the concept of power gain as applied to an antenna.

## 2.4 Antenna directivity, power gain and efficiency

We have already seen in Section 1.3 that the Hertzian dipole antenna has directional radiation properties, with its main power concentration occurring along the equatorial plane ( $\theta = 0^\circ$ ) of the antenna and an antenna field pattern null along the axis of the antenna at  $\theta = 90^\circ$ . Thus it follows that relative to an isotropic antenna radiating uniformly in all directions any antenna exhibiting directional characteristics will

exhibit power gain,  $G$ , at least in some directions of radiation, in relation to the isotropic antenna. This gain is defined as

$$G = \frac{\text{maximum power received (radiated) from a given antenna}}{\text{maximum power received (radiated) from a reference antenna}} \quad (2.47)$$

By the definition in equation (2.47), consider how the Hertzian dipole antenna can exhibit gain when compared with an isotropic source. For the Hertzian dipole from Section 1.2 we know that

$$E_{\theta} = \frac{60\pi \Delta \ell I \sin \theta}{\lambda r} \quad (2.48)$$

where  $I = I_0 e^{j(\omega t - \beta r)}$

Hence maximum  $E_{\theta}$  occurs at  $\theta = 90^\circ$

$$E_{\theta_{\max}} = \frac{60\pi \Delta \ell I}{\lambda r} \quad (2.49)$$

### Exercise 2.6

Calculate the maximum magnitude of the electric field radiated by a Hertzian dipole at a distance of 10 m. The dipole has length  $0.1\lambda$  and is centre-fed by a 1 A RMS current.

#### Solution

From equation (2.49):

$$E_{\theta_{\max}} = \frac{60\pi \times 0.1 \times 1}{10} = 0.6\pi = 1.9 \text{ V/m}$$

But we also know for a Hertzian dipole (Section 2.3) that

$$P_{\text{inst}} = 80\pi^2 I^2 \left( \frac{\Delta \ell}{\lambda} \right)^2 \quad (2.50)$$

so that by substituting (2.50) into (2.49) for the Hertzian dipole, we can write

$$E_{\theta_{\max}}^2 = \frac{60^2}{r^2} \frac{P_{\text{inst}}}{80} = \frac{45P_{\text{inst}}}{r^2 P} \quad (2.51)$$

But for the isotropic source we know from equation (2.46) that

$$E_{\theta_{\max}}^2 = \frac{30P_{\text{inst}}}{r^2} \quad (2.52)$$

Hence, by the definition given by equation (2.47), the power gain of a Hertzian dipole relative to an isotropic source is

$$G = \frac{45}{30} = 1.5$$

When expressed as a power gain, this gives  $10 \log_{10} 1.5$  or 1.76 dBi, where the ‘i’ denotes decibels relative to an isotropic source. This example demonstrates that even though the Hertzian dipole is very short it still has gain by virtue of the directional nature of its radiation characteristic when compared with that of an isotropic source.

As we have seen, antenna structures with non-zero length exhibit preferential energy radiation in a given direction  $(\theta, \phi)$ . This property can be defined as the antenna directive gain or directivity,  $D$ , given as the ratio of the radiation intensity for the antenna in some direction  $(\theta, \phi)$  to the average radiated power when the same power is radiated uniformly in all directions over the entire imaginary spherical shell placed some distance away from the antenna in its far field; or, stated another way

$$D = \frac{\text{radiation intensity in a given direction}}{\text{radiation intensity averaged over all directions}} \quad (2.53)$$

By noting that for a sphere the average radiation intensity is  $1/4\pi$  times the total power radiated by the antenna  $P_T$ , we can write

$$D = \frac{4\pi\Phi(\theta, \phi)}{P_T} \quad (2.54)$$

where  $P_T$  = total power radiated by the antenna and  $\Phi(\theta, \phi)$  = radiation intensity in a given direction  $(\theta, \phi)$ , i.e. the power per unit solid angle in that direction.

Here  $P_T$  can be found by integrating  $\Phi(\theta, \phi)$  over the whole sphere:

$$P_T = \int_0^{2\pi} \int_0^\pi \Phi(\theta, \phi) \sin\theta \, d\theta \, d\phi \quad (2.55)$$

hence

$$D = \frac{4\pi\Phi(\theta, \phi)}{\int_0^{2\pi} \int_0^\pi \Phi(\theta, \phi) \sin\theta \, d\theta \, d\phi} \quad (2.56)$$

This expression defines directivity with respect to an ideal isotropic antenna. If any other antenna type is used as the reference, then the directivity calculated will be reduced by the directivity of the reference antenna.

As suggested by equation (2.56), in a practical situation antenna directivity can be calculated by numerical integration of the measured radiation patterns for a given antenna type. For those cases where no azimuthal field variation exists, and if we assume that the maximum radiated power is unity, then a special case exists:

$$P_T = 2\pi \int_0^\pi \Phi(\theta) \sin\theta \, d\theta$$

$$\therefore D = \frac{2}{\int_0^\pi \Phi(\theta) \sin\theta \, d\theta} \quad (2.57)$$

For an antenna that is 100% efficient, i.e. has no losses, directivity and gain are the same; this issue is further discussed below.

Let us now calculate the directivity for a Hertzian dipole. Consider first a unit solid angle,  $\Omega$ , called a steradian, [8]. The surface area occupied per solid angle  $d\Omega$  is given by  $r^2 d\Omega$ , where  $r$  is the distance from the origin of the radiating source. Hence there are  $r^2$  square meters of surface area per unit solid angle.

Thus the radiation intensity  $\Phi(\theta, \phi)$  in a given beam direction can be derived from the power per unit solid as

$$\Phi(\theta, \phi) = r^2 P = \frac{r^2 E^2}{120\pi} \quad \text{W/steradian} \quad (2.58)$$

where  $P$  is the power flow per unit area.

Another term of fundamental importance to understanding antenna behaviour is radiation resistance; this will now be discussed.

From Section 2.2, for a plane wave propagating in free space  $P = EH$ , where  $E = 120 \pi H$ , and for a Hertzian dipole we know from equation (2.49) that

$$I = \frac{\lambda r E_{\theta_{\max}}}{60\pi \Delta \ell} \quad (2.59)$$

Thus we can write power as  $P = I^2 R_{\text{rad}}$ , where  $R_{\text{rad}}$  is called the radiation resistance of the antenna. This is a term of fundamental importance to antenna designers and requires definition.

The radiation resistance for an antenna is a fictitious resistance  $R_{\text{rad}}$  chosen such that the average power,  $P_{\text{av}}$ , dissipated in  $R_{\text{rad}}$  is the same as that dissipated by the antenna, hence

$$P_{\text{av}} = \frac{1}{2} I^2 R_{\text{rad}}$$

So, for a Hertzian dipole using equation (2.42), we obtain

$$R_{\text{rad}} = 80\pi^2 \left( \frac{\Delta \ell}{\lambda} \right)^2 \Omega \quad (2.60)$$

This resistance arises since in addition to the considerations given in Section 1.1 the charge on an electron can create its own electric field, which under dynamic conditions can produce a force that acts upon the electron itself. This occurs in such a way as to resist the motion of the electron. The drag force thus created is responsible for the creation of radiation resistance. In practice, radiation resistance will vary over the antenna length, and in the derivations presented here we find an aggregate value for radiation resistance over the entire antenna length. Current flowing against the radiation resistance is converted into electromagnetic energy. In addition, the motion of the electrons as they oscillate is impeded by collisions with atoms that lie in their path, causing heating or ohmic resistance. Ohmic and radiation resistance are necessary in order to define the radiation efficiency of an antenna.

### Exercise 2.7

Calculate the radiation resistance of a wire dipole of length  $0.01\lambda$ .

#### Solution

The wire is very short compared with a wavelength, therefore we can approximate it as a Hertzian dipole and apply equation (2.60). Thus

$$R_{\text{rad}} = 80\pi^2(0.01)^2 = 0.08 \Omega$$

From this it can be seen that the dipole has a very low radiation resistance and consequently it will not radiate very effectively.

Equation (2.60) is of fundamental importance, since it demonstrates that radiated power is proportional to the square of the length-to-wavelength ratio of the antenna; i.e. in order to be an efficient radiator the size of the antenna must be comparable with its wavelength. In effect, this shows why the Hertzian dipole,  $\Delta\ell \ll \lambda$ , is really of theoretical value only. Also, it clearly shows why conventional lumped element electronic components with dimensions at their operating frequency of  $< \lambda/20$  have radiation effects that are so small they are totally ignored in classical AC circuit theory.

For 1 W of total radiated power and using equation (2.60), we get

$$I = \frac{\lambda}{\sqrt{80\pi} \Delta\ell} \quad (2.61)$$

Equating (2.59) and (2.61) gives the field strength in the direction of maximum radiation as

$$E_{\theta_{\text{max}}} = \frac{60}{r\sqrt{80}} \text{ V/m} \quad (2.62)$$

and using equation (2.58) we get

$$\Phi(\theta, \phi) = \frac{60^2 r^2}{r^2(80)(120\pi)} = \frac{3}{8\pi} \quad (2.63)$$

Substituting this result into equation (2.56) yields

$$D = \frac{(4\pi) \frac{3}{8\pi}}{1} = \frac{3}{2} \quad (2.64)$$

The denominator in equation (2.64) is unity, since we are using the constraint of 1 W total radiated power as cited above. The result is the same as the one we obtained for the gain of a Hertzian dipole earlier in this section and is a consequence of the Hertzian dipole having a volumetric doughnut-shaped radiation pattern that fills only two-thirds of the entire solid angle of a sphere. Some typical directivity values for basic antenna types are listed in Table 2.1.

In equation (2.54), if total power input to the antenna instead of radiated power is used, then the antenna losses can be included and the power gain of the antenna,  $G$ ,

**Table 2.1** Typical antenna directivity values

Antenna type	Directivity
Isotropic	1
Short dipole	1.5
Half-wave dipole	1.64
Quarter-wave dipole over an ideal ground plane	3.28

calculated. Since the antenna power gain includes loss, it is always by definition going to be less than the directivity for the same antenna; hence we can write

$$G = \eta D \quad (2.65)$$

where  $\eta$  is the antenna efficiency factor and is less than, or at best equal to, unity.

We can now define antenna radiation efficiency as

$$\eta = \frac{R_{\text{rad}}}{R_{\text{rad}} + R_L} \quad (2.66)$$

so that

$$G = \eta + D \text{ (dB)} \quad (2.67)$$

Here  $R_{\text{rad}}$  is the radiation resistance of the antenna as defined above, and  $R_L$  is the antenna ohmic loss. For an antenna that is 100% efficient, i.e. has no losses, directivity and gain are the same.

For a circular cross-section dipole of radius  $a$  and length  $\ell$ ,  $R_L$  is mainly due to the sinusoidal current in the wire moving in a thin sheet near its surface. Approximately for a uniform current distribution, this can be written as

$$R_L = \frac{\ell}{4\pi a} \sqrt{\frac{\omega\mu_0}{2\sigma}} \text{ (}\Omega\text{)} \quad (2.68)$$

where  $\omega$  is the angular frequency of operation, and  $\sigma$  is the conductivity of the metal used to form the conductor.

### Exercise 2.8

What is the antenna efficiency factor for a dipole of length  $0.1\lambda$  operating at 1 GHz and constructed using 1 mm diameter copper wire, of conductivity  $6 \times 10^{-9}$  s/m.

#### Solution

Since  $\ell < \lambda$ , we will assume that the antenna can be approximated by a Hertzian dipole; thus equation (2.60) gives

$$R_{\text{rad}} = 0.8\pi^2 = 7.9 \text{ }\Omega$$

and from equation (2.68)

$$R_L = \frac{1}{4\pi 10^{-3}} \sqrt{\frac{2\pi \times 1 \times 10^9 \times 4\pi \times 10^{-7}}{2 \times 6 \times 10^{-9}}} = 0.065 \text{ }\Omega$$

Hence from equation (2.66) this antenna will have a theoretical efficiency,  $\eta$ , of

$$\eta = \frac{7.9}{7.9 + 0.065} = 99\%$$

showing that the use of copper as the constructional material for the antenna was a good choice due to its high conductivity hence low ohmic loss.

It is important to note that while efficiency is high, radiation resistance is low, so in practice both figures of merit need to be considered together before a proper assessment of antenna behaviour can be made.

For an antenna that is electrically short, i.e.  $\ell \ll \pi$ , the ohmic losses of the antenna become a critical issue. This is so since the antenna will be a poor radiator (c.f. equation (2.43)), and losses become critical in determining the efficiency of the antenna. In some applications, an electrically short antenna with efficiency of 30 to 50% may be useful where physical size is an issue, e.g. in HF or ruggedised systems.

The issue of electrically short antennas is a key concern for mobile wireless equipment. As we have already seen, antenna efficiency and gain decrease dramatically for  $\ell < \lambda$ ; this is accompanied by a decrease in bandwidth. All these features are undesirable in a practical antenna.

Key relationships that link the maximum gain (for a reasonable bandwidth),  $G_{\max}$ , and the minimum quality factor,  $Q_{\min}$  (itself a measure of bandwidth), are given in [9] for electrically short antennas radiating or receiving linearly polarised radiation. These are repeated here as

$$Q_{\min} = \frac{1}{(ka)^3} + \frac{1}{(ka)} \quad (2.69)$$

### Exercise 2.9

Calculate the  $Q$  factor of an electrically short dipole antenna of length  $0.02\lambda$ .

#### Solution

From equation (2.69), the minimum  $Q$  factor,  $Q_{\min}$ , is

$$\begin{aligned} & \frac{1}{\left(\frac{2\pi}{\lambda} \frac{0.02\lambda}{2}\right)^3} + \frac{1}{\left(\frac{2\pi}{\lambda} \frac{0.02\lambda}{2}\right)} \\ &= \frac{1}{(0.02\pi)^3} + \frac{1}{(0.02\pi)} = 4016 \end{aligned}$$

This shows that this antenna will have a very high  $Q$  factor and consequently narrow bandwidth. Indeed, since a Hertzian dipole appears capacitive below resonance and inductive above resonance and if ohmic losses are low, it can be approximated as a lossless series  $LC$  tuned circuit.

and

$$G_{\max} = (ka)^2 + 2ka \quad (2.70)$$

### Exercise 2.10

For the same parameters that were used in exercise 2.9, what is the maximum theoretical gain that this antenna can have?

### Solution

$$\begin{aligned} G_{\max} &= (2\pi \cdot 0.01)^2 + 2(2\pi \cdot 0.01) \\ &= 0.135 \text{ or } -9 \text{ dB} \end{aligned}$$

So the gain of the antenna is in fact negative and will become positive only when the antenna size is increased considerably.

where  $k = 2\pi/\lambda$ , and  $a$  is the radius of the smallest sphere enclosing the antenna. For very short antennas,  $G_{\max}$  will be reduced considerably, as mentioned above, by ohmic losses.

Using the concept of the near-field/far-field boundary, defined in Section 1.4 as  $\lambda/2\pi$ , Wheeler [10] suggested an approach whereby a metal shield could be placed over an electrically short antenna. Provided the shield was much bigger than the antenna but smaller than  $\lambda/2\pi$ , then the shield would prevent radiation while allowing dissipative ohmic losses to be measured. The composite ohmic and radiative losses can then be found by making a one-port impedance measurement on the antenna as it radiates into free space. In this way, the parameters in equation (2.66) can be identified and antenna radiation efficiency estimated.

Other methods exist, e.g. [11] for calculating antenna efficiency, namely directivity/gain and radiometric methods. These techniques are more broadly applicable than the Wheeler box approach above, but their use requires more specialised equipment.

### References

- [8] Karmel, P.R., Colef, G.D. and Camisa, R.L., *Introduction to Electromagnetic and Microwave Engineering*, Wiley Series in Microwave and Optical Engineering, John Wiley & Sons, 1998.
- [9] Skrivervik, A.K., Zürcher, J.F., Staub, O. and Mosig, J.R., PCS antenna design: the challenge of miniaturization, *IEEE Ant. and Prop. Mag.*, Vol. 43, No. 4, 2001, pp. 12–26.
- [10] Wheeler, H.A., Small antennas, *IEEE Trans. on Antennas and Propagation*, Vol. AP-23, No. 4, 1975, pp. 462–9.
- [11] Newman, E.H., Bohley, P. and Walter, C.H., Two methods for the measurement of antenna efficiency, *IEEE Trans. on Antennas and Propagation*, Vol. AP-23, No. 4, 1975, pp. 457–61.

**Problems**

---

- 2.1 Define from first principles the equations governing the radiation efficiency and power gain of a short linear dipole.
- 2.2 Use the equations derived in exercise 2.1 to establish the electric field strength at a receiver placed 100 km away from a  $50\ \Omega$  matched transmitting antenna of length 3 cm fed with a 1 GHz 0.25 A sine wave.
- 2.3 If the receive antenna in exercise 2.2 is also designed to be resonant at 1 GHz and has an effective length of 3 cm, what is the actual power available at the receiver input under matched conditions?  
What is the transmission loss in dB for this situation?

# Linear dipole antennas

---

In this chapter, the concepts previously defined for the Hertzian dipole are extended to encompass a straight wire antenna of finite length, the dipole antenna. The effects of current distribution on the radiation characteristics of dipole antennas of various lengths is established. In addition, general expressions for radiation resistance, gain and power transfer from a transmit antenna to a receive antenna are also discussed, as is the behaviour of electrically short dipole antennas.

### 3.1 Dipole antenna of finite length

We can use the concepts already developed for the Hertzian dipole (Chapter 1) to construct a model for a more general dipole type, i.e. a straight wire antenna of finite length. This type of antenna has many practical applications.

If we have a dipole antenna of length  $\ell$  consisting of two equal straight lengths of metal conductor,  $\ell/2$ , lying along the same axis and separated by a small gap  $\Delta$  we can form a centre-fed dipole antenna (Figure 3.1). Here because the antenna has a finite length the magnitude of the current distribution along its length will not be constant, but if the antenna is centre-fed the phase distribution along its length will be constant. Also due to its length, the radiation from different parts of the antenna will reach a far distant observation point P with different phase delays. Here the radiated wavefronts will add constructively or destructively, depending on their relative phase relationships.

An analysis of this situation is possible if we use the Hertzian dipole model as the basic building block. Assuming that the Hertzian dipole model is applicable over a short length  $dz$  (Figure 3.1), we can rewrite equation (1.16) using

$$dE_{\theta} = \eta dH_{\phi} \quad (3.1)$$

$$\text{where } dH_{\phi} = \frac{kI(z') dz'}{4\pi r'} \sin\theta' \exp(-jkr') \quad (3.2)$$

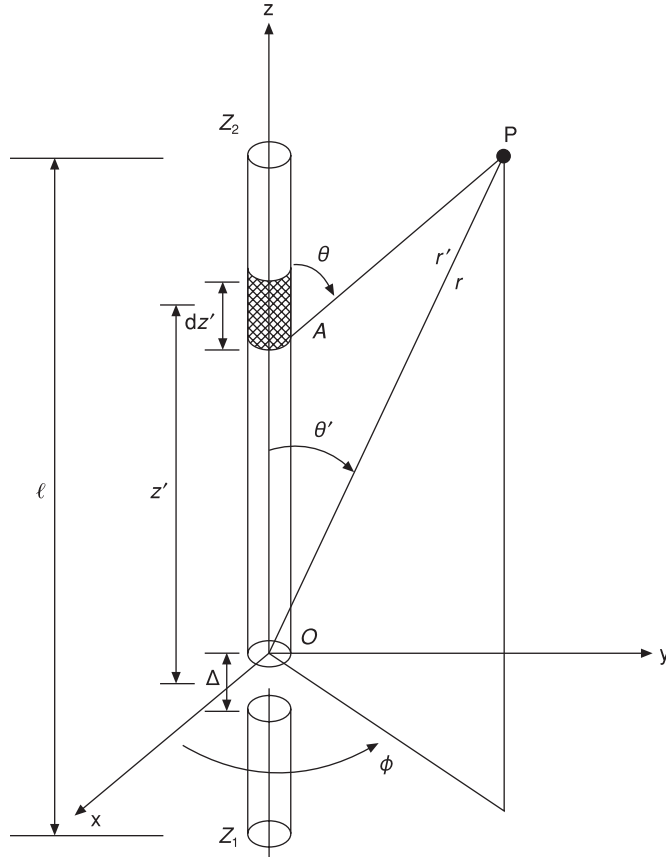


**Figure 3.1** Finite-length dipole

Here  $\exp(-jkr')$  is used as alternative exponent notation for  $\cos\omega(t - r'/c)$ , with the implicit assumption that we are concerned only with the real part of the exponent;  $k$  is the wavenumber, and  $\omega t$  is the radiation frequency.

If we are in the far field of the antenna, then lines AP and OP will be approximately parallel. Thus

$$r' = \sqrt{r^2 + z'^2 - 2rz'\cos\theta} \quad (3.3)$$

$$\therefore r' \approx r - z'\cos\theta \quad (3.4)$$

and

$$dH_\phi = \frac{kI(z') dz'}{4\pi(r - z'\cos\theta)} \sin\theta' \exp(-jk(r - z'\cos\theta)) \quad (3.5)$$

If we note that  $z'$  is much less than  $r$ , then  $r - z'$  is approximately equal to  $r$ , except in the exponent term, which remains as  $\exp(-jkr) \exp(jkz'\cos\theta)$ .

Hence

$$dH_\phi = \frac{k \sin\theta'}{4\pi r} \exp(-jkr) \exp(jkz' \cos\theta') \sin\theta' dz' \quad (3.6)$$

The total magnetic field at point P can now be found by summing incremental equation (3.6) over the entire length of the antenna:

$$H_\phi = \frac{k \exp(-jkr)}{4\pi r} \int_{z_1}^{z_2} \sin\theta' I(z') \exp(jkz' \cos\theta') dz' \quad (3.7)$$

where it is noted from Figure 3.1 that for far-field points  $\theta' \approx \theta$ .

The term in the integral is very important for antenna work and thus needs further consideration. As it stands, the integral has units of amperes per metre. If the integral was divided by the driving point current,  $I(0)$ , then the integral would have units of length. The resulting term is defined as the *effective length* (or *height*) for the antenna,  $h_e(\theta)$  [12] [13]:

$$h_e(\theta) = \frac{\sin\theta}{I(0)} \int_{z_1}^{z_2} I(z') \exp(jkz' \cos\theta) dz' \quad (3.8)$$

Hence we can write

$$H_\phi = \frac{k \exp(-jkr)}{4\pi r} h_e(\theta) I(0) \quad (3.9)$$

For a given current distribution, we can now compute the far-field pattern for any length of dipole. In effect, the use of the effective antenna length concept simply means that we need only evaluate the integral in equation (3.8) in order to find the far field radiation pattern, i.e. the integral is the quantity that identifies the characteristic radiation features of a particular length of dipole antenna.

### 3.2 Current distribution on a finite-length dipole (far-field effect of a sinusoidal current)

Consider a wire dipole antenna of length  $\ell$  that has a sinusoidal current distribution along its length, such that with reference to Figure 3.1

$$\begin{aligned} I(z') &= I_0 \sin\left[\frac{\omega}{c} \left[\frac{1}{2}\ell - z'\right]\right] z' > 0 \\ &= I_0 \sin\left[\frac{\omega}{c} \left[\frac{1}{2}\ell + z'\right]\right] z' < 0 \end{aligned} \quad (3.10)$$

See Figure 3.2.

$$\begin{aligned} \therefore h_e(\theta) &= I_0 \int_{-\ell/2}^0 \sin\left[\frac{\omega}{c} \left(\frac{1}{2}\ell + z'\right)\right] \exp(jkz' \cos\theta) dz' \\ &\quad + I_0 \int_0^{\ell/2} \sin\left[\frac{\omega}{c} \left(\frac{1}{2}\ell - z'\right)\right] \exp(jkz' \cos\theta) dz' \end{aligned} \quad (3.11)$$

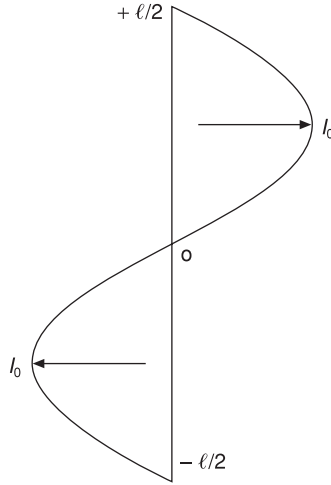


**Figure 3.2** Sinusoidal current distribution for a finite-length dipole

Fortunately, this is a standard integral, which can be expressed as

$$\int \exp(ax) \sin(c + bx) dx = \frac{\exp(ax)}{a^2 + b^2} [a \sin(c + bx) - b \cos(c + bx)]$$

After making the appropriate substitutions, i.e.  $a = jk \cos \theta$ ,  $b = k$  and  $c = 1/2 k \ell$  for the first integral and  $b = -k$  for the second integral in equation (3.11), we get

$$h_e(\theta) = \frac{2I_0}{kI(0)} F(\theta) \quad (3.12)$$

from which we can write

$$H_\phi = \frac{I_0}{2\pi r} \exp(-jkr) F(\theta) \quad (3.13)$$

where  $F(\theta)$  is called the pattern multiplication factor, and  $I_0$  is the maximum excitation current. Thus we obtain for a finite-length dipole with sinusoidal current distribution

$$F(\theta) = \frac{\cos\left(\frac{1}{2} k \ell \cos \theta\right) - \cos\left(\frac{1}{2} k \ell\right)}{\sin \theta} \quad (3.14)$$

Consider now some important cases.

### Case (1)

Let  $\ell = \lambda/2$ , i.e. a half-wave dipole

$$F(\theta) = \frac{\cos\left(\frac{\pi}{2} \cos \theta\right)}{\sin \theta} \quad (3.15)$$

Case (2)

Let  $\ell = \lambda$ , a full-wave dipole

$$F(\theta) = \frac{\cos(\pi \cos\theta) - 1}{\sin\theta} \quad (3.16)$$

Case (3)

Let  $\ell = 3\lambda/2$

$$F(\theta) = \frac{\cos\left(\frac{3}{2}\pi \cos\theta\right)}{\sin\theta} \quad (3.17)$$

Constructing the polar plots for each of these cases enables the 3 dB antenna beamwidths to be found; see Figure 3.3, which was constructed using the computer program given in Appendix 8.1. The half-power beamwidths (HPBW) quoted in Figure 3.3 are obtained as in Section 1.3.

---

**Exercise 3.1**

Calculate the half-power beamwidth for a half-wavelength centre-fed dipole antenna.

**Solution**

From equation (3.15), we can write

$$F(\theta) = \frac{1}{\sqrt{2}}$$

which yields

$$\cos\left(\frac{\pi}{2} \cos\theta\right) = \frac{\sin\theta}{\sqrt{2}}$$

which is satisfied with values of  $\theta$  of  $51^\circ$  and  $129^\circ$ , giving the HPBW as  $129^\circ - 51^\circ = 78^\circ$ .

From this result, we can show that the far-field radiation pattern from this antenna is more tightly focused than that of the Hertzian dipole (see exercise 1.3).

---

**Exercise 3.2**

Calculate the half-power beamwidth for a full-wave dipole.

**Solution**

Using equation (3.16), we get

$$1 + \frac{\sin\theta}{\sqrt{2}} = \cos(\pi \cos\theta)$$

which is satisfied when  $d = 255.5^\circ$  or  $284.5^\circ$ , giving  $\theta_{3dB} = 29^\circ$ .

Thus it can be seen that relative to exercise 3.1 by increasing the length of the dipole the antenna half-power beamwidth has decreased, i.e. it is producing more focused radiation. This situation cannot continue indefinitely.

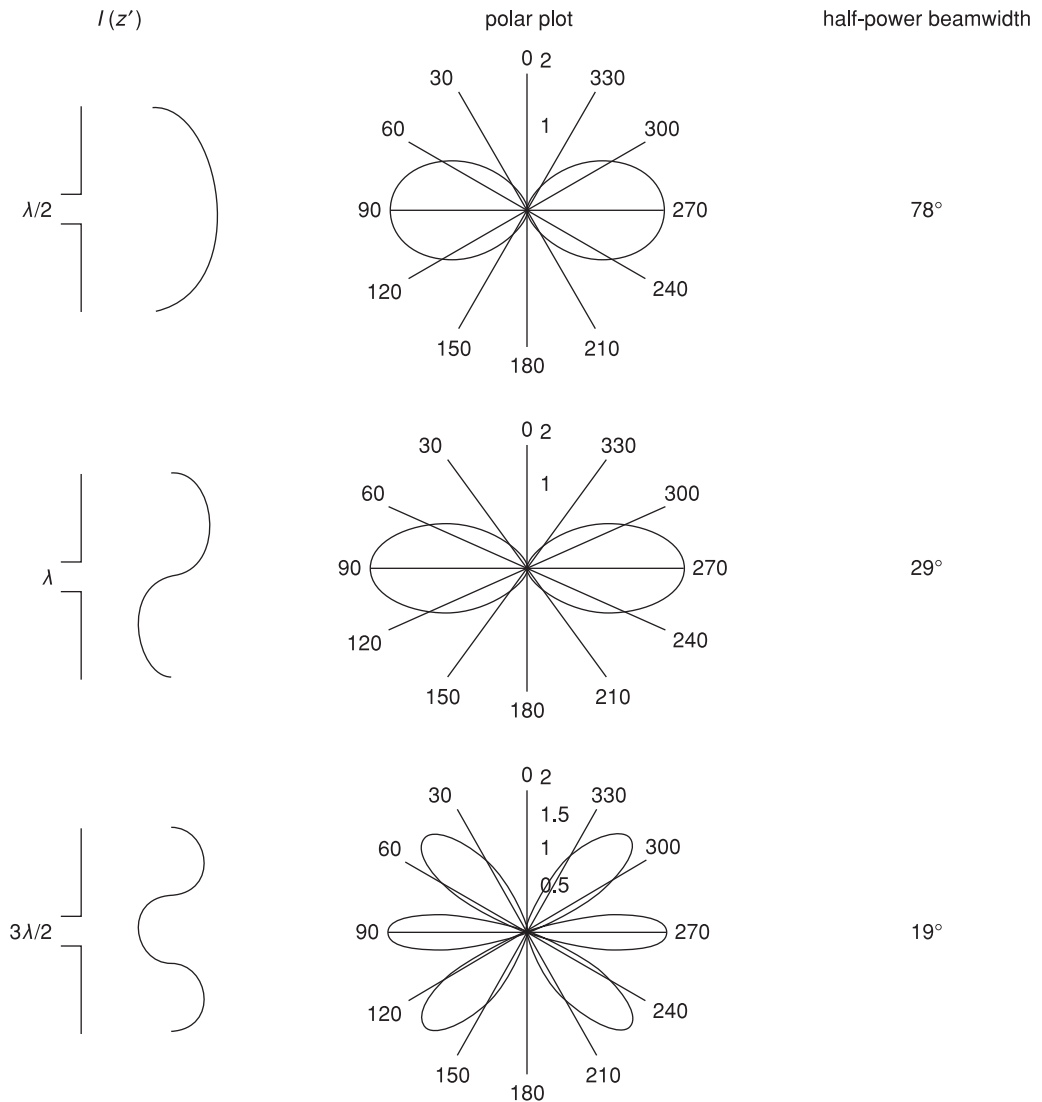


Figure 3.3 Typical polar plots for dipole antennas

From Figure 3.3, it can be seen that as the antenna length increases from  $\lambda/2$  to  $\lambda$  the gain associated with the main lobe radiation of the dipole increases. Above  $\lambda$  (at  $\ell = 1.2\lambda$ ) the antenna starts to present side lobes, which represent a loss of energy that would otherwise go into the main lobes of the antenna. This leads to a reduction of gain in the principal radiation directions of the antenna and also presents an opportunity for the antenna to pick up radiation from unwanted angles, i.e. along the directions of these side lobes.

### 3.3 Dipole antenna radiation resistance

Using the same procedure as was used in Section 2.3 for the Hertzian dipole based on Poynting's theorem, we can now find the power radiated by a straight wire dipole of length  $\ell$  with sinusoidal current distribution. Here, the average radiated power is

$$P_{\text{avg}} = \frac{1}{2} \int_0^{2\pi} \int_0^\pi E_\theta H_\phi r^2 \sin\theta \, d\theta \, d\phi \quad (3.18)$$

on using  $120\pi H_\phi = E_\theta$  and equation (3.13):

$$\begin{aligned} P_{\text{avg}} &= \frac{\eta I_0^2}{8\pi^2} \int_0^{2\pi} \int_0^\pi \frac{\left[ \cos\left(\frac{1}{2}k\ell \cos\theta\right) - \cos\left(\frac{1}{2}k\ell\right) \right]^2}{\sin\theta} \, d\theta \, d\phi \\ &= 30I_0^2 \int_0^\pi \frac{\left[ \cos\left(\frac{1}{2}k\ell \cos\theta\right) - \cos\left(\frac{1}{2}k\ell\right) \right]^2}{\sin\theta} \, d\theta \end{aligned} \quad (3.19)$$

But we know by definition that the average power at the input to this antenna,  $z = 0$ , is

$$P_{\text{avg}} = \frac{1}{2} I^2(0) R_{\text{rad}} \quad (3.20)$$

Hence the radiation resistance,  $R_{\text{rad}}$ , for a finite-length dipole antenna of length  $\ell$  is

$$R_{\text{rad}} = \frac{60I_0^2}{I^2(0)} \int_0^\pi \frac{\left[ \cos\left(\frac{1}{2}k\ell \cos\theta\right) - \cos\left(\frac{1}{2}k\ell\right) \right]^2}{\sin\theta} \, d\theta \quad (3.21)$$

Consider now the important special case of a half-wave dipole ( $\ell = \lambda/2$ ) that is centred. In this case  $I(0)$  must equal  $I_0$ , the maximum excitation current. Hence

$$R_{\text{rad}} = 60 \int_0^\pi \frac{\cos^2\left(\frac{\pi}{2} \cos\theta\right)}{\sin\theta} \, d\theta \quad (3.22)$$

The integral in this case can be evaluated only by numerical means; this evaluation results in a value of 1.22. Hence the radiation resistance for a half-wave linear dipole referred to the current at the centre feed point terminals at resonance (zero reactance term) is

$$R_{\text{rad}} = 60 \times 1.22 \approx 73 \, \Omega$$

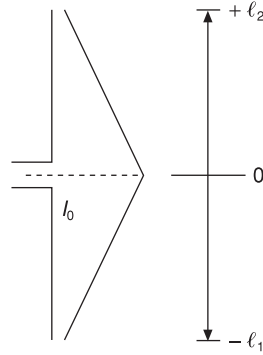


Figure 3.4 Short dipole with linear current distribution

### 3.4 Short dipole antenna

The Hertzian dipole antenna considered earlier had a uniform current distribution over its entire length. While theoretically this is useful, it does not represent accurately the physical situation for dipole antennas of finite but small physical length. In an actual case of a dipole antenna fed at the centre, the current at each end of the dipole must fall to zero, since that end is open-circuited. With this in mind a better model for the current distribution might be a linear distribution with its maximum at the centre, decreasing to zero at the ends (Figure 3.4). Here the antenna is considered to be short enough so that a sinusoidal current distribution cannot develop over the length of the antenna.

For the short dipole discussed here,  $\ell$  is assumed to be  $\ll \lambda_0$ . In addition, we will assume a current distribution:

$$I(z) = I_0 \left( 1 - \frac{z}{\ell_2} \right) \quad z \geq 0$$

and

$$I_0 \left( 1 + \frac{z}{\ell_1} \right) \quad z < 0 \quad (3.23)$$

such that the current goes to zero at each end of the short dipole and where  $\ell = \ell_1 + \ell_2$ .

Recalling equation (3.9) for the finite-length dipole, we get

$$H_\phi = \frac{k \exp(-jkr)}{4\pi r} \left[ \int_0^{\ell_2} I_0 \left[ 1 - \frac{z'}{\ell_2} \right] \exp(jkz' \cos\theta) dz' \right. \\ \left. + \int_{-\ell_1}^0 I_0 \left[ 1 + \frac{z'}{\ell_1} \right] \exp(jkz' \cos\theta) dz' \right] \quad (3.24)$$

using  $\int \exp(x) dx = \exp(x)$

and

$$\int x \exp(x) = \exp(x)(x - 1)$$

and also noting

$$k(\ell_1 + \ell_2) \ll 1$$

then

$$H_\phi = \frac{jk \exp(-jkr)}{4\pi r} \sin\theta \frac{I_0}{2} (\ell_1 + \ell_2) \quad (3.25)$$

which is an identical result to that obtained for the Hertzian dipole, equation (1.15), except that the excitation current is reduced by 50%. Thus the radiated power for a short dipole antenna with linear current distribution is reduced to 25% relative to the same quantity calculated for a Hertzian dipole. Hence the radiation resistance for a short dipole antenna  $R_{\text{rad}}$  is, after equation (2.60),

$$R_{\text{rad}} = 20\pi^2 \left(\frac{\ell}{\lambda}\right)^2 \Omega \quad (3.26)$$

### Exercise 3.3

Calculate the radiation resistance of a short dipole of length  $0.2\lambda$  supporting a linear current distribution.

#### Solution

Using equation (3.26):

$$\begin{aligned} R_{\text{rad}} &= 20\pi^2 0.04 \\ &= 0.8\pi^2 \Omega \end{aligned}$$

which is only one-quarter of what can be obtained from an antenna carrying a uniform current distribution.

We have seen that a Hertzian dipole is assumed to support a uniform current distribution (Figure 3.5a), while a short dipole can be approximated as supporting a linear current distribution (Figure 3.5b). The current distribution of the short linear dipole can be made to more closely approximate the uniform current distribution of the Hertzian dipole by adding circular metal plates to each end of the dipole (Figure 3.5c).

This forms a capacitive load for the antenna and, as a consequence, the antenna is termed a capacitor-plate or capacitor-loaded antenna. The current flow on the upper and lower plates is radially directed but in opposite senses for each plate. Hence the electromagnetic fields generated due to these currents cancel each other out and do not significantly influence the radiation pattern of the antenna. Thus the electromagnetic fields associated with the three parts of Figure 3.5, i.e. the Hertzian, short and capacitively loaded dipole antennas, are approximately equivalent.

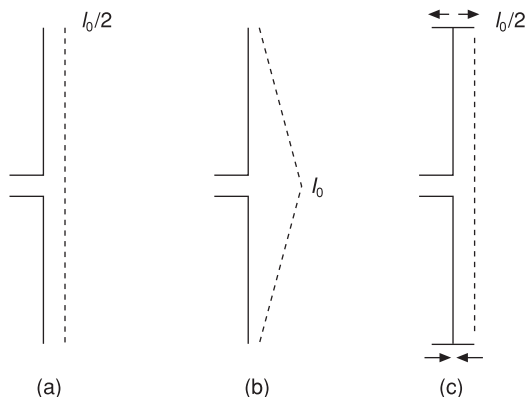


Figure 3.5 Approximately equivalent dipole antennas

### 3.5 Gain of a half-wave dipole relative to a Hertzian dipole and power transfer

For a half-wave dipole antenna, we have shown in Section 3.3 that its radiation resistance is  $73.2 \Omega$ , hence the instantaneous power radiated by the antenna is

$$P_{\text{inst}} = I_0^2 73.2$$

but for the half-wave dipole in the equatorial plane, we know from Section 3.2 that for  $\theta = 90^\circ$

$$E_{\theta_{\text{max}}} = \frac{60I_0}{r} \left( \frac{\cos(\pi/2(\cos 90^\circ))}{\sin 90^\circ} \right) = \frac{60I_0}{r}$$

Substituting for  $I_0$  gives

$$E_{\theta_{\text{max}}} = \frac{60\sqrt{P_{\text{inst}}}}{r\sqrt{73.2}} = 7\frac{\sqrt{P_{\text{inst}}}}{r} \quad (3.27)$$

and for an isotropic source (equation (2.52))

$$E_{\theta_{\text{max}}} = \frac{\sqrt{30P_{\text{inst}}}}{r} \quad (3.28)$$

#### Exercise 3.4

Calculate the maximum field strength at boresight radiated from a half-wavelength dipole, excited by a 1A RMS AC current measured at a range of 1 km.

#### Solution

Using equation (3.27), we find that

$$E_{\theta_{\text{max}}} = \frac{7\sqrt{73}}{1000} = 60 \text{ mV/m}$$

Hence by our previous gain definition (Section 2.4), assuming 100% efficiency the gain of an ideal half-wave dipole antenna relative to an isotropic radiator,  $G$ , is

$$G = \left( \frac{\frac{7\sqrt{P_{\text{inst}}}}{r}}{\frac{\sqrt{30}\sqrt{P_{\text{inst}}}}{r}} \right)^2 = 1.63 \quad (3.29)$$

or  $G = 10 \log_{10} 1.63 = 2.1$  dBi.

The purpose of an antenna is to deliver or to receive power in the form of an electromagnetic wave that is regarded as travelling through free space, although in general it may be propagating through any medium. From previous studies in Section 1.4, we saw that in the far field the electric field magnitude of the signal from the source varies in inverse proportion to its distance from the source,  $r$ , i.e. power varies according to  $1/r^2$ . This means that for reasonable separations between transmitter and receiver, only a very small amount of the transmitted power will be available at the receive antenna. Thus for best possible operation we need to make sure that maximum power is transferred from the propagating wave to the receive antenna, or vice versa. Figure 3.6a

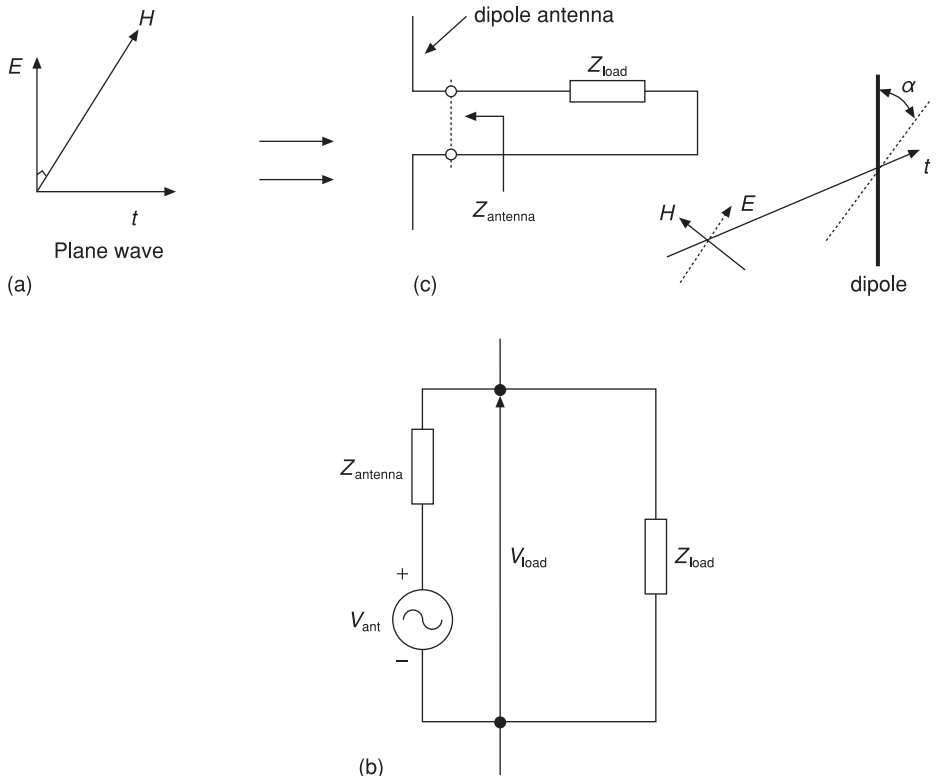


Figure 3.6 Receive antenna power transfer

shows a plane wave whose  $E$  field is incident on a receive dipole antenna; both have the same orientation (see Section 5.2). An electrical equivalent schematic for this arrangement is shown [14] in Figure 3.6b. In Figure 3.6,  $Z_{\text{antenna}}$  comprises the antenna loss mechanisms due to dielectric, ohmic and mismatch effects and a reactive component, which can be inductive or capacitive.

The external load  $Z_{\text{load}}$  sees an equivalent voltage source  $V_{\text{load}}$  placed across its terminals that has an internal impedance equal to the impedance of the antenna. For the optimal case, maximum power transfer to occur between antenna and external load,

$$Z_{\text{ant}} = Z_{\text{load}}^* \quad (3.30)$$

where the  $*$  indicates complex conjugation; hence

$$R_{\text{ant}} \pm jX_{\text{ant}} = R_{\text{load}} \mp jX_{\text{load}} \quad (3.31)$$

In this way, any reactance in the system is cancelled, leaving only real, lossy, components. Under the conjugate match condition

$$R_{\text{ant}} = R_{\text{load}} \quad (3.32)$$

so that

$$V_{\text{load}} = \frac{1}{2} V_{\text{ant}} \quad (3.33)$$

Hence the power delivered to the load,  $P_L$ , is

$$P_L = \frac{1}{4} V_{\text{ant}}^2 / R_{\text{load}} \quad (3.34)$$

In general

$$P_L = R_e \left[ \frac{1}{2} \frac{V_L^2}{Z_{\text{load}}} \right] \quad (3.35)$$

The equivalent circuit for the receive antenna given by Figure 3.6 is only approximate, since in general it should include additional sources to model the effects of scattering of the incident field by the receiving antenna. It should be noted that in most instances the current distribution along an antenna in transmit and in receive mode can be very different. However, their far-field patterns will be the same, since the combination of the re-radiated scattered and incident fields, on receive, add to yield the same far field as would have been obtained if the antenna had been used in transmit mode.

### Exercise 3.5

For the case when transmit and receive antenna current distributions are the same, show that under the matched condition i.e. when  $R_{\text{load}} = R_{\text{ant}}$  as much power is scattered as is absorbed by the antenna.

**Solution**

From Figure 3.6, the power absorbed in the terminating resistive load  $P_L$  is

$$P_L = \frac{V_{\text{ant}}^2 R_{\text{load}}}{(R_{\text{load}} + R_{\text{ant}})^2}$$

The power dissipated in the radiation resistance of the antenna itself, i.e. the power re-radiated from the antenna, is  $P_R$ , which by inspection of Figure 3.6 is

$$P_R = \frac{V^2 R_{\text{ant}}}{(R_{\text{load}} + R_{\text{ant}})^2}$$

now when  $R_{\text{load}} = R_{\text{ant}}$  and equation (3.34) results, i.e. the matched condition thus  $P_L = P_R$ .

Consequently, as much power is scattered as is absorbed. Note that this is a special case. In general, the amount of scattering may be, larger, smaller or equal to the power absorbed by a matched antenna operated in receive mode.

For an antenna driving into an open circuit

$$P_L = R_e \left[ \frac{1}{2} \left( \frac{V_{\text{oc}}}{2} \right)^2 \frac{1}{Z_{\text{load}}} \right] = \frac{V_{\text{oc}}^2}{8} R_e \left[ \frac{1}{Z_{\text{load}}} \right] \quad (3.36)$$

Now when an electric field is oriented relative to a receive antenna at some angle,  $\alpha$  (Figure 3.6c), the induced open-circuit voltage in the antenna is [13]

$$V_{\text{oc}} = h_e(\theta) E \cos \alpha \quad (3.37)$$

where  $E \cos \alpha$  is the component of electric field that lies along the axis of the antenna, and  $h_e(\theta)$  is the effective length of the antenna as defined in Section 3.2.

Thus we can say that under conjugate match conditions

$$P_L = \frac{1}{8} h_e^2(\theta) \frac{E^2 \cos^2 \alpha}{R_{\text{ant}}} \quad (3.38)$$

**Exercise 3.6**

Show that a linearly polarised receive antenna positioned in the far field and at right angles to a linearly polarised transmit antenna will receive no signal.

**Solution**

Using equation (3.37), we can see that if  $\alpha = 90^\circ$  then  $\cos \alpha = 0$  and no signal will be received.

Such situations imply that two orthogonal linearly polarised antennas can carry information at the same frequency without interfering with each other. This is a technique called polarisation diversity.

**Exercise 3.7**

Consider two half-wave dipoles aligned with their axes parallel. Find an expression for the maximum power that will be available at the receive antenna.

**Solution**

When the axes of both antennas are parallel,  $\alpha = 0$  ( $\cos\alpha = 1$ ). The power available at the second antenna can be calculated from equation (3.38) as

$$P = \frac{|h_c(\theta)|^2 |E|^2}{8R_{\text{rad}}} \quad (3.39)$$

**Exercise 3.8**

Calculate the effective length of a half-wave dipole at the position of maximum received power.

**Solution**

$$h_c(\theta) = \frac{2\cos\left(\frac{1}{2}\pi\cos\theta\right)}{k\sin\theta} \quad (3.40)$$

Noting that for maximum received power  $\theta = \pi/2$  so that for this example using

$$h_c\left(\frac{\pi}{2}\right) = \frac{\lambda}{\pi} = \frac{0.3}{\pi}$$

where  $\lambda = 30$  cm.

From equation (1.16), we can write  $E_\theta$  as

$$E_\theta = \frac{\eta I(0)}{2\pi\lambda r} \exp(-jkr) \quad (3.41)$$

Thus

$$|E_\theta| = \frac{\eta I(0)}{2\pi\lambda r} \quad (3.42)$$

Now  $I(0)$  is the current applied at the feed point to the centre-fed half-wave dipole; hence, if antenna ohmic losses are small, we can say that

$$I(0) = \left(\frac{2P_{\text{rad}}}{R_{\text{rad}}}\right)^{1/2} \quad (3.43)$$

**Exercise 3.9**

For 1 W average radiated power from a half-wave dipole, calculate the current applied at the antenna feed point and thus find  $E_\theta$ .

**Solution**

$$I(0) = \left( \frac{2 \times 1}{73.2} \right)^{1/2} = 165 \text{ mA}$$

Hence using equation (3.41) at the receive antenna:

$$|E_\theta| = \frac{(120\pi)(0.165)}{2\pi(0.3)1000} = 0.033 \text{ V/m}$$

**Exercise 3.10**

For the parameters defined in exercise 3.9, calculate the power available at the terminals of the receive antenna.

**Solution**

This can be found by applying equation (3.39):

$$P = \left( \frac{0.3}{\pi} \right)^2 (0.0332)/(8)(73) = 0.52 \text{ } \mu\text{W} \text{ or } -33 \text{ dBm}$$

where the unit dBm is defined as power relative to a 1 mW reference level:

$$\text{dBm} = 10 \log_{10} \left( \frac{P}{1\text{mW}} \right)$$

**References**

- [12] Stutzman, W.L. and Thiele, G.A., *Antenna Theory and Design*, John Wiley & Sons, 1998.
- [13] Kraus, J.D., *Antennas* (2nd edition), McGraw-Hill, 1988.
- [14] Kraus, J.D., *Antennas*, McGraw-Hill, 1950, pp. 254–6.

**Problems**

- 3.1** A dipole antenna has the following parameters: length  $0.7\lambda$ , excitation current 2 A and operating frequency 1 GHz. The radiation produced by the antenna is observed by a suitably equipped receiver at a distance of 200 m. For this arrangement, calculate
- the antenna radiation resistance;
  - the far field polar pattern for the dipole;
  - the electric field strength at the observation point; and
  - the gain of the dipole relative to an isotropic source.
- 3.2** What power must be fed to
- an isotropic antenna;
  - a half-wave dipole; and
  - a short dipole
- in order to maintain a field strength of 0.1 V/m at a distance of 1 km from the antenna? You may assume that the antennas are lossless and that they are operating at a frequency of 1 GHz.
- 3.3** Consider two half-wave dipoles aligned so that their axes are offset by  $30^\circ$ . If the transmit antenna radiates 1 W of power, find the maximum power that will be available at the receive antenna when they are placed 1 km apart at an operating frequency of 1 GHz. Plot the received power level as the axis of the receive antenna is rotated from  $0^\circ$  (both antennas parallel) to  $90^\circ$  (both antennas normal to each other). Comment on the engineering significance of these calculations.

# Antenna array techniques

---

In order to increase the gain of an antenna, several radiating elements are arranged in a systematic way to form an antenna array. Using geometrical considerations, this chapter illustrates how individual antenna elements can be grouped to form enhanced preferential radiation characteristics.

First, a simple situation comprising just two elements is used to describe the basic process for array factor calculation. Then the procedure is generalised for a one-dimensional linear array and then for a two-dimensional stacked array. The relationship that exists between the array aperture field distribution and the far-field radiation pattern of the array is then described. The far-field radiation characteristics of an array can be modified by using non-uniform excitation of the elements; this aspect of far-field radiation performance tailoring is introduced. Other important issues are also introduced, including antenna input impedance quantification, inter-element mutual coupling effects and the effect of a ground plane placed in proximity to a radiating element. The idea of electronically steering the far-field radiation pattern produced by an array is briefly discussed.

### 4.1 Radiation patterns for two antennas

We have previously seen that a single dipole antenna does not exhibit a high degree of directivity, and as a consequence its radiation is spread over a relatively large volume. Combinations of two or more antennas, called an antenna array, can be used if properly designed to enhance overall directivity hence gain response.

The simplest example of this is when two antennas are combined to form an array. Initially, we will assume the following:

- Both elements are identical.
- Both elements have the same spacial orientation.
- Both elements are excited with equal-magnitude in-phase currents.

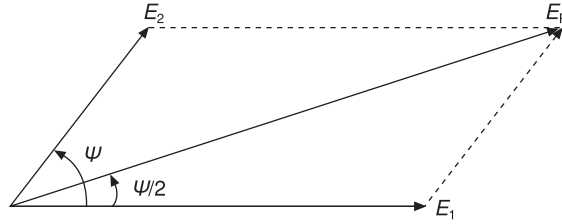


Figure 4.1 Vector summation of  $E$  fields

- There are no mutual coupling effects between antennas, i.e. the radiation pattern of each antenna remains undistorted by the presence of any other antenna.
- Initially, we will give both antennas that comprise the array the property of an isotropic radiator, i.e. non-preferential radiation in any direction.

If the electric field at some observation point in space due to a single antenna radiating power  $P$  is  $E(r, \theta, \phi)$ , then for a two-element array radiating the same total amount of power as the single element, each element in the array will be producing a resultant electric field strength of  $E(r, \theta, \phi)/\sqrt{2}$  or, on dropping the spherical coordinate notation,  $E/\sqrt{2}$ .

Due to the physical separation between elements, the fields produced by each element will not be in phase, even though their polarisations (see Section 5.4) will align. The phase delay due to the physical separation between elements is  $\psi$ ; the resultant field strength vector,  $E_R$ , is found by vector addition (Figure 4.1). The general case for a one-dimensional array will be covered in Section 4.2.

For the simplest case, i.e. a two-element array with equal amplitude and equal phase excitation, direct application of the parallelogram rule will suffice to gain an insight into the problem in hand. Thus

$$E_R^2 = E_1^2 + E_2^2 + 2E_1 E_2 \cos(\Psi) \quad (4.1)$$

If  $E_1 = E_2 = E/\sqrt{2}$ , as it does in our example of two identical but physically separated isotropic sources, the above expression reduces to

$$E_R^2 = E^2(1 + \cos(\Psi)) \quad (4.2)$$

by noting that  $\cos^2 \Psi = 1/2(1 + \cos 2\Psi)$  then  $E_R^2 = 2E^2 \cos^2 \Psi/2$ .

What is now required is to relate the phase delay, angle  $\Psi$ , to the physical separation between elements (Figure 4.2). In the figure, AC is the extra path length required for a signal sited at some position P in the antenna far field to reach position A on the array relative to position B, both of which are physically separated by distance  $d$ .

$$\begin{aligned} AC &= d \cos \theta \text{ meters} \\ &= \frac{d}{\lambda} \cos \theta \text{ wavelengths} \\ &= \frac{2\pi d}{\lambda} \cos \theta \text{ radians} \end{aligned} \quad (4.3)$$

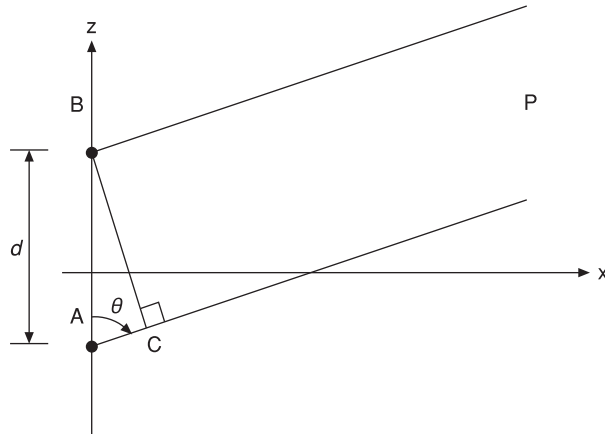


Figure 4.2 Two-element array factor geometry

Hence

$$E_R = E\sqrt{2} \cos\left(\frac{\pi d}{\lambda} \cos\theta\right) \tag{4.4}$$

Examination of this result shows that we have the original electric field description for the antenna element multiplied by a factor describing the geometry of the antenna array configuration. This second term is called the antenna array factor, or more simply the array factor, which for a co-phased two element array is

$$\sqrt{2} \cos\left(\frac{\pi d}{\lambda} \cos\theta\right) \tag{4.5}$$

This array factor can be plotted in polar form, as was previously done for the electric and magnetic field far field radiation patterns (Figure 4.3). Here, since there is no

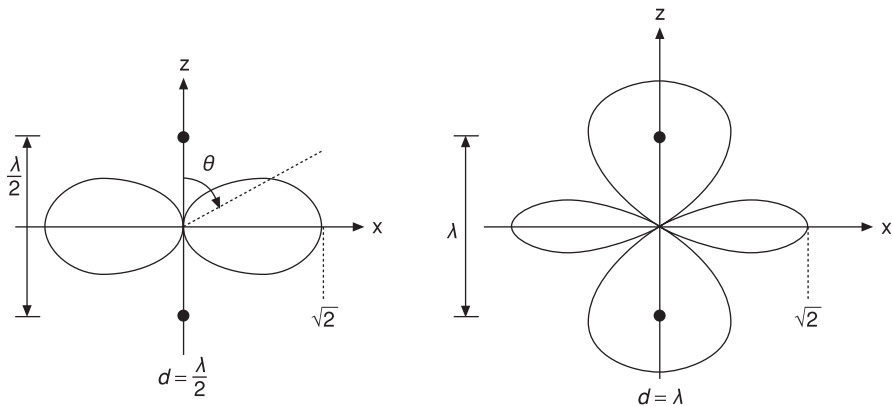


Figure 4.3 Isotropic source array factor plots

azimuthal variation with  $\phi$ , two-dimensional plots in the  $x$ - $z$  plane suffice in this case. From Figure 4.3, it can be seen that the array factor establishes the modification of the radiation pattern due to the radiated power from the two sources having a relative phase difference to be calculated in the far field.

### Exercise 4.1

Calculate the increase in gain that a two-element array has with respect to a single element when viewed along the antenna boresight direction.

### Solution

Using equation (4.5) for source separation  $d = \lambda/2$  in the broadside direction ( $\theta = 90^\circ$ ), the maximum radiated field strength is  $\sqrt{2}$ , so the power gain of this arrangement is 3 dB greater than that obtained from a single source. However, it should be noted that the increase in directivity obtained in one direction has to be compensated for by a reduction of radiation in another direction.

So far, since our antenna elements are isotropic sources, the array factor polar plot represents the composite array polar plot, or as it is often called, the resultant pattern.

$$\text{resultant pattern} = \text{element pattern} \times \text{antenna array factor} \quad (4.6)$$

In general, this multiplication must be carried out in both the  $\theta$  and  $\phi$  planes using the appropriate element and array pattern formulations.

If the array is driven with currents that are not in phase (i.e. are not co-phased), then we can add an additional factor to equation (4.4) to represent the effect that this additional phase angle  $\alpha$  has on the array pattern when introduced into the element drive current.

$$E_R = \sqrt{2} E \cos\left(\frac{\pi d}{\lambda} \cos\theta \pm \frac{\alpha}{2}\right) \quad (4.7)$$

Here the + sign indicates a phase lag and the – sign a phase lead with respect to the excitation phase of one of the elements, which has previously been selected to act as the reference element. Section 4.2 will describe in more detail the effect that the phase shift,  $\alpha$ , has on polar pattern response.

To see how the concept of the array factor facilitates a slightly more complex example, consider now the radiation pattern formed by two co-phased co-linear half-wave dipole antennas spaced one half-wavelength apart. The co-linear stipulation implies that both dipole antennas have their axes aligned, in our example along the  $z$ -axis as in Figure 4.4.

First, we plot the array factor polar pattern using equation (4.5); then we draw the dipole pattern, e.g. equation (3.15); and finally we compute by polar coordinate multiplication using equation (4.6) the resultant pattern for the array. These operations are illustrated in Figure 4.5. Note that for the dipole element case we have rotational symmetry in the  $x$ - $y$  plane. Notice also how the use of two elements in the array has

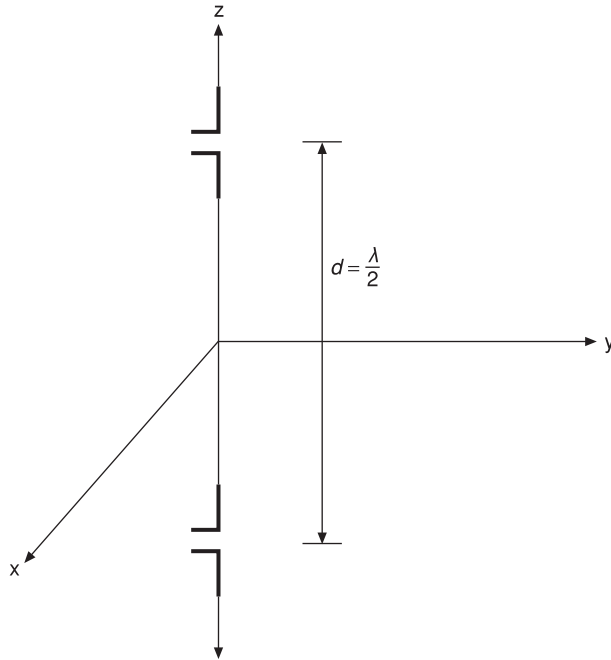


**Figure 4.4** Co-linear two-element dipole array

increased the relative field strength of a single dipole by a factor of  $\sqrt{2}$  due to the focusing action of the array described earlier.

## 4.2 One-dimensional linear arrays and far-field transformation

The two-element array technique previously discussed can be extended to represent a situation describing  $N$  elements placed in a one-dimensional or linear array. With the inclusion of specific radiating elements, the one-dimensional array can take several different forms (Figure 4.6).

### Co-linear array

The co-linear arrangement is shown in Figure 4.6a. Consider first the simplest case of  $N$  co-phased isotropic sources, each producing the same electric field and with negligible mutual coupling effects between antennas. If each isotropic source is separated by a distance  $d$  meters, then the resultant electric field,  $E_R$ , for the  $N$ -element linear array is found from Figure 4.7 using the same technique as before in Section 4.1. For example, for Figure 4.6a,

$$\psi = \frac{2\pi}{\lambda} d \cos\theta \quad (4.8)$$

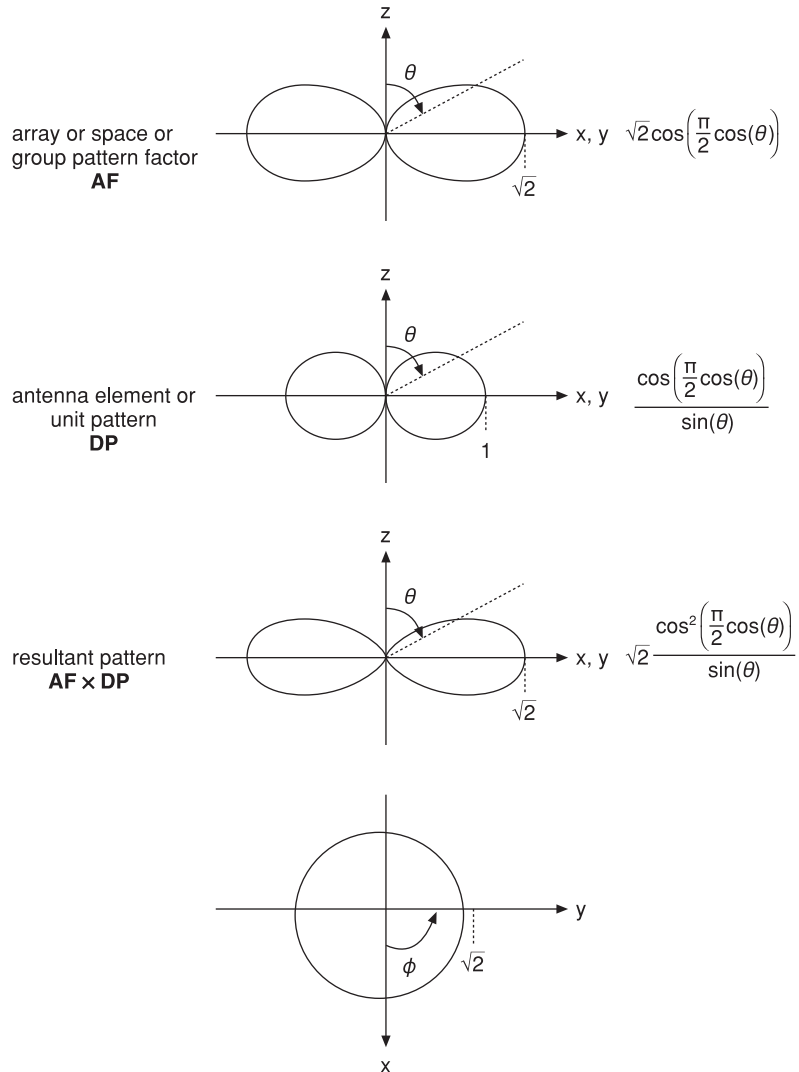


Figure 4.5 Group patterns for co-phased linear dipoles

with element 1 as the phase reference, the field from the  $(N - 1)$ th radiator will lag the  $N$ th radiator by  $\psi$  degrees. Thus

$$E_R = 2R \sin \frac{N\psi}{2} \tag{4.8}$$

and

$$E_1 = 2R \sin \frac{\psi}{2} \tag{4.9}$$

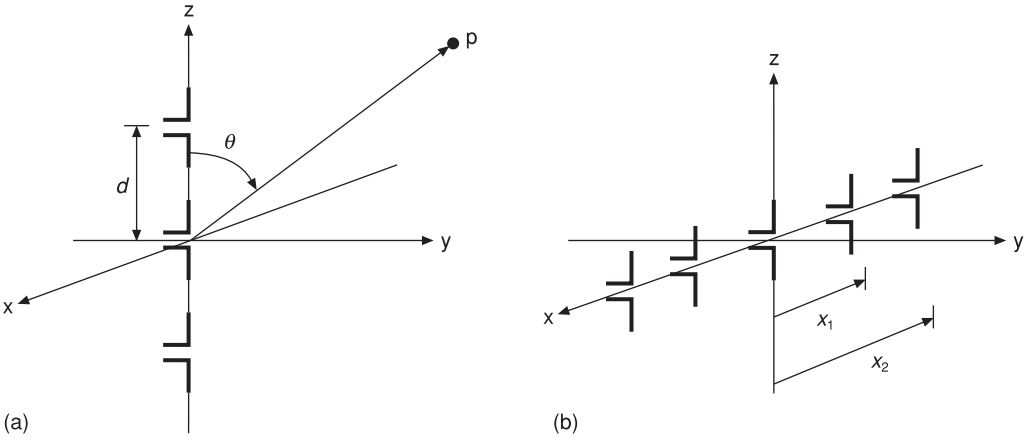


Figure 4.6 One-dimensional array configurations

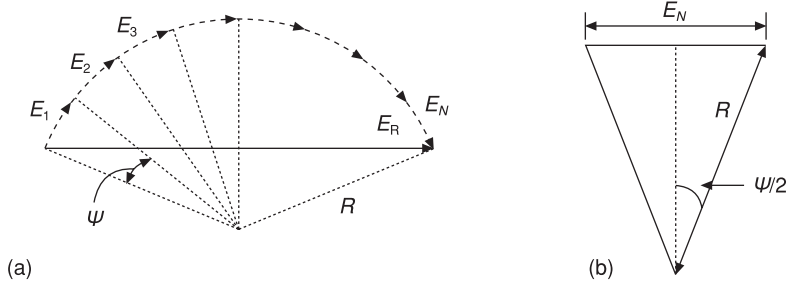


Figure 4.7 Vector plot for  $N$ -element array

Therefore

$$E_R = \frac{E_1 \sin\left(\frac{N\psi}{2}\right)}{\sin\left(\frac{\psi}{2}\right)} \quad (4.11)$$

on using equation (4.3)

$$E_R = \frac{E_1 \sin\left(\frac{N\pi d \cos\theta}{\lambda}\right)}{\sin\left(\frac{\pi}{\lambda} d \cos\theta\right)} \quad (4.12)$$

In the direction of maximum field strength  $\theta = 90^\circ$ , and since for a large number of array elements the array will have high directivity, i.e. the width of the main beam will be small, then using the small-angle approximation for the sine terms we get

$$E_R = NE_1 \quad (4.13)$$

Now if one radiator were to radiate the same amount of power as the entire array does, say  $E$  V/m, then in the array each element would need to radiate  $1/N$  W so that the electric field produced by each element in the array is  $E\sqrt{1/N}$  for the situation where each element is excited with equi-amplitude signals. Therefore, noting this equivalence, we can write

$$E_R = \frac{E}{\sqrt{N}} \frac{\sin\left(\frac{N\pi}{\lambda} d \cos\theta\right)}{\sin\left(\frac{\pi}{\lambda} d \cos\theta\right)} \quad (4.14)$$

from which the array factor or group pattern can be determined. Thus relative to a single element the maximum achievable power gain for an  $N$ -element array is  $N$  times that which can be achieved for a single radiator; the electric field strength magnification achievable is  $\sqrt{N}$ .

It is not unreasonable now to assume that since gain is enhanced, the beamwidth of the array will be reduced relative to that of a single element. Beamwidth can be calculated by locating the position of the nulls in equation (4.14).

### Exercise 4.2

Calculate the angle out to the first nulls for an array having a large number of elements an equally spaced distance  $d$  from each other.

#### Solution

Now since for a large number of elements directivity is high and the main lobe is along  $\theta = \pi/2$ , we can expect that the nulls will lie close to this position. Consequently, to find the angle out to the first nulls,  $\cos\theta$  in equation (4.14) can be replaced by

$$\cos\theta \approx \frac{\pi}{2} - \theta = \theta' \text{ radians}$$

which when substituted into equation (4.14) gives when set equal to zero (i.e. the first null condition)

$$\theta' \frac{N\pi}{\lambda} d \approx \pm\pi$$

or

$$\theta' \approx \pm \frac{\lambda}{Nd} \text{ radians} \quad (4.15)$$

*This is an important result, since it indicates that the longer the array is, the narrower the beamwidth to the first null, i.e. the antenna array is acting like a lens focusing the radiated electric and magnetic fields. The term  $Nd$  can be considered as the aperture of the co-linear array.*

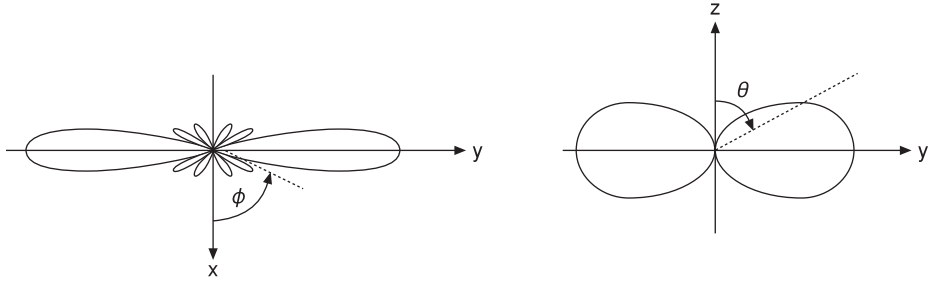


Figure 4.8 Group pattern for broadside array of half-wavelength spaced dipoles

In an  $N$ -element co-linear array (Figure 4.6a), the  $E$ -field component varies in the  $x$ - $z$  or  $y$ - $z$  plane as defined by the element  $E_\theta$  pattern multiplied by the group pattern above. As before, symmetry is preserved in the  $\phi$  plane.

### Broadside array

Figure 4.6b depicts the linear broadside array; here the situation is somewhat more complex. Even though the group pattern is the same as in the previous case, the radiation patterns exhibit different forms in the  $x$ - $y$  and  $y$ - $z$  planes (Figure 4.8). Any additional phase between array elements,  $\alpha$ , can be introduced in the same fashion as was used for the two-element array case in Section 4.1, namely

$$E_R = \frac{E_0}{\sqrt{N}} \frac{\sin\left(\frac{N\pi d}{\lambda} \cos\theta \pm \alpha\right)}{\sin\left(\frac{\pi d}{\lambda} \cos\theta \pm \alpha\right)} \quad (4.16)$$

As before, a + sign indicates lagging currents and a - sign indicates leading currents with respect to the drive current at the array reference element.

If we consider two currents phase-delayed by  $90^\circ$  and spacially separated by  $\lambda/4$ , we can see how the linear end-fire array (Figure 4.10a) can give preferential radiation in one direction (Figure 4.9).

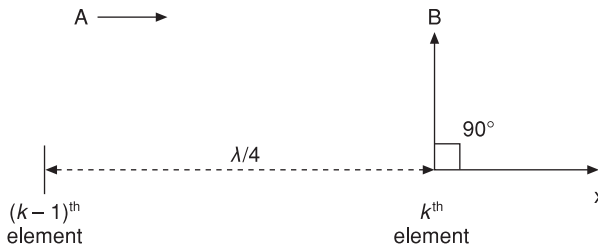
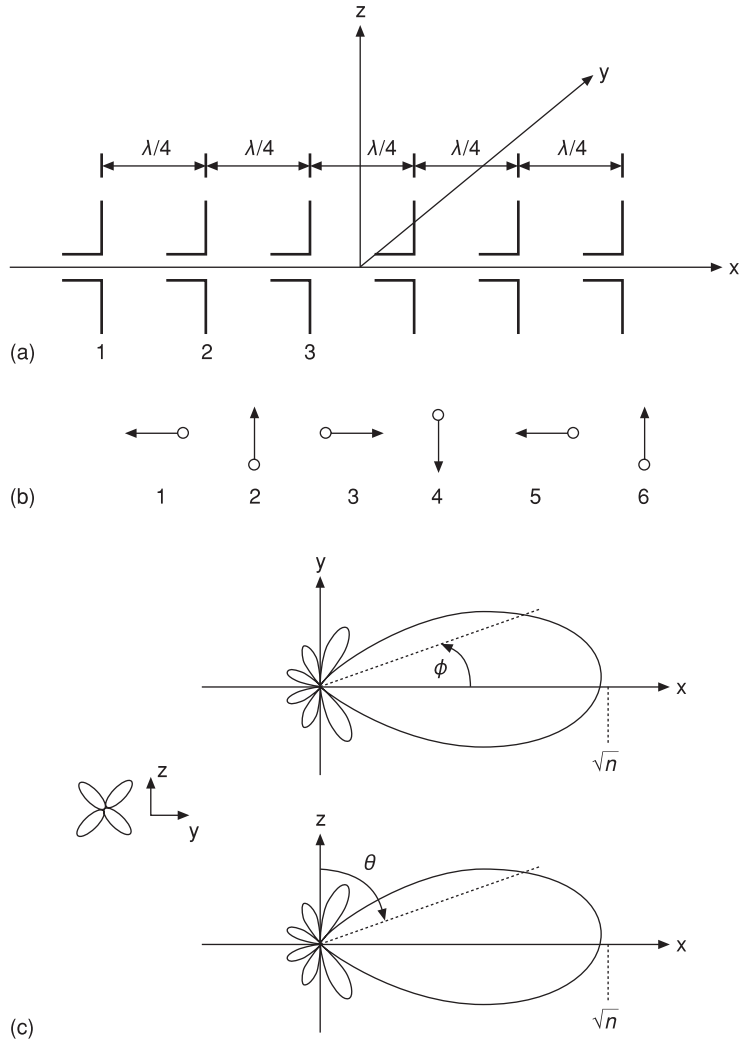


Figure 4.9 End-fire operation



**Figure 4.10** End-fire array of  $N$  half-wave dipole elements,  $d = \lambda/4$ : (a) end-fire arrangement; (b) phase relationship of excitation currents; (c) far-field patterns

### End-fire array

In Figure 4.9 and Figure 4.10b, as the electromagnetic wave induced by current vector  $A$  moves from left to right along the positive  $x$ -direction, it rotates through one-quarter of a wavelength (i.e.  $90^\circ$ ); therefore, it reinforces the field at position  $B$  provided that the current at  $B$  already lags the signal at  $A$  by  $90^\circ$ . Similarly, the field produced at  $B$  cancels the field at  $A$  along the negative  $x$ -direction. Hence, in general, a  $90^\circ$  lagging current at element  $k$  with respect to element  $k - 1$  will be reinforced in

the positive  $x$ -direction by virtue of the quarter-wavelength delay between elements. Moving from right to left across Figure 4.10a, the converse is true and destructive interference will occur in the reverse direction. Mathematically, stating this condition from equation (4.3),

$$\psi = \frac{\pi}{2} - \frac{2\pi d}{\lambda} \cos\theta$$

on setting  $d = \lambda/4$ , then

$$\psi = \frac{\pi}{2}(1 - \cos\theta) \quad (4.17)$$

so that after equation (4.14), the relevant group pattern becomes

$$\frac{1}{\sqrt{N}} \left( \frac{\sin\left(\frac{N\pi}{4}\right)(1 - \cos\theta)}{\sin\left(\frac{\pi}{4}\right)(1 - \cos\theta)} \right) \quad (4.18)$$

In the  $x$ - $z$  and  $y$ - $z$  planes, the pattern must be multiplied by the correctly oriented dipole figure-of-eight pattern, while in the  $x$ - $y$  plane the symmetrical circular pattern is used (see Figure 4.10).

### Exercise 4.3

Calculate the angle to the first null for a ten-element end-fire array with equal spacing of  $\lambda/4$  between each element.

#### Solution

Equation (4.18) governs this case. Thus we can determine the angle to the first null in the radiation pattern in the  $x$ - $y$  plane by calculating according to the angle  $\theta$  the condition that makes  $N\psi$  using equation (4.17) equal to

$$N \frac{\pi}{2} (1 - \cos\theta) = 2\pi$$

$$\theta = \cos^{-1} \left( 1 - \frac{4}{N} \right)$$

While this array does concentrate the radiated power mostly in one direction, it still does not produce a very focused beam; for example, if  $N$  is 10,  $\theta = 53^\circ$ .

---

The ratio of the radiated field in the positive  $x$ -direction to that in the negative  $x$ -direction is called the front-to-back ratio and is infinite for the ideal case cited here, i.e. this arrangement will be insensitive to signals coming from the negative

x-direction. In an actual end-fire array, mutual coupling effects will degrade the ideal front-to-back ratio (see Section 4.7 for more details).

## Phased array

A more general formulation for calculating the superimposed radiation from a series of radiating elements can be formed by discarding the parallelogram law and using complex exponent formulation. Thus if we wish to predict the vector summation of a series of radiators organised in a one-dimensional array, as for example in Figure 4.6b, then if we consider the electric field vector  $E(\theta)$ , we can write that for  $N$  elements, the summed electric field at some distant observation point P is

$$E(\theta) = A_1 e^{jkx_1 \cos \theta} + A_2 e^{jkx_2 \cos \theta} + \dots + A_N e^{jkx_N \cos \theta} \quad (4.19)$$

Here  $k$  is the free-space wavenumber,  $2\pi/\lambda$ , and  $A_N$  is a complex number representing the relative magnitude and phase of the excitation source applied to the  $N$ th radiating element. Distances  $x_1, x_2, \dots, x_n$ , are referenced from the centre of the array (see also Section 4.6). Hence with this model each element in the array can have arbitrary excitation and phase applied relative to the reference antenna. This equation is used as the basis for the MathCad general array program given in Appendix 8.1, which allows one-dimensional array factors to be calculated with arbitrary relative element excitation and phase applied.

By adjusting the relative phase angles between elements, an array can have its far field pattern scanned in azimuth or in elevation for a one-dimensional array, or in both azimuth and elevation for a two-dimensional array, without any mechanical movement of the position of the antenna. For a linear array, if the phase shift between array elements is allowed to vary progressively from element to element as  $\Delta\alpha$ , then the  $A_N$  weighting coefficients in equation (4.19) become  $A_0 e^{-jn\Delta\alpha}$  for uniform magnitude excitation  $A_0$ . Alternatively, on following the derivation of equation (4.14), the resultant field for  $N$  uniformly spaced elements  $d$  can be written as

$$|E|^2 = A_0^2 \frac{\sin^2[N/2(kd \cos \phi - \Delta\alpha)]}{\sin^2 \frac{1}{2}(kd \cos \phi - \Delta\alpha)} \quad (4.20)$$

from which the maximum far-field strength can be located as

$$\phi_{\max} = \cos^{-1} \left( \frac{\Delta\alpha}{kd} \right) \quad (4.21)$$

Equation (4.21) suggests that as  $\Delta\alpha$  is changed then  $\phi_{\max}$  will change, hence the array will be capable of electronically steering its far-field pattern.

Using the MathCad programme in Appendix 8.1, an example of a beam-scanned array is given in Figure 4.11. Here the array factor for an eight-element array of  $\lambda/2$  spaced isotropic sources is plotted as the progressive phase  $\Delta\alpha$  between adjacent elements is allowed to vary from 0 through  $360^\circ$  in  $30^\circ$  steps. This figure shows that scanning of the main antenna lobe is possible at the expense of the side-lobe responses by virtue of electronic control of the phases applied to the array elements.

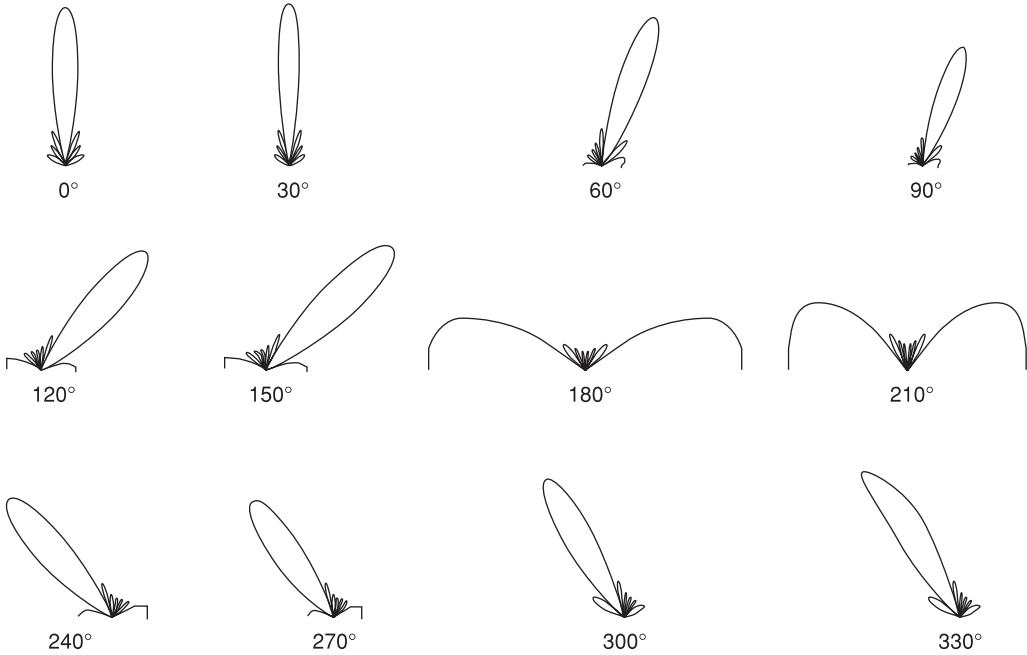


**Figure 4.11** Phased eight-element array of  $\lambda/2$  spaced isotropic elements;  $0^\circ$  to  $360^\circ$  in  $30^\circ$  steps

### Aperture distribution and far-field pattern relationship

Consider the electric field that would be produced by an incrementally small element of an array (Figure 4.12). Here  $OA = z \sin\theta$ , hence  $s = r - z \sin\theta$ .

The field  $dE$  produced by the element arrives later at some distant point P

$$dE = \frac{A}{s} e^{j\omega(t-s/c)} \tag{4.22}$$

Here  $A$  is the amplitude coefficient and  $c$  is the speed of light. Substituting  $s \approx r$  into the denominator and  $s = r - z \sin\theta$  into the exponential term to allow for any induced phase shifts, we get

$$dE = \frac{A}{r} e^{j\omega(t-r/c)} e^{j\omega z \sin\theta/c} \tag{4.23}$$

Assuming the field components by integration over the entire array length,  $a$ , gives the total electric field  $E(\theta)$  at any observation point P and can be written as

$$E(\theta) = \int_{-a/2}^{a/2} \frac{A}{r} e^{j\omega(t-r/c)} e^{j\omega z \sin\theta/c} dz \tag{4.24}$$

and using  $\omega = 2\pi f = 2\pi c/\lambda$  we get

$$E(\theta) = \int_{-a/2}^{a/2} A e^{j2\pi z \sin\theta/\lambda} dz \tag{4.25}$$

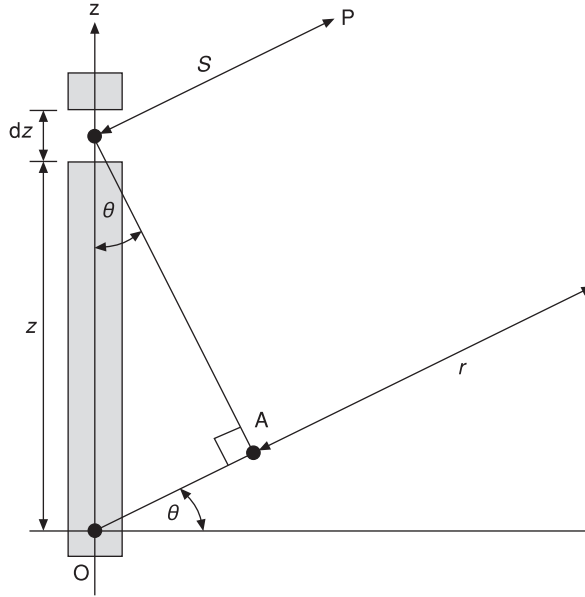


**Figure 4.12** Continuous linear array

For a non-uniform amplitude distribution  $A$  becomes a function of  $z$ , i.e.  $A(z)$ . A non-uniform phase distribution can also be incorporated into  $A$  if required. With the aid of equation (4.25) we can now calculate the far-field radiation pattern for any given aperture distribution. If  $A(z)$  is zero beyond  $-a/2 \leq z \leq +a/2$  then the limits of integration can be extended to  $\pm\infty$  without affecting the result.

$$E(\theta) = \int_{-\infty}^{\infty} A(z) e^{j2\pi z \sin\theta/\lambda} dz \quad (4.26)$$

This has the form of a Fourier integral, which together with its transformation properties is defined in [15]. One of these properties allows the inverse transformation of equation (4.26) to be established as

$$A(z) = \frac{1}{\lambda} \int_{-\infty}^{\infty} E(\theta) e^{-j2\pi z \sin\theta/\lambda} d\theta \quad (4.27)$$

Equation (4.27) allows a desired aperture distribution to be derived from a pre-specified far-field polar diagram.

Using this technique, equation (4.26) shows that for a uniformly excited aperture a  $\sin x/x$  response is obtained. Further investigation reveals that this distribution will always give the highest directivity of any type of aperture distribution [16]. Unfortunately, this aperture profile is accompanied by fairly high side lobes ( $-13$  dB down on the main lobe). Shaping the aperture distribution as shown in Section 4.4 can reduce the side lobe response at the expense of directivity [16]. In practice, since a finite aperture exists some field perturbation will occur if the aperture distribution is not tapered near to the aperture edges.

This technique for far field prediction or aperture distribution synthesis for a pre-specified far-field pattern is also extendable to two-dimensional aperture distributions and is a very powerful design tool for pattern synthesis.

### 4.3 Two-dimensional stacked arrays

Consider now a two-dimensional arrangement of array elements. Assume that these are equally spaced and fed with equi-amplitude co-phased signals (Figure 4.13). In the normal direction to the array, the electric field strength due to a column of  $N$  sources, each excited with equi-strength signals, will be determined according to equation (4.14) as

$$E_R \propto \frac{\sin\left(\frac{N\pi d_1}{\lambda} \sin\theta'\right)}{\sin\left(\frac{\pi d_1}{\lambda} \sin\theta'\right)} \tag{4.28}$$

where  $\sin\theta' = \cos(90 - \theta)$ . Here, for convenience, we have referenced the angle relative to the antenna boresight, i.e. along the  $y$ -direction, where the beam will be formed.

Similarly, for a single row with  $M$  elements

$$E_R \propto \frac{\sin\left(\frac{M\pi d_2}{\lambda} \sin\phi'\right)}{\sin\left(\frac{\pi d_2}{\lambda} \sin\phi'\right)} \tag{4.29}$$

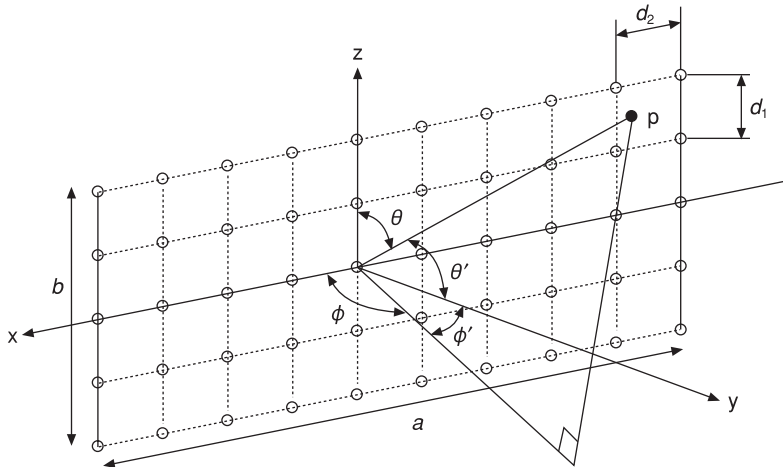
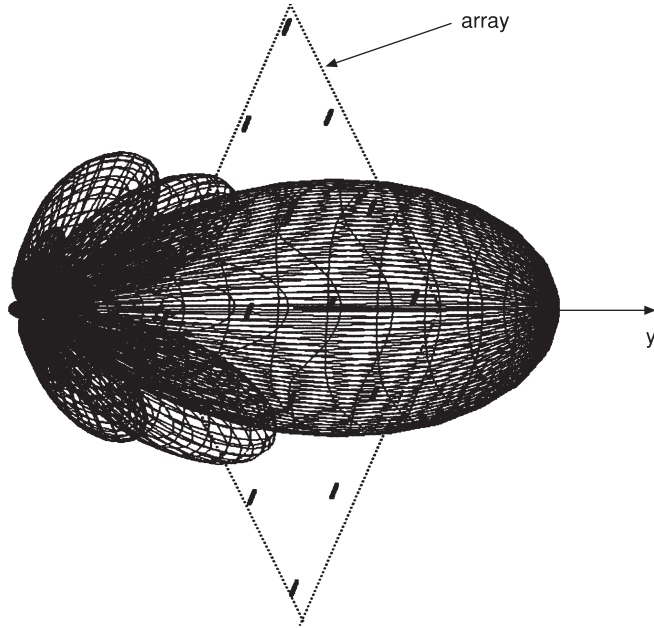


Figure 4.13 Stacked array



**Figure 4.14** Two-dimensional pencil beam

If the maximum radiated field strength is  $E_{\max}$ , then the expression governing the field for the stacked two-dimensional  $M \times N$  array is

$$E_R = E_{\max} \frac{\sin\left(\frac{N\pi d_1}{\lambda} \sin\theta'\right)}{\sin\left(\frac{\pi d_1}{\lambda} \sin\theta'\right)} \frac{\sin\left(\frac{M\pi d_2}{\lambda} \sin\phi'\right)}{\sin\left(\frac{\pi d_2}{\lambda} \sin\phi'\right)}$$

Thus the two-dimensional stacked array case exhibits  $\sin x/x$  responses in both vertical and horizontal directions. Hence, unlike the one-dimensional arrays discussed earlier, which can focus in only one plane, the stacked configuration can focus in two planes, giving rise to a pencil-like beam (Figure 4.14). For this situation, we can find the antenna array directive gain relative to an isotropic source by using the procedure given in Section 2.4.

Hence

$$G = \frac{4\pi E_{\max}^2}{\int_0^{2\pi} \int_0^\pi E^2(\theta, \phi) \cos\theta \, d\theta \, d\phi}$$

If there are many elements in the array, then the antenna aperture dimensions  $a$  and  $b$  will be large, hence the beam produced will be narrow and centred around the  $y$ -direction in Figure 4.13. Under these conditions,  $\sin\phi'$  and  $\sin\theta'$  will become approximately  $\phi'$  and  $\theta'$ , respectively, while  $\cos\theta'$  will tend towards unity; thus

$$E_R = E_{\max}^2 \int_0^{2\pi} \int_0^\pi \frac{\sin^2\left(\frac{\pi b \theta'}{\lambda}\right) \sin^2\left(\frac{\pi a \phi'}{\lambda}\right)}{\left(\frac{\pi b}{\lambda} \theta'\right)^2 \left(\frac{\pi a}{\lambda} \phi'\right)^2} d\theta d\phi \quad (4.30)$$

after noting that in Figure 4.13,  $Nd_1 = b$  and  $Md_2 = a$ .

Now since for a large  $M \times N$  array the beam is highly focused, i.e.  $\theta'$  and  $\phi'$  are small for large  $M$  and  $N$ , then the limits on the integral can be extended to  $\pm \infty$  without affecting the result. This approach leads to an analytical solution for equation (4.30) by noting that

$$\int_{-\infty}^{\infty} \frac{\sin^2 x}{x^2} dx = \pi$$

hence the denominator of the gain expression reduces to  $E_{\max}^2 \lambda^2/ab$ . Therefore

$$G = \frac{4\pi E_{\max}^2 ab}{E_{\max}^2 \lambda^2} = \frac{4\pi ab}{\lambda^2} \quad (4.31)$$

The above expression is valid for a stacked array that is uniformly excited, or for a uniformly illuminated aperture. This is valid for the uniformly illuminated aperture, since by Huygen's principle each point on a wavefront can be considered a source of a secondary spherical wavefront (an isotropic point source; see Section 7.5). These secondary wavefronts combine to form the overall radiation pattern. So a plane wavefront incident upon an aperture, say a rectangular hole in a sheet of metal, will illuminate the aperture and will produce a far-field radiation pattern according to equation (4.30).

Since the two-dimensional stacked array gives rise to a radiation pattern that is focused into a pencil beam in space, this beam can be steered in two dimensions using the techniques of phase control introduced in Section 4.2.

It should be noted that following the approach used in equation (4.19), the array factor for an  $M \times N$  element planar array with isotropic sources positioned on a rectangular grid can be written in a general way as

$$E(\theta, \phi) \propto \sum_{m=1}^M \left[ \sum_{n=1}^N A_{mn} e^{j[(m-1)kd_x \sin\theta \cos\phi + \Delta\alpha_{m,n}]} e^{j[(n-1)kd_y \sin\theta \cos\phi]} \right] \quad (4.32)$$

where  $d_x$  and  $d_y$  refer to isotropic element separations in the x- and y-directions, respectively.

#### 4.4 Non-uniform current excitation array

The uniform co-phased excitation cases discussed previously give greatest gain for a given length, but with this comes the  $\sin x/x$  far-field distribution, with its relatively high-value side lobes; e.g. for a ten-element array with  $0.5\lambda$  wavelength spacing, the first side lobe is approximately  $-13$  dB down on the level of the main beam. Sometimes these side lobes can be a problem, as they may give rise to pick-up from unwanted sources placed within the side-lobe envelope.

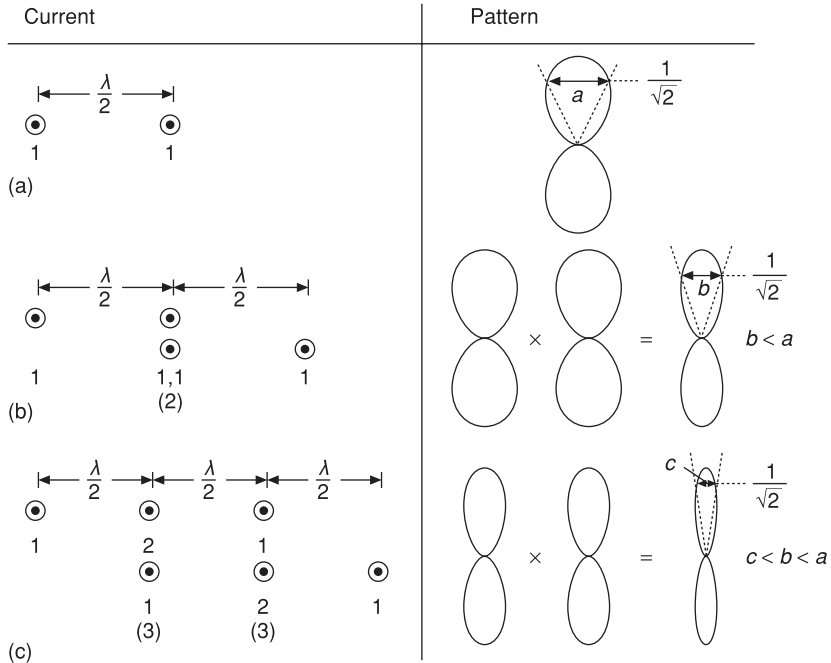


**Figure 4.15** Uniform excitation, binomial array

This figure is based on p. 195 and Figure 7.26 of *Applied Electromagnetism* by L. Shen and J. Kong © 1983. Reprinted with permission of Brooks/Cole, an imprint of the Wadsworth Group, a division of Thomson Learning.

By selecting a current distribution along a linear array that is not uniform, it is possible to modify the side lobe response of the antenna. The result is that while side lobes are reduced so is gain, and at the same time beamwidth is increased. The shape of the resultant far-field pattern is strongly determined by the details of the excitation currents used. In order to see how this works, consider now a two-element array with elements spaced one half wavelength apart and each fed with in-phase currents of equal magnitude; the resulting array pattern is shown in Figure 4.15a. Notice here how no side lobes are present in the array response. If two such arrays are overlapped, the result is shown in Figure 4.15b. Here a tighter beam pattern is exhibited, but still no side lobes are present. These two overlapped arrays are now equivalent to a single three-element array with a 1:2:1 feed current profile.

Continuing, we can overlap two three-element arrays to form a single four-element array with current distribution 1:3:3:1. Again no side lobes are present, and the resulting antenna array (Figure 4.15c) has a higher gain than before. Continuing this process yields the current distribution in Table 4.1 for this type of array. In general, the desired current ratios in the  $r$ th element  $r = 0, 1, 2, \dots$ , from one end of the array are obtained for an array  $N$  half-wavelengths long as the binomial coefficients

$$\frac{N!}{r!(N-r)!}$$

hence the term ‘binomial array’ is used [17].

Array size	Normalised current distribution					
$2 \times 1$	1	1				
$3 \times 1$	1	2	1			
$4 \times 1$	1	3	3	1		
$5 \times 1$	1	4	6	4	1	
$6 \times 1$	1	5	10	10	5	1

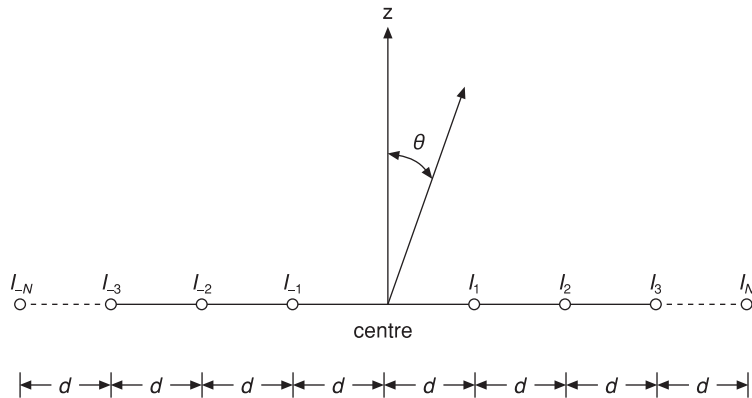


**Figure 4.16**  $2N$  broadside array definitions

For example, consider the development of the normalised current distributions needed for a variety of one-dimensional binomial arrays (Table 4.1). If a  $1 \times 1$  array were to be included in Table 4.1, the resulting coefficients would represent Pascal's triangle.

An array thus fed and consisting of  $\lambda/2$  element separation will exhibit no side lobes and is called a binomial array. Examination of Table 4.1 shows that binomial arrays with  $\lambda/2$  spacing require a large variation in amplitude coefficients. Another feature of this type of antenna is that their beamwidth is greater than that of the uniform or Dolph–Tchebyscheff array, considered next.

Consider now a more complex tapering distribution for the array element excitation current vector; as an example, we will look at the Dolph–Tchebyscheff distribution [18] [19]. An array fed with a current vector obeying this distribution has the property that it will produce the narrowest beamwidth for a given side-lobe level or, conversely, the lowest side-lobe level for a given beamwidth, for a given length of array. Consider Figure 4.16, in which the elements are symmetrically disposed around the centre of the array.

In the design process, the first step is to decide on the number of elements comprising the array, and the second step is to decide on the side-lobe ratio,  $r$ , required, such that

$$r = \frac{\text{main lobe maximum}}{\text{side-lobe level}} \quad (4.33)$$

The far-field radiation pattern,  $E(\theta)$ , can then be defined as

$$E(\theta) = T_{2N-1} \left( K_0 \cos \left( \frac{\pi d}{\lambda} \sin \theta \right) \right) \quad (4.34)$$

where  $T_{2N-1}$  is the Tchebyscheff polynomial order  $2N - 1$ ,  $d$  is the element separation ( $\lambda/2 \leq d < \lambda$ ), and  $K_0$  is defined in terms of the side-lobe ratio  $r$  as [19] [20]

$$K_0 = \cosh \left[ \frac{1}{2N-1} \cosh^{-1}(r) \right] \quad (4.35)$$

In order to compute  $T_{2N-1}(\cdot)$ , we use

$$T_{2N-1} \left( K_0 \cos \frac{\pi d}{\lambda} \sin \theta \right) = \begin{cases} \cos \left[ (2N-1) \cos^{-1} \left( K_0 \cos \frac{\pi d}{\lambda} \sin \theta \right) \right] & \left| K_0 \cos \frac{\pi d}{\lambda} \sin \theta \right| \leq 1 \\ \cosh \left[ (2N-1) \cosh^{-1} \left( K_0 \cos \frac{\pi d}{\lambda} \sin \theta \right) \right] & \left| K_0 \cos \frac{\pi d}{\lambda} \sin \theta \right| > 1 \end{cases} \quad (4.36)$$

The angles where the side-lobe response goes to zero,  $\theta_{k_0}$ , can be found as

$$\theta_{k_0} = \sin^{-1} \left[ \frac{\lambda}{\pi d} \cos^{-1} \left[ \frac{1}{K_0} \cos \frac{(2k-1)\pi}{2(2N-1)} \right] \right] \quad (4.37)$$

$$k = 1, 2, 3, \dots, N$$

The half-power beamwidth angle,  $\theta_{3dB}$ , is given as

$$\theta_{3dB} = \sin^{-1} \left[ \frac{\lambda}{\pi d} \cos^{-1} \left[ \frac{1}{K_0} \cosh \left( \frac{1}{2N-1} \cosh^{-1} \frac{r}{\sqrt{2}} \right) \right] \right] \quad (4.38)$$

As an example, for a four-element array the required excitation current vector is

$$I_{-2} = I_2 = K_0^3$$

$$I_{-1} = I_1 = 3I_2 - 3K_0$$

For a given ripple,  $K_0$  can be computed from equation (4.35) and the actual required current ratios found. For a given length of array greater than five wavelengths long and given side-lobe ratio, the half-power beamwidth 3 dB can be found from [4.5] and [4.6] as

$$\theta_{3dB} = \frac{K\lambda}{\ell} \quad (4.39)$$

where  $K$  is a function of side-lobe level  $r$  and is given in Table 4.2. The relationship in equation (4.39) applies for arrays of length greater than five wavelengths with element spacings between  $\lambda/2$  and  $\lambda$ .

Note: Figure 4.16 and equations (4.33) through (4.39) are based on H. Jasik (ed.), *Antenna Engineering Handbook*, 1st Edition, copyright © 1961 by McGraw-Hill Book Company, Inc. Reproduced with permission of the McGraw-Hill Companies.

**Table 4.2** Dolph–Tchebyscheff array coefficients

$r$ dB	$K$ rads
-20	0.89
-30	1.06
-40	1.18

## 4.5 Antenna input impedance

The bandwidth of an antenna will be governed primarily by operational requirements; for example, the modification of antenna radiation pattern with frequency resulting in gain modification or side-lobe response may be the dominant features that determine the operating bandwidth of the system. On the other hand, the antenna input impedance presented to a load or generator may be the main constraining feature; for example, for short antenna structures, i.e. less than half a wavelength, the limiting factor is variation in input impedance, while for end-fire antennas modification of radiation pattern with frequency is a primary issue.

A unique definition for the bandwidth of an antenna does not exist; for example, if antenna bandwidth in relation to its impedance characteristics is the main issue, then the objective is to minimise, over a range of frequencies, the voltage standing wave ratio (see Section 6.1) on the feed line connected to the antenna.

In general, the antenna input impedance will consist of a real part, normally assumed to be constant but which can vary over the frequency range of interest, and an imaginary part, whose value will vary with frequency. Consider a half-wavelength dipole antenna at resonance: input reactance is zero, and the current at its input terminals is in phase with the applied terminal voltage. In a little bit more detail, a resonance current applied to the centrally placed terminals of a half-wavelength dipole travels out one quarter wavelength ( $90^\circ$ ) to the open-circuited end of the antenna, where it undergoes a  $180^\circ$  phase reversal. The current then changes direction and propagates back  $90^\circ$ , until it reaches the antenna's terminals. Thus the total round trip for the current is  $360^\circ$ . During the time for this to occur, the excitation voltage at the terminals has also undergone a  $360^\circ$  phase change, so at the antenna terminals the current and voltage are in phase, and the load (the antenna) as seen by the generator appears as a resistance. If the antenna is made shorter than its resonant length, then following the logic above the reflected current arrives back at the terminals of the antenna earlier (since the round trip is shorter) than it would have done in the resonant case. Thus the current at the antenna terminals is phase-advanced with respect to the terminal voltage and the antenna appears, in addition to its resistive component, to have a capacitive reactive input component. If the antenna is longer than its resonant length, a phase lag between current and voltage occurs, and there is an inductive reactive antenna terminal component. An antenna designed to operate at resonance at a specific frequency will exhibit capacitive terminal reactance if the antenna is operated at frequencies below resonance (the antenna appears electrically shorter than its resonant electrical length, since the operating wavelength is longer) and inductive if the antenna is operated at frequencies above resonance (the antenna appears electrically longer than its resonant electrical length).

In such situations, it is useful to be able to determine what bandwidth can be achieved such that a given maximum tolerable voltage standing wave ratio (VSWR) can be adhered to or, vice versa, what minimum VSWR can be achieved for a given operating bandwidth.

Theoretical work [21] shows that the condition for maximum bandwidth occurs when the reflection coefficient presented by the antenna to be matched remains as uniform as possible. In practice this is not the case, so that less than optimum bandwidth realisation occurs. For an antenna with a high  $Q$  factor and large reactance variation, only a poor broadband impedance match can be realised. On the other hand, a low  $Q$  antenna can be matched with relative ease. For a parallel RC load with  $Q$  factor,  $Q_1$ , the magnitude of the minimum reflection coefficient magnitude  $|\Gamma_{\min}|$  is given by Fano's limit equation [21] as

$$|\Gamma_{\min}| = \exp(-\pi Q_2/Q_1) \quad (4.40)$$

where  $Q_1 = RC\omega_0 = 2\pi f_0$ ,  $Q_2 = f_0/\text{bandwidth}$ , and  $f_0$  is the centre frequency of operation for the antenna.

More generally, the input impedance at the antenna terminals can be represented at a spot frequency as a series LCR circuit giving at resonance an antenna input impedance that is purely real [22]. The input impedance for such an antenna equivalent circuit is

$$Z_{\text{in}} = R + j\left(\omega L - \frac{1}{\omega C}\right) \quad (4.41)$$

which for small frequency deviations from the resonant conditions,  $\delta\omega$ , yields using  $\omega = \omega_0(1 + \delta)$  and  $(1 + \delta)^{-1} \approx (1 - \delta)$  for small  $\delta$ .

Note: The treatment given here in equations (4.41) to (4.56) is based on p. 382 and pp. 387–8 of E.C. Jordan and K.G. Balmain, *Electromagnetic Waves and Radiating Systems*, 2nd edition, Prentice-Hall, 1968.

$$\delta Z = j(\delta\omega L + \delta\omega/\omega^2 C) \quad (4.42)$$

Hence the normalised change in input impedance relative to the resonant condition is

$$\frac{\delta Z}{R} = j\left(\frac{\delta\omega L}{R} + \frac{\delta\omega}{R\omega^2 C}\right) \quad (4.43)$$

or in terms of  $Q$  factor defined below as

$$Q = \frac{\omega_0(\text{energy stored in circuit})}{\text{average power loss}} = \frac{\omega_0\left(\frac{1}{2}I^2L\right)}{\left(\frac{1}{2}I^2R\right)} = \omega_0 \frac{L}{R} \text{ or } \frac{1}{\omega_0 RC}$$

Equation (4.43) becomes

$$\frac{\delta Z}{R} = j\left(\frac{Q\delta\omega}{\omega_0} + \frac{Q\delta\omega}{\omega_0}\right) = j2\frac{Q}{\omega_0}\delta\omega \quad (4.44)$$

which near resonance yields

$$\frac{\delta\omega}{\omega_0} = \frac{1}{2Q} \left| \frac{\delta Z}{R} \right| \quad (4.45)$$

Note here that when  $\delta Z = R$ , the power absorbed by the antenna reduces to one-half of its value at resonance. Thus the angular frequency difference at the half-power points  $\Delta\omega$  is

$$\Delta\omega = 2\delta\omega = \frac{\omega_0}{Q} \quad (4.46)$$

giving us a definition for relative bandwidth:

$$\frac{\Delta\omega}{\omega_0} = \frac{1}{Q} \quad (4.47)$$

In practice, for a real antenna  $R$ ,  $L$  and  $C$  vary with frequency, thus the simple  $LCR$  model above and the definitions based upon it are approximate.

We now need to find a method for evaluating  $L$ ,  $C$  and  $R$ . For low-loss uniform transmission lines (Section 6.1) we know that

$$Q = \frac{\omega L}{R} \quad (4.48)$$

$$Z_0 = \sqrt{\frac{L}{C}} \quad (4.49)$$

and

$$v = 1/\sqrt{LC} \quad (4.50)$$

where  $R$ ,  $L$  and  $C$  are the per unit length quantities defining transmission line resistance, inductance and capacitance, respectively, and  $Z_0$  and  $v$  are the line characteristic impedance and phase velocity, respectively.

From Section 6.6, for a resonant quarter-wavelength line that is open-circuited at one end, the input impedance is a resistance of value  $R_{in}$

$$R_{in} = \frac{R\lambda}{8} \quad (4.51)$$

and is equal to the radiation resistance of the  $LCR$  lumped equivalent circuit for the antenna.

Hence, since  $Q = \omega_0 L/R$ , then

$$QR = \omega_0 L = \frac{R\lambda}{8} \frac{2\pi Z_0}{\lambda R} = \frac{\pi Z_0}{4}$$

Also, since  $Q = 1/\omega_0 RC$ , then

$$\omega_0 C = \frac{4}{\pi Z_0}$$

Thus

$$L = \frac{Z_0}{8f_0} \quad (4.52)$$

$$C = \frac{2}{\pi^2 f_0 Z_0} \quad (4.53)$$

$$Q = \frac{\pi Z_0}{4R} \quad (4.54)$$

Here  $Z_0$  can be interpreted as the ‘average’ characteristic impedance, which for a centre-fed dipole of length  $\ell/2$  in free space [23] is defined as

$$Z_{0_{\text{avg}}} = \frac{2}{\ell} \int_0^{\ell/2} Z_0(r) dr \quad (4.55)$$

and is approximately equal [15] [22] to

$$Z_{0_{\text{avg}}} \approx 120 \left[ \ln\left(\frac{\ell}{a}\right) - 1 \right] \quad (4.56)$$

where  $a$  is the radius of the wire forming the dipole, and  $\ln$  denotes the natural logarithm.

It should also be noted that when the antenna is matched to a generator the total  $Q$ , i.e. the loaded  $Q$ , of the system is 0.5 times the unloaded  $Q$ . Thus in any calculations involving bandwidth the loaded  $Q$  factor should be used.

The real and imaginary components of the electric field component acting along the length of a linear dipole can be used to establish a more complete representation of the input or self-impedance of the antenna [24]. The mutual coupling impedances between antenna elements can be found by using the induced-emf method. For example, the mutual impedance between two antennas is given as (Section 4.6)

$$Z_{21} = \frac{V_{21}}{I_1(0)} \quad (4.57)$$

where  $I_1(0)$  is the current fed into the terminals of antenna 1, and the open-circuit voltage induced on the terminals of antenna 2,  $V_{21}$ , is defined as

$$V_{21} = -\frac{1}{I_2(0)} \int_0^{\ell_2} E_{z_{21}} I_2(z) dz \quad (4.58)$$

where  $I_2(z)$  is the current distribution along the second antenna, and  $E_{z_{21}}$  is the electric field along the axial direction of antenna 2 induced by antenna 1. Hence  $Z_{21}$  can be calculated from equation (4.57).

## 4.6 Induced-emf method and mutual coupling

In the array work reported so far in this chapter, we have ignored the effect that antenna elements have on each other. Mutual coupling effects between antenna elements will induce currents on adjacent and non-adjacent elements, which may result in the array

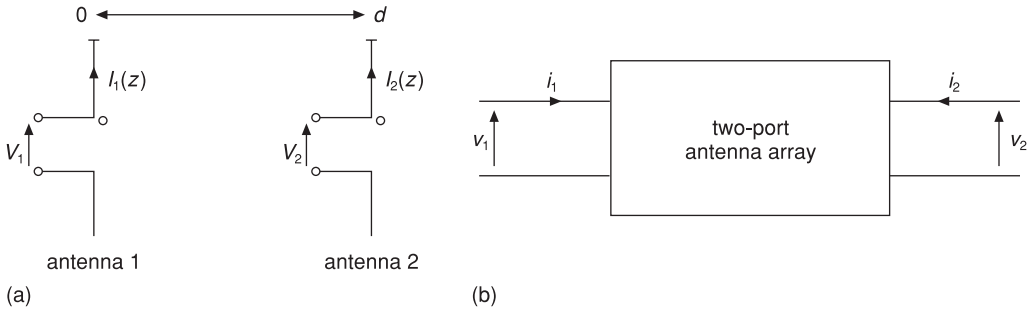


**Figure 4.17** (a) Mutually coupled antennas; (b) two-port Z-parameter mutual coupling model

far-field pattern being altered compared with the ideal situation, where no mutual coupling is included. With the induced-emf approach, the electric field produced in an antenna due to a known, or guessed, current distribution is used to calculate the voltage induced in each elemental section of the antenna. The reciprocity theorem (see Appendix 8.2) is then used to establish the voltage at the driving terminals of the antenna. This method, called the induced-emf method, is very important as it can be used to determine antenna radiation resistance, the mutual impedance between antenna elements or the self-reactance of a single antenna. The treatment of the induced-emf method and mutual coupling given here is based on [22].

Consider now how the technique is developed in order to compute mutual impedance between the two antennas separated by distance,  $d$ , as shown in Figure 4.17a. Here the antennas are assumed to be aligned along the  $z$ -axis. By definition (Figure 4.17b), the mutual impedance between elements (1) and (2) is [22]

$$Z_{21} = \frac{V_{21}}{I_1(0)} \quad (4.59)$$

Here,  $V_{21}$  is the open-circuit voltage at the terminals of antenna 2 due to the current introduced at the terminals of antenna 1, i.e. at position  $d = 0$  in Figure 4.17a.

Consider now the effect of a voltage  $V_1$  applied at the terminals of antenna 1 in order to produce a current  $I_1(0) = V_1/Z_{11}$  at the terminals of antenna 1 and current distribution  $I(z)$  along its length. Essentially, we are using antenna 1 as a transmitter. Here  $Z_{11}$  is the antenna impedance measured at the terminals of antenna 1.

If antenna 1 had voltage source  $V_1$  removed and was instead illuminated by an electromagnetic wave,  $E_z$ , a voltage,  $E_z dz$ , would be induced over a short length  $dz$  of the antenna at position  $z$  from the antenna terminals, i.e. here antenna 1 is used as a receiver. The induced voltage could then be represented by an ideal voltage generator placed in series with the element at that position. If the antenna terminals were short-circuited, then this voltage source would produce a current,  $dI_{sc}$ , across the shorting link (Figure 4.18).

In addition, the reciprocity theorem suggests that for equal terminating impedance values,  $Z_{12} = Z_{21}$  (see Appendix 8.2). Thus from Figure 4.17b and using Figure 4.18

$$V_1 = Z_{11} I_1 + Z_{12} I_2 \quad (4.60)$$

$$V_2 = Z_{21} I_1 + Z_{22} I_2 \quad (4.61)$$

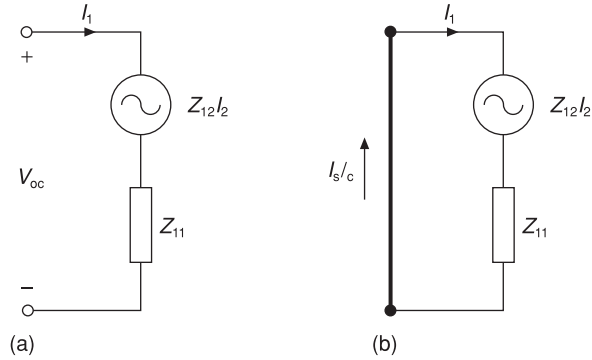


**Figure 4.18** Receive antenna equivalent circuits: (a) open-circuit terminals; (b) short-circuit terminals

and noting that when antenna 2 terminals are short-circuited,  $Z_{22} = 0$

$$V_2 = Z_{21} I_1 \quad (4.62)$$

and with antenna 1 terminals short-circuited,  $Z_{11} = 0$

$$V_1 = Z_{12} I_2 \quad (4.63)$$

thus

$$\frac{V_2}{V_1} = \frac{I_1}{I_2} \text{ or } V_2 I_2 = V_1 I_1 \quad (4.64)$$

By analogy with the reciprocity relationship

$$V_2 = E_z dz$$

$$I_2 = I(z)$$

$$I_1 = dI_{sc}$$

and denoting  $V_1 = V$  we get from equation (4.64)

$$E_z dz I(z) = V dI_{sc}$$

thus

$$dI_{sc} = \frac{E_z dz I(z)}{V} \quad (4.65)$$

Therefore the total short-circuit current is found by integrating over the entire length of the antenna:

$$I_{sc} = \frac{1}{V} \int E_z I(z) dz \quad (4.66)$$

If the short-circuit current is known, then the open-circuit voltage at the antenna terminals can be found by application of Thevenin's theorem, which states that

$$V_{oc} = -I_{sc} Z \quad (4.67)$$

Here a minus sign is included to keep the sign convention of current flow from high potential to low potential (c.f. Figure 4.17a and b). Combining equations (4.66) and (4.67) gives

$$V_{oc} = -\frac{Z}{V} \int E_z I(z) dz \quad (4.68)$$

hence

$$V_{oc} = -\frac{1}{I(0)} \int E_z I(z) dz \quad (4.69)$$

If the incident field strength is uniform along the length of the antenna, as it is for plane wave illumination, then  $E_z$  can be removed to outside the integral.

Returning now to the original situation given in equation (4.59), where

$$Z_{21} = \frac{V_{21}}{I_1(0)} \quad (4.70)$$

Where  $V_{21}$  is the open-circuit voltage at the terminals of antenna 2 produced as a result of current  $I_1(0)$  introduced into antenna 1 (see Figure 4.17).

We can now use the results derived in equation (4.69) to get an expression for  $V_{21}$  [22]:

$$V_{21} = -\frac{1}{I_2(0)} \int E_{z_{21}} I_2(z) dz \quad (4.71)$$

Where  $E_{z_{21}}$  is the component of the electric field incident on antenna 2 as result of a sinusoidal current applied at antenna 1. Thus, using equation (4.70), we can write

$$Z_{21} = -\frac{1}{I_1(0)I_2(0)} \int E_{z_{21}} I_2(z) dz \quad (4.72)$$

In order to find radiation resistance,  $R_{rad}$  by this method, we note that by allowing two identical antennas with the same spacial orientation to have zero separation then  $V_{21}$  becomes the voltage at the terminals of antenna 1 due to the current applied at  $I_1(0)$ . The zero separation criterion here means that the theoretical treatment is strictly valid only for dipoles that have an infinitesimally small diameter.

Therefore the self-impedance of an antenna of length  $\ell$  is equivalent to the mutual impedance between two identical antennas of length  $\ell$  when their separation is set equal to zero. Hence, using equation (4.72)

$$Z_{21} = -\frac{1}{I_{12}(0)} \int E_z I(z) dz \quad (4.73)$$

from which the radiation resistance,  $R_{rad}$ , can be found as real ( $Z_{21}$ ), since for zero separation distance  $V_{21}$ , the open-circuit voltage at antenna 2 due to a current  $I_1(0)$  at antenna 1, becomes the open-circuit voltage of antenna 1; hence  $Z_{21}$  becomes the self-impedance of antenna 1. Using this technique to find antenna input reactance requires special consideration, as does its application to finite-diameter dipoles; reference [22] gives more detail on these aspects.

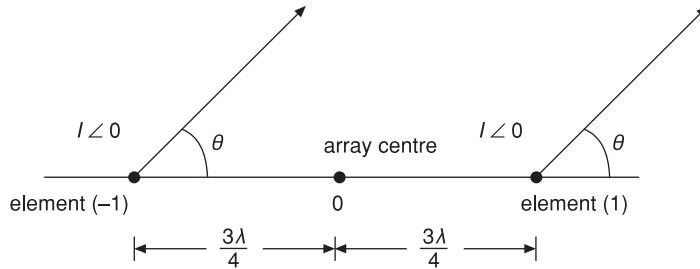


Figure 4.19 Mutual coupling example

It should be noted that the reactance of a dipole antenna calculated using this approach will be infinite except in cases where the dipole half length is  $(2n + 1)\lambda/4$ ,  $n = 0, 1, 2, \dots$ . To see how mutual coupling affects array behaviour, consider now two half-wave dipole antennas placed in a linear array (Figure 4.19) separated by  $3\lambda/2$  and fed with equal in-phase currents.

#### Exercise 4.4

Calculate the effect on the gain of a two-element array when mutual coupling between antennas is included. Assume that the input impedance of each element is  $73 \Omega$  and that the impedance between elements is  $-25 + 5j \Omega$ .

#### Solution

For this arrangement, the resultant electric field (after equation 4.19) with  $\lambda$  set equal to  $2\pi$  is

$$\begin{aligned} E_r &= E[e^{j3\pi/2} \cos\theta + e^{-j3\pi/2} \cos\theta] \\ &= 2E \cos\left[\frac{3\pi}{2} \cos\theta\right] \end{aligned}$$

since relative to position 0 in Figure 4.19, i.e. the array centre, the phase lag of the radiation at element 1 relative to element -1 is

$$\frac{2\pi}{\lambda} \frac{3\lambda}{4} \cos\theta$$

If  $v_1, i_1, v_2, i_2$  are the terminal voltages and currents at elements 1 and 2, respectively, then

$$v_1 = 73i_1 + (-25 + j5)i_2$$

$$v_2 = (-25 + j5)i_1 + 73i_2$$

but we have stated that  $i_1 = i_2 = I(0)$  i.e., in-phase current excitation, therefore we can write

$$v_2 = v_1 = 48 + j5$$

Thus if the power input to elements 1 and 2 are  $P_1$  and  $P_2$ , respectively, then

$$\begin{aligned} P_1 = P_2 &= 1/2 [v_1 I^* + v_1 I] \\ &= 1/2 |I|^2 [(48 + j5) + (48 - j5)] \\ &= |I|^2 48 \end{aligned}$$

$$\therefore \text{Total power } P_t = 96 |I|^2$$

If we say that (see Section 3.3) a reference dipole will radiate

$$P_t = |I_{\text{ref}}|^2 73$$

hence the field  $E$  at distance  $r$  from the reference dipole must be scaled as

$$E \frac{|I_{\text{ref}}|}{|I|} = \sqrt{\frac{96}{73}} E = 1.147E$$

giving the field strength of the array relative to the reference dipole (see Section 4.1) as

$$\frac{2E \left[ \cos\left(\frac{3\pi}{2} \cos\theta\right) \right]}{1.147E}$$

or 4.83 dB at  $\theta = 90^\circ$

Thus relative to the case where no mutual coupling between elements exists, the maximum gain has increased from 3 to 4.83 dB.

In the above example, the mutual impedance term here has acted to increase the gain of the array. This effect occurs because each dipole induces a voltage in the other by virtue of coupled free-space radiation. This manifests itself as an extra impedance in the source exciting the dipole. When both dipoles are excited by equiphase currents, this added impedance is the same for each dipole and the real part of  $Z_{12}$  is negative, indicating that an increase in current from the excitation source is required. This in turn gives rise to a stronger radiated field relative to the case where zero mutual coupling existed.

#### Exercise 4.5

Calculate the half-power beamwidth for the arrangement in exercise 4.4.

#### Solution

The half-power beamwidth can be obtained as

$$\begin{aligned} \cos\left(\frac{3\pi}{2} \cos\theta\right) &= \pm \sqrt{\frac{1}{2}} \\ \cos\theta &= \pm \frac{1}{6}, \pm \frac{1}{2}, \pm \frac{5}{6}, \pm \frac{7}{6} \end{aligned}$$

or

$$\theta = \cos^{-1}\left(\frac{\pm N}{6}\right) \quad N = 1, 3, 5, 7$$

the smallest  $\theta = \cos^{-1}(\pm 1/6)$  defines the half-power point for the main lobes as  $99.6 - 80.4 = 19.2^\circ$

---

#### Exercise 4.6

Calculate the array factor for the arrangement in exercise 4.4.

#### Solution

The array factor can be calculated as

$$\left| \frac{E_R}{E_{\text{ref}}} \right| = 1.74 \cos \left\{ \frac{3\pi}{4} \cos \theta \right\}$$


---

It should be noted that in the example given above the element spacing selected was  $3\lambda/2$ . As a general rule, in a uniform linear array once the spacing between elements exceeds  $\lambda$ , side lobes whose amplitude are equal to those of the main lobe appear in the spatial response of the antenna. This effect occurs because the element spacing can become large enough to allow in-phase radiation combination from each of the elements in more than one direction.

These lobes are called grating lobes and are normally undesirable, since they lead to a reduction in the gain of the array along the principle angle of operation and can make the array subject to influence by off-boresight interference signals by virtue of signal pick-up via the grating lobe response.

### 4.7 End-fire array example with mutual coupling

#### Exercise 4.7

Consider two centre-fed half-wavelength dipole antennas arranged to form a two-element end-fire array. The element separation is one-quarter wavelength, and the elements are supplied with phase quadrature equal power signals (Figure 4.20; see also Figure 4.17a). For this arrangement, we wish to find the ratio of the currents at the input terminals of the antennas – the gain of the array.

Assume that the self-impedance of each dipole is  $73 \Omega$  and that the mutual impedance between dipoles is  $40 - j30 \Omega$ , in practice, this can be measured or calculated (Section 4.6).

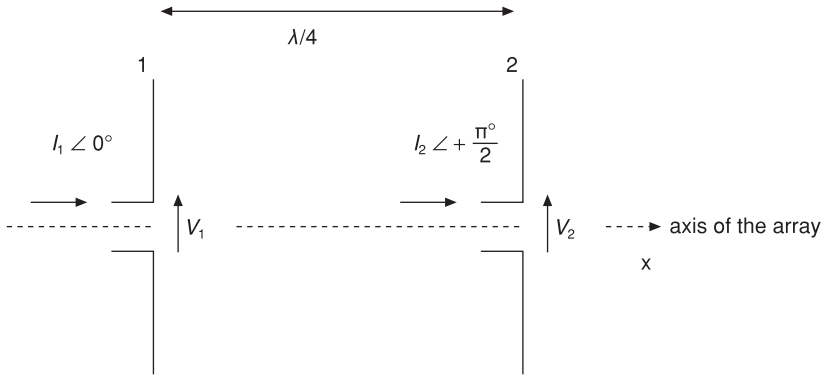


Figure 4.20 End-fire array

**Solution**

First we find the driving-point impedance of antenna 1 (Figure 4.20):

$$Z_1 = \frac{V_1}{I_1} = Z_{11} + Z_{12} \frac{I_2}{I_1} \quad (4.74)$$

$$Z_1 = 73 + j(40 - j30) \frac{I_2}{I_1}$$

$$\text{Let } \frac{I_2}{I_1} = k' \quad (4.75)$$

$$\therefore Z_1 = (73 + 30k') + j40k'$$

Next we find the driving point impedance of antenna 2

$$\begin{aligned} Z_2 &= \frac{V_2}{I_2} = Z_{22} + Z_{12} \frac{I_1}{I_2} \\ &= \left( 73 - \frac{30}{k'} \right) - j \frac{40}{k'} \end{aligned} \quad (4.76)$$

Then we find the power radiated by antenna 1 and 2, respectively:

$$P_1 = |I_1|^2 \text{Re}(Z_1) = |I_1|^2 (73 + 30k') \quad (4.77)$$

and

$$P_2 = |I_2|^2 \text{Re}(Z_2) = |I_2|^2 \left( 73 - \frac{30}{k'} \right) \quad (4.78)$$

But we have the stipulation that  $P_1 = P_2$ , hence

$$|I_1|^2 (73 + 30k') = |I_2|^2 \left( 73 - \frac{30}{k'} \right)$$

or

$$73(k')^2 - 60k - 73 = 0$$

thus

$$k' = \left( \frac{60}{73} + \sqrt{\left(\frac{60}{73}\right)^2 + 4} \right) / 2 = 1.49$$

$$\therefore \frac{I_2}{I_1} = 1.49 \quad (4.79)$$

We can now calculate gain relative to a  $\lambda/2$  dipole. We can do this by assuming that we have a  $\lambda/2$  dipole radiating the same power as the array:

$$\begin{aligned} (P_1 + P_2) &= 2P_1 \text{ (remember equal power levels)} \\ &= 2|I_1|^2 R_c(Z_1) \\ &= 2|I_1|^2 (73 + 30(1.49)) \\ &= 235|I_1|^2 \end{aligned} \quad (4.80)$$

Therefore we can say that for a reference dipole with  $(73 \Omega + j0)$  self-impedance:

$$73|I|_{\text{dipole}}^2 = 235|I_1|^2$$

hence

$$|I|_{\text{dipole}} = 1.8|I_1|$$

For the reference dipole, the maximum far-field radiated signal will be proportional to  $1.8|I_1|$ , while for the array the maximum far-field radiated signal will be proportional to

$$(1 + 1.49)|I_1| \quad (4.81)$$

Hence the gain of the array relative to a half-wave dipole will be

$$20 \log_{10} \left( \frac{2.5}{1.8} \right) = 2.85 \text{ dB}$$

### Exercise 4.8

For an antenna radiating preferentially into one-half space, we can define the front-to-back ratio as the ratio of the far-field strength along the array axis in the positive forward half space and negative reverse half space. Calculate the front-to-back ratio for the parameters given in exercise 4.4.

### Solution

The front-to-back ratio is defined as the ratio of the far-field strength along the array axis in the positive and negative directions; therefore, after equation (4.81), the front-to-back ratio =  $20 \log_{10}(2.49/0.49) = 14.1 \text{ dB}$ , where the minimum field strength is proportional to  $|I_1|(1.49 - 1)$ . Here, since the antenna elements are operated in phase

quadrature, with quarter-wavelength separation, radiation is cancelled along the end-fire direction since waves travelling from right to left will destructively reinforce, while waves moving from left to right constructively reinforce.

With no mutual coupling

$$Z_1 = \frac{V_1}{I_1} = Z_{11} = 73 \Omega$$

$$Z_2 = \frac{V_2}{I_2} = Z_{22} = 73 \Omega$$

Power radiated by antennas 1 and 2, respectively, is

$$P_1 = |I_1|^2 73 \text{ W}$$

$$P_2 = |I_2|^2 73 \text{ W}$$

$$P_1 = P_2 \therefore |I_1| = |I_2|$$

Hence by comparison with equation (4.79), one effect of mutual coupling is to unbalance the magnitudes of the feed currents.

Now  $(P_1 + P_2) = 2P_1 = 2|I_1|^2 73 \text{ W}$ , and for the reference dipole

$$|I|_{\text{dipole}}^2 73 = 146 |I_1|^2 \text{ W}$$

$$\therefore |I|_{\text{dipole}} = \sqrt{2} |I_1| \text{ A}$$

Hence the gain of the array relative to a half-wave dipole will be

$$20 \log_{10} \left( \frac{2}{\sqrt{2}} \right) = 3 \text{ dB}$$

Here the effect of the mutual impedance between array elements has been to reduce gain to 2.85 dB.

#### Exercise 4.9

Compute the front-to-back ratio for the ideal case, i.e. zero mutual coupling between antennas.

#### Solution

The front-to-back ratio for the case with no mutual coupling is

$$20 \log_{10} \left( \frac{2}{0} \right) = \infty \text{ dB}$$

i.e. perfect operation with no end-fire radiation; hence mutual coupling reduces the front-to-back ratio. The polar plots for this antenna arrangement with no mutual coupling included are given in Figure 4.21.

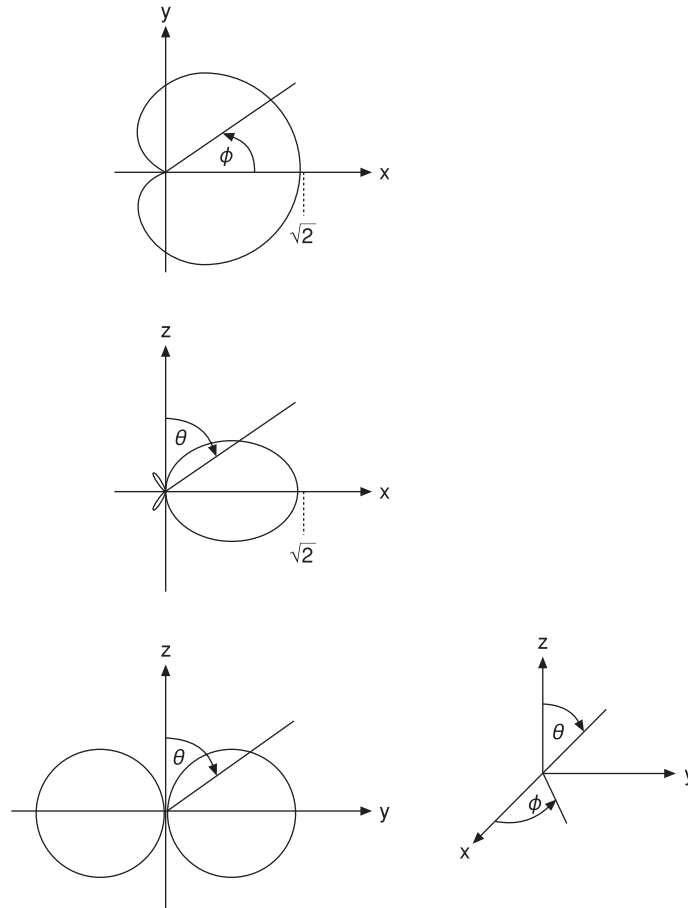


**Figure 4.21** Polar plots for two centre-fed half-wave dipoles forming a two-element end-fire array

#### 4.8 Dipole antennas in relation to a ground plane

If a perfectly conducting flat ground plane is introduced symmetrically into the equatorial plane of a dipole antenna, i.e. normal to the antenna axis, it would automatically be arranged that the electric field pattern associated with the dipole would remain unaffected by the presence of the ground plane. To see why this is so, consider Figure 4.22.

As can be seen from the figure, at some fixed instant the charge distribution on the antenna results in electric field lines running continuously from a positive charge to a negative charge (Figure 4.22a). If a perfect ground plane is introduced, then the electric field lines travel from the positive charge region to the ground plane and from the ground plane to the negative charge regions (Figure 4.22b). Thus the lines of flux terminate on charges on the conducting plane. As the field moves outwards and away

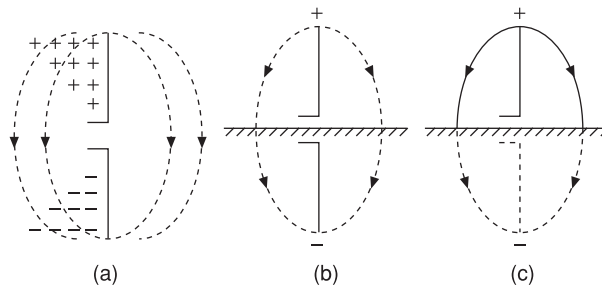


**Figure 4.22** Grounded vertical dipole  $E$ -field distributions

from the antenna, currents will be induced on the plane. The electric field lines intersect the ground plane, assumed here to be lossless, at right angles. Thus, as shown in Figure 4.22c, the part of the dipole below the conducting plane can be removed without affecting the fields above the plane. Hence a vertical dipole of length  $\ell$  placed above a perfectly conducting ground plane will have a field distribution equivalent to that which it would have had if it had been operating as an antenna of twice this length, i.e.  $2\ell$ , operated into free space.

When so arranged, the dipole antenna can be replaced by a single antenna mounted vertically normal to the ground plane (Figure 4.22c). In this configuration, the antenna is referred to as a unipole or monopole. Since this antenna is only half the length of its dipole equivalent, it will radiate only half of the total radiated power produced by the dipole. Due to this effect, its radiation resistance is only one-half of that of its equivalent dipole,  $36.5 \Omega$ . Extending this argument further, the power gain of a unipole antenna relative to an isotropic source is twice that of a centre-fed dipole antenna for the same amount of input power.

As previously discussed, continuity of the electric field lines must exist for a dipole antenna placed over a perfectly conducting ground plane. Let us now consider this in a little bit more detail (Figure 4.23). Here in each case the physical dipole above the ground plane has a mirror image below the ground plane placed here in the  $x$ - $y$  plane. Thus this arrangement means that the single dipole will behave as though it were a two-element array.

In Figure 4.23a and b, the dipole and its image are in phase, so they will act constructively to reinforce the radiated signal. In Figure 4.23c, the vertical components of the excitation current cause fields that can reinforce, while the horizontal components cancel. Finally, in Figure 4.23d, the currents are entirely horizontally disposed, and the resulting fields can act destructively upon each other, for example if the height of the horizontal dipole above the ground plane is small or close to one wavelength separation. If the horizontal dipole is placed at  $0.25\lambda$  above the ground plane, then the image dipole will act in ways to reinforce the broadside radiation of the virtual array in a similar fashion to the action of the end-fire array described in Section 4.2.

Consider the case in Figure 4.23b, where the antenna, assumed here to be an isotropic source, and its image are excited with in-phase currents. Figure 4.24 shows how the resultant field is formed at some far-field observation point P. Here, from Figure 4.24a

$$AC = 2h \cos\theta \text{ metres} = \frac{2h}{\lambda} \cos\theta \text{ wavelengths}$$

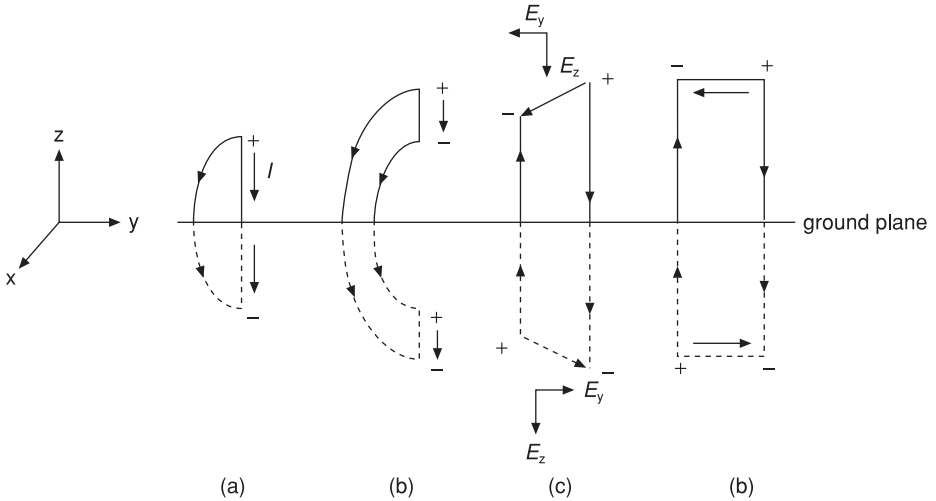


Figure 4.23 Dipole antennas above a conducting ground plane

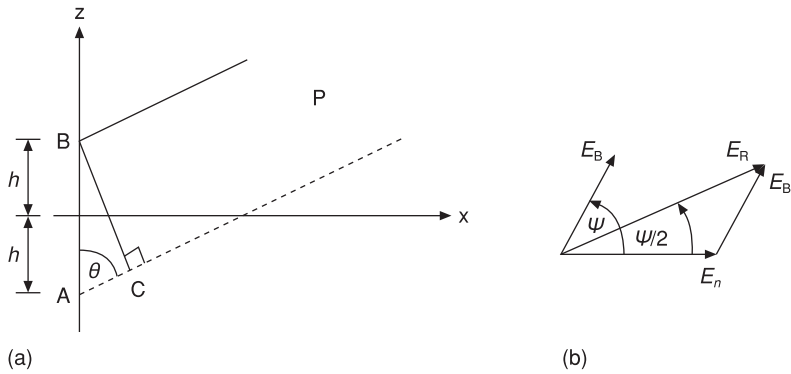


Figure 4.24 Array factor for in-phase source and image

or in terms of radians the phase delay between the field at A and the field at B is

$$\psi = \frac{2\pi(2h)}{\lambda} \cos\theta \text{ radians}$$

The resultant field from the source at B and the image at A is  $E_R$  and is found by vector addition, noting that in this case  $E_A = E_B$ . We can write

$$E_R = 2E_A \cos(\psi/2) = 2E_A \cos\left(\frac{2\pi h}{\lambda} \cos\theta\right)$$

so the array factor for this situation is  $2 \cos(2\pi h/\lambda \cos\theta)$ . Since only one antenna is really being excited, the apparent gain of this arrangement is twice what we would get from a two-element array driven with the same power in the boresight direction,  $\theta = 90^\circ$ ; this leads to a 6 dB power gain.

**Exercise 4.10**

Consider the effect that height  $h$  above a perfect infinite ground plane has on the side-lobe nulls of a vertically oriented dipole antenna.

**Solution**

If the height of the dipole is made to be  $\lambda/2$  above the ground plane then

$$E_R = 2E_A \cos(\pi \cos\theta)$$

which when plotted over the available physical space  $0 \leq \theta \leq 180^\circ$  yields a null at  $\cos\theta = 1/2$ , i.e.  $60^\circ$ . If  $h$  is made equal to  $\lambda$ , then two nulls exist, i.e.  $41^\circ$  and  $75^\circ$ . In general, the greater  $h$  is above the ground, the more nulls that exist. This means that the polar pattern for the antenna has more secondary side lobes that are radiating power. The overall effect is a reduction of power transmitted or signal received in the direction of maximum radiation. These side lobes are normally considered to be a nuisance, since they pick up stray signals when the antenna is operated in receive mode. The advantage or disadvantage of secondary side-lobe shape and spacial position is determined ultimately by the detail of the application specification into which the antenna array is to be used.

**References**

- [15] Kraus, A.D., *Circuit Analysis*, West Publishing Company, 1991.
- [16] Johnson, R.C. and Jasik, H., *Antenna Engineering Handbook*, 2nd edition, McGraw-Hill, 1984.
- [17] Shen, L.C. and Kong, J.A., *Applied Electromagnetism*, Brookes/Cole Engineering Division, 1983, 195–7.
- [18] Dolph, C.L., A current distribution for broadside arrays which optimises the relationship between beamwidth and sidelobe level, *Proc. IRE*, Vol. 34, pp. 335–48, 1946.
- [19] Jaskik, H., *Antenna Engineering Handbook*, McGraw-Hill, pp. 2–19, 2–25, 1961.
- [20] Stengen, R.J., Excitation co-efficients and beamwidths of Tchebyscheff arrays, *Proc. IRE*, Vol. 41, pp. 1671–4, 1952.
- [21] Fano, R.M., Theoretical limitations on the broadband matching of arbitrary impedances, *Journal of the Franklin Institute*, Vol. 249, pp. 57–83, Jan. 1960; also Feb. 1960, pp. 139–55.
- [22] Jordan, E.C. and Balmain, K.G., *Electromagnetic Waves and Radiating Systems*, 2nd edition, Prentice-Hall, 1968, pp. 387–8, 537–8.
- [23] Ramo, S., Whinnery, J.R. and Van Duzer, T., *Fields and Waves in Communication Electronics*, John Wiley & Sons, 1962, p. 712.
- [24] Slater, J.C., *Microwave Transmission*, McGraw-Hill, New York, 1942, pp. 218–19.

## Problems

- 4.1** Two short dipoles aligned parallel to the  $z$ -axis are spaced along the  $x$ -axis at separation  $d$  between each element. For this arrangement, plot the electric field patterns in the  $H$  plane ( $\theta = \pi/2$ ) of the array under element separation conditions  $d = \lambda/4$ ,  $\lambda/2$  and  $\lambda$ . You may assume that the elements are fed with equi-phase, equi-amplitude signals. What general conclusions can you draw about the effect of element spacing on boresight gain and side lobe pattern response for each of the element separations above?
- 4.2** For the same physical arrangement in exercise 4.1 but with element separation fixed at  $\lambda/4$  and a phase lag between excitation currents of  $-\pi/2$  predict the electric field patterns in the  $H$  plane ( $\theta = \pi/2$ ). What special property does the resultant far field electric field pattern possess that would make it useful in particular applications? State which applications you have in mind.
- 4.3** Show that for a uniformly spaced linear array its power gain is directly proportional to the number,  $N$ , of elements in the array. What happens to the half-power beamwidth of such an array as the number of elements used in its construction is increased?
- 4.4** Show that for a co-linear array of  $N$  elements constructed over a perfectly conducting ground plane inserted normal to the array, an apparent increase in power gain is available when compared with an equivalent  $2N$  element array operated without a perfectly reflecting ground plane being present. You may assume that both arrays are driven with a total input power of 1 W and that all excitation currents are in phase. What increase in gain along the direction of broadside radiation would you expect for a four-element array for the situation quantified above.
- 4.5** A uniform co-linear array (axial symmetry in the  $\phi$  plane) consisting of six half-wave dipoles spaced  $\lambda/2$  apart is fed with in-phase currents. Find the directions (in the  $\theta$  plane) along which the maximum electric fields occur. Find the half-power beamwidth in the direction of maximum radiation.
- 4.6** The situation described in exercise 4.5 is modified such that each element of the six-element array is fed with a progressive phase shift  $\psi$  and equi-amplitude signal. For this arrangement, show that maximum radiation in the  $\theta$  plane occurs when  $\psi + kd \sin\phi_{\max} = 0, 2\pi, \dots$ , where  $\phi_{\max}$  is the angle of the major lobe of the resulting electric far-field pattern for a given  $\psi$ .

This equation shows that when phase shift  $\psi$  is varied the antenna array can have its radiation pattern scanned over a wide angle. Sketch the radiation pattern responses for the array when  $\psi = 180^\circ, 135^\circ, 90^\circ, 45^\circ$  and  $0$ .

# Systems and characterisation considerations

---

This chapter deals with a variety of issues that arise when an antenna is to be deployed as part of a system. The idea of antenna effective length, as a figure of merit for establishing the quality of use of the antenna for radiation or collection of energy, is introduced and extended in order to allow aperture antennas to be quantified with respect to a similar figure of merit, the antenna effective aperture. Effective aperture and its relationship to the mechanisms associated with electromagnetic waves propagating through free space between a transmit and a receive antenna is also investigated. From these considerations, the free-space path loss equation used by microwave and wireless link designers is derived. Since an antenna can pick up radiation from many sources, including natural noise background radiation and thermal noise, techniques for including these effects and for establishing how this noise degrades wireless link transmitted signal integrity are included.

The concept of polarisation of an electromagnetic wave and its importance in terms of optimal signal transfer in an antenna system is discussed. The proximity of antennas to obstructions that might be encountered in a real-life situation may affect the free-space link calculations previously developed in this chapter. With this in mind, the topic of clearance is reviewed in order to provide a systems designer with an idea of how far the primary link path has to be removed from an obstruction so that the link appears as though it were operating in free space. In this way, the validity of the assumptions used in the derivation of the free-space link equation remain intact. Similarly, the problem of how close two antennas can be placed before the far-field separation assumptions used in the derivation of the path equation is also addressed.

The principal methods for testing for antenna far-field radiation characteristics and the definitions associated with these tests, together with the rules governing the construction of scale models for antennas, is also included, as are basic techniques for making calibrated electric field strength measurements.

### 5.1 Effective length of an antenna and reciprocity

In relation to a transmit antenna, the effective length of the antenna is defined as the length of an equivalent antenna,  $\ell_{\text{eff}_T}$ , that has a constant current distribution along its length and that radiates the same field strength normal to its axis as does the actual antenna when fed by a terminal current  $I(0)$ .

For an antenna of length  $\ell$ , in transmit mode [25] [26]:

$$I(0)\ell_{\text{eff}_T} = \int_{-\ell/2}^{+\ell/2} I(z) dz \quad (5.1)$$

thus

$$\ell_{\text{eff}_T} = \frac{1}{I(0)} \int_{-\ell/2}^{+\ell/2} I(z) dz \quad (5.2)$$

In receive mode, the open-circuit voltage  $V_{\text{oc}}$  across the antenna terminals for a known received field strength  $E_z$  obtained on receipt of a uniform field excitation defines the effective length in receive mode,  $\ell_{\text{eff}_R}$ , as

$$\ell_{\text{eff}_R} = \frac{V_{\text{oc}}}{E_z} \quad (5.3)$$

But from the induced emf method (Section 4.6), we know that

$$V_{\text{oc}} = -\frac{1}{I(0)} \int_{-\ell/2}^{+\ell/2} E_z I(z) dz \quad (5.4)$$

which for an incident  $E_z$  field excitation constant over the length of the antenna gives

$$\frac{V_{\text{oc}}}{E_z} = -\frac{1}{I(0)} \int_{-\ell/2}^{+\ell/2} I(z) dz$$

hence  $\ell_{\text{eff}_R} = \ell_{\text{eff}_T}$ . Therefore, the effective length of the antenna in transmit mode is the same as the effective length of the antenna in receive mode; i.e. reciprocity is maintained.

### 5.2 Antenna aperture and the free-space link equation

An antenna can be assigned an aperture area,  $A_e$ , that is not equivalent to its physical aperture and is such that the power absorbed by this area is equal to that absorbed by a perfectly matched antenna; i.e.

$$A_e = \frac{\text{power absorbed by load}}{\text{power density in incident wave}}$$

Consider a hypothetical aperture,  $A_e \text{ m}^2$ , which is placed parallel to a plane wave that is free to propagate through it. If the total power absorbed by area  $A_e$  is  $P_r$ , then

$$P_r = P_{\text{incident}} A_e \quad (5.5)$$

Also, the condition for maximum power transfer from an antenna to a real matched load is

$$P_L = \frac{V_{\text{ant}}^2}{4R} \quad (5.6)$$

For a plane wave propagating in free space, we know from Section 2.3 that the incident instantaneous power per unit area is

$$P_{\text{incident}} = EH \sin\theta \quad (5.7)$$

and from Section 2.2 that a plane wave propagating in the  $z$ -direction can be written as

$$E_x = R_e \left( E_0 \exp \left( j\omega \left( t - \frac{z}{c} \right) \right) \right) \quad (5.8)$$

also

$$H_y = R_e \left( E_0 \left( \frac{\epsilon_0}{\mu_0} \right)^{1/2} \exp \left( j\omega \left( t - \frac{z}{c} \right) \right) \right) \quad (5.9)$$

Thus if a surface is placed parallel to the plane wave, i.e.  $\theta = 90^\circ$  in equation (5.7), at  $z = 0$  then on using equation (5.7)

$$P_{\text{incident}} = E_0^2 \left( \frac{\epsilon_0}{\mu_0} \right)^{1/2} = \frac{E_0^2}{120\pi} \quad (5.10)$$

directed along the  $z$ -axis in the positive direction. Equating this with equations (5.5) and (5.6), we get

$$\frac{E_0^2 A_e}{120\pi} = \frac{V_{\text{ant}}^2}{4R} \quad (5.11)$$

which for a Hertzian dipole (i.e. uniform current distribution and length  $\ll$  wavelength) we can describe the voltage induced by the electric field  $E_0$  incident on the Hertzian antenna as

$$V_{\text{ant}} = E_0 \ell \quad (5.12)$$

so that

$$E_0^2 A_e / 120\pi = E_0^2 \ell^2 / 4R_{\text{rad}} \quad (5.13)$$

and we know  $R_{\text{rad}}$  for a Hertzian dipole from Section 2.4; therefore

$$\frac{E_0^2 A_e}{120\pi} = \frac{E_0^2 \ell^2}{4 \left( 80\pi^2 \left( \frac{\ell}{\lambda} \right)^2 \right)} \lambda^2$$

or

$$A_e = \frac{3}{8} \frac{\lambda^2}{\pi} \quad (5.14)$$

for the Hertzian dipole. In this derivation, we have assumed a lossless antenna with real matched load  $R$  and maximum received signal.

For a half-wave dipole, we can follow the same procedure as above. However, this time we must incorporate the non-uniform current distribution along the antenna (c.f. Section 3.2). For simplicity, we will assume that the current distribution along the half-wave dipole is given as

$$I(z) = I_0 \cos\left(\frac{\omega}{c} z\right) \quad (5.15)$$

from which we can find the voltage induced in the antenna as

$$\begin{aligned} V_{\text{ant}} &= \int_{-\lambda/4}^{\lambda/4} E_0 \cos\left(\frac{\omega}{c} z\right) dz \\ &= \frac{E_0 \lambda}{\pi} \end{aligned} \quad (5.16)$$

Here we have assumed that the voltage induced in a short length of dipole is directly proportional to the current flowing through it. Thus for a half-wave dipole whose  $73 \Omega$  radiation resistance at resonance is matched to its terminal impedance, the maximum power absorbed in the termination is found using equations (5.6) and (5.16).

Equating the result above with the  $z$ -directed power in a plane wave equation (5.11) yields

$$\frac{E_0^2 A_e}{120\pi} = \frac{E_0^2 \lambda^2}{4\pi^2 73}$$

giving

$$A_e = \frac{30}{73} \frac{\lambda^2}{\pi} \approx 0.13\lambda^2$$

### Exercise 5.1

Show that the effective aperture of a correctly terminated half-wave dipole is approximately the same as that of a rectangular section of a perfectly matched absorber approximately  $\lambda/4 \times \lambda/2$  in size.

#### Solution

From above, we see that for a correctly terminated half-wave dipole  $A_e = 0.13\lambda^2$  or  $0.25\lambda \times 0.5\lambda$ .

We know from Section 2.4 that the gain,  $G$ , of a Hertzian dipole with respect to an isotropic source is 1.5. Therefore we can deduce from equation (5.14) that

$$G = \frac{\text{Hertzian dipole}}{\text{isotropic source}} = \frac{3}{2} = \frac{3\lambda^2}{8\pi} / A_{\text{ei}} \quad (5.17)$$

where  $A_{ei}$  is the effective aperture of an isotropic source; i.e.

$$A_{ei} = \frac{\lambda^2}{4\pi}$$

Using this concept, we can express the gain of any antenna,  $G$ , with known effective aperture  $A_e$  relative to an isotropic source as

$$G = \frac{4\pi}{\lambda^2} A_e \quad (5.18)$$

From equation (5.5), we can write that the power at any receive antenna,  $P_r$ , is

$$P_r = P_{\text{incident}} A_{er} \quad (5.19)$$

where  $A_{er}$  is the effective aperture of the receive antenna and  $P_{\text{incident}}$  is the incident power in the wavefront, which if assumed to be a plane wave can be expressed using equation (5.10):

$$P_{\text{incident}} = \frac{E_0^2}{120\pi}$$

If  $A_{er}$  is the effective aperture of the receive antenna and  $E$  is the strength of the electric field, then

$$P_r = \frac{E_0^2}{120\pi} A_{er} = \frac{E_0^2 A_{er}}{30(4\pi)} \quad (5.20)$$

But from equation (5.18) we can write

$$P_r = \frac{E_0^2}{120\pi} \frac{G_R \lambda^2}{4\pi} = \frac{1}{30} \left( \frac{E_0 \lambda}{4\pi} \right)^2 G_R \quad (5.21)$$

However, we also know from Section 2.3 that the electric field strength at some distance  $r$  (far enough away from the source that the wavefront incident on the receive antenna is a plane wave) from an isotropic source transmitting an average power  $P_T$  is given by

$$E_0 = \frac{(30P_T)^{1/2}}{r} \quad (5.22)$$

so that if the transmitting antenna has gain  $G_T$ , then

$$E_0 = \frac{(30P_T G_T)^{1/2}}{r} \quad (5.23)$$

Combining these results yields

$$P_R = P_T G_T G_R \left( \frac{\lambda}{4\pi r} \right)^2 \quad (5.24)$$

This expression is generally written in terms of decibels as

$$P_R = P_T + G_T + G_R - 20 \log_{10} \left( \frac{4\pi r}{\lambda} \right) \text{dB} \quad (5.25)$$

Here the last term represents the free-space transmission loss, or path loss, of the signal after it has travelled distance  $r$ . Equation (5.25) is called the free-space path equation.

Often, when working with this path-loss equation, it is useful to define the term ‘effective isotropic radiated power’ (EIRP):

$$\text{EIRP} = P_T G_T \quad (5.26)$$

Here  $P_T$  is the actual power available for transmission at the transmitter antenna input terminals and includes any feed or connector losses between the transmitter and the feedpoint of the transmit antenna.

Equation (5.24) can also be recast in terms of the transmit and receive antenna effective apertures as

$$P_R = P_T A_{e_T} A_{e_R} \frac{1}{(\lambda r)^2} \quad (5.27)$$

which when expressed as a ratio gives

$$\frac{P_R}{P_T} = \frac{A_{e_T} A_{e_R}}{(\lambda r)^2} \quad (5.28)$$

in which form it is known as Friis transmission formulae. Equations (5.25) and (5.28) are important when doing system link budget calculations.

### Exercise 5.2

An 875 MHz signal is to be transmitted over a 1 km distance using half-wavelength dipole antennas. The transmitter has 1 W of power available at the input terminals of the transmit antenna, to which it is perfectly matched. Find the signal strength at the terminals of the receive antenna.

#### Solution

Using equation (5.25) we get

$$P_R \text{ (dBm)} = 30 \text{ (dBm)} + 2.15 \text{ (dBi)} + 2.15 \text{ (dBi)} - 91.3 \text{ dB}$$

where  $\lambda = 3 \times 10^8 / 875 \times 10^6 = 0.343 \text{ m}$ .

$$P_T = 10 \log_{10} \left( \frac{1000 \text{ mW}}{1 \text{ mW}} \right) = 30 \text{ dBm}$$

2.15 dBi = gain of half-wavelength dipole (Section 3.5)

$$\therefore \text{EIRP} = 32.15 \text{ dB}$$

$$\text{path loss} = 20 \log_{10} \left( \frac{4\pi 1000}{0.343} \right) = 91.3 \text{ dB}$$

$$\therefore P_R \text{ (dBm)} = -57 \text{ dBm}$$

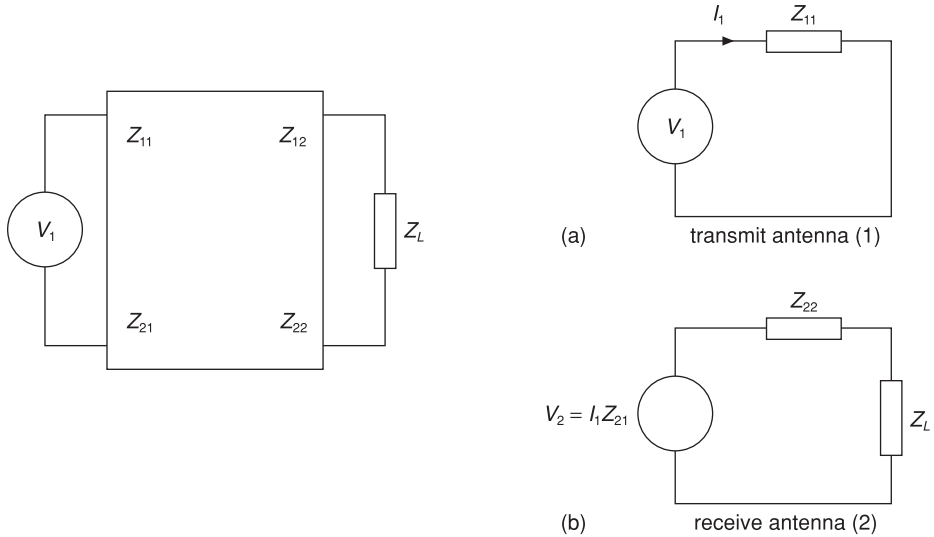


**Figure 5.1** Approximate equivalent transmit/receive antenna model

Based on the concepts of reciprocity discussed in Appendix 9.2, we will now illustrate that the polar pattern of a given antenna is the same on transmit as it is on receive. This means that for characterisation of an antenna the simplest physical arrangement, i.e. the antenna under test can be sited either as a transmit or more normally as a receive element in order to facilitate measurement of its characteristics (see Section 5.8), and that a single antenna design will exhibit identical transmit or receive functionality (see Section 5.1).

Consider a perfectly matched antenna model as shown in Figure 5.1a for the transmitter. Assume that the receive antenna does not create any backscattered radiation to the transmitter, i.e.  $Z_{12} = 0$ , and let  $Z_{21}$  represent the coupling between transmitter and receiver. Then Figure 5.1b represents a simple model for the receive antenna [27]. Here  $Z_{11}$  = transmitter input impedance,  $Z_{22}$  = receiver input impedance, and the general definitions for  $Z_{ij}$  are given in Section 4.6.

For maximum power transfer from transmitter to receiver  $Z_L = Z_{22}^*$ , where \* denotes the complex conjugate. Under this condition, the power delivered to the load is

$$P_{\text{load}} = \frac{1}{2} \cdot \frac{|I_1 Z_{21}|^2}{4} \cdot \frac{1}{\text{Re}(Z_{22})} \tag{5.29}$$

and the power delivered to the transmit element is

$$P_{\text{transmit}} = \frac{1}{2} |I_1|^2 \text{Re}(Z_{11}) \tag{5.30}$$

Hence the ratio

$$\frac{P_{\text{load}}}{P_{\text{transmit}}} = \frac{|Z_{21}|^2}{4\text{Re}(Z_{22}) \text{Re}(Z_{11})} \tag{5.31}$$

If the receive antenna is moved to a different position then in general, due to its directive response,  $P_{\text{load}}$  will change. Hence from equation (5.31) we can write for a constant transmit power level

$$\frac{P_{\text{load}_a}}{P_{\text{load}_b}} = \frac{|Z_{21}|_a^2}{|Z_{21}|_b^2} \quad (5.32)$$

where the subscripts a and b define two different spacial receive antenna positions. Similarly, if the roles of transmit and receive antenna are interchanged (in which case we assume  $Z_{21} = 0$  and  $Z_{12} \neq 0$ ) then we can write:

$$\frac{P^1_{\text{load}_a}}{P^1_{\text{load}_b}} = \frac{|Z_{12}|_a^2}{|Z_{12}|_b^2} \quad (5.33)$$

But from Appendix 8.2, we know that for reciprocity to hold  $Z_{12} = Z_{21}$  for equal terminating impedances, e.g. in a homogeneous bilateral transmission path such as free space. Therefore equation (5.32) must be equal to equation (5.33), and the same relative polar patterns are obtained in both transmit and receive mode, hence validating the assertion made above regarding the interchangeability of the roles of the antenna under test in a measurement set-up or in terms of transmit/receive functionality.

Note: The derivation of the reciprocity relationship given above is based on pp. 716–19 of S. Ramo, J.R. Winnery and T. van Duzer, *Fields and Waves in Communication Electronics*, copyright © 1965 by John Wiley & Sons Inc., reprinted by permission of John Wiley & Sons, Inc.

### 5.3 Effective temperature of an antenna and noise effects

An antenna will pick up noise from any source of radiation present in the bandwidth over which it operates. If pointed at the sky, the main antenna lobe may pick up one noise level, but the antenna side lobes may be pointing towards the ground and thus pick up a different noise level. This action may result in the antenna contributing a substantial amount of unwanted noise to the system to which it is connected. One method of combating this effect is to cover the ground around the antenna with a metal screen or mesh to reduce noise pick-up from the ground.

At temperatures above absolute zero, the free electrons available in metal conductors move randomly due to thermal agitation. Since each electron has a charge associated with it, as the electrons move their rate of change results in a randomly varying current being generated. Through conductor conductivity, this current gives rise to a randomly varying voltage across the ends of the conductor. The resulting noise voltage source is very broadband and ultimately may contain equal power density right across the frequency spectrum on a per unit bandwidth basis. If this is the case, then the noise is said to be ‘white noise’. The noise voltage,  $E$ , occurring at the open-circuited ends of such a conductor can be written as

$$E^2 = 4kTBR \quad (5.34)$$

where  $B$  = noise bandwidth (Hz),  $R$  = conductor resistance ( $\Omega$ ),  $k$  = Boltzmann’s constant ( $1.38 \times 10^{-23}$  J/K) and  $T$  = absolute temperature (K). Here the generally used standard reference temperature is 290 K.

When the conductor is connected to a load, some of this noise voltage becomes available to the load. The maximum power that can be transferred from the noise source to the load occurs when their respective impedances form a conjugate match. For a real noise source impedance, this occurs for a load resistance  $R$ , as defined by the maximum power transfer theorem. Under this condition, one-half of the noise voltage  $E$  will be delivered across the load resistance  $R$ :

$$\left(\frac{E}{2R}\right)^2 R = E^2/4R \quad (5.35)$$

Thus the available noise power  $P_n$  becomes

$$P_n = \frac{4kTB R}{4R} = kTB \quad (5.36)$$

Notice how this quantity is independent of the resistance producing it.

### Exercise 5.3

Calculate the available noise power in a 1 Hz bandwidth in dBm/Hz at 290 K.

#### Solution

From equation (5.36):

$$P_n = kT = 4 \times 10^{-21} \text{ W or } 4 \times 10^{-18} \text{ mW or } -174 \text{ dBm/Hz.}$$

Amplifiers are often used as the first component connected to an antenna. If an amplifier is placed in series with an equivalent noise generator, it will amplify the noise available at its input and will also produce additional noise itself. If a lossy element is connected to the antenna, it will attenuate the signal but will still add noise. The noise that is added due to the presence of the amplifier can be defined in terms of ‘effective noise temperature’. For an amplifier with gain  $G$  (gain here is defined as  $V_{\text{out}}/V_{\text{in}}$ , where, since the amplifier is an active device,  $V_{\text{out}}$  is generally greater than  $V_{\text{in}}$ ), connected to a matched resistor at its input, its output noise,  $n_o$ , will be

$$n_o = (KTB_n + n_a) G$$

where  $B_n$  is the amplifier noise equivalent bandwidth (see Appendix 8.3), and  $n_a$  is the noise added by the amplifier or lossy element. This noise when referred back to the input of the noise source can be written as

$$n_a = kT_e B_n \quad (5.37)$$

Here  $T_e$  is called the effective noise temperature and is a hypothetical quantity, since the contribution to noise produced by the amplifier itself may not be exclusively due to thermal noise.

Next consider the important case of the noise temperature of an attenuator with loss  $L$ , which may be connected in series with an antenna, e.g. a lossy coaxial feedline [28]. In order to find the effective noise temperature  $T_e$  of the attenuator held at temperature

$T$  when being fed from a matched resistor, e.g. the terminals of a resonant antenna, we must calculate the noise contributed by the attenuated input noise and the noise produced by the attenuator itself.

If we call the input resistor noise temperature  $T_1$ , the attenuated input noise will be  $kT_1 B_n L$ , and the total noise available at the output of the attenuator can be found if we first consider the noise characteristics of a series connection of  $N$  resistors,  $R_i$ , from the derivation presented in [29]. Total resistance  $R$  is

$$R = \sum_{i=1}^N R_i \quad (5.38)$$

For this arrangement, with different resistance temperatures  $T_i$  available for each resistor, the composite noise voltage is

$$E_n^2 = 4kB_n \sum_{i=1}^N R_i T_i \quad (5.39)$$

Thus the available noise power is by the definition in equation (5.36)

$$P_n = \frac{(E_n/2)^2}{\sum_{i=1}^N R_i} = \frac{4kB_n \sum_{i=1}^N R_i T_i}{4 \sum_{i=1}^N R_i} = kT_e B_n \quad (5.40)$$

from which the effective noise temperature  $T$  for a series connection of resistors is found as

$$T_e = \frac{\sum_{i=1}^N R_i T_i}{\sum_{i=1}^N R_i} \quad (5.41)$$

If we write the contribution of each resistance to the total effective noise temperature as

$$T_e = \sum_{i=1}^N \alpha_i T_i \quad (5.42)$$

then we can see from equation (5.41) that

$$\alpha_i = \frac{R_i}{\sum_{i=1}^N R_i} \quad (5.43)$$

This result is very useful, since we can treat the noise effects of power losses in a passive system as though they are due to the presence of attenuators. Hence we can model the overall noise temperature of the antenna system as the sum of all the pertinent passive noise mechanisms, i.e. component attenuation, body, sky and ground temperatures.

Returning once again to the attenuator problem, we can see from equation (5.43) for two resistors,  $R_1$ ,  $R_2$ , that

$$\alpha_1 = \frac{R_1}{R_1 + R_2}$$

and

$$\alpha_2 = \frac{R_2}{R_1 + R_2}$$

thus

$$\alpha_1 + \alpha_2 = 1 \quad (5.44)$$

hence from equation (5.42) to obtain the effective noise temperature of the attenuator and matched resistor arrangement,  $T_e$ , we assign the resistor an effective noise temperature  $T_1$  and the attenuator an effective noise temperature  $T_2$ . Thus

$$T_e = \alpha_1 T_1 + \alpha_2 T_2 \quad (5.45)$$

Now if  $\alpha_1 = L$ , then using this and equation (5.44) we can say that

$$T_e = T_1(L) + T_2(1 - L) \quad (5.46)$$

This equation enables the prediction of the effective noise temperature of an antenna being fed, or feeding, a matched attenuator to be made. This expression is very useful if we wish to determine how the presence of a lossy filter such as a duplexer attached to an antenna influences the overall effective noise temperature of the antenna assembly.

#### Exercise 5.4

If we have a 3 dB ( $\times 0.5$ ) loss introduced by a duplex filter operating at 290 K and the antenna to which it is matched sees a 4 K sky temperature, find the effective noise temperature of the arrangement.

#### Solution

From equation (5.46):

$$\begin{aligned} T_e &= 4 \times 0.5 + 290 \times 0.5 \\ &= 147 \text{ K} \end{aligned}$$

Thus the major noise contribution comes from the filter section.

We will now define the noise figure of a matched attenuator. The noise figure,  $N_f$ , is defined as  $10 \log_{10}$  (available signal-to-noise ratio, S/N, at the signal generator terminals at 290 K)/(available S/N at the network output). Alternatively it can be defined as  $10 \log_{10} F$ , where  $F$  is the noise factor. Thus

$$F = \frac{\left( \frac{S_i}{290k_B} \right)}{\left( \frac{S_o}{N_o} \right)} \quad (5.47)$$

where  $S_i$  is the signal at the network input terminals,  $S_o$  is the signal at the network output terminals and  $N_o$  is the output noise power.

Noting that  $S_o = GS_i$ , where  $G$  is the gain, or for  $G < 1$  the loss, of the network under investigation, then

$$F = \frac{N_o}{290k_B G} \quad (5.48)$$

or

$$N_o = 290k_B G F \quad (5.49)$$

for  $G < 1$ , i.e. an attenuator, we write  $G = L$ . Therefore

$$N_o = 290k_B L F \quad (5.50)$$

But from equations (5.46) and (5.36), we can write

$$N_o = k_B T_e \quad (5.51)$$

$$= k_B (290L + T(1 - L))$$

$$= k_B L \left( 290 + T \left( \frac{1}{L} - 1 \right) \right) \quad (5.52)$$

Comparing equations (5.50) and (5.52) yields

$$F = 1 + \frac{T}{290} \left( \frac{1}{L} - 1 \right) \quad (5.53)$$

If  $T = 290$  K, then

$$F = \frac{1}{L} \quad (5.54)$$

and

$$N_f = 10 \log_{10} \frac{1}{L} \quad (5.55)$$

Thus if a matched attenuator, e.g. an impedance-matched antenna downlead cable, is placed in front of an amplifier, the amplifier noise figure/factor will be increased by an amount exactly equal to the attenuator loss. This result is crucial when determining the sensitivity of a receiver system.

Consider now the noise figure of a cascaded system consisting of a number of components placed in series, such as might be encountered when an antenna is connected to an amplifier via a lossy cable. An example of a two-stage cascaded system is shown in Figure 5.2a, where  $G$  = gain of stage,  $F$  = noise factor,  $T_e$  = effective noise temperature,  $N_f$  = noise figure and  $T_0$  = reference noise temperature.

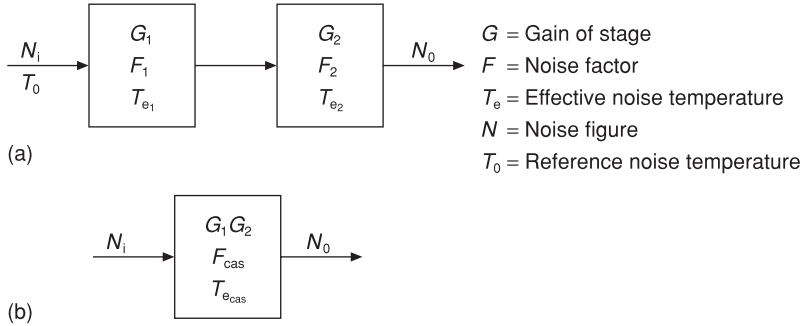


**Figure 5.2** (a) Cascaded two-stage receiver; (b) equivalent network

The output noise power,  $N_1$ , from the first stage of the system is

$$\begin{aligned} N_1 &= N_i + kT_{e_1}B_nG_1 \\ &= kT_0B_nG_1 + kT_{e_1}B_nG_1 \end{aligned} \quad (5.56)$$

The noise power at the output of the second stage is given by

$$\begin{aligned} N_0 &= N_1G_2 + kB_nT_{e_2}G_2 \\ &= kT_0B_nG_1G_2 + kT_{e_1}B_nG_1G_2 + kB_nT_{e_2}G_2 \\ &= G_1G_2kB_n\left(T_0 + T_{e_1}\frac{T_{e_2}}{G_1}\right) \end{aligned} \quad (5.57)$$

This system can also be treated as an equivalent single two-port network (Figure 5.2b):

$$\begin{aligned} N_0 &= kT_0B_nG_1G_2 + kB_nT_{e_{cas}}G_1G_2 \\ &= G_1G_2kB_n(T_0 + T_{e_{cas}}) \end{aligned} \quad (5.58)$$

Equations (5.57) and (5.58) yield the noise temperature of the cascaded system. Hence

$$T_{e_{cas}} = T_{e_1} + \frac{T_{e_2}}{G_1} \quad (5.59)$$

By definition,  $T_e = T_0(F - 1)$ . Hence the noise factor of the cascaded system is

$$F_{cas} = F_1 + \frac{F_2 - 1}{G_1} \quad (5.60)$$

Generalising this result for a cascaded system of  $n$  stages, the overall noise factor  $F_{cas}$  is given by

$$F_{cas} = F_1 + \frac{F_2 - 1}{G_1} + \dots + \frac{F_n - 1}{G_1G_2 \dots G_{n-1}} \quad (5.61)$$

where  $F_n$  = noise factor of each stage, and  $G_n$  = available gain of each stage.

### Exercise 5.5

Compute the overall noise factor of a cascaded three-stage amplifier system. The signal enters amplifier 1, gain 6 dB and noise factor 1.5, passes through amplifier 2, whose gain is 10 dB and noise factor is 3.0, and finally it exits via amplifier 3, gain 20 dB and noise factor 4.0. All amplifiers are impedance-matched.

#### Solution

Using equation (5.61), we can write

$$\begin{aligned} F &= F_1 + \frac{F_2 - 1}{G_1} + \frac{F_3 - 1}{G_1 G_2} \\ &= 1.5 + \frac{3 - 1}{4} + \frac{4 - 1}{4 \times 10} \\ &= 2.08 \end{aligned}$$

Finally, using the result obtained at equation (5.61), the overall system noise output  $N_{\text{sys}}$  can be written as

$$N_{\text{sys}} = Gk B_n F_{\text{cas}} T_0 \quad (5.62)$$

where  $G$  = overall system gain =  $G_1 G_2 \dots G_N$  and  $B_n$  = equivalent noise bandwidth of system (see Appendix 8.3).

From the result given in equation (5.61), it can be seen that the noise figure of the first stage contributes the maximum amount to the overall noise figure. Successive stages add noise that is reduced by the product of the gains of the preceding stages. If the stages have gain, then the noise figure will decrease, whereas lossy stages will increase the noise figure of the system.

Another important noise-related concept used mainly in satellite receiver antenna noise characterisation work is the gain to equivalent noise temperature ratio ( $G/T$ ), defined as

$$\frac{G}{T} = \frac{\text{receive antenna gain } (G)}{\text{equivalent noise temperature } (T_e) \text{ of the receiver}} \quad (5.63)$$

This quantity is often used in quantifying satellite or earth station receivers [30]. From equation (5.61), we saw that to minimise the noise figure a low-noise high-gain amplifier should, if possible, be located right at the receive antenna feedpoint, now defined to have gain  $G_R$ .

In this case, the  $G/T$  ratio becomes

$$\frac{G}{T} = \frac{G_R + G}{T_e} \quad (5.64)$$

or in dB after taking logs

$$\frac{G}{T} (\text{dBK}^{-1}) = G_R + G - T_e \quad (5.65)$$

Equation (5.65) is frequently used in satellite link budget calculations, since signal-to-noise ratio can be computed at the receiver using equations (5.25) and (5.26) as

$$\frac{S}{N} \text{ (dB)} = P_R - P_{\text{noise}} = \text{EIRP} - \text{path loss} - 10 \log_{10} k B_n + G + G_R - 10 \log_{10} T_e \quad (5.66)$$

hence

$$\frac{S}{N} \text{ (dB)} = \frac{G}{T} + \text{EIRP} - \text{path loss} - 10 \log_{10} k B_n \quad (5.67)$$

### 5.4 Polarisation of plane electromagnetic waves

The polarisation of an electromagnetic wave is defined by the direction in which its electric field vector is oriented over at least one cycle of oscillation [31].

In the general case, the tip of the electric field vector maps out an ellipse (Figure 5.3 when viewed end-on as the electromagnetic wave propagates). In Figure 5.3a, the coordinate system used is referenced to (x, y), while in Figure 5.3b it is referenced to the principal axis of the ellipse (x', y').

The shape of the ellipse is defined by its axial ratio, |AR|:

$$|AR| = \frac{\text{major axis of ellipse}}{\text{minor axis of ellipse}} = \frac{|E_{\text{max}}|}{|E_{\text{min}}|} \quad (5.68)$$

here  $|E_{\text{max}}| = |E_{\text{co}}| + |E_{\text{cross}}|$  and  $|E_{\text{min}}| = |E_{\text{co}}| - |E_{\text{cross}}|$ , where  $E_{\text{co}}$  is the antenna cross-polarisation level and  $E_{\text{cross}}$  is the antenna cross-polarisation level.

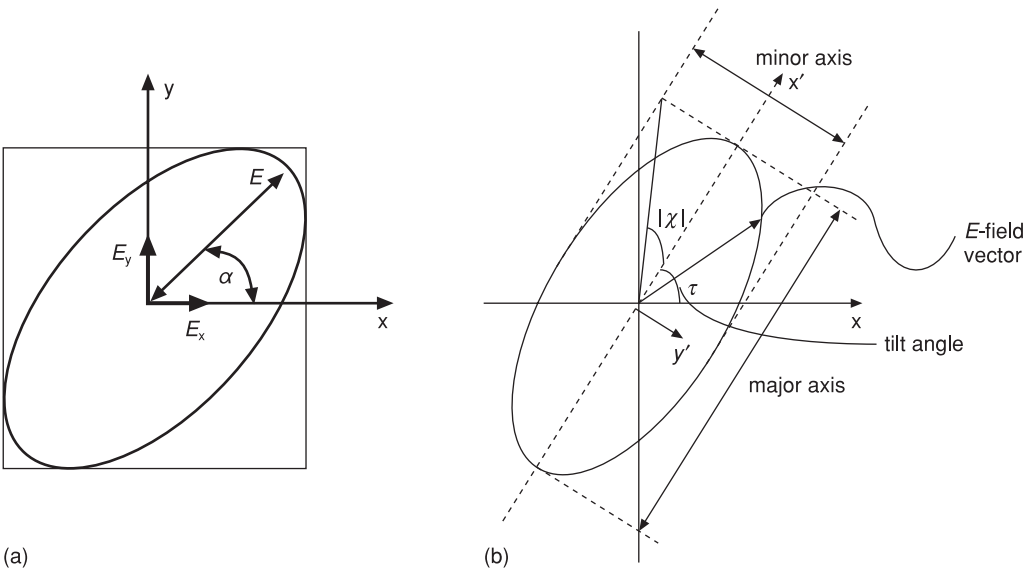


Figure 5.3 Polarisation ellipse

Rewriting using equations (5.69) and (5.70) gives  $E_{\text{co}} = (E_x + jE_y)$  and  $E_{\text{cross}} = (E_x - jE_y)$  such that the total  $E$  field,  $\mathbf{E}$ , is  $\mathbf{E} = (E_{\text{co}} \hat{c} + E_{\text{cross}} \text{cross}\hat{s})$ ; here  $\hat{c}$  and  $\text{cross}\hat{s}$  are orthogonal unit vectors. The axial ratio is normally expressed in dB as  $20 \log_{10} |AR|$ . The orientation of the polarisation ellipse is defined by the tilt angle, i.e. the angle,  $\gamma$ , between the major axis and the horizontal axis (Figure 5.3b). Two special cases exist for the polarisation ellipse; the first is when the minor axis reduces to zero, i.e. the axial ratio goes to infinity and we have linear polarisation. The second case is when both major and minor axis are identical, i.e. 0 dB ellipticity; this is the case of circular polarisation. From these observations, the definitions of linear and circular polarisation can be formed.

A linearly polarised wave is a transverse electromagnetic wave whose electric field vector lies along a straight line at all times, while a circularly polarised wave is a transverse electromagnetic wave whose electric field vector describes a circle with time. A linearly polarised wave is said to be vertically or horizontally polarised if aligned in parallel with the vertical or horizontal axis, respectively.

A circularly polarised wave has the important property that if rotation of the electric field vector occurs the reception strength of the wave by a circularly polarised receiver polarised with the same sense will not be affected by a rotation of the wave. A circularly polarised wave can be polarised in a right- or left-hand sense. To define the hand of polarisation, we say that for an observer looking in the propagation direction, if the rotation of the electric field vector is clockwise as time advances then we have right-hand polarisation, and if it rotates in the anticlockwise direction as time advances we have left-hand polarisation.

An elliptically polarised wave can be constructed from two linearly polarised waves orthogonal to each other and with a phase delay between them. This technique is used for example to synthesise a circularly polarised wave; here we have two options using linearly polarised waves, each of the same magnitude. In the first case, these can be fed with equi-phase equi-magnitude signals positioned orthogonally and displaced in space by  $90^\circ$  (Figure 5.4a), or by equi-magnitude  $90^\circ$  phase-shifted signals displaced orthogonally but co-located in space (Figure 5.4b).

The situation in Figure 5.4b can be realised in numerous ways and represents a physically compact solution, for example if the input impedance of the dipole whose terminals are AA in Figure 5.4b is made to be  $73 + j73 \Omega$  at its frequency of operation (i.e. the dipole is made slightly longer than its resonant length; Section 4.5). Now if the element whose terminals are at BB is made to have input impedance  $73 - j73 \Omega$  (slightly shorter than its resonant length), then the current at dipole BB terminals will be  $90^\circ$  out of phase with that at terminals pair AA, since

$$\tan_{\text{AA}}^{-1}(73/73) - \tan_{\text{BB}}^{-1}(-73/73) = 90^\circ$$

In order for maximum energy transfer to occur between a transmitter and a receiver, both transmit and receive antennas should have identical polarisation type senses. It should also be noted that for any polarisation type another polarisation can exist such that the wave coming from the transmitter will cause no signal to be received at the reception antenna: for example, vertical and horizontal linear polarisation or left- and right-hand circular polarisation. In these cases, the antennas are said to have orthogonal polarisation. This effect can be exploited in a technique using multiple

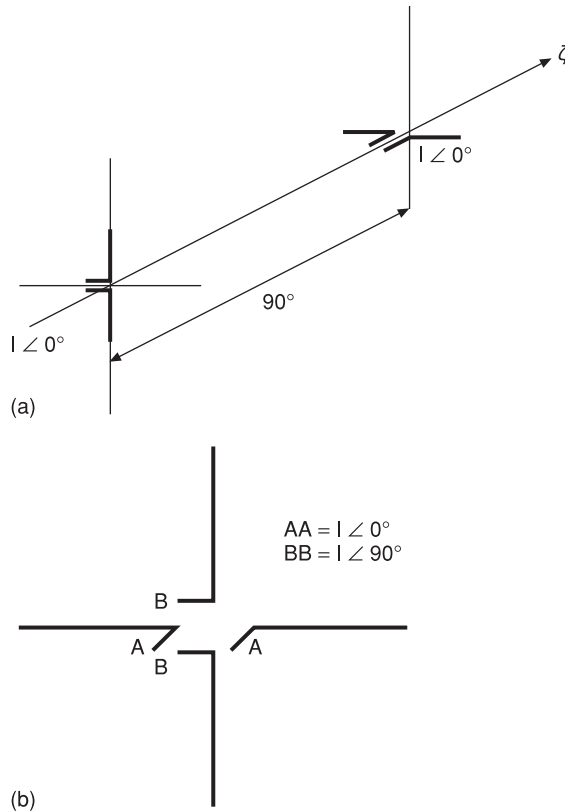


**Figure 5.4** Methods for generating circular polarisation

polarisation orientations called polarisation diversity, and it can be used to increase the amount of information transmitted in a wireless system without increasing bandwidth. In cases where polarisation rotation of a signal over its transmission path is expected, then circular or elliptical polarisation is normally used. In situations such as these, the change of the state of polarisation of the propagating wave is defined using the Poincaré sphere in conjunction with a classification scheme (useful when randomly polarised waves are to be expected) known as Stokes parameters. Readers interested in these aspects and in the polarisation of electromagnetic waves should consult [31] for more details.

It is known that the wave equation is a linear equation and consequently any complicated electromagnetic wave distribution can be synthesised or analysed using superposition of individual plane waves of appropriate relative magnitudes, phases and directions of travel. For example, a linear combination of plane waves with arbitrary relative magnitude and phase and all propagating in the same direction gives an unpolarised wave, while a linear combination of two plane waves with unequal magnitudes, the same direction of propagation and arbitrary relative phase  $\psi$  gives rise to an elliptically polarised wave. Here a phase lead or lag determines right- or left-hand polarisation in the same fashion as occurs for a circularly polarised wave.

Consider how we can decompose an elliptically polarised signal into its two component linearly polarised waves, one with its  $E$  vector lying in the  $x$ -direction, the other with its  $E$  vector oriented in the  $y$ -direction, denoted here as

$$E_x = E_1 \cos(\omega t - \beta z) \quad (5.69)$$

and

$$E_y = E_2 \cos(\omega t - \beta z + \psi) \quad (5.70)$$

Now for any plane transverse to the direction of propagation, say at  $z = 0$ , equations (5.69) and (5.70) reduce to

$$E_x = E_1 \cos(\omega t) \quad (5.71)$$

and

$$E_y = E_2 \cos(\omega t - \psi) \quad (5.72)$$

which are the parametric equations for an ellipse [31]. If  $E_x = E_y$  and  $\psi = \pi/2$ , then the locus of the resultant  $E$  vector ( $E = E_x^2 + E_y^2 = E_1^2$ ) maps out a circularly polarised wave.

The instantaneous angle  $\alpha(t)$  between the  $E$  vector and the  $x$ -axis in Figure 5.3a can be found as

$$\alpha(t) = \tan^{-1} \left( \frac{E_y}{E_x} \right) \quad (5.73)$$

$$= \tan^{-1} \left( \frac{\mp E_1 \sin \omega t}{E_1 \cos \omega t} \right) = \mp \omega t \quad (5.74)$$

Thus the resultant vector rotates at a uniform rate of  $2\pi f$ . If  $\psi$  is  $-\pi/2$  it rotates clockwise when observed in the direction of propagation as time progresses, i.e. right-hand CP, and when  $\psi = +\pi/2$  in a counter-clockwise direction, i.e. left-hand CP.

It turns out that an elliptically polarised wave can also be synthesised using two circularly polarised waves, such that in complex notation [32]:

$$E_{\text{ccw}} = E_1' e^{j(\omega t - \beta z)} \quad (5.75)$$

$$E_{\text{cw}} = E_2' e^{-j(\omega t - \beta z + \psi)} \quad (5.76)$$

where ccw indicates counter-clockwise and cw indicates clockwise propagation.

Hence on decomposing equations (5.75) and (5.76) into real and imaginary parts,

$$E_x = E_1' \cos(\omega t - \beta z) + E_2' \cos \left( \omega t - \beta z + \frac{\pi}{2} \right) \quad (5.77)$$

and

$$E_y = E_1' \sin(\omega t - \beta z) - E_2' \sin \left( \omega t - \beta z + \frac{\pi}{2} \right) \quad (5.78)$$

When  $E_1' = E_2'$  and  $\psi = \pi/2$ , circular polarisation occurs. When  $\psi = 0$  and  $E_1' = E_2' = 0$ , linear polarisation occurs. With reference to Figure 5.3b, the tilt angle  $\tau$  can be found as

$$\tau = \frac{1}{2} \tan^{-1} \left( \frac{2E_1 E_2 \cos \Psi}{E_1^2 - E_2^2} \right) \quad (5.79)$$

where  $E_1$  and  $E_2$  refer to the magnitude of the two linear  $E$  vectors forming the ellipse (equations (5.69) and (5.70)).

### 5.5 Distance to antenna far field

In Section 1.4, we saw that the electromagnetic fields behave differently close to the antenna (near-field or Fresnel region) compared with their behaviour far from the antenna (far field). By geometric consideration, an approximation for the distance required from the antenna to the far-field, or Fraunhofer region can be determined as follows.

It is commonly assumed that plane wave illumination of the receive antenna (Figure 5.5) occurs when the phase difference of the transmitted wavefront as measured between the centre and edge of a receiver or test antenna is no greater than  $\lambda/16$ . In doing this, we are suggesting that the wavefront incident on the receive antenna is approximately a plane wave, i.e. a wave whose wavefront is an equi-phase surface. From the geometry of the problem as defined from Figure 5.5 by Pythagoras' theorem

$$(R + \delta)^2 = R^2 + \left( \frac{d}{2} \right)^2 \quad (5.80)$$

$$R^2 + \delta^2 + 2R\delta = R^2 + \left( \frac{d}{4} \right)^2$$

for  $R \gg \delta \ll d$ .

Then  $\delta^2 \cong 0$ , so that  $2R\delta = d^2/4$ , or

$$R = \left( \frac{d^2}{8\delta} \right) \quad (5.81)$$

which becomes for  $\delta = \lambda/16$

$$R \geq \frac{2d^2}{\lambda} \quad (5.82)$$

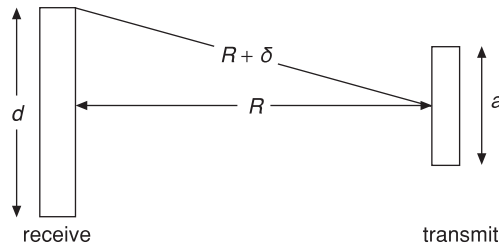


Figure 5.5 Calculation of far-field distance

where  $d$  is length (or largest dimension) of the receive antenna, i.e. the antenna under test in the test set-up. Thus for accurate measurement, i.e. illumination of the test antenna by a plane wave, the condition stipulated by equation (5.82) should be adhered to.

If too short a distance for  $R$  is used when making measurements on the test antenna, then broader radiation patterns, higher side lobes and shallower nulls between side lobes will be measured than if a much greater value of  $R$  is used. It should be noted that for large antennas operated at very high frequencies the wavelength can be very short and the minimum range defined by equation (5.82) can be large.

Furthermore, in making the decision on the value of  $R$  to be used for a measurement it is essential that near-field (induction field) energy levels are kept low in order to prevent excessive mutual coupling between the antenna under test and the receive antenna in Figure 5.5. Consider equation (5.83) and Section 1.4 for a Hertzian dipole:

Note: Equations (5.69) through (5.79) are based on the polarisation presentation given in H. Jasik, *Antenna Engineering Handbook*, McGraw-Hill, 1961, pp. 34–29 and 34–30, and equations 5.80–5.82, pp. 34–14 and 34–15, reproduced with permission The McGraw-Hill Companies, © 1961 The McGraw-Hill Companies.

$$H\phi = \frac{I_0 \Delta \ell}{4\pi} \sin\theta \left[ \frac{\omega}{cR} \cos\omega \left( t - \frac{R}{c} \right) + \frac{1}{R^2} \sin\omega \left( t - \frac{R}{c} \right) \right] \quad (5.83)$$

The ratio between the components in brackets (the largest components) is  $\omega R/c = 1/kr$ ,  $k = 2\pi/\lambda$ ; thus for  $R = 10\lambda$  the ratio becomes  $-36$  dB, which is considered low enough to ensure that mutual coupling between the elements is small compared with the radiated field. The criterion  $R > 10\lambda$  is useful when the antenna under test is physically short and/or the wavelength of operation is long, e.g. VHF/UHF antennas; in which case the distance to the far field predicted by equation (5.82) may be considered an underestimate.

### Exercise 5.6

An antenna test range of length 10 m is available, and it is required to characterise the far-field radiation pattern of a dipole antenna of length 30 cm operating at 500 MHz. Is the antenna test range suitably long for an accurate measurement to be made?

#### Solution

Using  $R \geq \frac{2d^2}{\lambda}$  we get

$$\frac{2 \times 0.3 \times 0.3}{0.6} = 0.3 \text{ m}$$

and using  $R > 10\lambda = 6$  m. Therefore, since the range is 10 m, we can make the desired measurement.

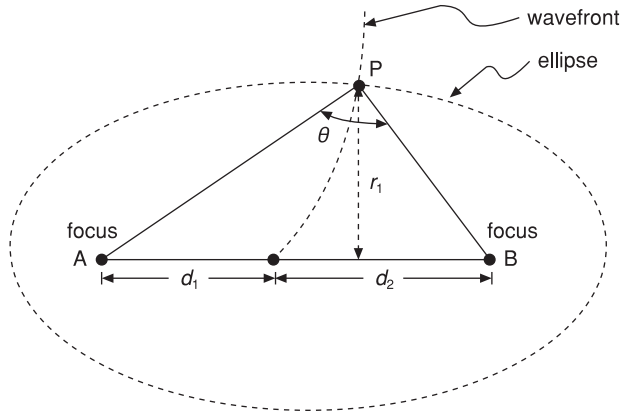


Figure 5.6 Fresnel zone calculations

**5.6 Clearance**

When designing an RF radio path or making antenna test measurements, it is important to make sure that the line-of-sight path over which transmission is to occur is sufficiently clear of any obstructions so that the free-space path-loss equations derived in Section 5.2 remain valid, or that destructive interference does not occur due to multiple re-reflected multi-path signals combining out of phase.

A transmitting system will issue energy that travels outwards from the source as a wavefront expanding with distance (Section 2.2). Huygen’s principle says that each element of this wavefront acts as a new source of radiation energy, each of which in turn propagates secondary wavefronts, and so on. The secondary radiation from these radiators sum to form a new wavefront, such that the field received is the vector sum of all these wavefronts. At any point on the summed wavefront, say P in Figure 5.6, only a proportion of the energy produced from the secondary source at P will reach the receiver placed at B. This amount will depend on the separation between A and B and also on angle  $\theta$ , which can lie in the range 0 to 180°. The cosine of angle  $\theta$  is called the ‘obliquity factor’, and energy arriving along path APB will arrive later than energy along the most direct path, AB.

If the difference between these two paths is 180° (one half wavelength), the two signals will completely cancel each other out. If they differ by 360° (one wavelength), the indirect ray via PB will add constructively to the direct ray AB and they will reinforce each other.

Taking P as the locus of a circle extending out of the page such that  $AB = d_1 + d_2$  and  $APB = d_1 + d_2 + \lambda/2$ , i.e. the condition for signal cancellation between path APB and path AB, then a solid ellipsoid with foci at A and B is formed, such that

$$(d_1^2 + r_1^2)^{1/2} + (d_2^2 + r_1^2)^{1/2} = d_1 + d_2 + \frac{\lambda}{2} = d_1 \left( 1 + \left( \frac{r_1}{d_1} \right)^2 \right)^{1/2} + d_2 \left( 1 + \left( \frac{r_1}{d_2} \right)^2 \right)^{1/2} \tag{5.84}$$

Since  $r_1 \ll d$ , the binominal expansion  $(1 + x)^n \approx (1 + nx)$  can be used to approximate equation (5.84) as

$$d_1 \left( 1 + \frac{1}{2} \left( \frac{r_1}{d_1} \right)^2 \right) + d_2 \left( 1 + \frac{1}{2} \left( \frac{r_1}{d_2} \right)^2 \right) = d_1 + d_2 + \frac{\lambda}{2}$$

thus

$$d_1 + \frac{d_1 r_1^2}{2d_1^2} + d_2 + \frac{d_2 r_1^2}{2d_2^2} = d_1 + d_2 + \frac{\lambda}{2}$$

hence

$$\frac{r_1^2}{2d_1} + \frac{r_1^2}{2d_2} = \frac{\lambda}{2}$$

from which

$$\frac{2d_2 r_1^2 + 2d_1 r_1^2}{4d_1 d_2} = \lambda$$

giving

$$\frac{d_1 r_1^2 + d_2 r_1^2}{2d_1 d_2} = \frac{\lambda}{2}$$

and

$$r_1^2 = \frac{d_1 d_2}{d_1 + d_2} = \lambda$$

from which the clearance radius  $r_1$  can be approximately found:

$$r_1 = \left( \frac{d_1 d_2 \lambda}{d_1 + d_2} \right)^{1/2} \quad (5.85)$$

This locus is called the first Fresnel zone. The second Fresnel zone, the locus for which the difference between the direct and indirect rays is  $d + 2\lambda/2$ , is given as

$$r_2 = \sqrt{2} r_1 \quad (5.86)$$

and the  $n$ th Fresnel zone ( $d + n\lambda/2$ ):

$$r_n = \sqrt{n} r_1 \quad (5.87)$$

A detailed investigation of equations (5.85) to (5.87) shows that the area of the annular ring enclosed by each of the different zone boundaries e.g.  $d + 2\lambda/2$ ,  $d + 3\lambda/2$ , relative to the area of the next ring e.g.  $d + 3\lambda/2$  relative to  $d + 4\lambda/2$ , are approximately equal. This means that the energy flowing through each ring for normal incidence is nearly equal.

However, even though we have already stated that each zone has nearly the same area, the contributions from adjacent zones may act to cancel each other because of their relative phase relationships. The practical situation is made even more complex because, due to the obliquity factor, higher-order zones contribute less energy than lower-order zones. The overall picture is that at the receiver the total field from all other zones is about 50% of that from the first zone alone. Thus clearance of the radiated field to the first Fresnel zone is very critical if an unobstructed transmission

path is to be approximated and equation (5.25) is to be valid. Normally, it is assumed that diffraction of the beam, hence attenuation, will occur if more than 57% of the first Fresnel zone is obstructed [28]. To see how this result is obtained, consider the following: if we consider the ratio of actual path clearance radius  $r_n$  to the first Fresnel zone radius  $r_1$  to be  $\sqrt{n} = r_n/r_1$  and let the attenuation relative to free space,  $\alpha$ , be defined as

$$\alpha = -20 \log_{10}(E/E_0) \quad (5.88)$$

where  $E$  is the received signal strength when transmitted over a plane surface (which is acting as an imperfect reflector/absorber), and  $E_0$  is the received signal strength when transmitted through free space, then from [27] for a perfectly reflecting plane surface and small grazing angle:

$$\alpha = -6 - 10 \log \left( \sin^2 \left( \frac{n\pi}{2} \right) \right) \text{dB} \quad (5.89)$$

Examination of equation (5.89) shows that at  $n = 0$  attenuation is infinite, i.e. the signal is at grazing incidence to the reflecting surface.

When no Fresnel zone obstruction occurs due to lack of proximity to a plane reflecting surface, i.e. the free-space condition, we have 0 dB attenuation, thus from equation (5.89)

$$n = \frac{2}{\pi} \sin^{-1} \sqrt{10^{-6/10}} = 0.334 \text{ or } (n)^{1/2} = 0.578 \quad (5.90)$$

giving the 57% rule suggested above.

### Exercise 5.7

Consider a link design where an obstruction is placed halfway along a point-to-point line of sight with a length of 1 km operating at 10 GHz. For this situation, calculate the minimum clearance required for the obstruction to lie outside of the first Fresnel zone.

#### Solution

If the indirect ray strikes the ground approximately halfway between transmitter and receiver then the clearance required is given by equation (5.85):

$$d_1 = d_2 = d \quad (5.91)$$

$$r \approx \left( \frac{d\lambda}{2} \right)^{1/2} \quad (5.92)$$

$$= \sqrt{(400 \times 0.03)}$$

$$= \sqrt{12}$$

$$= 3.5 \text{ m}$$

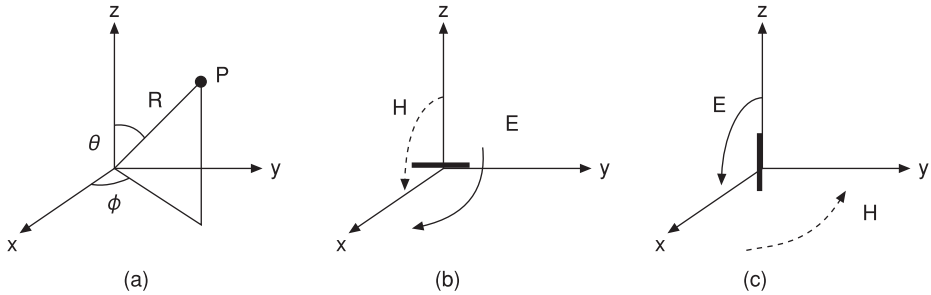


Figure 5.7 Three dimensional Cartesian polar coordinate system definitions

## 5.7 Antenna characterisation principles

In order to define the performance of an antenna, factors such as radiation pattern, beamwidth, bandwidth and gain have to be assessed.

To ascertain the beamwidth of the antenna under test, ideally it is necessary to map its radiated energy over the three-dimensional sphere enclosing the antenna in its far field as defined by the polar coordinate system in Figure 5.7. This assessment enables factors such as side lobe levels to be found. Other features such as gain, beamwidth and polarisation response can also be determined.

Normally, far-field assessment is carried out on an open-area test site or in an anechoic chamber. In an anechoic environment, RF-absorbing materials are used to simulate open-area test conditions, which can be reproduced approximately subject to the conditions given in Sections 5.5 and 5.6. Where the available measurement space is limited, a compact antenna range lined with radar-absorbing material can be used [33].

Full three-dimensional volumetric assessment of the far-field radiation pattern is very time-consuming, and it requires massive data storage and good graphic visualisation tools. For this reason, antenna characterisation is normally carried out over sectional cuts through the sphere; in particular, two principal, or cardinal, planes are often used to characterise the performance of the antenna under test. This reduces the amount of measurement data required.

With reference to Figure 5.7a, these planes are the azimuth pattern ( $x$ - $y$ ) plane, or, phi ( $\phi$ ) cut, here  $\theta = 90^\circ$  and  $360^\circ \leq \phi < 0^\circ$ , and the elevation pattern ( $x$ - $z$ ) or theta ( $\theta$ ) cut, i.e.  $\phi = 0^\circ$ ,  $360^\circ \leq \theta < 0^\circ$ . Under these conditions, polarisations are defined as  $E_\theta$  for vertical polarisation and  $E_\phi$  for horizontal polarisation.

For a linear horizontally polarised antenna oriented along the  $x$ -axis, the  $E_\phi(\theta, \phi = 0^\circ)$  cut corresponds to the  $H$ -plane pattern, while the  $E_\theta(\theta = 90^\circ, \phi)$  corresponds to the  $E$ -plane pattern (Figure 5.7b). For a purely linear vertically polarised antenna oriented along the  $z$ -axis, the  $E_\theta(\theta, \phi = 0^\circ)$  far-field radiation is the  $E$ -plane pattern, while the  $E_\phi(\theta = 90^\circ, \phi)$  pattern is the  $H$ -plane pattern (Figure 5.7c).

Radiated energy that is transmitted and received in the same polarisation plane is called co-polar radiation, while energy received with the orthogonal polarisation response is termed cross-polarisation. The amount of cross-polarisation radiation found in a practical situation helps to define the degree to which the polarisation purity of an antenna has been corrupted due to imperfections in its design, manufacture or characterisation.

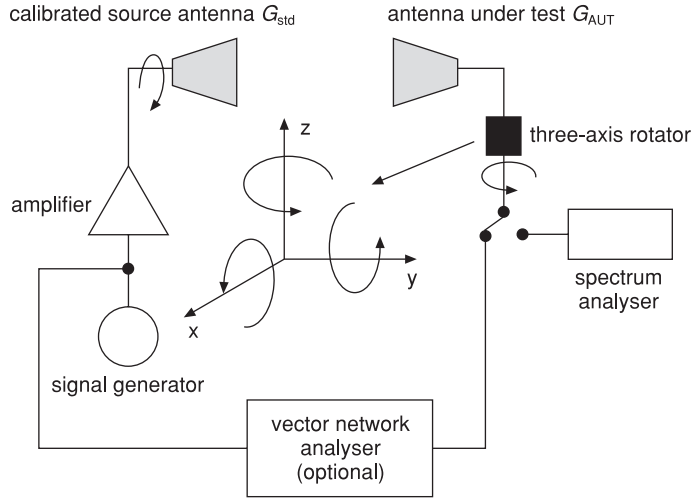


**Figure 5.8** Antenna test set-up

In order to determine the far-field radiation characteristics of the antenna under test (AUT) in Figure 5.8, i.e. its far-field radiation pattern, two antennas are required: the one being tested, which is normally free to rotate and which is connected to a receiver; and one that is normally fixed and is connected as the transmitter. The AUT is rotated by a positioner, which can have one, two or three degrees of freedom of rotation (Figure 5.8).

As the AUT is rotated, the received field strength is measured by a spectrum analyser or power meter, or after suitable down conversion by a tuned receiver. Alternatively, a vector network analyser can be used to measure the input impedance to the AUT,  $S_{11}$ , and the transmission path,  $S_{12}$ ,  $S_{21}$ , between source and test antennas (see Appendix 8.4 for the definitions of  $S$ -parameters).

For circularly polarised antenna measurements, a spinning dipole technique can be used, in which case the source antenna is rotated at high speed as the position of the AUT is varied. Here the envelope of the radiation pattern of the AUT gives information on polarisation ellipsicity [34]. Other schemes exist for the measurement of circularly polarised elements: the main variants are known as the linear component method and the circular component method [33]. In general, in point-to-point communication systems not only should the transmit and receive antennas be polarisation-matched but also the tilt angle should be aligned for maximum coupling and hence power transfer.

The complex voltages in the horizontal and vertical planes,  $E_H$  and  $E_V$ , can be combined to express the RHCP and LHCP wave components [33]:

$$E_{RHCP} = \frac{1}{\sqrt{2}}(E_H + jE_V) \quad (5.93)$$

$$E_{LHCP} = \frac{1}{\sqrt{2}}(E_H - jE_V) \quad (5.94)$$

The radiation patterns that are generated by a CP antenna can therefore be obtained by combining the amplitude and phase response of two orthogonal linearly polarised waves at each measurement angle using equations (5.93) and (5.94). Here the phases of the two field components are measured relative to the signal generator providing excitation to the antenna under test. By making separate horizontal and vertical plane measurements, rectangular horn antennas (due to their low cross-polarisation characteristics) can be used in an actual experimental set-up.

Horn antennas, section 7.7, unlike circularly polarised antennas, exhibit very low levels of cross-polarisation over broad frequency bands, thereby eliminating a major source of error in the measurement of circular polarisation (CP). Equations (5.93) and (5.94) can be expanded to give simple expressions that can be used to convert from dual linear to co-polar and cross-polar CP power at each measurement angle. Let the real and imaginary components of the horizontal and vertical response be expressed as

$$E_H = E_{H_r} + jE_{H_i} \quad (5.95)$$

$$E_V = E_{V_r} + jE_{V_i} \quad (5.96)$$

where

$$E_{H_r} = H_{AMP} \cos(H_{PHASE}) \quad (5.97)$$

$$E_{H_i} = H_{AMP} \sin(H_{PHASE}) \quad (5.98)$$

$$E_{V_r} = V_{AMP} \cos(V_{PHASE}) \quad (5.99)$$

$$E_{V_i} = V_{AMP} \sin(V_{PHASE}) \quad (5.100)$$

Here the horizontal and vertical amplitude ( $H_{AMP}$ ,  $V_{AMP}$ ) and phase ( $H_{PHASE}$ ,  $V_{PHASE}$ ) components are the quantities that are measured at each angle  $\theta$  in the far field of the antenna with the source horn positioned at angles  $\phi = 0^\circ$  and  $90^\circ$ , Figure 5.8. Inserting into equations (5.93) and (5.94) gives the relative field in the orthogonal polarisations:

$$E_{LHCP} = \frac{1}{\sqrt{2}} \left\{ \begin{array}{l} [H_{AMP} \cos(H_{PHASE}) + V_{AMP} \sin(V_{PHASE})] \\ + j[H_{AMP} \sin(H_{PHASE}) - V_{AMP} \cos(V_{PHASE})] \end{array} \right\} \quad (5.101)$$

$$E_{RHCP} = \frac{1}{\sqrt{2}} \left\{ \begin{array}{l} [H_{AMP} \cos(H_{PHASE}) - V_{AMP} \sin(V_{PHASE})] \\ + j[H_{AMP} \sin(H_{PHASE}) + V_{AMP} \cos(V_{PHASE})] \end{array} \right\} \quad (5.102)$$

### Exercise 5.8

The radiation from a circularly polarised antenna is measured using an  $E$ -plane horn antenna. The vertical electrical field component is measured to be  $1.20E - 3 \angle -35^\circ$  while the horizontal electric field is  $1.28E - 3 \angle 112^\circ$ . Construct the left- and right-hand circular polarisation components of field from the vertical and measured field horizontal components.

**Solution**

Using equations (5.97) to (5.100), we calculate that  $E_{H_i} = -4.8E - 4$ ,  $E_{H_i} = 1.187E - 3$ ,  $E_{V_i} = -9.8E - 4$ ,  $E_{V_i} = -6.9E - 4$ .

Upon applying equations (5.101) and (5.102)

$$E_{\text{LHCP}} = \frac{1}{\sqrt{2}}[-11.7E - 4 + j2.07E - 4]$$

$$E_{\text{RHCP}} = \frac{1}{\sqrt{2}}[2.1E - 4 + j2.17E - 3]$$

thus

$$|E_{\text{LHCP}}| = 1.2E - 3, |E_{\text{RHCP}}| = 2.18E - 3$$

thus RHCP is dominant.

The power in each component can be expressed by

$$P(\text{dB}) = 10 \log_{10} \left( \frac{V^2}{377} \right) \quad (5.103)$$

where  $377 \Omega$  is the wave impedance in free space, and voltage  $V$  represents the individual co-polar and cross-polar field components that are expressed in equations (5.101) and (5.102). The far-field radiation pattern in each antenna polar-pattern cut ( $\phi$ ) is generated by plotting the parameters  $\theta$  (deg),  $P_{\text{RHCP}}$  (dB) and  $P_{\text{LHCP}}$  (dB). At a given angle  $\theta$  in the antenna radiation pattern, cross-polarisation is defined as the difference in the power level (equation (5.103)) between the RHCP and LHCP components. For a perfectly circular polarised pattern, this is  $-\infty$  dB (axial ratio = 0 dB), and for a linearly polarised signal, where the two CP signals are of identical magnitude, this is 0 dB (axial ratio =  $\infty$  dB).

**Exercise 5.9**

Calculate the axial ratio for the situation given in exercise 5.8.

**Solution**

Using equation (5.68)

$$|AR| = \frac{|E_{\text{co}}| + |E_{\text{cross}}|}{|E_{\text{co}}| - |E_{\text{cross}}|} \text{ etc.}$$

where  $E_{\text{co}}$  = LHCP or RHCP depending on the result from exercise 5.8, in this case RHCP. Hence

$$|AR| = \frac{2.18 + 1.2}{2.18 - 1.2} = 3.4$$

For antenna gain measurements the following approach is useful; from Section 2.4, we recast for convenience the antenna directivity as

$$\begin{aligned}
 D &= \frac{\text{maximum radiation power density}}{\text{average radiation intensity}} \\
 &= 4\pi \frac{\text{maximum radiation power density}}{\text{total power radiated}} \\
 &= \frac{4\pi E_{\max}^2(\theta, \phi)}{\iint E^2(\theta, \phi) d\Omega}
 \end{aligned} \tag{5.104}$$

where  $\iint d\Omega$  indicates integration over a volume, and  $\Phi(\theta, \phi)$  (Section 2.4) is proportional to the square of field pattern electric field strength.

Now if field pattern is used instead of power density, and this is itself normalised to its own peak level, then we can write

$$D = \frac{4\pi}{\iint E^2(\theta, \phi) d\Omega} \tag{5.105}$$

However, noting that  $E(\theta, \phi)$  is the total field at any point and is made up of two orthogonal components,  $E_1(\theta, \phi)$  and  $E_2(\theta, \phi)$ ,

$$D = \frac{4\pi}{\iint [E_1^2(\theta, \phi) + E_2^2(\theta, \phi)] d\Omega} \tag{5.106}$$

Thus, to find the antenna directivity from measured patterns, two polarisations must be measured over an entire sphere and,  $E_1(\theta, \phi)$ ,  $E_2(\theta, \phi)$  found. This can be done by taking a series of appropriate  $\phi$  cuts for different  $\theta$  values.

Antenna gain can be measured by a comparison method, subject to the clearance and antenna separation criteria established in Sections 5.5 and 5.6. Antennas operating at low frequencies and with broad radiation patterns are among the most difficult to measure. A known radiation power level is radiated from a source antenna and is received by the antenna under test, which is assumed to be perfectly matched. The value of the received signal,  $S_{R1}$ , is noted and the test antenna is replaced with a standard reference antenna (normally a half-wave dipole, absolute gain 2.5 dBi) whose gain is known at the same operating frequency of the antenna under test and the new received signal strength,  $S_{R2}$ , noted. Again the reference antenna is assumed to be perfectly matched to the transmit or receive instrumentation; hence the resultant gain  $G$  can be obtained as

$$G = 10 \log_{10}(S_{R2}/S_{R1}) \tag{5.107}$$

from which the gain of the antenna under test relative to an isotropic source can be found as

$$G_{\text{AUT}} = 10 \log_{10}(1.64G) \text{ dBi}$$

If two identical antennas exist, then the absolute gain technique described below can be used. Here the Friis transmission formula given in Section 5.2 is used, since

$$\frac{P_r}{P_t} = \frac{A_{er}A_{et}}{\lambda^2 r^2} \quad (5.108)$$

For identical antennas,  $A_{er} = A_{et} = A_e$  = effective area of the antenna(s) and subscripts t and r denote transmit and receive, respectively.

$$A = G_{\text{AUT}} \frac{\lambda}{4\pi} \quad (5.109)$$

where  $G_0$  is the antenna(s) under test gain relative to an isotropic source. Then

$$\frac{P_r}{P_t} = \frac{G_{\text{AUT}}^2}{(4\pi)^2 r^2} \quad (5.110)$$

or

$$G_{\text{AUT}} = 4\pi r \sqrt{\frac{P_r}{P_t}} \quad (5.111)$$

Hence the gain of the antenna is forthcoming.

The gain substitution method is one of several techniques that can be used to provide an accurate measurement of the absolute gain of a CP antenna [33]. This requires the beam and axial ratio peak of the antenna under test (AUT) to be located and the power level compared when the AUT is replaced with a gain-standard  $G_{\text{std}}$ , which is referenced to an isotropic source (Figure 5.8). Above 1 GHz, linearly polarised horns are normally used for both the source and gain reference antennas. The gain,  $G_{\text{AUT}}$ , of the AUT referenced to a linear isotropic source, 'il', is determined from the difference in the measured power level  $\Delta$  thus:

$$G_{\text{AUT}} (\text{dBil}) = G_{\text{std}} - \Delta \quad (5.112)$$

For a polarisation-pure AUT, the absolute gain of the antenna referenced to a circularly polarised isotropic source, 'ic', can then be expressed as

$$G_{\text{AUT}} (\text{dBic}) = G_0 + 3 \quad (5.113)$$

The 3 dB increase in gain in equation (5.113) represents the difference in the power received by a linear isotropic and a circular isotropic antenna when these are illuminated by a polarisation-pure CP signal wave. However, practical antennas generate cross-polar power, which results in an elliptically polarised field pattern. Therefore a correction factor  $G_C$  must be applied to compensate for the finite axial ratio  $AR$ , which is measured at the beam peak. Thus

$$G_C (\text{dB}) = 20 \log_{10}[0.5(1 + 10^{-AR/20})] \quad (5.114)$$

hence antenna gain can be calculated using the expression

$$G_{\text{AUT}} (\text{dBic}) = G_{\text{AUT}} + G_C + 3 \quad (5.115)$$

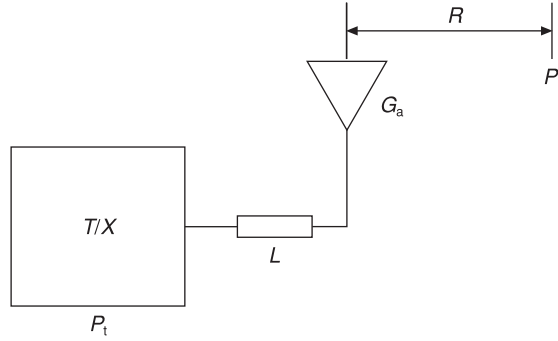


**Figure 5.9** Electric field strength assessment for transmitter

For equipment calibration, absolute field strength measurements are often required. Consider the measurement set-up shown in Figure 5.9 [35]; here the power density at a distance  $r$  from the transmitting antenna is, according to Section 5.2,

$$P_r = \frac{P_T G_a L}{4\pi R^2} \text{ (W/m}^2\text{)} \quad (5.116)$$

where  $P_r$  = received power,  $P_T$  = transmitted power,  $R$  = distance to observation point,  $L$  = cable loss and  $G_a$  = transmit antenna gain.

We know that time-averaged power is  $|E^2|/\eta$  (Section 2.3), thus the field strength at a distance  $r$  from a source is

$$E = 19.4\sqrt{P_r} \text{ (V/m)} \quad (5.117)$$

which in dB yields

$$P_r = -11 - 20 \log_{10} R + P_T + G_a - L \text{ (dBW/m}^2\text{)} \quad (5.118)$$

from which

$$E = 15 - 20 \log_{10} R + P_T + G_a - L \text{ (dBV/m)} \quad (5.119)$$

Subtracting these and converting power density to field strength, we get

$$E = 26 + P \text{ (dBW/m}^2\text{)} \quad (5.120)$$

Thus we can express the power density from the transmitting antenna in terms of electric field intensity. It is also possible to convert the power received to field strength; Figure 5.10 shows the model used. Here the received power density is given by

$$P_r = \frac{4\pi P_T}{\lambda^2 G_a L} \text{ (W/m}^2\text{)} \quad (5.121)$$

As before, field strength  $E$  is

$$E = 19.4\sqrt{P_r} \text{ (V/m)}$$

Hence

$$P_d = 11 - 20 \log_{10} \lambda + P_r - G_a - L \text{ (dBW/m}^2\text{)} \quad (5.122)$$

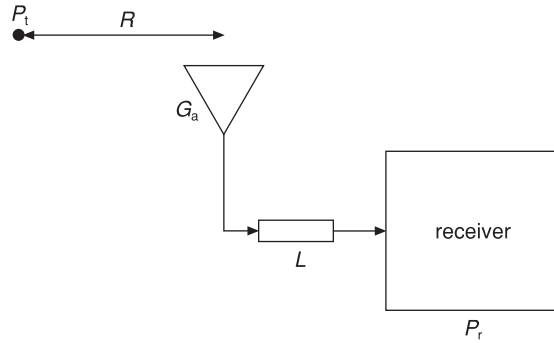


**Figure 5.10** Electric field strength assessment for receiver

and

$$E = 37 - 20 \log_{10} \lambda + P_r - G_a - L \text{ (dBV/m)} \quad (5.123)$$

To convert received signal voltage to field strength or to power density, let us define the input power incident on a field strength measuring instrument as

$$P_r = \frac{V^2}{Z_\ell} \text{ (W)} \quad (5.124)$$

where  $Z_\ell$  is the input impedance of the field strength measuring apparatus (normally this will be  $50 \Omega$ ) and  $V$  is the rms voltage reading on the field strength measuring instrument, in which case power density at the antenna aperture,  $P_T$ , is

$$P_T = \frac{4\pi V^2}{50} \frac{1}{\lambda^2 G_a L} \text{ (W/m}^2\text{)} \quad (5.125)$$

and the electric field strength at the antenna aperture is

$$E = \frac{4\pi V}{\lambda G_a} \frac{30}{L Z_\ell} \text{ (V/m)} \quad (5.126)$$

From the above two equations:

$$P_d = -6 - 20 \log_{10} \lambda - G_a + V - L \text{ (dBW/m}^2\text{)} \quad (5.127)$$

and

$$E = 19.8 - 20 \log_{10} \lambda - G_a + V - L \text{ (dBV/m)} \quad (5.128)$$

### Exercise 5.10

A receive antenna has 10 dB gain and is connected to an antenna using a cable with 3 dB loss. The cable, antenna and intensity meter are impedance-matched, and the received signal frequency is 1 GHz. Calculate the electric field intensity at the aperture of the receiving antenna for a measured intensity reading of  $20 \text{ dB}\mu\text{V}$ .

**Solution**

Using equation (5.128) to obtain electric field intensity at the receive antenna aperture:

$$20 \text{ dB}\mu\text{V} = 10 \mu\text{V} \text{ or } -100 \text{ dBV}$$

$$\begin{aligned} E &= 19.8 - 20 \log(0.3) - 10 - 3 - 100 \\ &= -103.7 \text{ dBV/m.} \end{aligned}$$

The first three terms in equation (5.128) constitute the antenna factor, which is widely used in instrumentation for laboratories characterising field strength levels in electromagnetic compatibility (EMC) problems:

$$\text{antenna factor} = 19.8 - 20 \log_{10} \lambda - G_a \text{ (dB)} \quad (5.129)$$

Once the antenna factor is known, by calculation or from the antenna manufacturer's data sheet for a calibrated antenna, then electric field strength can be found as

$$E = \text{antenna factor} + V - L \text{ (dBV/m)} \quad (5.130)$$

Thus the antenna factor is very important in making calibrated radiated electric field strength measurements.

Due to the linear properties of the equations governing electromagnetism, i.e. Maxwell's equations, an antenna operating at a known frequency  $f$  will have identical behaviour at another frequency  $kf$ , provided that a number of criteria are adhered to [36]:

- All linear dimensions are scaled by  $1/k$ .
- Relative dielectric constant values in the antenna structure should remain the same at both frequencies, i.e. should not be a function of frequency.
- Relative permeability values should remain the same at both frequencies, i.e. should not be a function of frequency.
- All material conductivity values should scale by  $k$ .

In general, all of these parameters can be scaled relatively easily, with the exception of conductivity; however, the operation of many antenna structures does not rely critically on conduction losses.

Theoretically, a perfectly constructed scale model will exhibit the same radiation and impedance characteristics as its full-size counterpart. Imperfections in the scaling process will affect impedance levels much more than radiation properties, and as such the impedance values normally derived from a scale model are considered to be approximate. In general, each case has to be carefully investigated in this respect.

Note: Equations 5.116 through 5.130, and Figures 5.9 and 5.10, are from *Engineering Applications of Electromagnetic Theory* by S. Liao © 1988. Reprinted with permission of Brooks/Cole, an imprint of the Wadsworth Group, a division of Thomson Learning.

**References**

- [25] Jordan, E.C. and Balmain, K.G., *Electromagnetic Waves and Radiating Systems*, 2nd edition, Prentice Hall, 1968, pp. 350–3.
- [26] Kraus, J.D., *Antennas*, 2nd edition, McGraw-Hill International Editions, 1988, p. 42.
- [27] Ramo, S., Whinnery, J.R. and Van Duzer, T., *Fields and Waves in Communication Electronics*, John Wiley & Sons, 1967, pp. 715–19.
- [28] Townsend, A.A.R., *Analog Line-of-Sight Radio Links (A Test Manual)*, Prentice Hall, 1987, pp. 129–32.
- [29] Mumford, W.W. and Scheibe, E.H., *Noise Performance Factors in Communications Systems*, Horizon House, 1968.
- [30] Benoit, H., *Satellite Television, Techniques of Analogue and Digital Television*, Arnold Co., published by John Wiley & Sons, 1999.
- [31] Smith, G.S., *An Introduction to Classical Electromagnetic Radiation*, Cambridge University Press, 1997.
- [32] Jasik, H., *Antenna Engineering Handbook*, McGraw-Hill, 1961, pp. 34–29, 34–30.
- [33] Evans, G.E., *Antenna Measurement Techniques*, Norwood, Mass., Artech House, 1990.
- [34] *Antenna Measurements*, Hewlett-Packard Application Note 374-1, 1998.
- [35] Liao, S.Y., *Engineering Applications of Electromagnetic Theory*, West Publishing Company, 1988, pp. 406–11.
- [36] Balanis, C.A., *Antenna Theory Analysis and Design*, 2nd edition, John Wiley & Sons, 1997.

**Problems**

- 5.1 A radio station operating at 300 kHz has a vertical antenna placed over a perfectly conducting ground plane. The height of the antenna is 106 m. The antenna is excited between its base and the ground plane. Calculate the effective length of the antenna and its radiation resistance as referenced to the feed point. You may assume that the current distribution along the antenna is linear, going from a maximum at the base to zero at the top of the antenna. How appropriate is this assumed linear current distribution assumption?
- 5.2 For the problem given in 5.1, when a radial set of horizontal wires is attached to the antenna the current at the top of the antenna increases to 25% of the base current. Calculate the effective height and radiation resistance for the modified antenna.
- 5.3 A satellite is in geosynchronous orbit around the Earth, i.e. it is positioned at 36,000 km above the equator and is equipped with a 100 W transmitter operating at 12 GHz. Calculate the effective isotropic radiated power (EIRP) if the parabolic

satellite transmit antenna has a 1 m diameter and is assumed to be 90% efficient. Assuming that the receive antenna also has 1 m diameter and 90% efficiency, calculate the power available at the output from the receive antenna.

- 5.4** For the problem in 5.3, the receiver connected to the output of the receive antenna needs to produce a signal-to-noise ratio of 12 dB to guarantee service operation for 99.9% of the time. What is the minimum G/T ratio required for the system? You may assume that channel bandwidth is 27 MHz and that the low-noise receiver has an equivalent noise temperature of 160 K.
- 5.5** In areas of weak television reception, it is sometimes necessary to mount the receive antenna on a mast. The antenna is connected to the television receiver by a lossy coaxial cable. If the cable has 3 dB loss and the television receiver has 90 dB gain and 12 dB noise figure, calculate the overall noise figure for the system. If a high-gain low-noise pre-amplifier (gain 20 dB, 4 dB noise figure) is introduced between the antenna and its connection to the coaxial cable, calculate the improvement in overall system noise figure that results.
- 5.6** An electromagnetic wave propagating in the z-direction has its electric field vector  $\mathbf{E}$  defined as

$$\mathbf{E} = 4 \sin(\omega t - \beta z) \mathbf{i} + 6 \sin\left(\omega t - \beta z - \frac{\pi}{4}\right) \mathbf{j}$$

For this wave, calculate the inclination angle of the polarisation ellipse, the sense of rotation of the wave and the axial ratio of the ellipse. What modifications would be required to the amplitude and phase relationships of the describing equation to produce a left-hand circularly polarised signal?

- 5.7** What is the first Fresnel zone radius about the main beam at 1 km for an antenna on a 10 km single-link hop if the frequency of the carrier signal is 2.4 GHz?
- 5.8** Calculate the antenna calibration factor for a half-wave dipole designed to operate at 1 GHz. When this antenna is connected to a cable having 0.5 dB loss, the power available at the receiver input terminals is  $-10$  dBm. Under these conditions, what is the measured electric field strength in dBV/m?

# Antenna-matching techniques

---

In order for an antenna or antenna array to be useful, it must be connected to a transmitting or receiving device. Often the terminal impedance of a transmitter or receiver is either 50 or 75  $\Omega$ . However, the same cannot be said for the input terminal impedance of the antenna element, which can exhibit, particularly off-resonance, a reactive component, which can be capacitive or inductive, in conjunction with a resistive part, both of which can change over a wide range of values as frequency varies. Therefore, what is usually required is to create an electrical network that can interface the antenna to the transmitter or receiver such that maximum power transfer can occur. This is achieved by transforming by impedance matching the input impedance of the antenna or array to that of the device to which it is to be connected. Normally, this is done at the band centre, or resonant frequency, of the element or array for a narrowband antenna or over a preselected bandwidth for a wideband antenna. In the later case, more elaborate matching networks are required than for the former case.

With this in mind, in this chapter we first establish the terminology then the figures of merit used to define the properties of a uniform transmission line. This investigation leads to the fundamental concepts of transmission line propagation velocity, attenuation and reflection coefficients, hence voltage standing wave ratio (VSWR). This last quantity, VSWR, can then be used to define the quality of power transfer from antenna to load.

The concept of an attenuator or pad as a resistive matching technique is then introduced. Lossless matching methods using lumped circuits are developed. These methods, while narrowband, are generally adequate for matching resonant antennas with a few per cent bandwidth and have the advantage that for ideal elements they do not introduce additional noise into the system.

Dipole and other types of balanced antenna structures often have to be fed or to feed equipment with unbalanced, coaxial connections. To facilitate this, the operation of a variety of balanced to unbalanced transformer types, baluns, are described. When creating arrays of antennas, it is necessary to excite the individual elements

comprising the array with currents whose relative amplitude and phases are known in advance and whose values have been prescribed by the required application. This involves creating a feed network for the array chosen to set the required current amplitudes. These are then interconnected with suitably adjusted lengths of uniform transmission lines selected to give the necessary phase distribution. The basic techniques used to create the power splitting (combiners) that is required for these networks are discussed.

Classically, and currently the most powerful graphical method for designing a wide variety of impedance matching networks is the Smith chart, invented in 1939 by P.H. Smith, then an engineer at Bell Telephone Laboratories. Elementary applications of the Smith chart are described in conjunction with stub and quarter-wavelength transformer matching based on the philosophy of sending end impedance.

## 6.1 Transmission line principles

An appreciation of transmission line techniques is important when studying antennas, since ultimately a connection between the antenna and the receive/transmit electronics is required for an operational system to be realised. The purpose of this section is to introduce some useful concepts that will facilitate the design of the antenna/system or in the case of an antenna array the antenna/harness interface.

A section of uniform transmission line for use as a guiding medium for electromagnetic energy can be described approximately by decomposing a finite section of the line into very short segments. Each segment has length  $\Delta\ell$  and is composed of a series loss resistance,  $R$ , representing conductor loss. Support dielectric material losses are represented by a shunt conductance,  $G$ . The series inductance and shunt capacitance of the line are represented by  $L$  and  $C$ , respectively.  $L$ ,  $C$  and  $G$  are normally defined on a per unit length basis (Figure 6.1).

In Figure 6.1a, for an infinitely long uniform transmission line  $V_1/I_1 = V_2/I_2 = Z_0$ , where  $Z_0$ , the characteristic impedance of the line, is defined below. In general,  $Z_0$  is frequency-dependent and can be complex. Under the condition when the line is terminated in an impedance of  $Z_0$ , the line is said to be perfectly matched, i.e. no energy is reflected from the termination.

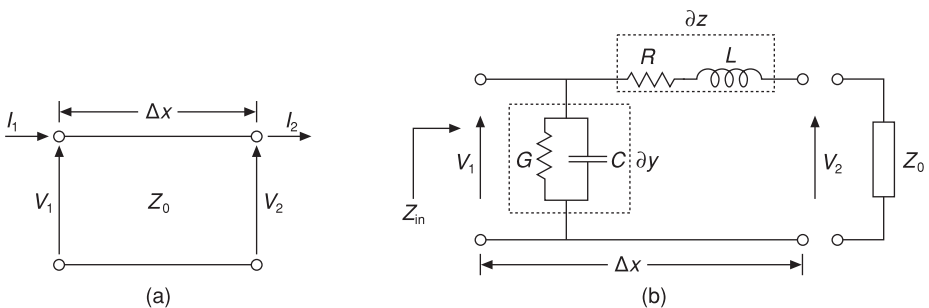


Figure 6.1 Lumped transmission line

For the  $L$  section shown in Figure 6.1b terminated in impedance  $Z_0$ , its input impedance,  $Z_{in}$ , is the parallel combination of the series impedance components  $Z_0$  and  $\partial z$  and the shunt admittance component  $\partial y$  (shunt impedance  $1/\partial y$ ).

$$Z_{in} = \frac{(Z_0 + \partial z)}{\partial y} \bigg/ (Z_0 + \partial z + 1/\partial y)$$

$$Z_{in} = \frac{Z_0 + \partial z}{1 + Z_0 \partial y} = Z_0 \quad (6.1)$$

where  $\partial z \partial y \cong 0$  as  $\partial y$  and  $\partial z$  tend to zero. Hence

$$Z_0 = \left( \frac{\partial z}{\partial y} \right)^{1/2} \quad (6.2)$$

from Figure 6.1,  $\partial z = R + j\omega L$  and  $\partial y = G + j\omega C$ . Therefore

$$Z_0 = \left( \frac{R + j\omega L}{G + j\omega C} \right)^{1/2} \Omega \quad (6.3)$$

At very low frequencies  $\omega \approx 0$ , so

$$Z_0 \approx \left( \frac{R}{G} \right)^{1/2} \Omega \quad (6.4)$$

while at very high frequencies, where for high-quality transmission line materials  $\omega L \gg R$  and  $\omega C \gg G$ ,

$$Z_0 \approx \left( \frac{L}{C} \right)^{1/2} \Omega \quad (6.5)$$

Now, from Figure 6.1b, the voltage drop  $\Delta V$  across one incremental line segment  $\Delta x$  is

$$\Delta V = V_2 - V_1 = -I(R + j\omega L)\Delta x \quad (6.6)$$

or in the limit as  $\Delta x$  tends to zero:

$$\frac{\partial V}{\partial x} = -I(R + j\omega L) \quad (6.7)$$

Similarly, for the shunt arm

$$\frac{\partial I}{\partial x} = -V(G + j\omega C) \quad (6.8)$$

Differentiating equation (6.7) and substituting equation (6.8) yields the one-dimensional wave equation:

$$\frac{\partial^2 V}{\partial x^2} = -\psi^2 V \quad (6.9)$$

where

$$\psi = ([R = j\omega L][G + j\omega C])^{1/2} \quad (6.10)$$

This is called the propagation constant for the line and is generally expressed as

$$\psi = \alpha + j\beta \quad (6.11)$$

Here  $\alpha$  is the line attenuation per unit length, and  $\beta$  is the phase shift per unit length ( $2\pi/\lambda_g$ );  $\lambda_g$  is the wavelength of the guided signal, which will be different from the wavelength for a free-space factor by a slowing factor determined by the permittivity of the dielectric filling material of the line. In general, this slowing factor is inversely proportional to the square root of the dielectric constant filler material.

The voltage across the line inductance will lead the current  $I$  across it by some angle  $\partial\beta$ , such that

$$\partial\beta = \tan^{-1}\left(\frac{\omega L I \partial x}{I Z_0}\right) \quad (6.12)$$

For small angles  $\tan\theta \approx \theta$ , so for a small length  $\partial x$

$$\partial\beta \approx \frac{\omega L}{Z_0} \partial x$$

or

$$\partial\beta \approx \frac{\omega L}{(L/C)^{1/2}} \partial x = \omega(LC)^{1/2} \partial x$$

So the phase change per unit length  $\beta$  is equal to

$$\beta \approx \omega\sqrt{LC} \quad (6.13)$$

This can be worked further, since we know from Section 2.2 that the velocity of propagation, denoted now as  $v_p$ , the phase velocity of the phase front of a propagating signal, is given as

$$v_p = f\lambda_g = \frac{\omega}{2\pi} \lambda_g \quad (6.14)$$

By definition

$$\lambda = \frac{2\pi}{\beta}$$

hence

$$v_p = \frac{\omega}{\beta} \text{ m/s} \quad (6.15)$$

or

$$v_p = \frac{1}{(LC)^{1/2}} \text{ m/s} \quad (6.16)$$

Also for a lossy line using Figure 6.1a, we note that since for a uniform transmission line whose impedance,  $Z_0$ , the characteristic impedance of the transmission line, is constant with length:

$$\frac{V_1}{I_1} = \frac{V_2}{I_2} = \dots = \frac{V_n}{I_n} \quad (6.17)$$

and  $I_{n+1} = kI_n$ , where  $k$  is a constant related to attenuation. Therefore, as the signal progresses along the line, we can write

$$Z_0 = \frac{V_1}{I_1} = \frac{V_2}{kI_1} = \frac{V_3}{k^2I_1}, \text{ etc.} \quad (6.18)$$

so that

$$V_{n+1} = V_1 k^n \quad (6.19)$$

or

$$\log_e \left( \frac{V_{n+1}}{V_1} \right) = \log_e k^n \quad (6.20)$$

If  $k$  is made equal to  $\exp(-\alpha x)$ , the left-hand side of equation (6.20) becomes  $-n\alpha x$ . Thus the total attenuation of the line is  $n\alpha x$  and is given in units called *nepers*.

If we now say that the power delivered to the load is  $P_L$  and the power input to the line is  $P_i$ , then the line loss or attenuation in decibels must be

$$\text{loss (dB)} = 10 \log_{10} \frac{P_L}{P_i} \quad (6.21)$$

but

$$P_L = V_L I_L \text{ and } P_i = V_i I_i$$

so

$$\frac{P_L}{P_i} = \frac{V_L I_L}{V_i I_i} \quad (6.22)$$

Using equation (6.20) with the exponential decay factor included, we see that

$$\exp(-\alpha x) = \frac{V_L}{V_i} \quad (6.23)$$

Alternatively

$$\exp(-\alpha x) = \frac{I_L}{I_i} \quad (6.24)$$

Inserting equations (6.23) and (6.24) into equation (6.22) gives

$$\frac{P_L}{P_i} = \exp(-2\alpha x)$$

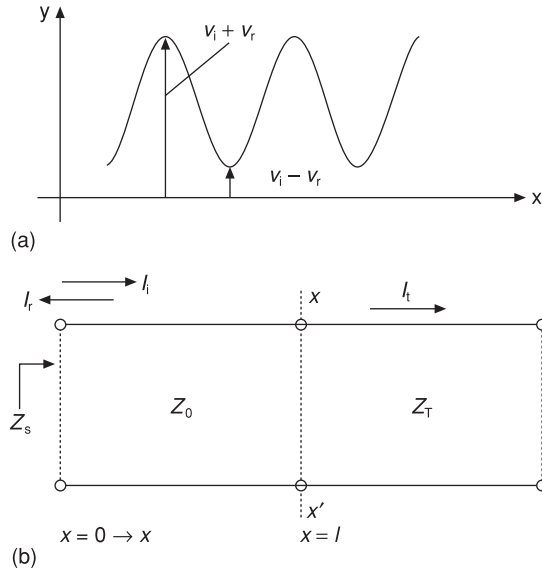


**Figure 6.2** Standing wave formation in an unmatched transmission line

or in more familiar units

$$\begin{aligned}
 \text{loss (dB)} &= 10 \log_{10}[\exp(-2\alpha x)] \\
 &= -20\alpha x \log_{10}(\exp(1)) \\
 &= -8.686\alpha x
 \end{aligned} \tag{6.25}$$

thus 1 neper =  $-8.686$  dB.

If the line is not perfectly terminated in its own characteristic impedance it is said to be mismatched, and as a result, some of the energy in the signal incident on the load will be reflected back along the line; if the line is resonant then a standing wave will be formed. Here energy travelling in the forward direction along the line and energy travelling in the reverse direction along the line act to form field maxima (nodes) and field minima (antinodes) at specific (stationary with respect to distance) positions along the line. We will see later that this situation can be very problematical when the transmission line load is an antenna.

In Figure 6.2a, let  $v_i$  be the incident wave and  $v_r$  the reflected wave; the ratio of antinode to node voltage is called the VSWR or voltage standing wave ratio and is defined from Figure 6.2 as

$$\text{VSWR} = \frac{|v_i| + |v_r|}{|v_i| - |v_r|}$$

VSWR is a unitless quantity ranging between 1 (no reflected signal) and  $\infty$  (all incident signals reflected) in value; peak or RMS voltage values can be used with equal facility.

Inspection of Figure 6.2b shows that across boundary  $x-x'$  for current continuity

$$I_t = I_i - I_r$$

where  $I_t$  denotes current transmitted through the boundary, and  $I_r$  and  $I_i$  denote reflected and incident currents, respectively. In terms of the line impedances, we write this as

$$\frac{v_i}{Z_0} - \frac{v_r}{Z_0} = \frac{v_T}{Z_T} \quad (6.26)$$

where  $v_T$  denotes total voltage amplitude. We also note that at boundary  $x-x'$

$$v_i + v_r = v_T$$

Hence we can define a new term, the reflection coefficient  $\Gamma$ , as being the ratio  $v_i/v_r$  at this interface. Between unequal impedance levels, this quantity must therefore be

$$\Gamma = \frac{v_i}{v_r} = \frac{Z_T - Z_0}{Z_T + Z_0} \quad (6.27)$$

where  $Z_T$  is the terminating impedance.

For a perfectly matched line,  $Z_T = Z_0$  and the reflection coefficient is zero, while for a short-circuit termination  $Z_T = 0$  hence  $\Gamma = -1$ , and for an open-circuit termination  $Z_T = \infty$ , giving  $\Gamma = +1$ . The reflection coefficient can also be expressed in decibels, as  $10 \log_{10} \Gamma$ , in which case it is referred to as return loss. It can also be expressed in terms of the VSWR as

$$\Gamma = \frac{\text{VSWR} - 1}{\text{VSWR} + 1} \quad (6.28)$$

### Exercise 6.1

Calculate the VSWR for a  $50 \Omega$  transmission line terminated in an antenna with impedance of  $73 - j32 \Omega$ .

#### Solution

From equation (6.27)

$$\Gamma = \frac{73 - j32 - 50}{73 - j32 + 50} = \frac{23 - j32}{123 - j32}$$

hence using equation (6.28)

$$\text{VSWR} = \frac{1 + |\Gamma|}{1 - |\Gamma|} = \frac{1 + 0.31}{1 - 0.31} = 1.9$$

Further more, if we observe that the incident power,  $P_i$ , in the transmission line must always be equal to the sum of the power lost to the line through dissipation,  $P_L$ , and reflection,  $P_r$ , then we can say that

$$\frac{P_L}{P_i} = \frac{P_i - P_r}{P_i} = 1 - \left( \frac{\text{VSWR} - 1}{\text{VSWR} + 1} \right)^2 = \frac{4\text{VSWR}}{(1 + \text{VSWR})^2} \quad (6.29)$$

This expression allows the amount of power delivered to the load for a given mismatch to be readily assessed. For example, a line VSWR of 2 implies that 89% of the available power reaches the load. Thus the lowest possible VSWR is highly desirable for maximisation of power transfer to the load. Also a low VSWR is important if an antenna is to be connected to the transmission line, since any received or transmitted energy will be reduced in all cases where  $VSWR \neq 1$  and system sensitivity or range are reduced as a consequence. In addition, any line mismatch will cause standing waves on the transmission line. In some situations, this may cause the antenna connecting cable to act as a secondary radiating element, leading to unpredictable results (see Section 6.4). In some high-power transmission applications, too high a VSWR may result in transmission line dielectric overvoltage breakdown as a large-amplitude standing wave is formed. This could be a potential problem in the feeder section to a high-power transmit antenna.

Another useful figure of merit in antenna systems design is insertion loss. Consider Figure 6.3, in which the insertion loss of a two-port network,  $L_1$ , is defined as

$$L_1 = 10 \log \frac{P_b}{P_a} \text{ dB} \quad (6.30)$$

where  $P_b$  is the power delivered to a load  $Z_L$  from a generator with impedance  $Z_g$  before connection of the network under test (Figure 6.3a), and  $P_a$  is the power delivered to the same load from the same generator but this time with the network under test connected (Figure 6.3b). It should be noted that insertion loss is given as a power ratio between quantities measured across the same terminals or network port.

The insertion loss of a two-port network may be positive, or it may be negative. The second situation occurs when the load impedance and generator impedance are not matched. Under these circumstances, a lossless matching network introduced between the load and generator will increase the power delivered to the load; thus  $P_a$  is larger

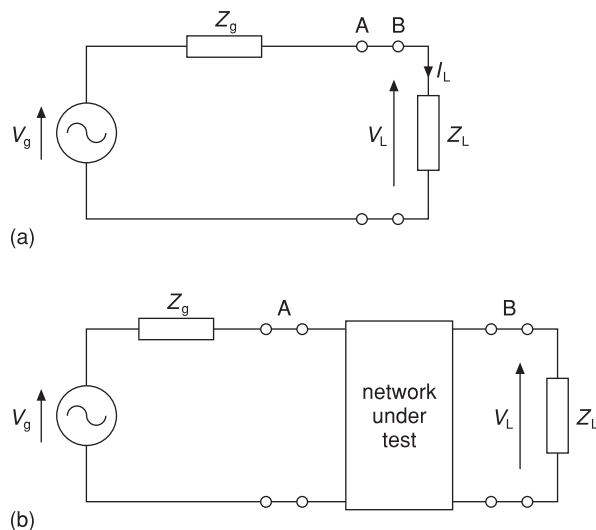


**Figure 6.3** Insertion loss: (a) network under test removed; (b) network under test connected

than  $P_b$ , giving a negative value for insertion loss. Sometimes this is considered to be an insertion gain, which for a passive network does not mean a gain in the classical sense, i.e. amplification; it simply means a more effective coupling of power to the load than would have occurred if the intervening network was not connected. For more elaborate formulations to deal with this situation, see [37].

In the following sections, we will consider how to design networks that provide impedance matching between input and output ports and that have known insertion loss characteristics.

## 6.2 Lumped matching circuits

Lumped matching circuits are useful at low frequencies where minimised area or hybrid matching circuits are to be provided. This class of circuit can consist of purely real or reactive components, or a mixture of both real and reactive components.

### Resistive L matching

Resistive matching necessitates low power loss and therefore provides a way of producing controlled attenuation between a transmitter and antenna or an antenna and a receiver; each can have different impedance levels.

To illustrate the approach, consider the simplest case of a resistive  $L$  section matching network (Figure 6.4). Here we wish to match two pure resistances,  $R_g$  and  $R_L$ , while introducing a known attenuation into the network; subscripts  $g$  and  $L$  refer to generator and load resistances, respectively.

For an impedance match on the input:

$$R_g = R_1 + \frac{R_2 R_L}{R_2 + R_L} \quad (6.31)$$

while for an impedance match on the output

$$R_L = \frac{R_2(R_1 + R_g)}{R_1 + R_2 + R_g} \quad (6.32)$$

Expanding equations (6.31) and (6.32) and letting  $R_g R_L = R_1 R_2$  yields

$$R_1 = (R_g(R_g - R_L))^{1/2} \quad (6.33)$$

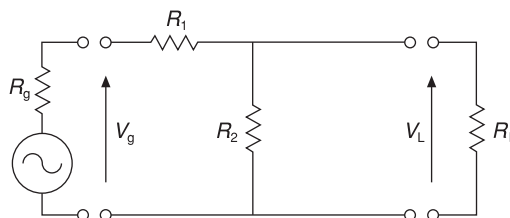


Figure 6.4 Resistive L-matching network

and

$$R_2 = \left( \frac{R_g R_L^2}{R_g - R_L} \right)^{1/2} \quad (6.34)$$

Here  $R_g > R_L$  and numerical values for  $R_g$  and  $R_L$  are normally specified at the outset.

By defining the attenuation of the circuit as  $V_g/V_L$ , we can write

$$\text{attenuation} = 20 \log_{10} \left[ \frac{V_g}{V_L} \right] = 20 \log_{10} \left[ \frac{R_2 R_L}{R_L(R_1 + R_2) + R_1 R_2} \right] \text{ dB} \quad (6.35)$$

A circuit designed according to these principles will act as a matched attenuator and is useful for setting power levels in a system or for protecting sensitive instrumentation from overload. However, it should be noted that this type of matching network will also add to the noise figure of the system into which it is inserted (Section 5.3). These attenuator networks, called pads, are sometimes used in antenna systems to reduce unwanted signal reflections. In addition, purely resistive networks have the advantage that they introduce zero phase shift to a signal passing through them.

### Exercise 6.2

An asymmetrical resistive matching network is to be used to match a  $75 \Omega$  generator to a  $50 \Omega$  characteristic impedance transmission line. Calculate the attenuation that occurs when the matching network is deployed.

#### Solution

From equations (6.31) through (6.35), we calculate that for  $R_g = 50 \Omega$ ,  $R_L = 75 \Omega$ , from equation (6.33)

$$R_1 = 43.3 \Omega$$

and from equation (6.34)

$$R_2 = \left( \frac{(50) \times (75)^2}{(75 - 50)} \right)^{1/2} = 106 \Omega$$

Hence, using equation (6.35)

$$\begin{aligned} \text{attenuation} &= 20 \log_{10} \left[ \frac{106 \times 50}{50(43.3 + 106) + (43.3 \times 106)} \right] \\ &= -7 \text{ dB} \end{aligned}$$

In a normal design situation, the characteristic impedance of the line into which the attenuator is to be inserted is specified. Generally, a characteristic impedance that has only a real component,  $50 \Omega$  or  $75 \Omega$ , with the  $50 \Omega$  level being the most common impedance level associated with a wide variety of communications equipment, is selected. For an air dielectric coaxial cable, the ratio of outer to inner radius,  $b/a$ , is 3.6 for the

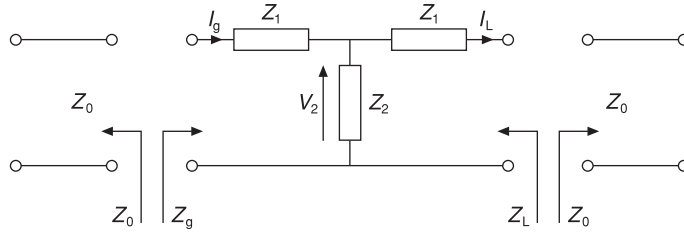


**Figure 6.5** General symmetrical T-network

minimum power loss condition. This ratio  $b/a$  corresponds to an air-spaced coaxial cable with  $77\ \Omega$  characteristic impedance (c.f.  $75\ \Omega$  used for low-loss TV downlead applications), while maximum power-handling capability occurs for an air dielectric coaxial cable when  $b/a = \sqrt{\epsilon}$ , i.e.  $30\ \Omega$  characteristic impedance. The average of these two values is  $53.5\ \Omega$ , thus the compromise impedance level used in most communications systems is the rounded-down value of  $50\ \Omega$ .

Consider a generalised representation of the attenuator design problem, now cast as a symmetrical T network (Figure 6.5). Using the same approach as above for the resistive L network

$$Z_g = Z_1 + \frac{Z_2(Z_1 + Z_L)}{Z_1 + Z_2 + Z_L} \quad (6.36)$$

We now wish to insert this network into a transmission line of characteristic impedance  $Z_0$ , such that  $Z_g = Z_L = Z_0$ . First we must establish an equivalent analogue between Figure 6.5 and a uniform transmission line of characteristic impedance  $Z_0$ . For a matched network

$$I_L = \left( \frac{Z_2}{Z_1 + Z_2 + Z_0} \right) I_g \quad (6.37)$$

but from basic transmission line theory (Section 6.1)

$$\frac{I_g}{I_L} = \exp(-\psi\ell) \quad (6.38)$$

where  $\psi$  is the propagation coefficient of a section of uniform transmission line of length  $\ell$ . Hence

$$\exp(-\psi\ell) = \frac{Z_2}{Z_0 + Z_1 + Z_2} \quad (6.39)$$

Solving equation (6.36) for  $Z_1$  with  $Z_g = Z_L = Z_0$  gives

$$Z_1 = Z_0 \frac{1 - \exp(-\psi\ell)}{1 + \exp(-\psi\ell)} \quad (6.40)$$

or

$$Z_1 = Z_0 \tanh\left(\frac{\psi\ell}{2}\right) \quad (6.41)$$

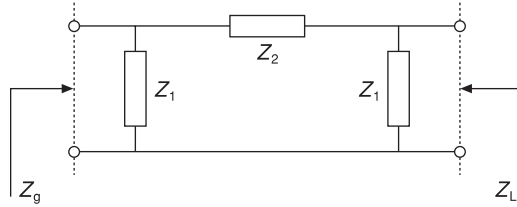


**Figure 6.6** Symmetrical PI-network

Similarly, solving for  $Z_2$  gives

$$Z_2 = Z_0 / \sinh(\psi \ell) \quad (6.42)$$

Equations (6.41) and (6.42) link lumped element impedances to uniform transmission line elements.

For the symmetrical PI model of a transmission line shown in Figure 6.6, the uniform transmission line equivalences are obtained using the same procedure as above:

$$Z_1 = Z_0 / \tanh\left(\frac{\psi \ell}{2}\right) \quad (6.43)$$

$$Z_2 = Z_0 \sinh(\psi \ell) \quad (6.44)$$

Now if we are interested in designing attenuators, we can exploit these equivalences.

We are dealing only with resistive components, so

$$Z_1 = R_1 = Z_0 \tanh\left(\frac{\alpha \ell}{2}\right) \quad (6.45)$$

Remember that a resistive component does not introduce a phase shift, so  $j\beta = 0$ , hence  $\psi = \alpha + j\beta$  reduces to  $\alpha$ , i.e. a loss only. After expanding the tanh term in equation (6.45) into exponent form, we get

$$R_1 = Z_0 \frac{\exp(\alpha \ell) - 1}{\exp(\alpha \ell) + 1} \quad (6.46)$$

Now because of the exponential term in equation (6.46) it is best to express attenuation not in decibels but in nepers,  $N$ , where by definition (Section 6.1),  $N = \exp(\alpha \ell)$ .

Where, as in this case,  $\ell$ , the length of a component, is very small compared with a wavelength at the lowest operating frequency, the component is assumed to be lumped. Thus for the symmetrical T network:

$$R_1 = Z_0 \left( \frac{N - 1}{N + 1} \right) \quad (6.47)$$

and

$$R_2 = Z_0 \left( \frac{2N}{N^2 - 1} \right) \quad (6.48)$$

By similar reasoning for the symmetrical PI network:

$$R_1 = Z_0 \left( \frac{N + 1}{N - 1} \right) \quad (6.49)$$

and

$$R_2 = Z_0 \left( \frac{N^2 - 1}{2N} \right) \quad (6.50)$$

So that if we specify the characteristic impedance of the line into which the attenuator is to be fitted, and we also specify how much loss we require, we have a complete specification for a design.

---

### Exercise 6.3

Design a single-section symmetrical PI, T network attenuator giving 20 dB attenuation for use in a 50  $\Omega$  system.

#### Solution

$$Z_0 = 50 \Omega$$

$$N = 10^{20/20} = 10$$

Thus for a PI network use equations (6.49) and (6.50):

$$R_1 = 50 \left( \frac{11}{9} \right) = 61 \Omega$$

$$R_2 = 248 \Omega$$

For a T network:

$$R_1 = 41 \Omega$$

$$R_2 = 10 \Omega$$


---

### Exercise 6.4

In general, when designing attenuators we must use preferred resistor values, i.e. the closest available values. This will mean that we cannot exactly realise our design specification. The selection of preferred-value components has two main effects: (1) the impedance match will be altered; and (2) the amount of attenuation obtained will be altered. For the T example above with preferred values used, the nearest value to 41  $\Omega$  becomes 47  $\Omega$ ; compute the implication that this has for the performance of the matching network in exercise 6.3. To see the implication of this, consider equation (6.36) with real components only.

**Solution**

$$Z_0 = R_1 + \frac{R_2(R_1 + R_2)}{R_1 + R_2 + Z_0}$$

Hence

$$Z_0 = (R_1^2 + 2R_1R_2)^{1/2} \quad (6.51)$$

and by defining attenuation using equation (6.38), then

$$\exp(\alpha\ell) = \frac{I_g}{I_L} = \frac{Z_0 + R_1 + R_2}{R_2}$$

After some manipulation, substituting this into equation (6.51) yields

$$\alpha\ell = \cosh^{-1}\left(1 + \frac{R_1}{R_2}\right)$$

or, on using the inverse cosh expansion [38],

$$\alpha\ell = \log_e \left\{ \left(1 + \frac{R_1}{R_2}\right) + \left[ \left(1 + \frac{R_1}{R_2}\right)^2 - 1 \right]^{1/2} \right\} \text{ nepers} \quad (6.52)$$

It should be noted that since 8.686 nepers is equal to 1 dB (equation (6.25)), multiplication of  $\alpha\ell$  by 8.686 converts this quantity into decibels. A similar result occurs for the PI case, where

$$\alpha\ell = \cosh^{-1}\left(1 + \frac{R_2}{R_1}\right)$$

Hence, returning to our example from equation (6.51),  $Z_0$  becomes 56  $\Omega$ , giving a VSWR of about 1.1 and 21 dB attenuation.

Another important factor in attenuator design is an assessment of how much power is dissipated in each of the resistive elements in the attenuator. This allows final component power ratings to be made.

Consider the T example. For an input power of  $P_{in}$  W the input voltage  $V_{in}$  must be

$$V_{in} = (Z_0 P_{in})^{1/2} \quad (6.53)$$

but

$$I_g = V_{in} / \left[ R_1 + \frac{(R_1 + Z_0)R_2}{R_1 + R_2 + Z_0} \right] \quad (6.54)$$

Now the power dissipated in the leftmost series resistance of  $R_1$  (Figure 6.31) is

$$P_1 = I_g^2 R_1 \quad (6.55)$$

while the power dissipated in resistor  $R_2$  is

$$P_2 = \frac{V_2^2}{R_2} \quad (6.56)$$

where  $V_2$  is the voltage across  $R_2$ , and  $V_2 = V_{in} - I_g R_1$ .

The last resistance,  $R_1$ , on the right-hand side of the attenuator must dissipate power

$$P_3 = \left( \frac{V_2}{R_1 + R_0} \right)^2 R_1 \quad (6.57)$$

### Exercise 6.5

For the parameters identified in exercise 6.3, calculate the power rating for each of the resistors in the resistive T matching network.

#### Solution

Returning to the example above, we see that for  $R_1 = 41 \Omega$  and  $R_2 = 10 \Omega$ , then for 1 W input power,  $V_{in} = 7.1 \text{ V}$ ,

$$I_{in} = 7.1 / \left[ R_{in} + \frac{(41 + 50)10}{(41 + 50 + 10)} \right] = 140 \text{ mA}$$

$$\therefore V_2 = 7.1 - (0.14)(41) = 1.36 \text{ V}$$

Hence

$$P_1 = (0.14)^2(41) = 0.8 \text{ W}$$

$$P_2 = 0.19 \text{ W}$$

$$P_3 = 0.01 \text{ W}$$

yielding a total power dissipation of 1 W.

This calculation shows that the bulk of the power in the input signal is dissipated in the first resistor of the attenuator network. Thus this component, together with the other components used to construct the attenuator circuit, must be properly power rated.

## 6.3 Reactive matching circuits

Networks comprising only ideal reactive components have the advantage of not dissipating RF energy. Simple designs have the disadvantage of being able to give a perfect match at a single frequency only. Let us investigate the procedures involved in the design of the simplest of these types of network. The approach adopted here will involve adjusting the quality factor  $Q$  of the matching network so that unequal resistive terminations can be matched to each other [38].

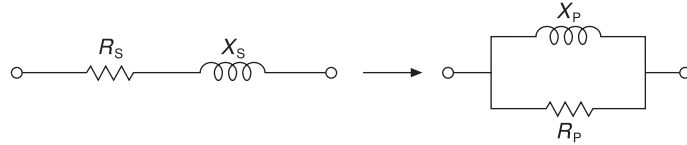


**Figure 6.7** Equivalence of LR circuits

The working definition for the  $Q$  factor as used here is

$$Q = \omega_0 \frac{\text{stored energy in a network}}{\text{energy lost per second}} \quad (6.58)$$

where  $\omega_0$  is the operating frequency in rad/s.

From Figure 6.7, for the series  $LR$  circuit

$$|Z| = (R_S^2 + X_S^2)^{1/2} \quad (6.59)$$

For the parallel  $LR$  circuit:

$$|Z| = \frac{X_P R_P}{(R_P^2 - X_P^2)^{1/2}} \quad (6.60)$$

For a simple series connected circuit consisting of an inductor and a resistor,  $L_S$  and  $R_S$ , the  $Q$  factor can be written as

$$Q = \frac{X_S}{R_S} \quad (6.61)$$

where  $X_S = \omega_0 L_S$ , while for the parallel connected circuit

$$Q = \frac{R_P}{X_P} \quad (6.62)$$

thus

$$Q = \frac{R_P}{X_P} = \frac{X_S}{R_S} \quad (6.63)$$

Since equations (6.57) and (6.58) are equivalent equations, (6.60) and (6.61) can be recast as

$$|Z| = \frac{R_P}{(1 + Q^2)^{1/2}} = R_S(1 + Q^2)^{1/2} \quad (6.64)$$

Hence

$$\frac{R_P}{R_S} = 1 + Q^2 \quad (6.65)$$

thereby indicating that control of the  $Q$  factor can expedite an impedance match between unequal resistive terminations,  $R_P$  and  $R_S$ .

The simplest topology we can use as an impedance-matching network is an L–C network, which can take two forms (Figure 6.8). Here  $R_P$  is assumed to be greater than  $R_S$ .

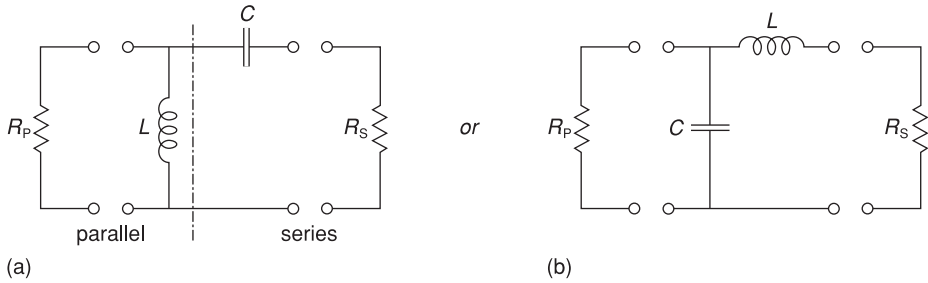


**Figure 6.8** L-section matching network

### Exercise 6.6

Match a  $500\ \Omega$  load to a  $300\ \Omega$  generator using an L–C network.

#### Solution

Using equation (6.65):

$$\frac{R_P}{R_S} = 1 + Q^2 = \frac{300}{50} = 1 + Q^2$$

$$\therefore Q = 2.24$$

Now using equation (6.61):

$$X_S = QR_S = 112\ \Omega$$

and equation (6.60):

$$X_P = \frac{R_P}{Q} = 134\ \Omega$$

from which for a known frequency of operation  $C$  and  $L$  the matching circuit components can be found.

The choice of Figure 6.8a or Figure 6.8b is generally dictated by whether we require AC decoupling and/or a DC path to ground, in which case Figure 6.8a would suit best. Alternatively, if DC biasing to the load is required, then use Figure 6.8b. For example, the circuit in Figure 6.8b can be used if impedance matching is required and DC bias to a masthead preamplifier (Section 5.3) is supplied via the centre conductor of the coaxial cable used to connect them. In addition, Figure 6.8b is useful for rejecting unwanted harmonic content in the signals.

For the example given above, we can now realise the actual component values for Figure 6.8a at a given operating frequency of 458 MHz:  $X_C = 112\ \Omega$ ,  $C = 3.1\ \text{pF}$ ,  $X_L = 134\ \Omega$  and  $L = 0.46\ \text{nH}$ . For Figure 6.8b, the component values are  $X_C = 181\ \Omega$ ,  $C = 2.0\ \text{pF}$ ,  $X_L = 112\ \Omega$  and  $L = 0.4\ \text{nH}$ .

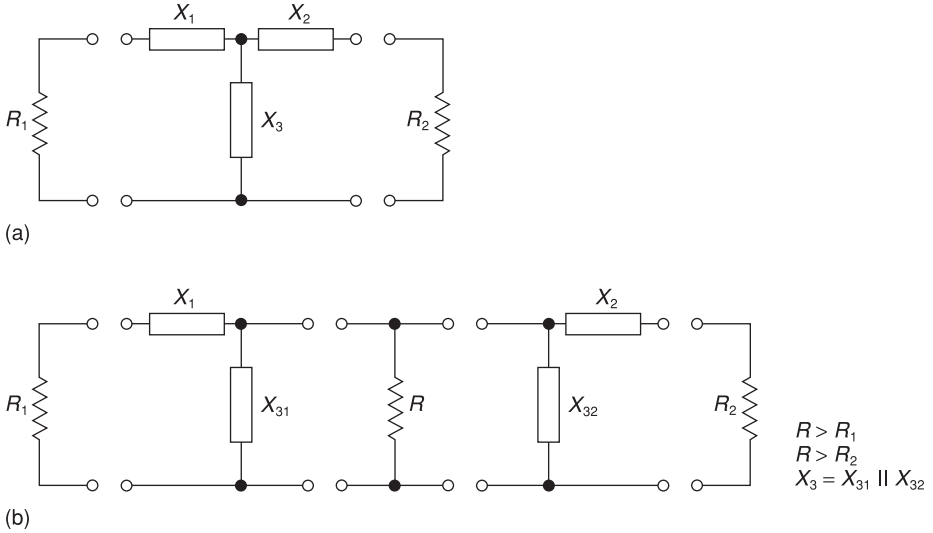


**Figure 6.9** T-section matching network

A major problem exists with L-section matching circuits designed by this approach: namely, the  $Q$  factor is determined by the ratio of the termination resistances to be matched. This results in a low  $Q$  factor, which means that harmonic suppression of unwanted signals is inherently poor.

By switching to the T configuration in Figure 6.9a, this problem can be overcome. Here the T configuration is conceptualised as two-back-to-back L networks, terminated in a virtual resistance,  $R$  (Figure 6.9b). This resistance is selected so that it has a value greater than the actual resistances to be matched. This is necessary since above we showed that for an L-section network (equation (6.65))

$$Q^2 = \frac{R}{R_{1,2}} - 1 \quad (6.66)$$

Assuming for the moment that  $R_1$  and  $R_2$  are known, then we can write for  $R_1$

$$\frac{R}{R_1} = Q_1^2 + 1 \quad (6.67)$$

where  $Q_1$  is the  $Q$  factor of the first L section. For an assumed value of  $Q_1$ ,  $R$  can now be found. If  $R$  is less than  $R_2$ , increase  $Q_1$  and try again.

Once  $Q_1$  has been selected, we can find  $X_{31}$  and  $X_1$

$$X_{31} = \frac{R}{Q_1} \quad (6.68)$$

and

$$X_1 = R_1 Q_1 \quad (6.69)$$

Similarly, for the second L section

$$\frac{R}{R_2} = Q_2^2 + 1 \tag{6.70}$$

Since, at this point, R and R<sub>2</sub> are known quantities, we can find Q<sub>2</sub> = Q<sub>1</sub> = Q. Once Q<sub>2</sub> is established, then

$$X_{32} = \frac{R}{Q_2} \tag{6.71}$$

and

$$X_2 = Q_2 R_2 \tag{6.72}$$

The design is completed by noting that X<sub>3</sub> is the parallel combination of X<sub>31</sub> and X<sub>32</sub>.

**Exercise 6.7**

Match a 50 Ω source to 300 Ω load using a reactive T network at an operating frequency of 458 MHz.

**Solution**

Assume a value of 10 for Q; R<sub>1</sub> = 50 Ω, R<sub>2</sub> = 300 Ω, f = 458 MHz and R = 50(101) = 5050 Ω > R<sub>1</sub>R<sub>2</sub>. Next, from equation (6.68)

$$X_{31} = 505 \text{ } \Omega$$

and from equation (6.69):

$$X_1 = 500 \text{ } \Omega$$

Compute using equation (6.70):

$$Q_2 = \left( \frac{5050}{300} - 1 \right)^{1/2} = 4$$

Hence X<sub>32</sub> = 1263 Ω and X<sub>2</sub> = 1200 Ω. Thus X<sub>3</sub> = 361 Ω.

The actual component values can now be realised for either of the networks shown in Figure 6.10. Here the circuit in Figure 6.10a allows a DC through connection, while the arrangement in Figure 6.10b blocks DC.

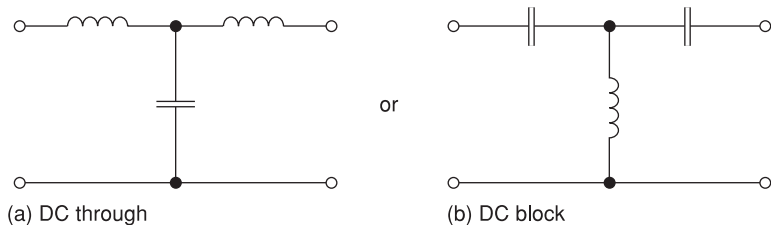


**Figure 6.10** T-network schematic

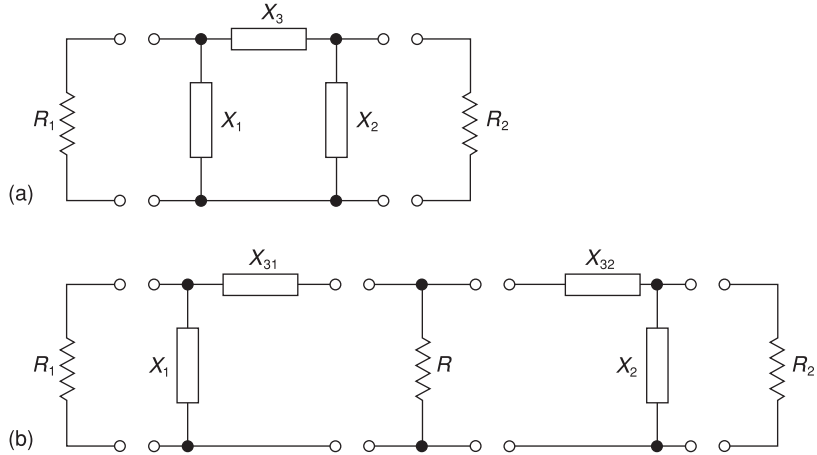


**Figure 6.11** PI-section matching network

This methodology can now be extended to the PI configuration shown in Figure 6.11. Here we assume that  $Q_1$ , the  $Q$  factor of the first section to be matched, is known and that  $R_1$  and  $R_2$  have already been specified. Then

$$X_1 = \frac{R_1}{Q_1} \quad (6.73)$$

and

$$\frac{R_1}{R} = Q_1^2 + 1 \quad (6.74)$$

Thus

$$R = \frac{R_1}{Q_1^2 + 1} \quad (6.75)$$

Again we check to ensure that the value of  $R$  calculated is greater than both  $R_1$  and  $R_2$ . If not, decrease  $Q_1$  and try once more.

Then compute

$$X_{31} = RQ_1 \quad (6.76)$$

Next find  $Q_2$  as

$$Q_2^2 = \frac{R_2}{R} - 1 \quad (6.77)$$

Hence

$$X_{32} = R_2Q_2 \quad (6.78)$$

$$X_2 = \frac{R_2}{Q_2} \quad (6.79)$$

and finally calculate  $X_3 = X_{31} + X_{32}$ .

## 6.4 Balun matching

If a centre-fed dipole antenna is fed with a parallel conductor transmission line, both radiating elements are balanced with respect to each other. However, as is more normally the case, if the antenna is to be fed with a coaxial cable, a balanced feed no longer exists, since one radiator is connected to the shield of the coaxial cable (normally grounded), while the other end is connected to the coaxial cable inner conductor. This is a problem, since on the side connected to the shield currents can flow down the outside of the outer coaxial cable, thereby giving rise to secondary radiation. Thus the shielding properties of the coaxial cable are lost. Antenna radiation far-field patterns can also be distorted as a result of secondary radiation from the outer coaxial cable screen.

Circuits that minimise or disrupt this phenomenon are known as balun (balanced to unbalanced) transformers. Their need comes from the fact that for most transmitting equipment their final output stages have one side grounded (unbalanced), since with this type of arrangement common-mode interference can be minimised.

A coaxial cable connection scheme for a dipole antenna is shown in Figure 6.12a. With this arrangement, for dipole element A, current will flow in the centre conductor of the coaxial cable and will be returned along the inner side of the coaxial screen, while, for dipole element B, fed in anti-phase relative to ground with respect to element A, a current is produced on the outer side of the coaxial cable screen. This causes a current imbalance in the system. If these two currents, i.e. the current on the coaxial inner conductor and external screen surface are equal in magnitude, then since they are in anti-phase they will cancel each other. However, the coupling of the fields between inner conductor and outer shield is weak due to the presence of the shield, so total cancellation cannot occur, and in fact only rather poor cancellation actually occurs. The effect of this current imbalance is that residual current flowing on the coaxial conductor outer shield may be re-radiated, causing distortion of the normal far-field radiation behaviour of the antenna.

Two possibilities exist for rectifying this problem. First, we could more strongly couple the coaxial centre conductor to the outer shield of the coaxial cable, perhaps

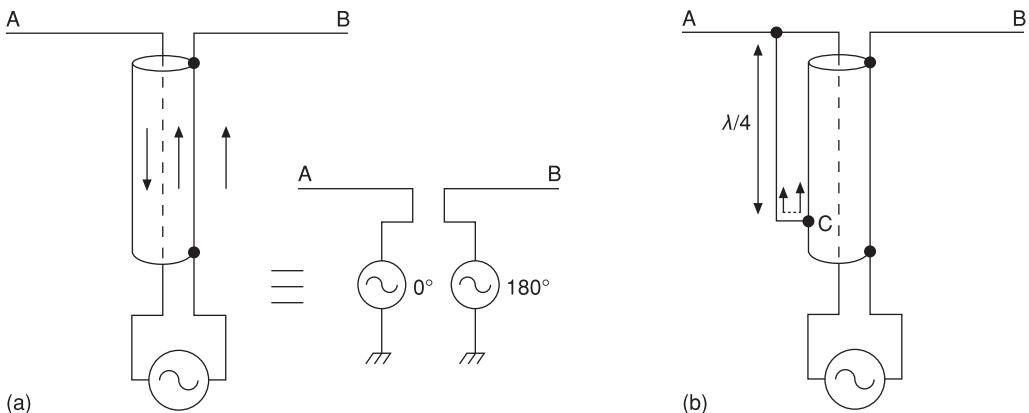


**Figure 6.12** Basic balun construction: (a) dipole connected to coaxial cable; (b) quarter-wavelength balun

(in the extreme) by a short circuit placed between them. If directly implemented, however, this would inhibit the operation of the antenna. What we need is a more indirect way of achieving the same result. This can be done by placing a secondary transmission line between the outer conductor and the centre conductor of the coaxial cable. This section of line is short-circuited at one-quarter wavelength from element A in Figure 6.12b; at this position, it is directly connected to the coaxial cable outer screen. A quarter-wavelength section of line short-circuited at one end has the property that at the other end it appears as an open circuit (see Section 6.6). Thus a physical connection can be made between these positions that electrically does not disrupt the normal current and voltage distributions at radiating elements A and B (Figure 6.12b), and the balanced current in the coaxial centre conductor is unaffected by the connection. However, unbalanced current on the outside of the coaxial screen, because of the direct connection that now exists between it and the coaxial centre conductor, has an equal but opposite current flowing on the secondary conductor, which negates its effect. At the position where the two are connected, (position c in Figure 6.12b), the resultant current is zero since they are in phase opposition. As a result, no current flows on the remainder of the transmission line outer conductor, so the rest of the interconnecting line has no effect on the system.

A shielded variant of the above approach is shown in Figure 6.13. Here an oversized outer sleeve forms the outer conductor of a coaxial cable, while the outer conductor of the inner coaxial cable forms the inner conductor of the oversized coaxial cable. The open-circuit end at the antenna terminal inhibits unbalanced current flow on the outside of the oversized coaxial cable conductor. Thus this conductor acts as a choke, stopping the unbalanced current from affecting the rest of the line. With both of the arrangements above, the presence of the quarter-wavelength transformer makes the bandwidth of the system quite small, normally less than 5%.

For many applications, especially at lower frequencies, it is preferable to make a balun using a transformer and a series parallel connection of transmission lines (Figure 6.14). Here two lines, each with characteristic impedance  $Z_0$ , are connected in parallel at A–A' and in series at B–B'. The two  $Z_0$  lines in parallel give an input

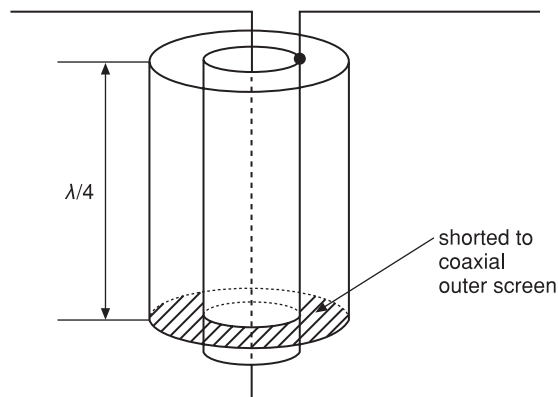
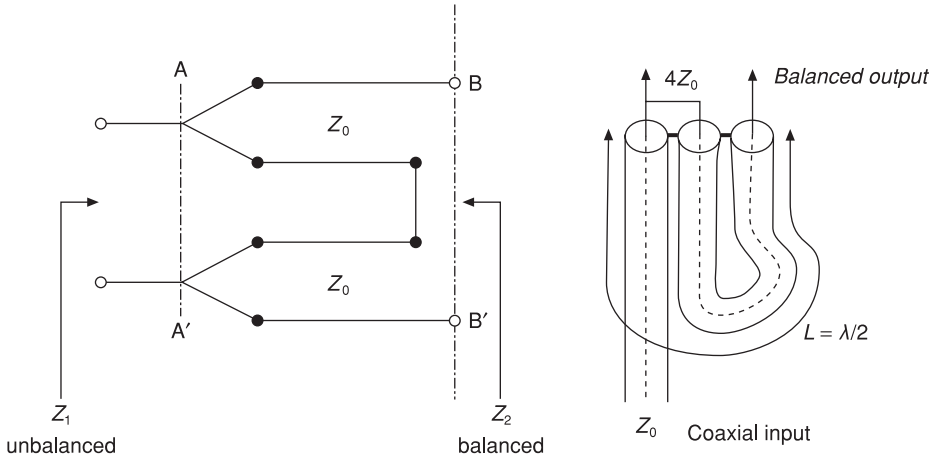


Figure 6.13 Shielded balun



**Figure 6.14** Impedance-transforming balun

impedance  $Z_1$  of  $Z_0/2$ , while the two  $Z_0$  impedances in series give a  $Z_2$  equal to  $2Z_0$ . Thus the impedance ratio between the input and output of this structure is

$$\frac{Z_2}{Z_1} = \frac{2Z_0}{Z_0/2} = 4 \tag{6.80}$$

Therefore this type of configuration allows the possibility for a four-to-one impedance transformation as well as balun action.

When wound as a coil as in Figure 6.15, the additional series inductance appended by the coil winding acts to increase the decoupling between input and output; thus the overall length for this arrangement is not critical, and the system can operate over a

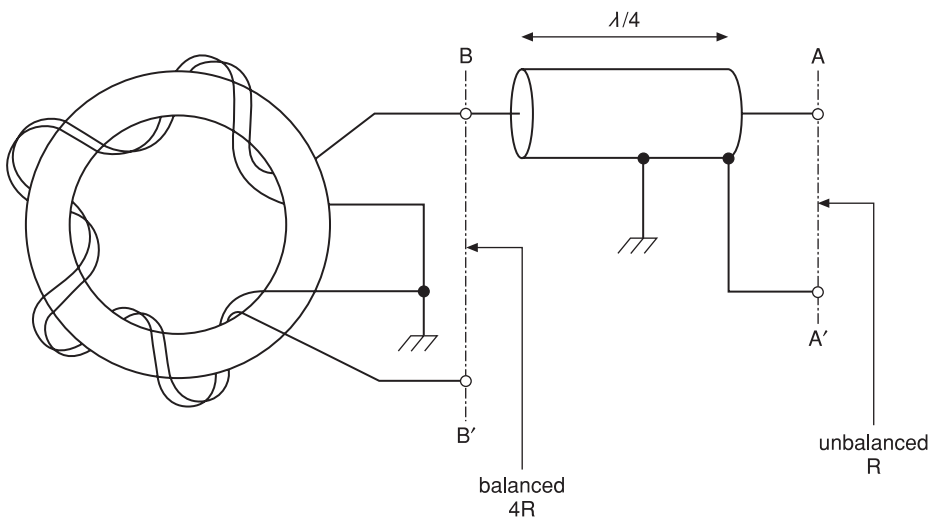


**Figure 6.15** Torodial wire transformer

relatively broad frequency range. However, in order for one side, A–A', of this configuration to be connected to ground, the arrangement must be such that the length of the transmission line A–B is one quarter-wavelength long.

Many other balun configurations exist; see for example [39].

## 6.5 Power splitting/combining networks

In its simplest manifestation, if we want a high-gain antenna array with the main beam pointing in the broadside direction, we need to feed all the elements with in-phase excitations (Section 4.2). The array can have an amplitude taper if required in order to shape the far-field side lobe response of the antenna array (Section 4.4). The basic circuit building block for this type of array feed structure is the power splitter, or when operated in receive mode the power splitter connections are reversed and it is used as a power combiner.

The simplest power divider/combiner consists of a T junction (Figure 6.16a). The circuit shown in Figure 6.16a has poor isolation between ports 2 and 3 but is very simple. This arrangement can be improved on by using the circuit shown in Figure 6.16b, which is designed to match to the source and load of  $Z_0$  characteristic impedance. Here we get a good impedance match between both output arms when the input is correctly matched. As before, this type of circuit has fairly poor isolation between output ports whenever a mismatch exists at these ports. In addition, the resistors used in the T junction will increase the insertion loss of the circuit and will also introduce additional noise into the system. An advantage of this type of circuit is that, provided that resistors with low parasitics are used, the circuit should be extremely broadband. Other lumped component variations of the power splitter/combiner exist; see, for example, Figure 6.17.

The lumped hybrid power splitter circuit shown in Figure 6.17 is useful for monolithic realisation, where it can be designed for use at microwave frequencies. The structure has good impedance-matching properties and also good isolation. The

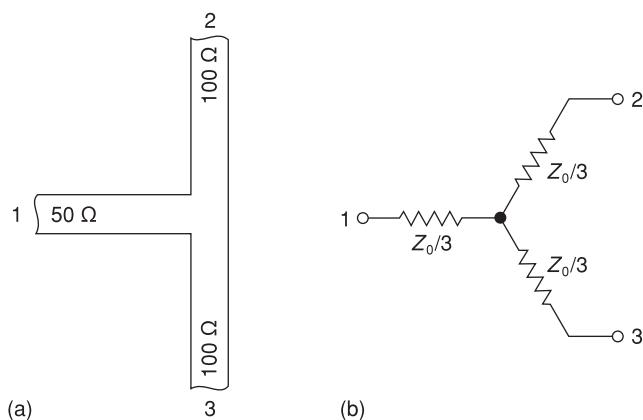


Figure 6.16 Simple power splitter/combiner types

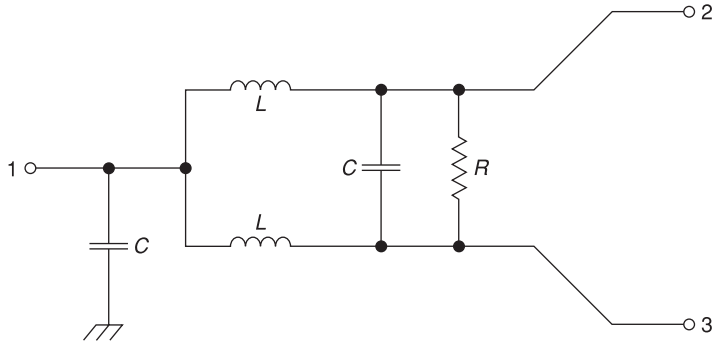


Figure 6.17 Lumped power splitter/combiner

design equations for use in a system with  $Z_0$  characteristic impedance and equal power split are as follows:

$$C = \frac{1}{2\omega Z_0}; L = \frac{Z_0}{\omega}; R = 2Z_0$$

Distributed versions of this splitter called a Wilkinson power splitter/combiner are used at higher frequencies (Figure 6.18) [40] [41]. The power split can be made equal ( $Z_{02} = Z_{03}$ ) or unequal ( $Z_{02} \neq Z_{03}$ ), and the circuit can be made to match unequal impedances [42]. By cascading stages, the bandwidth of the splitter/combiner can be made broader [40]. The design equations for this arrangement are

$$\frac{\text{power at port 2}}{\text{power at port 3}} = \frac{1}{\Delta^2} \tag{6.81}$$

Here  $\Delta$  is used to represent the coupling factor between output ports:

$$Z_{02} = Z_0[\Delta(1 + \Delta^2)]^{1/2} \tag{6.82}$$

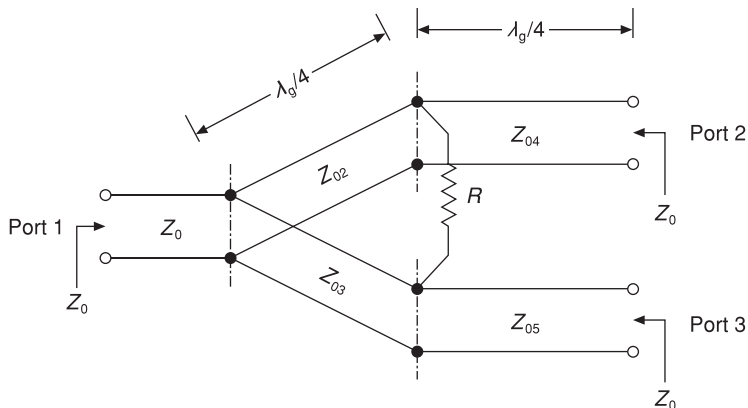


Figure 6.18 Wilkinson power splitter/combiner

$$Z_{03} = Z_0 \frac{(1 + \Delta^2)^{1/2}}{\Delta^3} \quad (6.83)$$

$$Z_{04} = Z_0(\Delta)^{1/2} \quad (6.84)$$

$$Z_{05} = Z_0/(\Delta)^{1/2} \quad (6.85)$$

$$R = Z_0(1 + \Delta^2)/\Delta \quad (6.86)$$

This class of circuit is narrowband (typically 5% bandwidth) by virtue of the quarter-wavelength matching sections used.

### Exercise 6.8

Consider now the design of a 3 dB 50  $\Omega$  Wilkinson coupler.

#### Solution

Since we have a 3 dB equal power split between ports 2 and 3, then using equation (6.81):

$$\Delta^2 = \frac{P_2}{P_3} = \frac{1}{2} / \frac{1}{2} = 1$$

thus using equations (6.82) and (6.83):

$$Z_{02} = Z_{03} = Z_0\sqrt{2} \quad (\text{all lengths} = \lambda_g/4)$$

and equations (6.84) and (6.85):

$$Z_{04} = Z_{05} = Z_0 = 50 \Omega$$

and finally equation (6.86):

$$R = 2Z_0 = 100 \Omega$$

## 6.6 Impedance matching and the Smith chart

The Smith chart was developed to assist in the solution of transmission line matching problems [43]. The chart is a plot of normalised sending-end impedance (equation (6.93)) or admittance as a function of angle in a unit circle. The chart in impedance form is shown in simplified form in Figure 6.19 and has the following key properties:

- The upper half of the normalised impedance chart represents resistance and inductive reactance.
- The lower half of the normalised impedance chart represents resistance and capacitive reactance.
- One revolution of the chart represents one half-wavelength distance travelled along the transmission line, clockwise towards the signal generator, anticlockwise towards the load.
- Points A and B represent short-circuit and open-circuit positions, respectively.

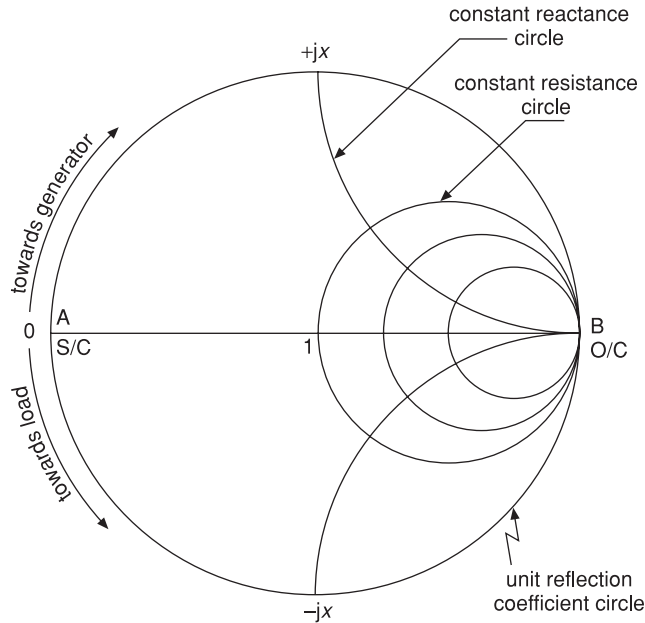


**Figure 6.19** Normalised impedance Smith chart, simplified

We know from Section 6.1 that a uniform transmission line terminated in its own characteristic impedance will absorb or transmit energy without reflection. For maximum power transfer to occur, a conjugate match between source and load impedances must exist. Thus in order to match a complex load impedance to a transmission line with given characteristic impedance (usually a real quantity), conjugate matching is required.

### Exercise 6.9

We wish to match an antenna with input impedance  $40 + j30 \Omega$  to a  $50 \Omega$  feeder line using only a section of  $50 \Omega$  transmission line (assumed lossless) and a series reactance (Figure 6.20b). It should be noted that for multiport circuits, scattering or parameters are often used to define port and port-to-port interaction (see Appendix 9.4). Here, since we are working with one-port matching, we will use input impedance. We can use the Smith chart shown in Figure 6.20a to facilitate a graphical solution to this problem, i.e. to determine the element values of the required matching network.

### Solution

The solution proceeds as follows: first, normalise the antenna input impedance to the impedance of the feed line, normally  $50 \Omega$ .

$$\frac{40 + j30}{50} = 0.8 + j0.6$$

Point A on the Smith chart in Figure 6.20a.

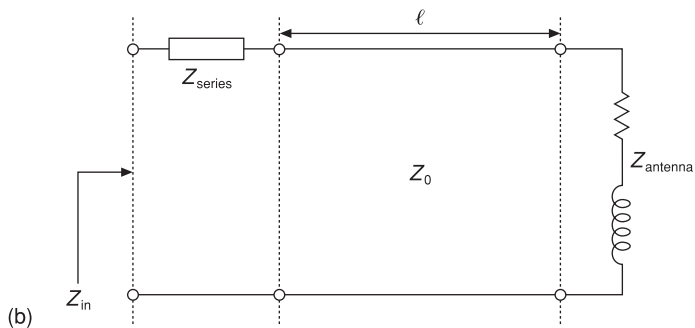
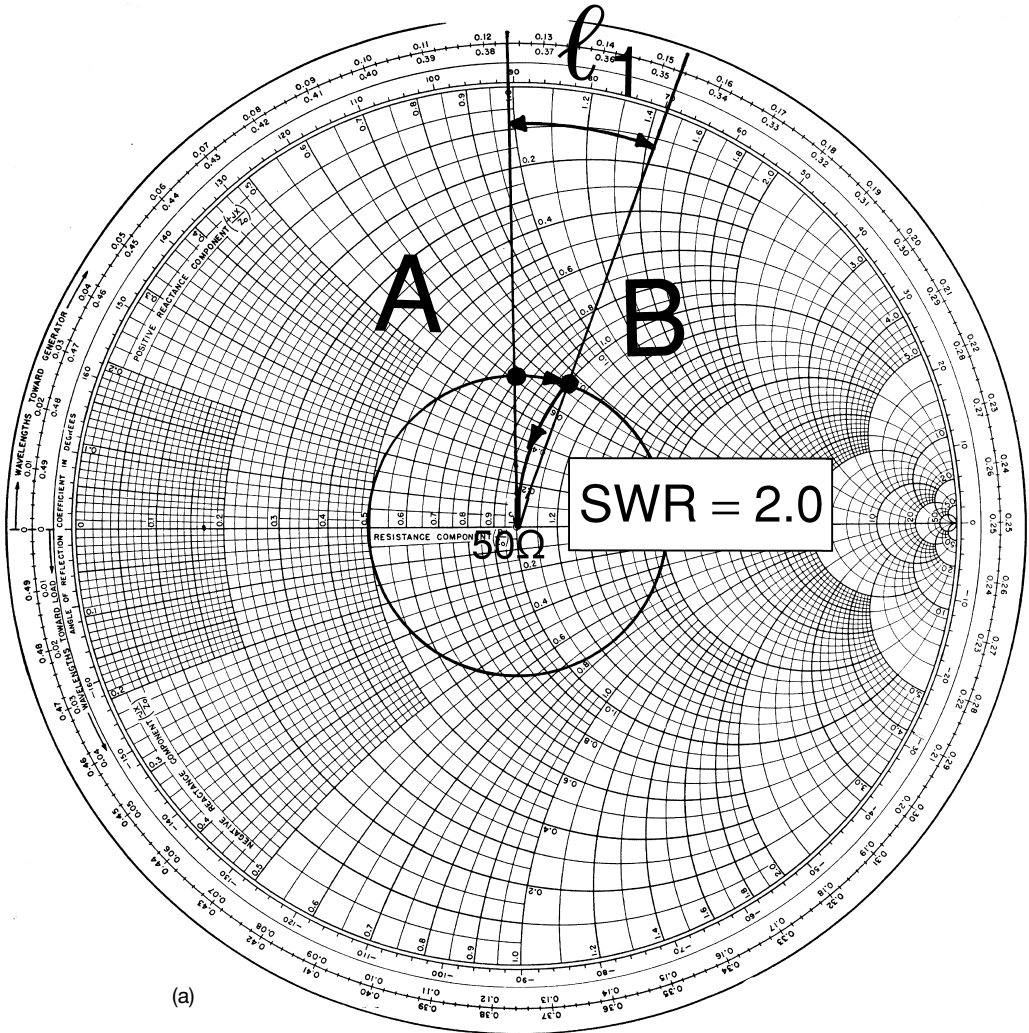


Figure 6.20 Series impedance matching

First we must select line length  $\ell$  such that the normalised real part of the input impedance at A is unity. To achieve this, we draw an SWR circle through point A and rotate it clockwise (towards the generator, since we are impedance matching the generator) until it touches the unity conductance circle; i.e. since we are matching the load to the generator, move towards the generator in a circle centred at (1.0, 0), which passes through the  $0.8 + j0.6$  circle, until the 1.0 constant conductance circle is intercepted, i.e. point B. Consequently,  $\ell$  must equal  $(0.152 - 0.124)\lambda = 0.028\lambda$ . At this point, the normalised impedance is  $1.0 + j0.7$ . The series value of  $j0.7$  is inductive and can be cancelled to achieve  $Z_{in} = 1 + j0$  by placing a capacitor of normalised reactance value  $-j0.7 \Omega$  in series with the section of connecting line. Hence, after denormalisation, at  $Z_{in}$  we are left with a  $50 \Omega$  input impedance when looking into the antenna at the frequency of interest. Thus we have synthesised the desired matching network.

As an alternative to impedance matching with lumped elements, we can also match by using open- or short-circuited transmission line stubs.

By considering the same approach as was used in Section 6.1 for a uniform section of transmission line, some very important and useful results can be obtained that will ultimately facilitate the design of distributed matching circuits.

To see how matching using distributed circuits can be made to occur, consider equation (6.9):

$$\frac{\partial^2 V}{\partial x^2} = -\psi^2 V$$

A working solution for this second-order differential equation is that the voltage or current at any position  $x$  along the uniform line segment in Figure 6.1 is

$$V(x) = A \exp(-\psi x) + B \exp(+\psi x) \quad (6.87)$$

or

$$I(x) = \frac{A}{\psi_0} \exp(-\psi x) - \frac{B}{\psi_0} \exp(+\psi x) \quad (6.88)$$

where a + sign indicates a wave travelling in the negative  $x$ -direction and a - sign indicates a wavefront travelling in the positive  $x$ -direction along the transmission line.  $A$  and  $B$  are as yet unknown coefficients, which if necessary can be found by considering the transmission line boundary conditions. The  $-B$  coefficient in equation (6.88) arises since from Figure 6.2 we know that the total transmitted current,  $I_t$ , through the interface between a uniform transmission line of characteristic impedance  $Z_0$  and mismatched termination  $Z_T$  is equal to

$$I_t = I_i - I_r \quad (6.89)$$

where  $I_i$  is the incident current and  $I_r$  is the reflected current at the interface, therefore the terminating mismatch impedance  $Z_T$  can be written using equations (6.87) and (6.88). Hence at position  $x = \ell$

$$Z_T = \frac{V_t}{I_t} = \frac{A \exp(\psi \ell) + B \exp(+\psi \ell)}{A \exp(-\psi \ell) + B \exp(+\psi \ell)} Z_0 \quad (6.90)$$

rearranging gives

$$\frac{B}{A} = \exp(-2\psi\ell) \frac{Z_T - Z_0}{Z_T + Z_0} \quad (6.91)$$

while at position  $x = 0$  with reference to Figure 6.2b

$$Z_S = \frac{V_s}{I_s} = \frac{A + B}{A - B} Z_0 \quad (6.92)$$

here  $Z_S$  is the sending end impedance seen looking into the transmission line towards the load, substituting equation (6.91) into equation (6.92) we get

$$\frac{Z_S}{Z_0} = \frac{Z_T [1 - \exp(-2\psi\ell) + Z_0[1 + \exp(-2\psi\ell)]]}{Z_T [1 + \exp(-2\psi\ell) + Z_0[1 - \exp(-2\psi\ell)]]}$$

hence

$$\frac{Z_S}{Z_0} = \frac{\left[ \frac{Z_T}{Z_0} + \tanh(\psi\ell) \right]}{\left[ 1 + \frac{Z_T}{Z_0} \tanh(\psi\ell) \right]} \quad (6.93)$$

From equation (6.93), it can be seen that if  $Z_T = Z_0$  then no mismatch exists and the sending-end impedance of the line,  $Z_S$ , is equal to the characteristic impedance  $Z_0$  of the transmission line, i.e. the line is matched and no reflection occurs.

If the line is lossy or has very little associated loss, then  $\psi = 0$  and equation (6.93) can be rewritten as

$$\frac{Z_S}{Z_0} = \frac{\left[ \frac{Z_T}{Z_0} + j \tan(\beta\ell) \right]}{\left[ 1 + \frac{Z_T}{Z_0} j \tan(\beta\ell) \right]} \quad (6.94)$$

Now consideration of equation (6.94) shows that

$$Z_S = Z_T \quad (6.95)$$

only when  $j \tan(\beta\ell) = 0$ . This condition occurs only when  $\beta\ell = n\pi$ , where  $n = 1, 2, 3$ , etc. Also, since  $\beta = 2\pi/\lambda_g$  the above condition is equivalent to

$$\ell = \frac{n\lambda_g}{2} \quad (6.96)$$

This result shows that, when a half-wavelength section of transmission line is located between a source and a load impedance, irrespective of its characteristic impedance, the sending-end impedance is transformed to the source impedance, or vice versa. This result when plotted on a Smith chart indicates that one-half guide wavelength is equal to a full  $360^\circ$  rotation on the chart, i.e. impedance values repeat every time a half-wavelength section of very low-loss line (called a half-wavelength transformer) is introduced between load and generator. This concept is useful when one is trying to separate a source from a load for reasons of physical convenience while trying to preserve the electrical transparency of the connecting circuit at a spot frequency.

Another very important property of the half-wavelength transformer is that it introduces a  $180^\circ$  phase shift between its ends. This effect is very useful when designing phasing harnesses for antenna array applications.

In equation (6.94), if  $\beta\ell$  is made equal to  $n\pi/2$  radians, i.e.  $\ell$  is an odd multiple of a quarter-wavelength, where  $n = 1, 3, \text{etc.}$ , then  $j \tan(\beta\ell)$  goes to infinity, and

$$\frac{Z_S}{Z_0} = \frac{Z_0}{Z_T} \quad (6.97)$$

from which

$$Z_0 = (Z_S Z_T)^{1/2} \quad (6.98)$$

This is the condition for a quarter-wavelength transformer, the utility of which is that a low impedance can be matched to a higher impedance by placing a quarter-wavelength section of transmission line of appropriate characteristic impedance given by equation (6.98) between the source and load terminations that are to be matched. Normally, quarter-wavelength transformers are used for matching impedances that have had their reactive component neutralised, as was done for example in Figure 6.20. In general, for a complex load, for this condition to be realised residual reactance can be cancelled by using tuning stubs (see later in this section).

Like half-wavelength transformers, quarter-wavelength transformers are very frequency-sensitive, hence narrowband. Techniques for making the quarter-length transformer more broadband by cascading a number of appropriately designed sections are given in [44].

### Exercise 6.10

Use transmission lines to design a matching harness with  $50 \Omega$  input impedance for two  $75 \Omega$  antennas to be co-phased in a half-wavelength separated array configuration.

#### Solution

Use quarter-wavelength transformers to match a  $75 \Omega$  antenna impedance to  $100 \Omega$ . We choose  $100 \Omega$  so that the two  $100 \Omega$  termination impedances combine in parallel from a  $50 \Omega$  load impedance, which can then be transferred to a  $50 \Omega$  generator placed some distance away. From equation (6.96)

$$Z_0 = 75^2/50 = 112.5 \approx 100 \Omega$$

here for convenience we use standard  $75 \Omega$  characteristic impedance cable and accept the resultant mismatch so that cost can be minimised. Combining impedances  $Z_0$  in parallel we get an input impedance  $Z_{in}$  of

$$Z_{in} = \frac{(112.5)^2}{2(112.5)} = 56.2 \Omega$$

which results in a VSWR of 1.125.

Since two quarter-wavelength transformers have been used, the separation between the antennas is one half-wavelength as stipulated.

The next important thing to know about distributed transmission line techniques is their use as tuning stubs for the purpose of cancelling out residual reactance in a circuit. Consider once again equation (6.93). This time, if the transmission line in Figure 6.2 is terminated in a short circuit, i.e.  $Z_T = 0$ , then

$$Z_{S_{sc}} = Z_0 \tanh \psi \ell \quad (6.99)$$

and for an open circuit

$$Z_{S_{oc}} = Z_0 = \frac{Z_0}{\tanh \psi \ell} \quad (6.100)$$

Inspection of equation (6.99) shows that for a lossless line

$$Z_{S_{sc}} = j Z_0 \tan \beta \ell \quad (6.101)$$

that is, the full range of inductive sending-end reactances from  $0 \Omega$  at  $\ell = 0$  to infinity at  $\ell = \lambda_g/4$  are available. At  $\ell = \lambda_g/8$ , the reactance is a pure inductance and has the value  $+j Z_0 \Omega$ .

Similarly, for equation (6.100) we can approximate a lossless line section as

$$Z_{S_{oc}} = -j Z_0 \cot \beta \ell \quad (6.102)$$

That is, the full range of capacitive sending-end reactances are available; e.g. at  $\ell = \lambda_g/8$  the reactance is  $-j Z_0 \Omega$ .

This means that in practice lengths of open or circuit transmission line can be used to synthesise capacitive or inductive elements, which can be used as components in distributed filters or as components in impedance-matching networks.

### Exercise 6.11

Using a transmission line network, match a dipole antenna with  $73 - j25 \Omega$  to a  $50 \Omega$  low-loss balanced cable. The design frequency is 1 GHz, and the signal travels in the cable at a velocity of 0.7 times the speed of light due to the dielectric filling of the cable.

#### Solution

Consider the Smith chart shown in Figure 6.21, in which  $f = 1$  GHz,  $\lambda_0 = 30$  cm,  $\lambda_g = 30 \times 0.7$  cm,  $Z_0 = 50 \Omega$  and  $Z_L = 73 - j25 \Omega$ . Low loss, hence attenuation is approximately 0 dB.

1. Normalise  $Z_\ell$  to  $50 \Omega$ :

$$Z_\ell = \frac{73 - j25}{50} = 1.46 - j0.5 \quad (\text{point A on the chart}).$$

2. Since we are assuming zero loss, we can draw an SWR circle through point A (SWR = 1.75).
3. Convert point A to a normalised admittance value point B by rotating it by  $180^\circ$ , so that  $y_\ell = 1/z_\ell = 0.65 + j0.25$ .

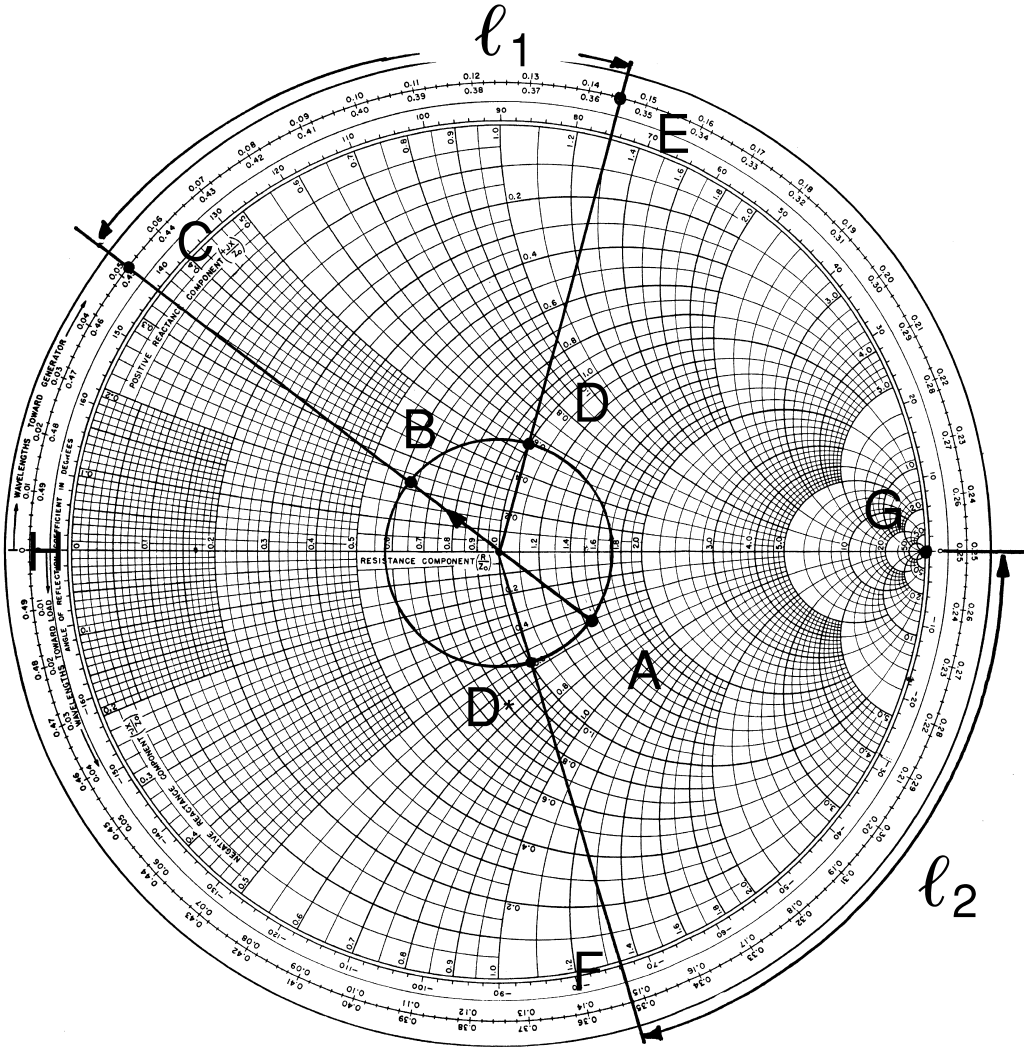


Figure 6.21 Stub matching

4. Extend the radial line between A and B to the chart periphery and read off the wavelength generator scale the position of point C,  $0.054\lambda_g$  (remember that we are matching a load to the generator, so we will be moving towards the generator).
5. Next, note the circle described by the intersection of the SWR radial where it intersects unit conductance circle, point D, and extend a radial from the centre of the chart through point D to point E on the chart periphery ( $0.146\lambda_g$ ).
6. Note the distance along the chart periphery from C to E, i.e.  $\ell = 0.146\lambda_g - 0.054\lambda_g = 0.09\lambda_g$ . This value gives the distance from the load to the stub along the transmission line connection such that we will have unit normalised (to  $50\ \Omega$ ) plus some residual reactance. We must now cancel this reactance. In order to do this, we must work out the length of the stub needed to complete the design.

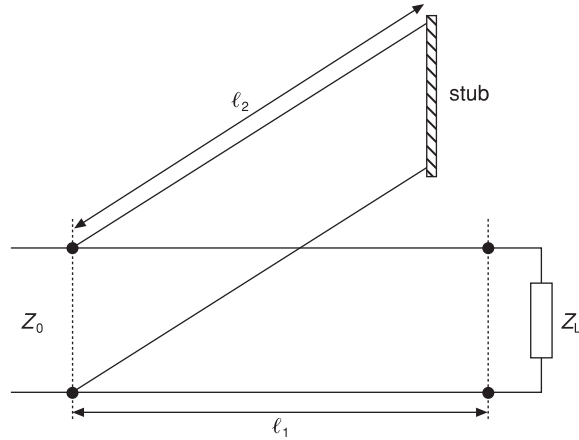


Figure 6.22 Single-stub impedance matching

7. To do this, we locate point  $D^*$  (where  $*$  denotes the complex conjugate value of  $D$ ), and extend a radial from the chart centre through  $D^*$  to point  $F$  on the chart periphery ( $0.35\lambda_g$ ).
8. If we wish to use a short-circuit tuning stub to obtain the desired match, then we locate the short-circuit position, point  $G$  on the chart ( $0.25\lambda_g$ ), and rotate clockwise towards the generator until we reach point  $F$ . If we wished to use an open-circuit stub, then we would start at point  $H$  ( $0\lambda_g$ ) and rotate to position  $F$  in a clockwise direction or simply add one quarter-wavelength line to the short-circuit solution.
9. Assuming that we require a short-circuited stub, we now translate periphery distances  $CE$  and  $GF$  to physical lengths:

$$\ell_1 = CE = 0.1\lambda_g = 0.1 \times 30 \times 0.7 = 2.1 \text{ cm}$$

$$\ell_2 = GF = 0.01\lambda_g = 0.21 \text{ cm}$$

Thus the resultant matching structure is as shown in Figure 6.22.

For more sophisticated examples of the use of the Smith chart, and for more complex lumped and distributed matching scenarios, see references [43] and [44].

## References

- [37] Matthai, G.L., Young, L. and Jones, E.M.T., *Microwave Filters, Impedance Matching Networks and Coupling Structures*, McGraw-Hill, New York, 1964.
- [38] Fusco, V.F., *Microwave Circuits, Analysis and Computer-Aided Design*, Prentice Hall International, 1987.
- [39] Jasik, H., *Antenna Engineering Handbook*, McGraw-Hill, 1961, pp. 31–3.
- [40] Parad, L.I. and Moynihan, R.L., Split tee power divider, *IEEE Trans on MTT*, Vol. 13, No. 1, pp. 91–5, 1965.

- [41] Wilkinson, E.J., An  $n$ -way hybrid power divider, *IRE Trans on Microwave Theory and Techniques*, Vol. 8, pp. 116–18, 1960.
- [42] Taub, J.J. and Kurpis, G.P., A more general  $n$ -way hybrid power divider, *IEEE Trans on MTT*, Vol. 17, pp. 406–8, 1969.
- [43] Smith, P.H., *Electronic Applications of the Smith Chart in Waveguide, Circuit and Component Analysis* McGraw-Hill, 1969.
- [44] Thomas, R.L., *A Practical Introduction to Impedance Matching*, Artech House, 1976.

## Problems

- 6.1 A parallel-wire transmission line is used to provide a balanced feed to a half-wavelength dipole antenna. If the characteristic impedance of the transmission line is  $73 - j32 \Omega$  at 100 MHz and the dipole has  $73 \Omega$  input impedance, calculate the magnitude and phase of the input current and the actual power delivered to the antenna terminals. You may assume that an AC signal of 10 V RMS is used to excite the cable.
- 6.2 A 1 GHz frequency source is connected to the input of a cable with low loss. The length of the cable is 3 m, and it is terminated with a load whose value is identical to its own characteristic impedance. If the wavelength of the signal when propagating along the line is 0.2 m, calculate the time delay from connection of the generator to receipt of the signal at the other end of the cable. What is the phase difference between the input signal, taken as being the phase reference, and the output signal, once steady-state conditions have been reached?
- 6.3 A lossless transmission line has a characteristic impedance of  $73 \Omega$  and when connected to a load exhibits a VSWR of 3.5. The distance between successive voltage minima on the resulting standing wave on the line is 35 cm. Calculate the value of the load impedance used to terminate the line and also calculate the guide wavelength of the transmission line.
- 6.4 An antenna is to be designed to operate at 1 GHz and have an input impedance of  $73 \Omega$  at that frequency. The signal source used to power the array has a balanced output impedance of  $50 \Omega$  and is located 2 m from the array. Design a quarter-wavelength transformer, using a parallel-wire transmission line to connect the generator and the antenna with minimum impedance mismatch. The cable has a phase velocity which is 95% of that of free space.
- 6.5 What value of matched attenuator is required to reduce a VSWR of 4 to a VSWR of 1.2?
- 6.6 Design a single-stage Wilkinson power splitter that provides 6 dB power division at 1 GHz. Assume that air-spaced coaxial cable is to be used to form the transmission line elements of the splitter.
- 6.7 Design a resistive network that will provide 10 dB attenuation in a  $50 \Omega$  system.

- 6.8** Using simple network theory, design a reactive circuit that can be used to match a  $50\ \Omega$  generator to a  $75\ \Omega$  load at 400 MHz.
- 6.9** Repeat exercise 6.8, but this time use a Smith chart to facilitate the design process.
- 6.10** Use the Smith chart to find the load reflection coefficient and VSWR along a 10 cm length of  $75\ \Omega$  line that is terminated with a load impedance of  $50 + j20\ \Omega$ . Find the impedance and admittance at the sending end of the cable and at a point 3 cm from the load. The line exhibits 3 dB/m loss, and the operating frequency is 1 GHz.  $\lambda_g = 0.9\lambda_0$ .
- 6.11** By using a Smith chart, find the position and length of an ideal short-circuited matching stub that will enable a  $100\ \Omega$  characteristic impedance transmission line terminated in a  $150 - j200\ \Omega$  impedance to be matched to a  $100\ \Omega$  generator.

# Basic antenna types

---

The number of different types of antennas that currently exist is bewildering, but most are designed specifically to fit a pre-specified application. In this chapter, we will confine discussion to a subset of available antennas. The discussion will be necessarily brief and will not consider the subtleties of any of the generic types of antenna discussed as these can be found in specialists texts given in the bibliography.

In order to address some of the major types of antenna element in current use, we have confined the discussion to the following classes of antenna. First, the properties of a small rectangular loop antenna such as could be used in electromagnetic near-field sensing equipment is described. Then the complementary antenna to the straight-wire dipole, the slot antenna, is discussed. This is followed by a description of the operation of the Yagi antenna. This class of antenna is extremely important in a variety of UHF and microwave applications where low wind loading and good electrical gain and polar pattern requirements need to be addressed simultaneously. The area of planar printed antennas is explored briefly by establishing the operating mechanisms and basic design equations for a printed circuit board antenna type, the rectangular microstrip patch antenna. Such antennas find use in many applications where low profile and adherence to the mounting structure shape (conformal construction) are required.

Reflector antennas are covered next. For the simplest of these, the parabolic reflector, we describe the properties of the parabola as a surface that can convert a plane wave to a spherical wave on reception and that can focus this spherical wave to a single point; the converse is true on transmission. This type of antenna finds wide application at microwave frequencies, where as wavelength becomes small relative aperture size increases, hence narrow beamwidth and attendant high gains can be readily achieved. The fundamentals of helical antennas are discussed, and the conditions under which a helical antenna will operate in axial end-fire radiation mode are given. Next the fundamentals of horn antennas are described, since they are simple to construct and find application as calibration antennas in measurement test set-ups due to their predictable gain and radiation performance. Wire-based travelling-wave antennas are described in

order to illustrate how non-resonant, travelling-wave antennas operate. This is followed by a brief exposition on the properties of the planar inverted F or PIFA antenna. This antenna is widely used in mobile wireless handsets. Dielectric antennas have small dimensions due to the high dielectric constant of the material from which they are constructed, and consequently they are of interest in applications such as hand-held PIFA antennas. An additional feature of dielectric antennas is that depending on which antenna mode is excited, different far-field radiation patterns suitable for terrestrial or satellite tracking using a single antenna are possible. Another interesting class of antenna, the reflect-array, suitable for microwave and millimetre-wave applications, where element-fed losses are high, is described. In addition, ultra-wideband planar spirals and compact multiband fractal antennas are also discussed. It is hoped that consideration of these generic antenna types will promote further independent research into the specific issues related to each class of antenna structure discussed in summary in this chapter.

## 7.1 Small rectangular loop antennas

The idea of using opposing currents to cause field cancellation is a useful one in antenna work. This is illustrated by an analysis, using the techniques we have previously developed in Section 1.4, but applied this time to a small rectangular loop antenna. Antennas such as these are useful for coupling energy into and out of cavities and also for various field-sensing operations such as are required in electromagnetic compatibility measurement equipment.

In Figure 7.1, if  $\ell_1$  and  $\ell_2$  are small when compared with a wavelength of the radiated energy, then we will model the current in each arm of the loop as being uniform and in phase around the loop. In this way, we will consider the small loop antenna to be an assembly of four Hertzian dipole antennas with known phase relationships. In Figure 7.1a, dipoles 2 and 4 are symmetrically placed with opposing currents flowing in them. As a result, the electromagnetic fields produced completely cancel each other at all points in the  $x$ - $y$  plane. On the other hand, dipoles 1 and 3 produce field components  $E_\theta$  and  $H_\phi$  in the  $x$ - $y$  plane. From Figure 7.1b, the path length difference  $CB = \ell_1 \cos\phi$  metres, for which a phase difference  $\psi$  exists such that  $\Psi = 2\pi\ell_1/\lambda \cos\phi + 180^\circ$ , where the  $180^\circ$  results from the currents in arms 1 and 3 being in antiphase. Hence the resultant electric field at some distance point P can be found by vector summation as

$$\begin{aligned} E_{\theta_r} &= E_\theta \cos \frac{\Psi}{2} \\ &= E_\theta \cos \left( \frac{\pi\ell_1}{\lambda} \cos\phi + 90^\circ \right) \\ &= -2E_\theta \sin \left( \frac{\pi\ell_1}{\lambda} \cos\phi \right) \end{aligned} \quad (7.1)$$

if  $\ell_1 \ll \lambda$ , then  $\sin(\alpha) \approx \alpha$  for small  $\alpha$ , and on using  $\cos\phi = j \sin\phi$  we get

$$E_{\theta_r} = -2jE_\theta \left( \frac{\pi\ell_1}{\lambda} \sin\phi \right) \quad (7.2)$$

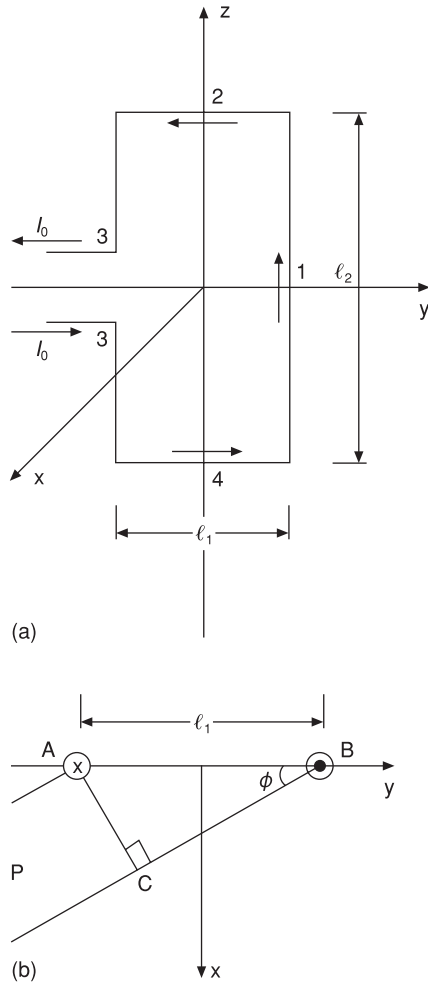


Figure 7.1 Small rectangular loop antenna

Substituting this into the expression for the  $E_\theta$  field for a Hertzian dipole (Section 1.2) (we can do this since we have assumed that  $\ell_1$  is very small) we get

$$E_{\theta_R} = 2 \left( \frac{60\pi I_0 \ell_1}{\lambda r} \sin\theta \right) \exp\left( j\omega \left( t - \frac{r}{c} \right) \right) \left( \frac{\pi \ell_1}{\lambda} \sin\phi \right) \quad (7.3)$$

$$= \frac{120\pi^2 I_0 \ell_1^2 \sin\theta \sin\phi \exp\left( j\omega \left( t - \frac{r}{c} \right) \right)}{\lambda^2 r} \quad (7.4)$$

This expression has its maximum value in the equatorial plane, i.e. when  $\theta = 90^\circ$ ; also if  $\ell_1 = \ell_2$  then  $\ell_1^2$  is equal to the area of the loop, i.e.  $A$ .

$$|E_{\theta_{R_{\max}}}| = \frac{120\pi^2 I_0 A}{\lambda^2 r} \sin\phi \quad (7.5)$$

By noting that

$$|H_{\phi_{R_{\max}}}| = \frac{|E_{\theta_{R_{\max}}}|}{120\pi} \quad (7.6)$$

we can calculate the power radiated from the small loop antenna by using Poynting's theorem (Section 2.3) as

$$\begin{aligned} P &= EH \sin\phi \\ &= \frac{120\pi^3 I_0^2 A^2 (\sin\phi)^2}{\lambda^4 r^2} \sin\phi \end{aligned} \quad (7.7)$$

from which the instantaneous power radiated can be found. We can write the instantaneous radiated power as

$$P_{\text{inst}} = \frac{120\pi^3 I_0^2 A^2}{\lambda^4 r^2} \int_0^\pi \int_0^{2\pi} r^2 (\sin\phi)^2 \sin\phi \, d\theta \, d\phi \quad (7.8)$$

Thus the average power level is

$$P = \frac{120\pi^3 I_0^2 A^2}{2\lambda^4 r^2} 2\pi r^2 \int_0^\pi (\sin\phi)^2 \sin\phi \, d\phi \quad (7.9)$$

$$= 160\pi^4 I_0^2 \left(\frac{A}{\lambda^2}\right)^2 \quad (7.10)$$

from which the radiation resistance of the small loop antenna is determined as

$$R_{\text{rad}} = 320\pi^4 \left(\frac{A}{\lambda^2}\right)^2 \quad (7.11)$$

which for a very small loop, say  $\lambda/10$ , gives a radiation resistance of only  $3 \, \Omega$ . This result is in line with our expectation that electrically small circuits do not radiate effectively.

In order for this antenna to operate correctly, it is necessary for it to be connected to a matching circuit. However, even when properly resonated its efficiency will be low, due to low radiation resistance and its ohmic losses (which have not been included above). In general, for electrically small antennas, bandwidth can to a limited extent be traded for efficiency, such that a relatively efficient electrically short antenna will exhibit an extremely narrow bandwidth.

## 7.2 Slot antennas

If a slot is cut into a metal sheet, then the resulting aperture can be made to radiate electromagnetic energy (Figure 7.2). This type of antenna can be considered as the dual of a dipole antenna. Here the electric fields of the dipole antenna are swapped for

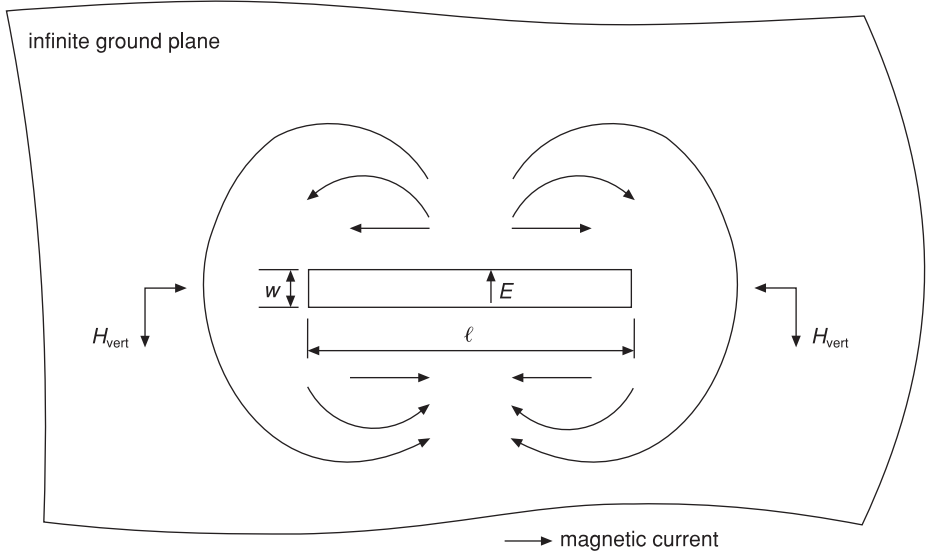


Figure 7.2 Slot in infinite ground plane

the magnetic fields in the slot antenna. Using this duality concept, then from Section 3.1 the  $E$  and  $H$  fields for a half-wavelength slot antenna are given as

$$E_{\phi} = \frac{jI_0 e^{-j\beta r}}{2\pi r} \left[ \frac{\cos\left(\frac{\pi}{2} \cos\theta\right)}{\sin\theta} \right] \tag{7.12}$$

and

$$H_{\theta} = \frac{j60I_0 e^{-j\beta r}}{r} \left[ \frac{\cos\left(\frac{\pi}{2} \cos\theta\right)}{\sin\theta} \right] \tag{7.13}$$

For this type of antenna to radiate, an electric field stimulus,  $E$ , should be placed to provide a feed across the slot aperture. With this arrangement, the magnetic field is partially aligned along the slot edge. If the width of the slot  $W$  is made much less than a wavelength, the long edges of the slot carry equal and opposite current so that fields radiated from these edges act to cancel. If the slot length is  $\lambda/2$ , then at the short edges of the slot the currents are in phase, but since the slot width is much less than a wavelength these ends do not radiate efficiently. However, since the currents also spread out over the metal sheet, then at some distance from the narrow slot edges the vertical components of the  $H$  field in Figure 7.2 reinforce to give far-field radiation. For efficient radiation, the extent of the ground plane should be at least one wavelength around the slot; ideally it will be of infinite extent, although for reasonable polar patterns an  $8\lambda \times 8\lambda$  or larger ground plane is often used.

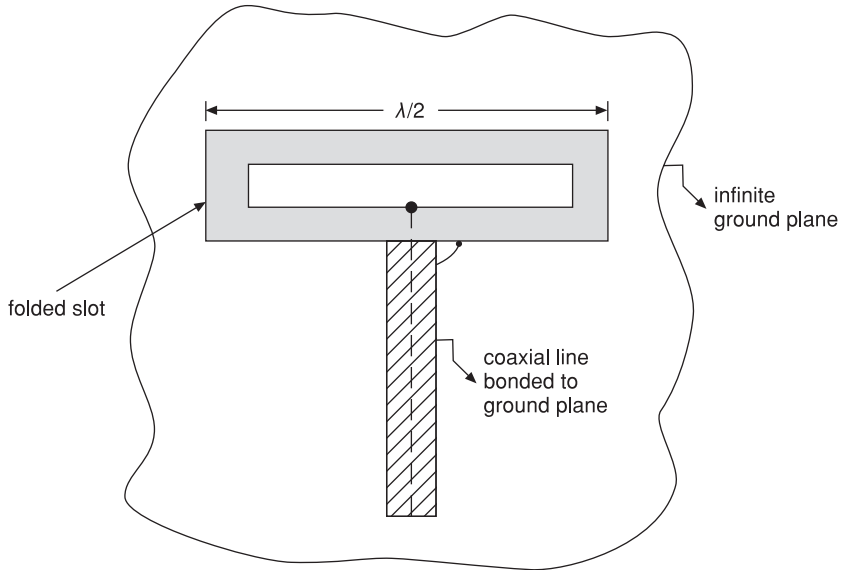


**Figure 7.3** Folded slot antenna

The radiation resistance of the slot antenna,  $R_{\text{rad}_s}$ , [45], can be expressed in terms of driving-point impedance and its dual, dipole antenna radiation resistance,  $R_{\text{rad}_d}$ , as

$$\sqrt{R_{\text{rad}_s} R_{\text{rad}_d}} = \frac{\eta_0}{2} \quad (7.14)$$

Hence

$$R_{\text{rad}_s} = \frac{\eta_0^2}{4R_{\text{rad}_d}} \quad (7.15)$$

If the slot is short, then by duality with a short dipole (Section 3.4) and using equation (7.15), we can write

$$R_{\text{rad}_s} = 180(\lambda/\ell)^2 \quad (7.16)$$

By folding the slot as shown in Figure 7.3, it is possible to lower the slot impedance by a factor of 4, helping to facilitate impedance matching to a 50  $\Omega$  line.

It is possible to make the slot antenna radiate only on one side of the metal sheet by reflecting energy from the other side back into the slot so that radiation in the forward direction can be reinforced. This is achieved by placing a metal reflecting sheet a quarter of a wavelength behind the aperture so that the total path length from slot to reflector and back again is half a wavelength, thus cancelling any radiation in the unwanted direction [46]. This type of arrangement also increases the radiation resistance of the slot by a factor of 2. In addition, the directivity and effective aperture of the slot are increased by a factor of 2 when this technique is employed.

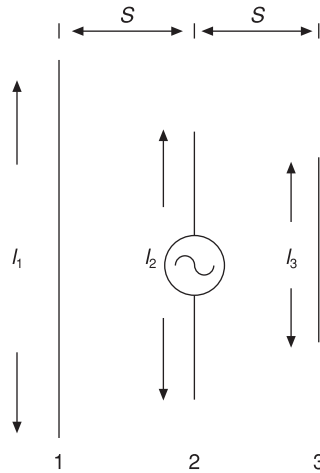


Figure 7.4 Three-element Yagi array

### 7.3 Yagi antennas

The Yagi or Yagi–Uda antenna, named after Hidet Sugu Yagi (1926), is a linear array with only one driven element [47]. This is a very important antenna structure and is used in a wide variety of applications where a directional transmit or receive far-field polar pattern is required. Consider the three-element transmitting Yagi antenna shown in Figure 7.4. Here, element 2, the driven element, is a half-wave dipole antenna. Element 1 is arranged to be slightly longer than element 2 in order to accommodate the inductive reactance caused by the mutual coupling due to the  $0.25\lambda$  spacing between elements 1 and 2. The other elements are shorter than the driven element since they are at a spacing of greater than  $0.25\lambda$ , typically  $0.37\lambda$ . This makes these elements appear capacitive, and they function as signal directors.

Consider now a simple Yagi array with one driven element and an undriven second element acting as either a reflector or as a director; in general, the undriven element is called the parasitic element (Figure 7.5). From the figure, it can be seen that the voltage induced in element 2 due to the presence of current flowing in the resonant element, element 1, is (Section 4.6)

$$V_2 = -I_1 Z_{12} \quad (7.17)$$

where  $Z_{12}$  is the mutual coupling between the element, and the negative sign indicates that the voltage induced in element 2 is in phase opposition to that in element 1.

If element 2 is longer than element 1 by an appropriate amount, i.e. inductive, the current in it,  $I_2$ , will lag  $E_2$  by some angle,  $\phi$ , hence it will lag  $I_1$  by  $180^\circ - \phi$  and so will act to produce end-fire operation.

If element 2 is shorter than element 1 by an appropriate amount, i.e. capacitive, then  $I_2$  will lead  $E_2$  by  $\phi$  and hence will lag  $I_1$  by  $180^\circ + \phi$ , so that the direction for end-fire is reversed with respect to the previous case, i.e. maximum radiation is directed from element 1 to element 2. Here the parasitic reflector acts as a director;

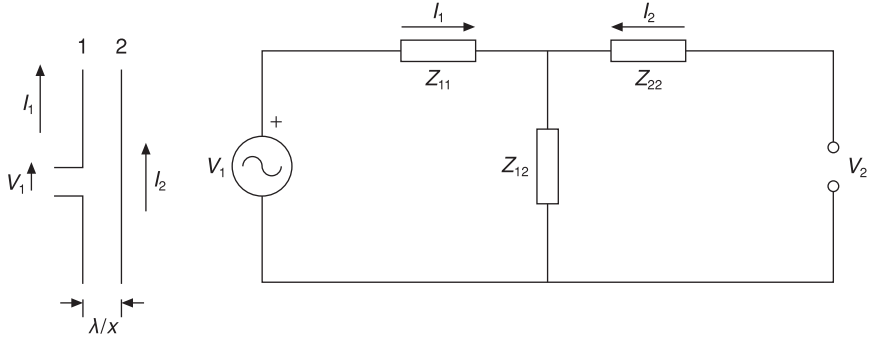


**Figure 7.5** Two-element Yagi array

in the previous case it acted as a reflector. The spacing between elements is usually between  $0.15$  and  $0.25\lambda$ .

The primary advantage of the Yagi arrangement over an end-fire array is that the feed arrangement is very simple. If the parasitic element is made to be reactive then little power is wasted in it, and it can be directly attached to a metal supporting mast without the need for insulation. Consequently, very little current will be induced in the mast, which simplifies the installation arrangements needed for this type of antenna.

As more parasitic director elements are introduced into the antenna, they are gradually shortened as we move away from the driven element so that they have greater reactance; thus correct phasing of the parasitic component can be ensured so that directed end-fire radiation is guaranteed.

With reference to Figure 7.5, if the impedance of the driven element is

$$Z_d = \frac{V_1}{I_1} \quad (7.18)$$

where  $V_1 = Z_{11}I_1 + Z_{12}I_2$ , then

$$Z_d = \frac{V_1}{I_1} = Z_{11} + Z_{12} \frac{I_2}{I_1} \quad (7.19)$$

Then, since element 2 is parasitic,

$$V_2 = 0 = Z_{21}I_1 + Z_{22}I_2 \quad (7.20)$$

Hence

$$\frac{I_2}{I_1} = -\frac{Z_{21}}{Z_{22}} \quad (7.21)$$

Thus

$$\frac{V_1}{I_1} = Z_d = Z_{11} - \frac{Z_{12}Z_{21}}{Z_{22}} \quad (7.22)$$

Now from Appendix 9.2 for a reciprocal network with equal terminating impedances

$$Z_{12} = Z_{21}$$

thus

$$Z_d = Z_{11} - \frac{Z_{12}^2}{Z_{22}} \quad (7.23)$$

This result shows that the input impedance of the Yagi antenna is reduced by the factor  $Z_{12}^2/Z_{22}$  relative to the self-impedance of the driven element. Hence the radiation resistance of the driven element has been lowered and a reactive component introduced. The reactive part is normally compensated for by making the driven element slightly longer or shorter than the resonant length, depending on whether the excess reactance is inductive or capacitive.

With a two-element Yagi, about 3 dB gain over a half-wavelength dipole can be obtained with a front-to-back ratio of about 12 dB. The introduction of additional parasitic elements further increases the gain of the Yagi antenna [47].

#### 7.4 Rectangular microstrip patch antennas

Many applications require antennas that are capable of conforming to the shape of the surface on to which they are mounted or that for aesthetic or wind-resistance criteria need to have a planar profile. In such applications, microstrip patch antennas are a useful low-cost route, since they can be manufactured using standard printed circuit techniques [48]. On the negative side, they have low radiation efficiency and narrow bandwidth (typically only a few percent).

A microstrip patch antenna normally consists of a thin metal patch separated from a ground plane by a low-loss dielectric material. The far-field radiation from the patch antenna is directed normally to the patch surface. The length of the patch,  $L$ , is normally chosen to be approximately one-half guide wavelength; this parameter controls its operating frequency. The width of the patch,  $W$ , controls its radiation resistance; typically,  $W$  is selected to be just under one half free-space wavelength [48]. Figure 7.6a shows the arrangement. For the simplest mode of excitation,  $TM_{010}$ , Figure 7.6b shows that in the  $y$ -direction, the electric fringe field components sum, while in the  $x$ -direction they cancel. The  $y$ -directed field component constitutes the radiated field from the patch antenna. Using the coordinate system of Figure 7.6a, we define the field distribution shown in Figure 7.6c. Examination of this diagram shows that the magnetic surface current vectors cancel along each side of the patch in the  $y$ -direction and reinforce in the  $z$ -direction. Thus under ideal conditions in the  $TM_{010}$  mode, the antenna is said to radiate along edges,  $W$ , and have no radiation from edges,  $L$ .

The thicker the substrate selected combined with the lower the dielectric constant of the material used, the better the performance of the antenna will be in terms of bandwidth. The penalty paid for this is the larger size of the antenna. In addition, it should be noted that surface wave losses (energy will be lost to the substrate) will increase with increased substrate thickness, resulting in reduced antenna efficiency and distorted far-field radiation patterns [49].

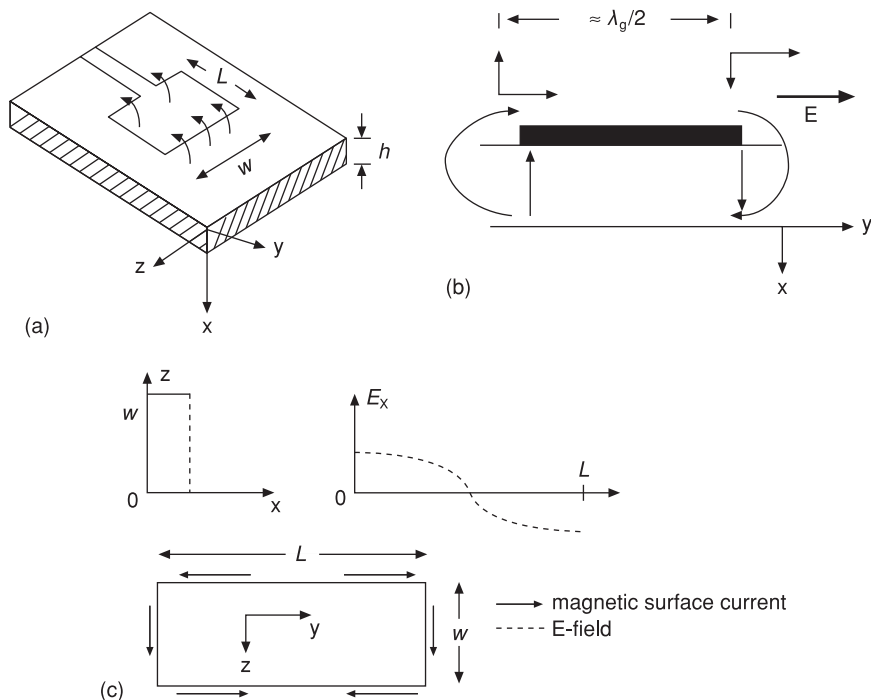


**Figure 7.6** Microstrip patch antenna  $TM_{010}$  mode

The principal approach used for feeding the antenna is to use a microstrip feedline attached to the radiating edge of the antenna, or tapped internal to it, in order to facilitate impedance matching. Alternatively, a coaxial connection can be made internal to the radiating patch (Figure 7.7). Impedance matching for the microstrip feedline approach is available by modifying both line width and tap-in position but for the coaxial case by modifying tap-in position only. The use of the microstrip feedline solution may impact on the cross-polarisation performance of the antenna, since higher-order modes generated by the connection of the feedline to the patch may cause spurious radiation to occur.

The simplest method used that allows the design of a rectangular microstrip patch antenna is the transmission line model [49]. This model is represented in its simplest form in Figure 7.8. Reference [50] gives a useful refinement of the model where mutual coupling between end slots is taken into account. Here each of the antenna radiating edges is represented as a slot antenna (see Figure 7.9, which is drawn with reference to Figure 7.6a). The slot reactance is  $jB$  and its conductance is  $G$  for physical width  $W$  and substrate thickness,  $h$ , see Figure 7.8).

The fringing fields at the slots are accounted for by using an effective dielectric constant value,  $\epsilon_{\text{eff}}$ , in the antenna calculations. This leads to the requirement for a slight foreshortening of the physical length of the antenna by an amount,  $\Delta\ell$ , to preserve the correct resonant frequency by virtue of the patch being half a wavelength at resonance in order to phase the slot radiation as shown in Figure 7.6b.

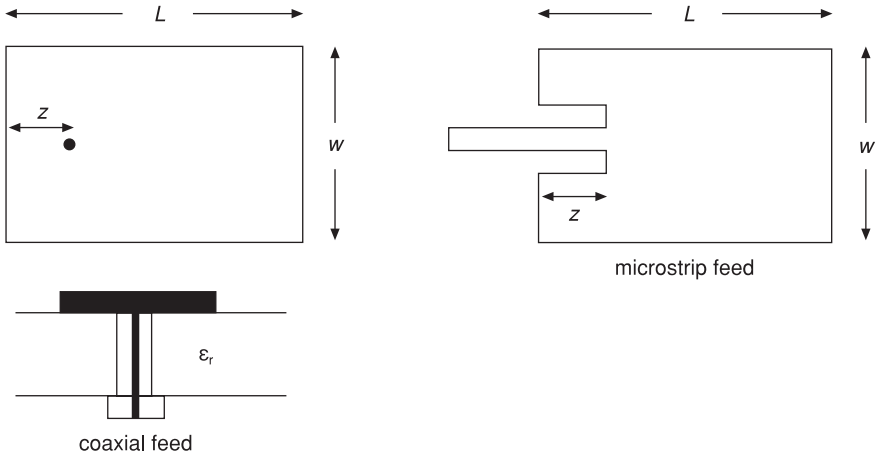


Figure 7.7 Microstrip patch antenna feed arrangements

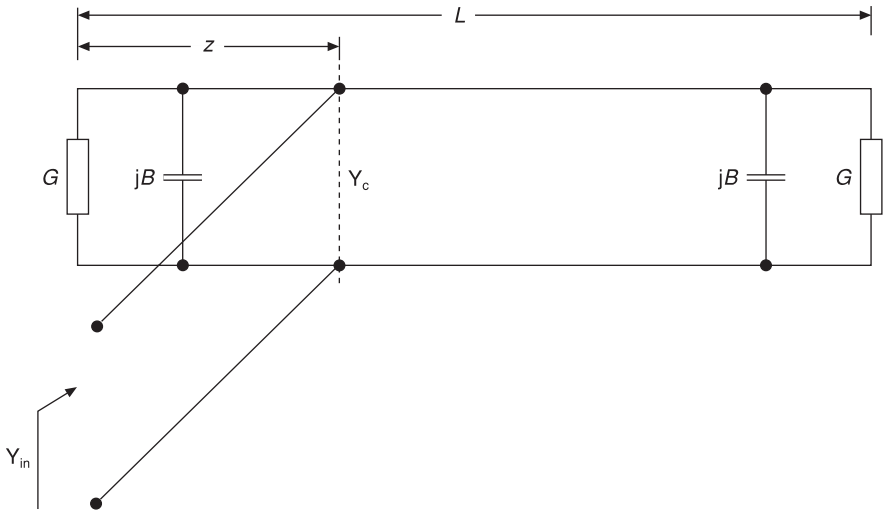


Figure 7.8 Microstrip patch antenna: transmission line model with variable tap-in point,  $z$

Under these conditions, an approximate design for the rectangular patch antenna follows from [49] as

$$L = \frac{\lambda_0}{2\sqrt{\epsilon_{\text{eff}}}} - 2\Delta\ell \tag{7.24}$$

where, approximately,

$$\epsilon_{\text{eff}} = \frac{\epsilon_r + 1}{2} + \frac{\epsilon_r - 1}{2} \left[ 1 + \frac{12h}{W} \right]^{-1/2} \quad \text{for } W/h > 1 \tag{7.25}$$

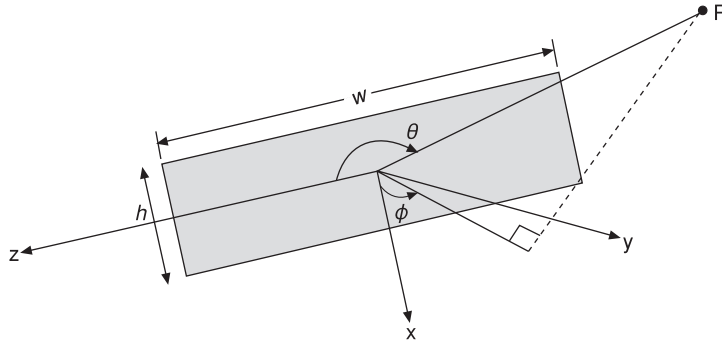


**Figure 7.9** Microstrip patch antenna radiating slot definitions

$$\Delta\ell = 0.412h \frac{(\epsilon_{\text{eff}} + 0.3)(W/h + 0.264)}{(\epsilon_{\text{eff}} - 0.258)(W/h + 0.8)} \quad (7.26)$$

and empirically for near optimum radiation:

$$W = \frac{\lambda_0}{2} \frac{1}{\sqrt{\frac{\epsilon_r + 1}{2}}} \quad (7.27)$$

with the input admittance presented along a radiating edge, at resonance, at tap-in point,  $Z$ , given as [51]. Using Figure 7.8, it is possible to select a position internal to the patch,  $z$ , such that an impedance match is facilitated, (c.f. Figure 7.7); this is achieved using equation (7.28) [52].

$$Y_{in}(Z) = 2G[\cos^2(\beta Z) + \frac{G^2 + B^2}{Y_0^2} \sin^2(\beta Z) - \frac{B}{Y_0} \sin(2\beta Z)]^{-1} \quad (7.28)$$

Where the radiation conductance  $G$  is, for small  $h$

$$G = \frac{1 - \frac{(k_0 h)^2}{24}}{120\lambda_0} \quad (7.29)$$

Other useful parameters are

$$Z_0 = \frac{\eta_0}{\sqrt{\epsilon_{\text{eff}}}} \left( \frac{w}{h} + 1.393 + 0.667 \log_e \left( \frac{w}{h} + 1.444 \right) \right)^{-1} \quad (7.30)$$

and

$$jB \approx jk_0 \Delta\ell \frac{\sqrt{\epsilon_{\text{eff}}}}{Z_0} \quad (7.31)$$

also

$$Y_0 = 1/Z_0, \quad \beta = 2\pi\sqrt{\epsilon_{\text{eff}}/\lambda_0} \quad (7.32)$$

It should be noted that transmission line models also exist that allow arrays of rectangular microstrip patch antennas to be designed [53]. In addition, other modelling techniques and shapes of microstrip patch radiating elements are available [54] that can give the designer additional flexibility or other advantage in a particular application.

The far-field radiation patterns for this type of antenna can be found from the analysis of radiation from the equivalent slot antennas formed along the radiating edges  $W$  of the microstrip antenna (Figure 7.9). This is achieved by assuming the field distribution along the slot as given in Figure 7.6c, i.e. a uniformly illuminated aperture (see Section 4.3), which for two slots placed  $L$  apart from each other gives the  $E$ -plane cut,  $x$ - $y$  plane ( $\theta = 90^\circ$ ;  $0^\circ \leq \phi \leq 180^\circ$ ) radiation pattern as

$$E(\phi) = \frac{\sin\left(\frac{k_0 h \cos\phi}{2}\right)}{\left(\frac{k_0 h \cos\phi}{2}\right)} \quad (7.33)$$

and the  $H$ -plane cut  $y$ - $z$  plane ( $\phi = 90^\circ$ ,  $0^\circ \leq \theta \leq 180^\circ$ ) as

$$H(\theta) = \frac{\sin\left(\frac{k_0 W}{2} \cos\theta\right)}{\frac{k_0 W}{2} \cos\theta} \sin\theta \quad (7.34)$$

where  $k_0$  is the free space wave number  $2\pi/\lambda_0$ .

The directivity,  $D$ , of this arrangement is approximately [7.6]

$$D = 6.6 \quad W \ll \lambda_0 \quad (7.35)$$

$$D = 8 \left(\frac{W}{\lambda_0}\right) \quad W \gg \lambda_0 \quad (7.36)$$

and half-power beamwidths for the  $E$  and  $H$  planes are approximately

$$\theta_E \approx 2 \cos^{-1} \sqrt{\frac{7.03\lambda_0^2}{4(3L^2 + h^2)\pi^2}} \quad (7.37)$$

$$\theta_H \approx 2 \cos^{-1} \sqrt{\frac{1}{2 + k_0 W}} \quad (7.38)$$

Here it has been assumed that the antennas are printed on to an infinitely large flat ground plane. Finite ground and curved ground planes will lead to a variety of pattern aberrations [52].

### Exercise 7.1

Consider now a design example. Let the design frequency be 1 GHz, the dielectric constant of the substrate material be 2.36 and  $h = 0.15$  mm. Then, using equations

(7.24),  $L = 9.6$  cm, and (7.27),  $W = 11.93$  cm, and at the radiating edge,  $z = 0$ , after equation (7.28):

$$Y_{in}(0) = 2G = 0.66 \text{ mS}$$

giving

$$Z_{in}(0) \approx 1515 \Omega$$

Note: The material in this section is based on *Microstrip Antennas* by I.J. Bahl and P.B. Bhartia, Artech House, Norwood, Mass., USA; [www.artechhouse.com](http://www.artechhouse.com). Reprinted with permission.

## 7.5 Reflector antennas

As frequency increases wavelength decreases, hence it becomes possible to construct antennas that are of moderate physical size but that are electrically large with respect to a wavelength. This allows the possibility of constructing antennas with a large aperture (c.f. Section 4.3), hence with high gain and narrow beamwidth. This type of radiation behaviour allows the antenna to be deployed in radar and point-to-point microwave links.

A very convenient way of achieving this behaviour at microwave frequencies is to use shaped metal reflectors. We will now show below that if an aperture (i.e. a plane area through which the antenna energy is transmitted or received) has a maximum dimension  $D$  in any given plane, then the minimum angle  $\theta$  (radians) in which radiated or received energy can be focused in that plane is approximately

$$\theta \approx \frac{\lambda_0}{D} \quad (7.39)$$

One of the best ways to obtain a narrow beam for a given aperture is to use a parabolic metal reflector (Figure 7.10). This type of reflector has the property that a point source placed at its focus will produce a plane wavefront at some distance from the antenna (along line  $XX'$ ).

In order for this to occur, it is necessary that the distance along each path to the aperture plane is constant:

$$EO + OF = EA + AD = EB + BC = \text{etc.}$$

Rotation of the parabolic section in Figure 7.10 about axis OF generates the paraboloid surface. Such a surface will in principle generate a parallel beam when excited with a source of spherical waves placed at its focus. We will show below using array theory that the ideal situation calculated above by geometrical optics considerations, i.e. a perfectly collimated beam, does not in fact occur and as a consequence there will be some beam divergence.

We showed previously in Section 4.2 that for a linear array of  $n$  isotropic elements the resultant electric field vector  $E$  can be found as

$$E = E_1 \frac{\sin((n\pi d/\lambda) \sin\theta)}{\sin((\pi d/\lambda) \sin\theta)} \quad (7.40)$$

where  $E_1$  is the field from an individual point source.

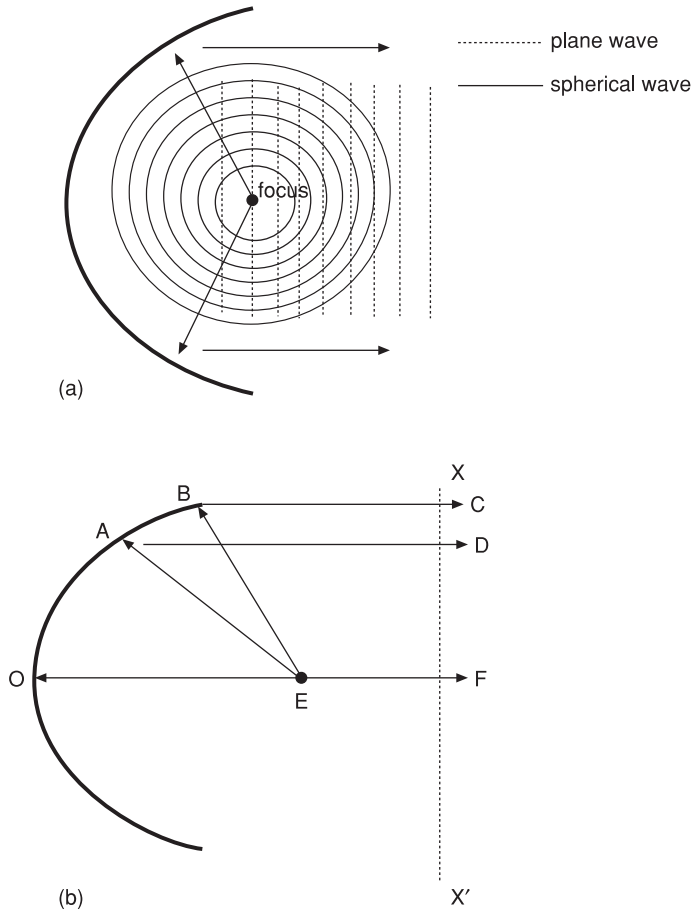


Figure 7.10 (a) Parabolic reflector; (b) ray diagram

For a large number of point sources the beamwidth will be narrow, so  $\sin\theta$  in equation (7.40) can be replaced with  $\theta$ , so that at the position of the first nulls

$$\frac{\sin \frac{n\pi d}{\lambda} \theta}{\sin \frac{n\pi d}{\lambda} \theta} \approx 0$$

$$\frac{n\pi d}{\pi} \theta \approx \pm\pi$$

$$\theta \approx \pm \frac{\lambda}{nd} \text{ radians} \tag{7.41}$$

If the field distribution is continuous across the radiating aperture, then  $n$  tends to infinity and  $d$  tends to zero, so that  $nd = a$ ; thus equation (7.41) becomes

$$\theta \approx \pm \frac{\lambda}{a} \text{ radians} \quad (7.42)$$

Hence the larger the aperture the narrower the beam that is formed.

At boresight (i.e. when  $\theta = 0$ ), maximum field strength occurs and  $E$  becomes  $E_{\max} = nE_1$ . Consequently, using equation (7.40), the field strength relative to the maximum is given by

$$E = \frac{E_{\max}}{n} \frac{\sin\left(\left(\frac{n\pi d}{\lambda}\right)\sin\theta\right)}{\sin\left(\left(\frac{\pi d}{\lambda}\right)\sin\theta\right)} \quad (7.43)$$

Now as  $d$  tends to zero and using small angle approximations

$$E = E_{\max} \frac{\sin\left(\left(\frac{a\pi}{\lambda}\right)\sin\theta\right)}{\left(\frac{\pi a}{\lambda}\right)\sin\theta} \quad (7.44)$$

for a rectangular aperture distribution, dimensions  $a \times b$  (Section 4.3). Using the same procedure used to obtain equation (7.44) (see also Section 4.2), we can derive the total electric field as

$$E = E_{\max} \frac{\sin\left(\left(\frac{a\pi}{\lambda}\right)\sin\theta\right) \sin\left(\left(\frac{b\pi}{\lambda}\right)\sin\phi\right)}{\left(\frac{\pi a}{\lambda}\right)\sin\theta \left(\frac{\pi b}{\lambda}\right)\sin\phi} \quad (7.45)$$

Now, since the gain of an antenna,  $G$ , (Section 2.4) is defined as

$$G = \frac{\text{maximum power received from a given antenna}}{\text{maximum power received from a reference antenna}}$$

we can calculate gain relative to an isotropic radiator (Section 2.4):

$$G = \frac{4\pi E_{\max}^2}{\int_{-\pi/2}^{\pi/2} \int_{-\pi/2}^{\pi/2} E^2 \cos\theta \, d\theta \, d\phi} \quad (7.46)$$

If the aperture is large,  $\theta$  and  $\phi$  become small, so  $\cos\theta$  tends to unity and  $\sin\theta$  and  $\sin\phi$  become  $\theta$  and  $\phi$ , respectively. Therefore, equation (7.46) becomes

$$G = \frac{4\pi E_{\max}^2}{E_{\max}^2 \int_{-\pi/2}^{\pi/2} \int_{-\pi/2}^{\pi/2} \frac{\sin^2(\pi a\theta/\lambda)}{(\pi a\theta/\lambda)^2} \frac{\sin^2(\pi b\phi/\lambda)}{(\pi b\phi/\lambda)^2} \, d\theta \, d\phi} \quad (7.47)$$

Since the beam is narrow (large aperture) then contributions at angles greater than those defining the main beam will be small. This means that the integral in equation (7.47) can be replaced by the standard integral:

$$\int_{-\infty}^{\infty} \frac{\sin^2 x}{x^2} dx = \pi$$

Hence equation (7.47) becomes

$$G = \frac{4\pi}{\lambda^2/ab}$$

making the gain of a rectangular aperture relative to an isotropic source

$$G = \frac{4\pi ab}{\lambda^2} \quad (7.48)$$

This expression is generally true for any uniformly illuminated aperture and can be written as

$$G = \frac{4\pi}{\lambda^2} \text{area of aperture} \quad (7.49)$$

From this, it can be seen that the larger the aperture the greater the gain of the antenna.

For a circular aperture of diameter  $D$ , the area of the aperture is  $\pi D^2/4$ , giving a gain of  $(\pi D/\lambda)^2$  relative to an isotropic source or dividing by 1.63 (see Section 3.5). The gain for a circular aperture of diameter  $D$  relative to a half-wave dipole becomes

$$G = 6 \left( \frac{D}{\lambda} \right)^2 \quad (7.50)$$

Since the dimensions of the feed used to illuminate a reflector antenna are not negligible compared with the aperture of the antenna, the point source approximation suggested by Figure 7.10 is not entirely accurate and consequently the beam formed by the parabolic reflector will be divergent. Thus the polar pattern will exhibit a narrow main lobe with small side lobes. In addition, with practical feed networks the provision of perfect uniform illumination is impossible, and some energy spills over the edge of the reflector and is lost, thereby reducing the efficiency of the antenna.

A simple feed network for a parabolic reflector antenna is shown in Figure 7.11. Here a two-element dipole arrangement of the type suggested in Section 7.3 is used with a reflector element to direct radiation from the dipole towards the reflector (Figure 7.11a). This feed arrangement produces a half-power beamwidth that is approximately 25% greater than that of a circular parabolic reflector. This leads to gain reduction of around 35% on that predicted by equation (7.50). However, this tapering of illumination can be used to advantage to provide side-lobe reduction of up to 20 dB (see Section 4.4); this arrangement also requires a balun (Section 6.4).

The focal length of the parabolic reflector is also of importance (see Figure 7.11b). If the focal length is small, thereby forcing the feed to be positioned inside the aperture (Figure 7.11b (i)), then uniform illumination will be very difficult to achieve. With

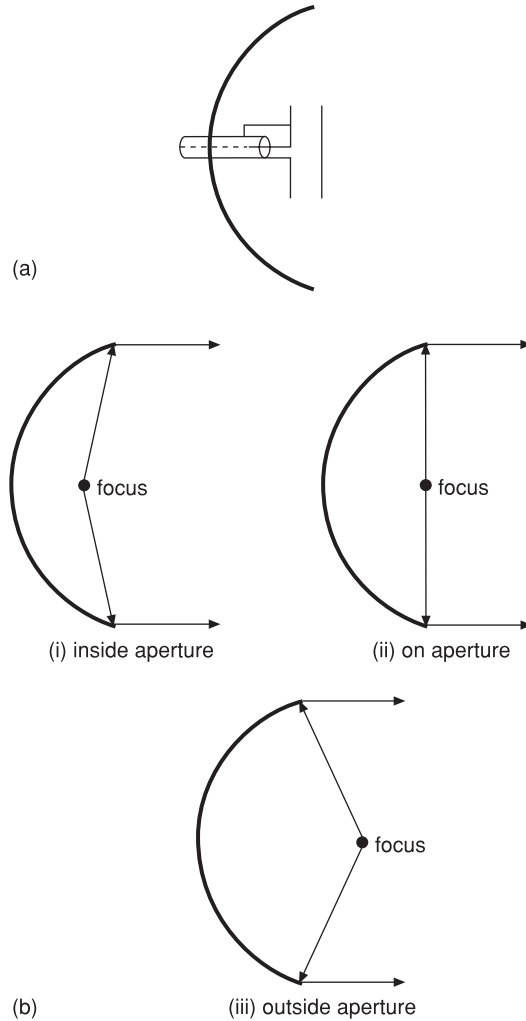


**Figure 7.11** Parabolic feed arrangements: (a) dipole feed; (b) feed positions

the focus placed outside the aperture, feed radiation spillover is difficult to prevent (Figure 7.11b (ii)). The focal length feed configuration that yields maximum gain is when the focus is placed at the aperture (Figure 7.11b (iii)).

Other types of arrangement that use waveguide feeders are popular. In many cases, these take the form of a waveguide flared at the end into a small horn antenna (Section 7.7). The feed arrangement can be offset from the reflector to prevent aperture blockage by the feed.

In addition to parabolic reflectors, a reflector can have its shape deformed in order to produce specialised radiation patterns. Such beam-shaped antennas find use in a variety of applications, including radar, remote sensing and direct broadcast radiation footprint design. In addition, by varying the position of the feed network relative to

the focus of the parabola, it is possible to scan the beam produced by the antenna. These and other considerations related to reflector antennas are discussed in more detail in reference [55].

## 7.6 Helical antennas

Helical antennas are formed by winding a helix or helices from a single or multiple conductor. This type of antenna is a natural choice for producing radiation that is circularly polarised. The antenna operates by setting up travelling waves on the conductors forming the helix. This class of antenna exhibits other useful operational features, such as nearly real input impedance and wide bandwidth.

The helix can radiate in a number of different modes (Figure 7.12). Of these, the axial mode in Figure 7.12b is widely used for point-to-point communication as it provides focused radiation along the z-axis. This mode occurs when the helix circumference is about one wavelength long. When the helix circumference is small relative to the operating wavelength, normal-mode radiation occurs (Figure 7.12a). This mode of operation is useful in mobile communications equipment such as telephone handsets. Higher-order modes such as the conical mode in Figure 7.12c occur when the circumference of the helix is greater than a wavelength.

Figure 7.13 defines the helix geometry used in this section. The following dependencies exist for the parameters shown in Figure 7.13 for a cylindrical helix.

$$L^2 = (\pi D)^2 + S^2 \quad (7.51)$$

$$\alpha = \tan^{-1} \frac{S}{\pi D} \quad (7.52)$$

$$\ell = nS \quad (7.53)$$

where  $n$  is the number of turns and  $S$  is the pitch of the helix.

The helix can of course be flared to form a conical helix with an increasing or decreasing flare angle in order to alter its performance; for more detail see [56]. Due to the complexity of this situation, this aspect will not be further discussed here.

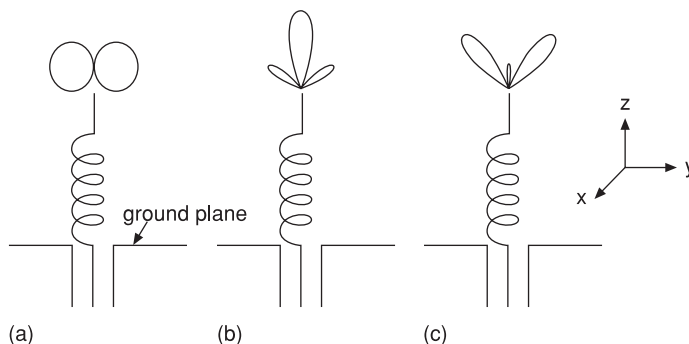


**Figure 7.12** Helical antenna operating modes: (a) normal (omnidirectional) mode; (b) axial mode; (c) conical mode

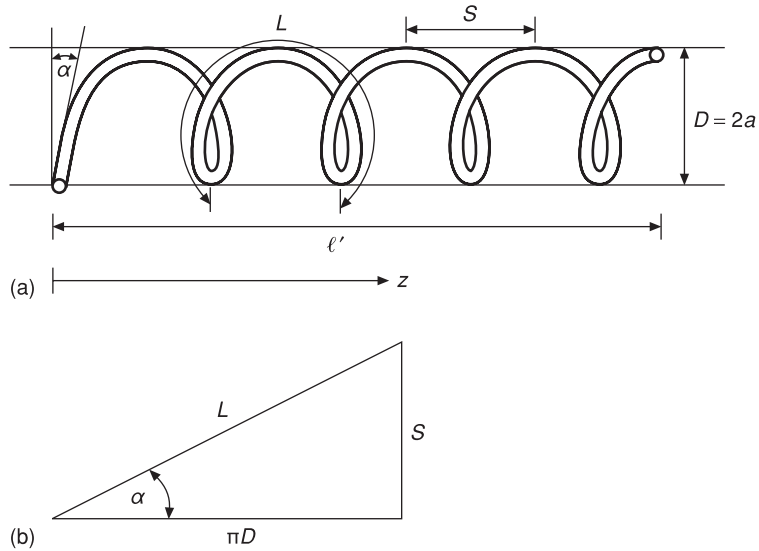


Figure 7.13 Simple helix geometry

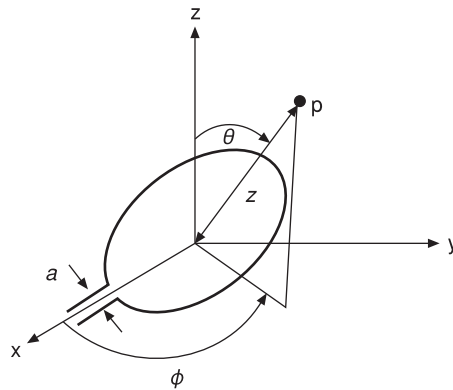


Figure 7.14 Single-turn geometry

Consider now the condition necessary to realise axial radiation. The relative strengths of axial versus normal-mode radiation for a helical antenna are discussed in considerably more detail than the treatment given here in [57]. Consider a single turn of the helix in which  $\alpha$  in figure 7.13a is set equal to zero, i.e. a circular loop (Figure 7.14). Assume that a standing wave has been set up on the turn with an antinode at  $x = a$ . For  $L/\lambda \ll 1$  and  $L/\lambda = 1$ , the  $x$  and  $y$  components of current can be sketched (Figure 7.15a and b), respectively. In the  $L/\lambda \ll 1$  case, the current distribution is almost constant around the loop. Thus from Figure 7.15a:

$$-I_{x_A} = I_{x_C} \tag{7.54}$$

$$-I_{x_B} = I_{x_D} \tag{7.55}$$

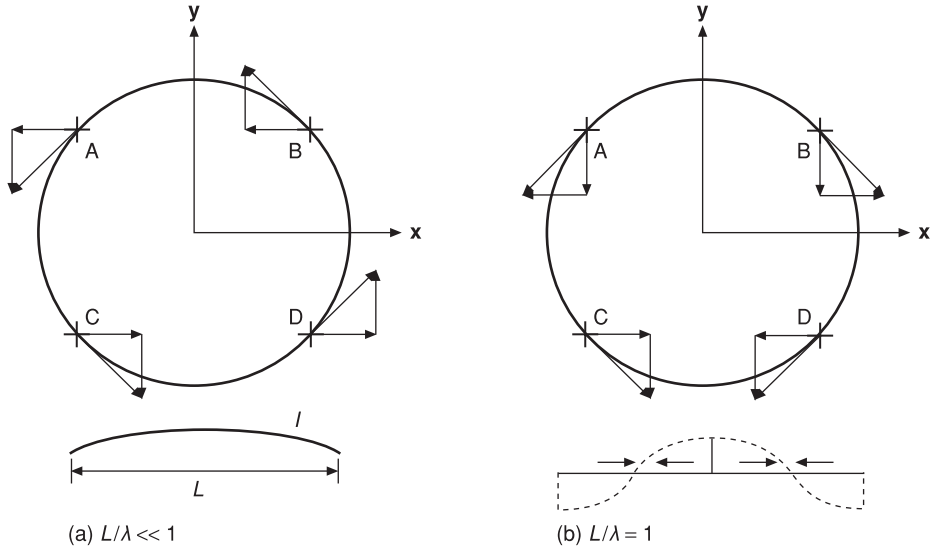


Figure 7.15 Loop current distributions

Hence there can be no  $x$  component of the  $E$  field and the resulting radiation is linearly polarised with its  $E$  field vector parallel to the  $y$ -axis.

For the  $L/\lambda = 1$  case (Figure 7.15b)

$$I_{yA} = I_{yC} = I_{yB} = I_{yD} \tag{7.56}$$

and for  $L/\lambda \ll 1$

$$I_{yA} = I_{yC} = -I_{yB} = -I_{yD} \tag{7.57}$$

Hence we would expect that the axial radiation for the  $L/\lambda \ll 1$  case should be less than for the  $L/\lambda = 1$  case.

Consider the radiation field for a single loop as defined in Figure 7.14. Following the procedure adopted in Section 1.4, we can find the radiation in the axial direction as [57]

$$\begin{aligned} E_y &= \frac{30kI_0}{z} e^{-jkz} 2 \int_0^\pi \cos(ma\phi) \cos(\phi) a \, d\phi \\ &= \frac{60I_0}{z} e^{-jkz} (ka)^2 \frac{\sin\pi ka}{(1 - (ka)^2)} \end{aligned} \tag{7.58}$$

Here  $I_0$  is the maximum current on the loop and  $a$  is its radius, Figure 7.13a.

For  $L/\lambda = 1$ , equation (7.58) becomes

$$E_y = \frac{60I_0}{z} e^{-kz} \frac{\pi}{2} \tag{7.59}$$

assuming a cosine current distribution necessary for the standing wave condition mentioned above. Along  $\phi = 90^\circ$

$$E_y = \frac{60I_0}{z} e^{-jkz} \int_0^\pi \cos\phi \sin(\sin\phi) \sin\phi \, d\phi = 0 \quad (7.60)$$

Comparing equation (7.60) with (7.59) shows that for  $L/\lambda = 1$  the radiation in the axial direction is much stronger than that in the direction normal to the axis. For other angles of  $\phi \neq 90^\circ$ , the value of the normal field will increase. However, for an assumed cosine distribution it never rises above 0.65 times the axial field value [57].

The field in the plane normal to the axial direction is further attenuated when a ground plane is introduced, as in Figure 7.12. Essentially then for the axial mode to be formed in a helical structure, the current in each segment of each turn must be suitably phased for end-fire radiation to occur; for example, see Section 4.7. Hence if the spacing between turns,  $S$  (Figure 7.13a), is approximately  $\lambda/4$  the phase of the second element should lag by  $\lambda/4$ . This condition can be met by making the length of the turn  $(\lambda + \lambda/4)$ . Hence a pitch of  $\lambda/4$  and a turn length  $L$  of  $5\lambda/4$  should give a usable antenna. Since the  $\lambda/4$  condition is only approximate due to mutual coupling effects, let the length be  $\ell'$ . Thus the diameter  $D$  of the helix can be written using equation (7.51) as

$$D = \sqrt{\frac{L^2}{\pi} - \frac{S^2}{\pi}} \quad (7.61)$$

$$\frac{D}{\lambda} = \frac{\sqrt{(1 + \ell')^2 - \ell'^2}}{\pi} = \frac{\sqrt{1 + 2\ell'}}{\pi} \quad (7.62)$$

With this type of antenna, the axial mode can be maintained over a frequency range of typically 1.7:1 without significant perturbation of the far-field pattern.

Empirical equations that approximate the characteristics of a single-wire helical antenna consisting of  $n$  turns when operated in axial mode are listed below [56].

- the half power angle:

$$2\theta_{3\text{dB}} = \frac{52}{\frac{L}{\lambda} \sqrt{\frac{nS}{\lambda}}} \text{ degrees} \quad (7.63)$$

- the angle to the first zero in the polar pattern:

$$2\theta_0 = \frac{115}{\frac{L}{\lambda} \sqrt{\frac{nS}{\lambda}}} \quad (7.64)$$

- the gain of the antenna:

$$G = 15 \left( \frac{L}{\lambda} \right)^2 n \frac{S}{\lambda} \quad (7.65)$$

- the input impedance of the antenna:

$$Z_{\text{in}} \approx R_{\text{in}} = 140 \frac{L}{\lambda} \quad (7.66)$$

## 7.7 Horn antennas

It is possible to construct an antenna by flaring the aperture of a rectangular to circular waveguide such that the impedance of the waveguide is made to match that of free space. A rectangular waveguide can be made to flare in the  $E$  plane (sectorial  $E$ -plane horn) or the  $H$  plane (sectorial  $H$ -plane horn) with a rectangular aperture, or in both  $E$  and  $H$  planes (pyramidal horn) with a square aperture (Figure 7.16). In a horn antenna, the wavefront near the horn can be shown to be spherical [58].

Sectorial  $H$ -plane horns give slightly wider beamwidth than sectorial  $E$ -plane types. This is mostly due to the near uniform  $E$  field distribution that can be obtained over the aperture in the sectorial  $E$ -plane horn antenna. Unfortunately, for all types, since the length of the taper  $\ell_T$  (Figure 7.16) is greater than the open end of the aperture, a phase distribution across the aperture occurs. This results in gain reduction due to increased side-lobe production.

As with a reflector antenna, the larger the radiating aperture the larger the directivity and unwanted non-uniformity in the phase distribution across the aperture. For a pyramidal horn antenna, the power gain  $G$  is given approximately as

$$G = \frac{7.5A}{\lambda^2} \quad (7.67)$$

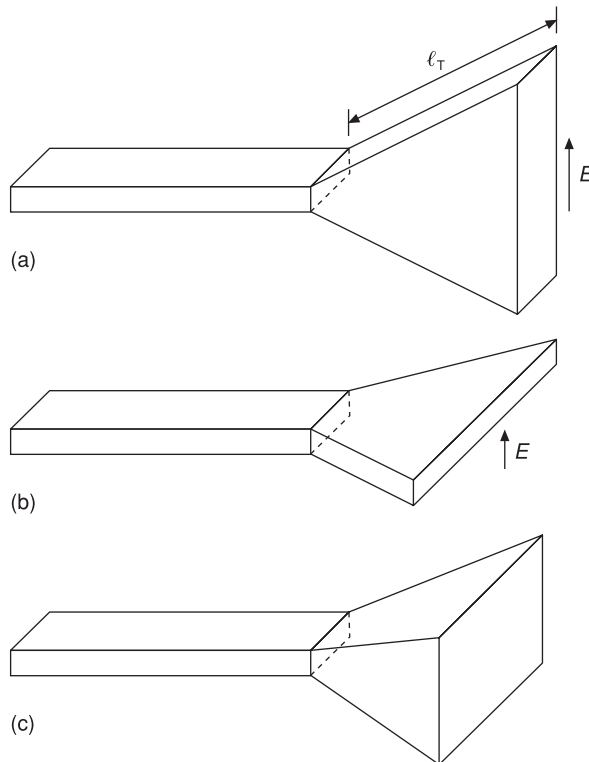


**Figure 7.16** Basic horn antenna types: (a)  $E$ -plane horn; (b)  $H$ -plane horn; (c) pyramidal horn

and its 3 dB beamwidth  $B$  is

$$B = \lambda/d \text{ radians} \quad (7.68)$$

where  $A$  is the area of the horn antenna aperture, and  $d$  is the aperture width in the plane of the beamwidth measurement.

Since this type of antenna is easy to fabricate, can have large gain and is easy to feed, it tends to be used as a favoured antenna type for calibration standards by which other high-gain antennas are characterised. The design procedure by which the dimensions for a *standard-gain horn antenna* can be calculated are given in reference [58]. In [59], detailed design nomographs are given, which greatly facilitate the practical design of rectangular horn antennas.

## 7.8 Straight-wire travelling-wave antennas

Resonant antennas have narrow bandwidth operation, typically only a few percent. When there is a need for wider bandwidth operation, a non-resonant or travelling-wave antenna affords a possible solution. In this solution methodology, the antenna ideally operates with a uniform current distribution and progressive phase lag along its length. To see what effect these conditions have on the radiation characteristics of a straight wire isolated from ground plane effects, consider Figure 7.17. Here the antenna is excited by a generator, producing current. Residual power at the end of the wire that has not been radiated is arranged to be absorbed in a matching resistor  $R$  to prevent its reflection and unwanted subsequent re-radiation.

If we assume that the straight wire in Figure 7.17 is comprised of many elements of length  $dx$ , then from equation (7.69), valid for an elementary Hertzian dipole (Section 1.2), we can write

$$dE_{\theta} = \frac{60\pi I_0 e^{-j\beta x} dx \sin\theta}{\lambda r} \quad (7.69)$$

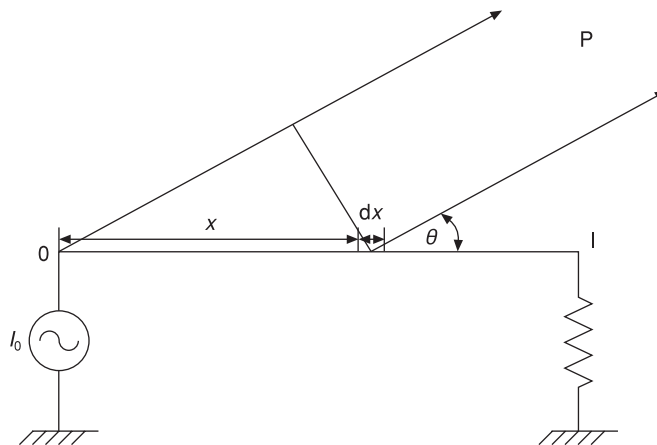


Figure 7.17 Straight-wire travelling-wave antenna

where  $I_0$  is the RF current produced by the generator, and  $\beta = 2\pi/\lambda$  is the current lag per unit along the wire.

If we assume that the generator, located at position 0 in Figure 7.17, represents the reference phase position, the radiated field associated with element  $dx$  will be  $(2\pi x/\lambda) \cos\theta$ , or  $\beta x \cos\theta$  with respect to the reference position. Hence the total field can be obtained by integrating equation (7.69) over the entire length of the straight wire,  $\ell$  (see equation (7.70)).

$$E_\theta = \int_0^\ell e^{j\beta x \cos\theta} dE_\theta \tag{7.70}$$

$$\begin{aligned} &= \frac{60\pi I_0}{\lambda r} \int_0^\ell e^{-j\beta x} e^{j\beta x \cos\theta} \sin\theta \, dx \\ &= \frac{60\pi I_0}{\lambda r} \int_0^\ell e^{-j\beta x(1-\cos\theta)} \, dx \\ &= -\frac{60\pi I_0}{\lambda \beta r} \frac{\sin\theta}{(1-\cos\theta)} [e^{-j\beta x(1-\cos\theta)}]_0^\ell \end{aligned} \tag{7.71}$$

$$= \frac{60\pi I_0}{2r} \frac{\sin\theta}{(1-\cos\theta)} [e^{-j(2\pi\ell/\lambda)(1-\cos\theta)} - 1] \tag{7.72}$$

Hence

$$|E_\theta| = \frac{60I_0}{r} \frac{\sin\theta}{(1-\cos\theta)} \sin \frac{\pi\ell}{\lambda} (1-\cos\theta) \tag{7.73}$$

Equation (7.73) can then be used to obtain the polar pattern for the straight single-wire travelling-wave antenna. Figure 7.18 shows a typical pattern for the cases when the length of the wire,  $\ell$ , ranges from  $0.5\lambda$  to  $4\lambda$ . From these patterns, it can be seen that the antenna is radiating end-fire with a null in the forward,  $\theta = 0$ , direction. As the length of the wire increases, the main lobe becomes narrower and is directed at a shallower angle  $\theta$ .

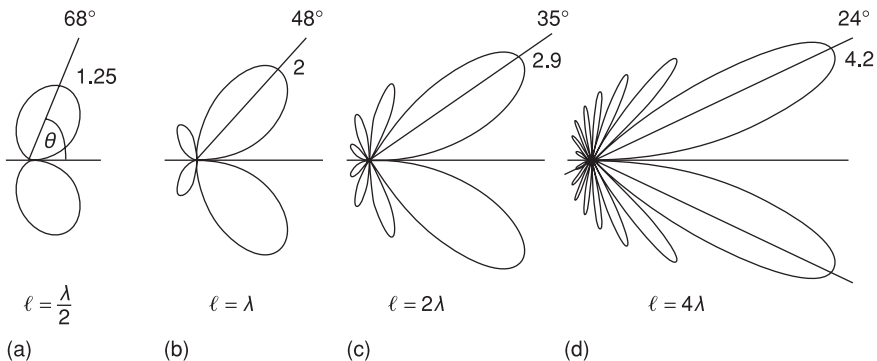
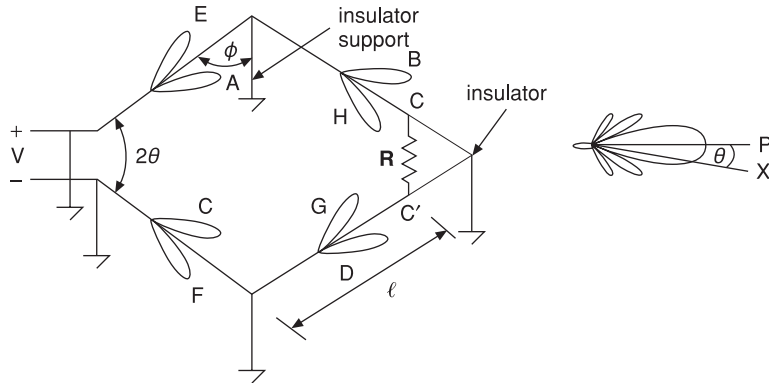


Figure 7.18 Far-field patterns for travelling-wave radiator



**Figure 7.19** Four-wire travelling-wave radiator rhombic antenna

For a single-wire travelling-wave antenna of the type illustrated in Figure 7.17, it is necessary to ensure that the end of the terminating resistance not connected to the straight wire is made to be at a low impedance with respect to its surroundings; this can be achieved by connecting it to a quarter wavelength stub. Otherwise, a second wire is needed to provide a ground return path. The presence of this second wire will affect the behaviour of the single-wire antenna in a similar fashion to that reported in Section 4.8 for a dipole antenna placed over a conducting ground plane.

Another alternative for travelling-wave wire antennas exists in which the return conductor is deformed such that a rhombus is formed (Figure 7.19). Here four straight-wire travelling-wave antennas fed by a balanced line are arranged so that the wires are far enough apart that each wire produces a radiation characteristic such as that shown in Figure 7.19. Here the wire separation is such that lobes A, B, C and D reinforce to give additional gain. Lobe pairs E and F and G and H are designed to cancel each other. Resistor A connected between points C and C' absorb residual energy, and the structure is held above a ground plane on insulated supports. Due to the low angle forward lobe formation, such structures have been traditionally used for low-frequency long-distance communications, where a low angle of incidence signal occurs due to ionospheric reflection [55].

The design of this type of antenna consists of optimising three main parameters: height  $h$ , length  $\ell$  and tilt angle  $\phi$  (Figure 7.19). Height  $h$  mainly controls the elevation angle  $\theta$ , and  $\ell$  and  $\phi$  control the maximum gain available from the antenna in association with  $h$ .

If we make  $\theta = 90 - \phi$ , then equation (7.73) can be used to establish the contribution of wire AB, in Figure 7.19, along the main axis. The contribution from A'B' will be the same and in phase with that from AB, since the currents at equivalent positions in the two wires are in antiphase. Hence twice the field strength predicted by equation (7.19) will occur due to the constructive contributions of wires AB and A'B'. For non-optimal values of  $\theta$ , the principal lobe in the horizontal plane will broaden, and eventually addition with a partial null along the main axis will occur.

Since the current at B lags the current at A by  $2\pi\ell/\lambda$  and the current at B' lags by another  $\pi$  radians because it is in antiphase, and in addition, since B'C' is  $(2\pi\ell \cos\theta)/\lambda$  closer to observation point P in Figure 7.19 then the field at P due to AB and BC' is

$$\frac{2\pi\ell}{\lambda} + \pi - \frac{2\pi\ell \cos\theta}{\lambda} \quad (7.74)$$

Therefore, if  $E_{AB}$  is the field due to lag AB, then the resultant field will be

$$2E_{AB} \cos 1/2 \left( \frac{2\pi\ell}{\lambda} + \pi - \frac{2\pi\ell}{\lambda} + \pi - \frac{2\pi\ell \cos\theta}{\lambda} \right) \quad (7.75)$$

hence the factor by which the contribution from wire AB must be multiplied to give the field from AB and B'C' and similarly for A'B' and BC combined is

$$2 \sin \left( \frac{\pi\ell}{\lambda} (1 - \cos\theta) \right) \quad (7.76)$$

Thus the total field strength,  $E$ , along the main axis is obtained by using equations (7.73) and (7.76):

$$E_{\theta} = \frac{120I_0}{r} \frac{\sin\theta}{(1 - \cos\theta)} \sin \left( \frac{\pi\ell}{\lambda} (1 - \cos\theta) \right) 2 \sin \left( \frac{\pi\ell}{\lambda} (1 - \cos\theta) \right) \quad (7.77)$$

$$= \frac{240I_0}{r} \frac{\sin\theta}{(1 - \cos\theta)} \sin^2 \left( \frac{\pi\ell}{\lambda} (1 - \cos\theta) \right) \quad (7.78)$$

or

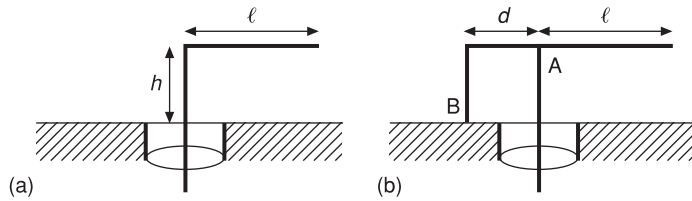
$$E_{\theta} = \frac{240I_0}{r} \frac{\cos\phi}{(1 - \sin\phi)} \sin^2 \left( \frac{\pi\ell}{\lambda} (1 - \sin\phi) \right) \quad (7.79)$$

Here the factor of 4 (i.e.  $4 \times 60$ ) signifies the contribution from all four wire elements comprising the array. When equation (7.79) is plotted against  $\phi$  for various values of  $\ell$ , the optimum tilt angle for maximum gain along the boresight can be obtained.

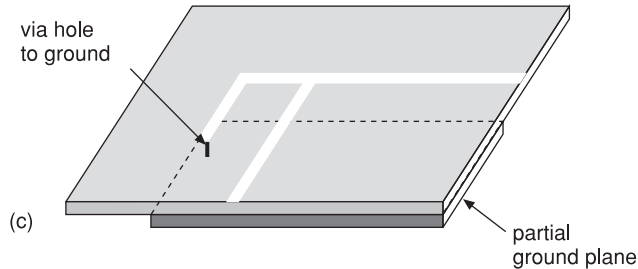
## 7.9 Planar inverted-F antennas

Figure 7.20 shows the basic configurations of L and F antenna types. These antennas, which offer low profile and narrow bandwidth, are widely deployed in cars and aircraft. In the L antenna (Figure 7.20a), the vertical section provides a short monopole antenna, which is capacitively loaded to produce a more uniform current distribution (Section 3.4), typically  $h + \ell \ll \lambda/4$ . The presence of the capacitive wire reduces the height of the monopole while creating a lower resonant frequency than could otherwise be obtained for a short monopole of the same height. With this type of antenna, the vertical section produces omnidirectional radiation, with only minor radiation occurring from the horizontal section due to image cancellation (Section 3.4).

In the F antenna (Figure 7.20b), the addition of section AB to the L antenna permits a means for impedance matching by inductive tuning of the antenna; typically



□



**Figure 7.20** Inverted antennas: (a) L type; (b) F type; (c) printed F

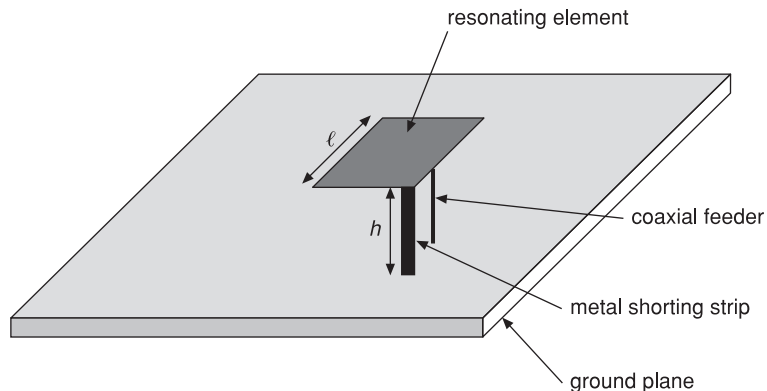


**Figure 7.21** Basic PIFA antenna:  $h \ll \lambda$  and  $\ell + h \approx \lambda/4$

$h + \ell \approx \lambda/4$  and  $d \ll \lambda$ . Such an antenna can be implemented in microstrip without the need for a balun. When printed on to a substrate with  $\epsilon_r > 1$ , then size can be reduced. With this antenna, parasitic elements can be added to provide an increase in bandwidth or to introduce dual- or multiple-band frequency operation. With the arrangement shown in Figure 7.20c, radiation is omnidirectional. The  $Q$  factor is also lowered when compared with a resonant microstrip antenna, hence bandwidth is larger.

For mobile handset applications, the F antenna is modified to form a printed F (Figure 7.20c) or a planar inverted-F or PIFA antenna (Figure 7.21). The size and radiation characteristics of this type of antenna make them attractive for mobile handset applications, since they can be readily incorporated into the handset case, which provides

a finite ground plane and which in turn leads to preferential radiation away from the user. This is considered to be a desirable feature in a personal mobile wireless handset.

The impedance bandwidth of the PIFA antenna is related to height,  $h$ , of the resonating patch above the ground plane; the greater the value of  $h$  the larger the radiation bandwidth of the PIFA. The PIFA radiates both vertical and horizontally polarised signals, again an attractive feature for handheld mobile applications, where the precise orientation of the antenna cannot be guaranteed. Dual- and triple-band variations have been reported [60], and the impedance bandwidth of the basic PIFA on a small ground plane can be as much as 10%.

### 7.10 Dielectric resonator antennas

A dielectric resonator consists of a three-dimensional geometrically regular shape of ceramic material with a high dielectric constant, typically  $\epsilon_r \approx 40$ . Due to the large discontinuity between the inside and outside of the resonator, normally air  $\epsilon_r = 1$ , reflection of energy at the interface occurs, and there are a variety of resonant modes. When operated without a shielding enclosure, sufficient energy is lost from the resonator to make them useful as an antenna. The actual mode type depends on the size and shape of the resonator, which is usually hemispherical, cylindrical or rectangular, and also on the method and frequency of excitation selected. The primary advantages of the use of a high-permittivity dielectric as a radiating element are that the material losses are low, consisting only of dielectric losses; the antenna can also be miniaturised, since the dielectric wavelength is proportional to  $1/\sqrt{\epsilon_r}$  times the free-space wavelength. In addition, this type of antenna can have high radiation efficiency, since it does not suffer from conductor or surface wave losses.

A further significant advantage occurs because resonators can support several different modes; hence, in principle, various radiation patterns for different applications can be realised with a single antenna, depending on how it is excited. Consequently, far-field radiation patterns can be made to be broadside or omnidirectional, the actual quality of the far-field pattern ultimately being determined by the size and shape of the ground plane upon which the dielectric resonator radiating element is mounted. 2.1 VSWR bandwidth can vary between a few percent for high  $\epsilon_r$  to 20% for low  $\epsilon_r$  materials; for example, it can be 10% for  $\epsilon_r \approx 10$  material.

One particular geometry that has been thoroughly studied is a dielectric cylindrical resonator mounted above a ground plane (Figure 7.22). The far-field radiation pattern for this configuration when operated in  $TM_{110}$  mode is similar to that of a dipole positioned parallel to and one quarter of a wavelength above a ground plane (see Section 4.8). This mode is of particular interest, since it is the fundamental mode of a cylindrical resonator radiating element and thus has the lowest resonant frequency,  $f_{TM_{110}}$ , for given resonator dimensions:

$$f_{TM_{110}} = \frac{1}{2\pi a \sqrt{\mu_0 \epsilon_r}} \sqrt{(1.841)^2 + \left(\frac{\pi a}{2d}\right)^2}$$

where  $a$  is the radius of the cylinder and  $d$  its height.

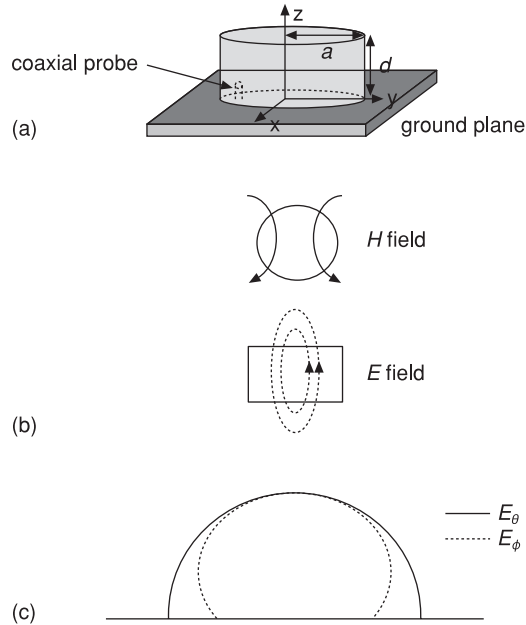


**Figure 7.22** Coaxial probe-fed dielectric resonator antenna

This type of mode can be excited by using a coaxial feed probe placed internally and near to its circumference in order to excite the  $TM_{110}$  mode of the dielectric resonator element (Figure 7.22). Figure 7.22b shows the electric and magnetic field distributions for this mode, while Figure 7.22c shows sketches of the resulting ideal far-field patterns for this mode. It can be seen that when the dielectric resonator is positioned over a ground plane, the far-field pattern will be similar to that of a  $TM_{010}$  rectangular microstrip patch antenna.

## 7.11 Reflectarray antennas

In order to produce a plane wavefront from a source producing a spherical wavefront, it is necessary to introduce appropriate phase compensation across the spherical wavefront. In Section 7.5, this was achieved by using the intrinsic phasing properties of a curved parabolic dish. In a reflectarray antenna, the objective is to construct a planar antenna array that is capable of scattering an incident wavefront with suitable phasing superimposed such that a planar wavefront is collimated along some predetermined direction (Figure 7.23). In this way, the normal parabolic dish antenna can be replaced by a flat reflector or by a conformal surface. A second benefit of the reflectarray concept is that the corporate feed arrangement normally associated with a planar array is eliminated in favour of a spatial feed. This arrangement is much easier to construct at millimetre wavelengths, where corporate feed losses can become unacceptably high. Thus reflectarrays can offer a variety of antenna configurations that have electrical, aesthetic and ergonomic benefits.

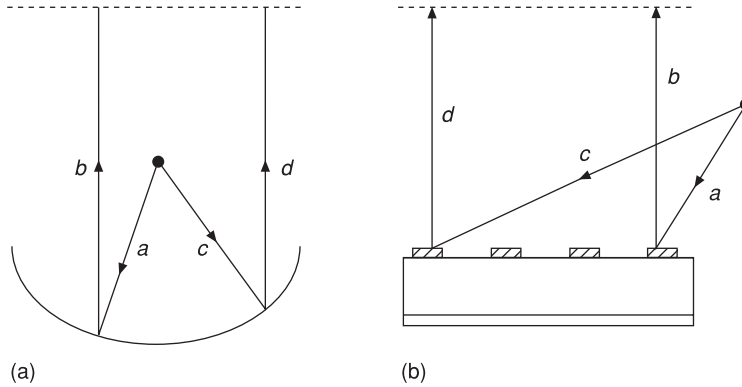


**Figure 7.23** Reflectarray concept: (a) parabolic dish  $a + b = c + d$ ; (b) microstrip patch reflectarray  $a + b = c + d$

The basic principle underpinning the operation of a reflectarray is the means by which to make the constituent elements of the array scatter the incident signal with the appropriate phases necessary for plane wave formation. Like the parabolic dish reflector, the basic design philosophy for a reflectarray requires that the total phase delay from the feed to a fixed aperture plane is constant for all elements (Figure 7.23). A simple narrowband method for achieving this was proposed in [61].

The method is based on the fact that a dipole antenna short-circuited at its feed terminals will at resonance reflect a signal that is  $180^\circ$  out of phase with the incident signal. Off resonance, the phase of the reflected signal can be made to lie anywhere between  $0^\circ$  and  $360^\circ$ . The same effect can be made to occur by keeping frequency constant and varying dipole length about the length required for resonance. Figure 7.24

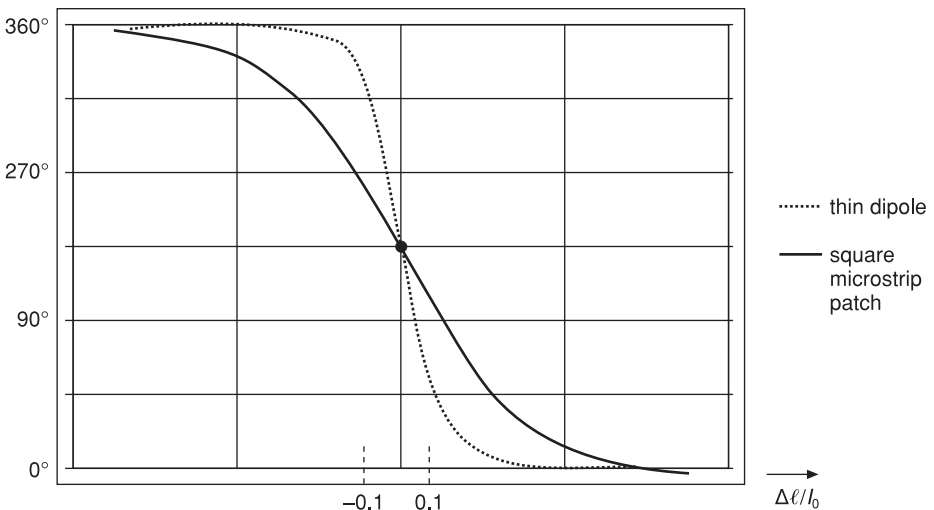


**Figure 7.24** Reflectarray phase

indicates how the phase of the reflected signal varies for a thin wire dipole mounted over a ground plane. Here, due to the steep slope of the reflected phase response, it can be seen that accurately controlling the reflected phase from a thin wire dipole would be extremely difficult. By replacing the dipole with a square microstrip patch antenna, the same effect occurs but in a more controlled manner, i.e. the phase response is a less steep function of element length. With microstrip patch elements the bandwidth is about 2%. This is less than a parabolic antenna but is better than a basic corporate-fed planar microstrip array.

Variants on the basic design permit dual and circular polarisation to occur; in addition, other elements based on stacked microstrip patches or ring geometries can offer better bandwidth responses than those obtained from a single microstrip patch [62]. A significant advantage of the reflectarray is that with appropriate phasing it can be made to produce a main beam that can be squinted off broadside, allowing the antenna to be mounted vertically with its main far-field lobe aligned to a predetermined direction in the forward half-space of the antenna.

## 7.12 Equi-angular spiral antennas

A number of modern communication applications, for example surveillance receivers, require extremely broadband antennas. A class of antennas was proposed in [63] that in principle have unlimited bandwidth, with ratios of 10:1 common; these antennas are known as frequency-independent antennas. The operating principle for this class of antenna relies on the ability to construct a structure whose geometry can be defined entirely by angles and not by any particular dimension. If this is the case, then arbitrary scaling applied about the feed point of the structure will result in a new structure that is identical to the old one but is rotated about the same axis passing through the feed point of the antenna. If this is the case, then the new structure will operate efficiently at a different frequency  $kf$  relative to the original frequency  $f$ .

Rumsey showed that the axis of rotation must be independent of  $k$  and must be proportional to

$$\rho = e^{a(\phi-\delta)}$$

where  $a$  and  $\delta$  define the rate of the resulting spiral, and  $\rho$  and  $\phi$  are the normal polar coordinate notation. If this condition is adhered to, then a frequency-independent antenna can be constructed. A planar two-spiral suitability tapered with distance is shown in Figure 7.25. Here the edges of the arms are defined by

$$e_1 = ke^{a\phi} \text{ and } p_2 = ke^{a(\phi-\delta)} \text{ for arm 1}$$

and

$$e_1^1 = ke^{a(\phi-\pi)} \text{ and } p_2^1 = ke^{a(\phi-\pi-\delta)} \text{ for arm 2}$$

In this type of spiral, the angle between the spiral and the radius vector is constant for all points, hence its name, the equi-angular spiral. An important property of this type of spiral is that it retains its frequency-independent properties when it is truncated.

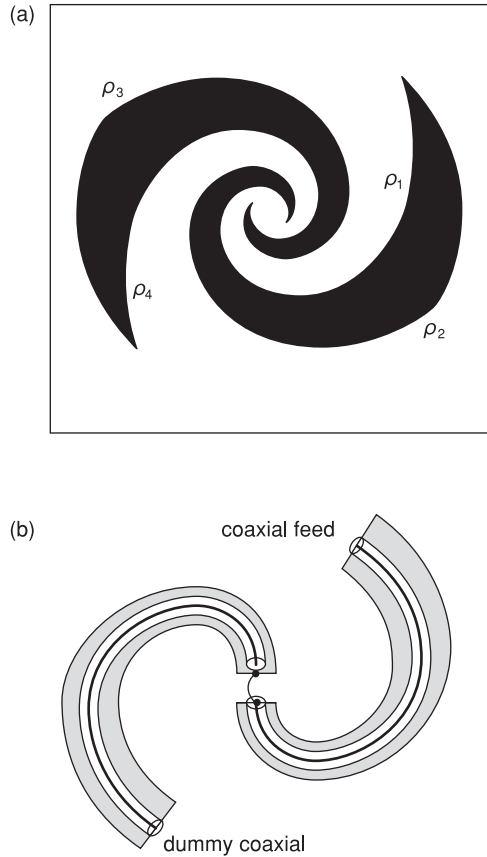


**Figure 7.25** Finite equiangular spiral antenna

The antenna is fed with a balanced voltage applied to the spiral arms. As the currents on the spiral flow outwards they suffer little attenuation until they reach a region of the spiral where the gap is resonant and energy is radiated; this region is known as the active region. The active region moves inwards or outwards as frequency is increased or decreased, respectively, thus the radiating aperture of the antenna is modified automatically so that in principle the same terminal impedance and radiation pattern is achieved at all frequencies. However, it is important to remember that since the active area is rotated with angle about the antenna axis, the radiation from the antenna is also rotated. Radiation occurs in the forward and back hemispheres, and the pattern generally has the best axial ratio for high spiral rates.

A preferred method for feeding the antenna is to use a coaxial cable attached to one arm of the spiral, and for symmetry a second identical dummy cable is attached to the other arm of the structure (Figure 7.25). Since the current decreases exponentially along the spiral, the presence of these cables has very little effect on the far-field radiation patterns.

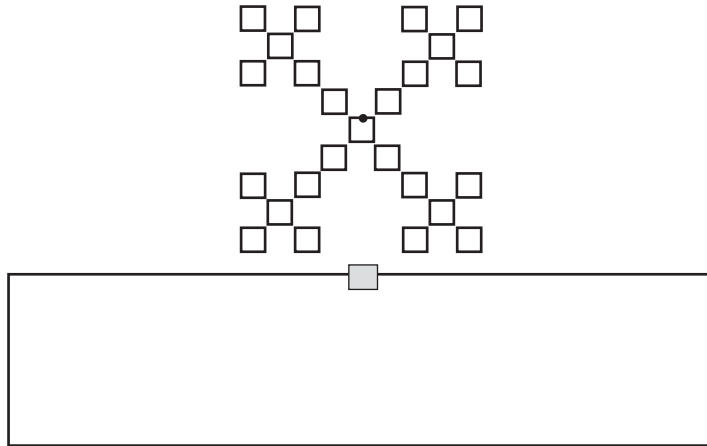


Figure 7.26 Fractal loop (top) and folded dipole antenna (bottom)

### 7.13 Fractal antennas

In an attempt to achieve multifrequency operation while simultaneously reducing antenna size, workers have started to combine the disciplines of fractal geometry [64] and antenna theory. In the 1970s, B. Mandelbrot defined the term ‘fractal’ to describe a set of geometrical objects that have self-similar shapes. An important property that a fractal must have is its fractional dimension. This is a mathematical means for defining how effectively the object fills space. Fractal curves have the mathematical property that they fill a given space better than any classical Euclidean surface, and this property is the key to obtaining antennas that occupy a small space.

The 1990s brought the first reports of multiband and reduced-size antennas exploiting this discipline [65]. In Section 7.12, it was shown that in order for an antenna to work effectively across a range of frequencies it should be symmetrical about a point, and it must be self-similar; that is to say, it must have the same general appearance at every scale. In some sense, it is appropriate to describe this as a characteristic of a fractal. A fractal curve is a set of self-similar broken curves, consequently fractal antenna area reduction of two to four times relative to its classical counterpart is not uncommon (Figure 7.26). The properties of this type of antenna include multiband performance at non-harmonic frequencies and matched input impedance, which helps to reduce the complexity of matching circuitry. As such, fractal antennas are essentially self-matching; furthermore, far-field radiation patterns are generally similar with frequency.

Due to the potential for size reduction, considerable activity has been devoted to realising usable designs for personal handheld terminals operating between 800 MHz and 1800 MHz, with the fractal design methodology being applied to dipoles and monopoles in an attempt to obtain a single antenna that can operate over the entire frequency band. A fractal antenna is constructed entirely by many copies of itself at different scales, e.g. Figure 7.27. Consider now one particular example of a fractal antenna, the Sierpinski monopole antenna [65]. The shape of this antenna evokes another

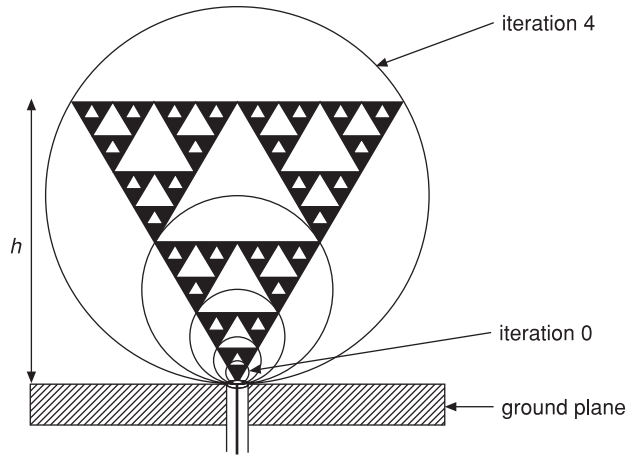


**Figure 7.27** Five-iteration Sierpinski monopole antenna

wideband antenna type, the bow-tie antenna [66], itself a broader band version of the dipole antenna. With the version shown in Figure 7.27, the Sierpinski fractal algorithm has been iterated five times. Neglecting the holes (white areas), each iteration gives rise to a self-scaled version of a simple bow-tie antenna. Each of these structures operates at its own resonant frequency. Across the bandwidth, in [65] it was shown that the structure was approximately matched at logarithmic frequencies  $f_m$ , such that

$$f_m \approx 0.26 \frac{c}{h} \delta^n$$

where  $c$  is  $3 \times 10^8 \text{ ms}^{-1}$ ,  $h$  is the height of the largest gasket,  $\delta$  is the log period (two in this case), since at iteration 4 we have  $2^4$  black triangles. The far-field radiation patterns at each of these frequencies for  $h = 88.9 \text{ mm}$  was reported in [65] and shown to be broadly similar at each frequency to those that would be obtained from appropriately sized bow-tie antennas positioned over a finite ground plane.

## References

- [45] Jordan, E.C. and Balmain, K.G., *Electromagnetic Waves and Radiating Systems*, 2nd edition, Prentice Hall EE Series, 1968.
- [46] Jasik, H., *Antenna Engineering Handbook*, McGraw-Hill, 1961.
- [47] Yagi, H., Beam transmission of ultra short waves, *Proc. IRE*, Vol. 16, pp. 715–41, 1928.
- [48] Munson, R.E., Conformal microstrip antennas and microstrip phased arrays, *IEEE Trans. on Ant. and Prop.*, pp. 74–8 Jan. 1974.

- [49] Pues, H. and van de Capelle, A., Accurate transmission-line model for the rectangular microstrip antenna, *IEEE Proceedings*, Vol. 131, pt. H, No. 6, pp. 334–9, 1984.
- [50] Bahl, I.J., Build microstrip antennas with paper-thin dimensions, *Microwaves*, pp. 50–61, Oct. 1979; also Bahl, I.J. and Bhartia, P., *Microstrip Antennas*, Artech House, 1980, Chapter 2.
- [51] Derneryd, A.G., Linearly polarised microstrip antennas, *IEEE Trans. AP*, pp. 846–51, Nov. 1976.
- [52] Huang, J., The finite ground plane effect on microstrip antenna radiation patterns, *IEEE Trans. AP*, Vol. AP-31, No. 4, pp. 649–53, July 1983.
- [53] Demuyneck, F., Nauwelaers, B. and van de Capelle, A., Arrays of coaxially fed rectangular microstrip antennas: analysis with a PC, *Microwave Engineering Europe*, pp. 49–55, Dec./Jan. 1992.
- [54] Pozar, D.M. and Schaubert, D.H. (eds), *Microstrip Antennas: The Analysis and Design of Microstrip Antenna Arrays*, IEEE Press, 1995.
- [55] Johnston, R.C. and Jasik, H. (eds), *Antenna Engineering Handbook*, 2nd edition, McGraw-Hill, 1984.
- [56] Kraus, J.D., *Antennas*, 2nd edition, McGraw-Hill, Chapter 7, pp. 265–339.
- [57] Fradin, A.Z., *Microwave Antennas*, Pergamon Press, 1961, pp. 623–8.
- [58] Balanis, C.A., *Antenna Theory Analysis and Design*, 2nd edition, John Wiley & Sons, 1997.
- [59] Milligan, T., Scales for rectangular horns, *IEEE Antennas and Propagation Magazine*, Vol. 42, No. 5, 2000, pp. 79–83.
- [60] Rowell, C.R. and Murch, R.D., A compact PIFA suitable for dual-frequency 900/1800 MHz operation, *IEEE Trans. on Ant. and Prop.*, Vol. 46, No. 4, pp. 596–8, 1998.
- [61] Pozar, D.M., Design of Millimeter Wave Microstrip Reflectarrays, *IEEE Trans. on Ant. and Prop.*, Vol. 45, No. 2, pp. 287–95, 1997.
- [62] Tasi, F.E. and Bialkowski, M.E., Designing a 161-element Ku-band microstrip reflectarray of variable size patches using an equivalent unit cell waveguide approach, *IEEE Trans. on Ant. and Prop.*, Vol. 51, No. 10, pp. 2953–62, 2003.
- [63] Rumsey, V.H., *Frequency Independent Antennas*, Academic Press, New York, 1966.
- [64] Falconer, K., *Fractal Geometry, Mathematical Foundations and Applications*, John Wiley & Sons, New York, 1990.
- [65] Puente-Baliarda, C., *et al.*, On the behavior of the Sierpinski multiband fractal antenna, *IEEE Trans. on Ant. and Prop.* Vol. 46, No. 4, pp. 517–25, 1998.
- [66] Shluge, K.L., Smith, G.S. and Maloney, J.G., Optimization of bow-tie antennas for pulse radiation, *IEEE Trans. on Ant. and Prop.*, Vol. 42, No. 7, pp. 975–82, 1994.

**Problems**

- 7.1 Sketch the  $\theta$  plane far-field electric field pattern for a single-turn square loop antenna whose sides are  $\lambda/10$ .
- 7.2 Show that the real part of the driving-point impedance for an ideal half-wavelength slot antenna on an infinite ground plane when operated at resonance is approximately  $418 \Omega$ .
- 7.3 Show that the real part of the input impedance of a folded half-wave dipole is approximately  $300 \Omega$ .
- 7.4 Design a microstrip patch antenna using a substrate of relative permittivity 2.3 and thickness 0.254 mm to operate at 10 GHz in fundamental  $TM_{010}$  mode.  
Sketch the E- and H-field far-field radiation patterns for the antenna and predict its half-power beamwidth. What is the effect of a finite ground plane on the radiation characteristics of this type of antenna?
- 7.5 A reflector antenna consisting of a parabolic cylinder aperture with dimensions of  $0.5 \times 0.2$  m is fed with nearly 100% efficiency from an idealised distributed line source. Calculate the half-power beamwidth of the antenna, its side-lobe levels in decibels and its directivity, also in decibels.
- 7.6 Design a single-conductor cylindrical helical antenna that produces 12 dBi gain in the axial direction.  
Compute the half-power angle and input impedance of the antenna.
- 7.7 A travelling-wave antenna is to be used for reception of horizontally polarised signals arriving at elevation angles of  $45^\circ$  and  $70^\circ$ . One end of the antenna is matched to the receiver while the other end is matched to a load termination such that no reflections occur.  
If the antenna is  $10\lambda_0$  long, calculate the dB ratio of the voltages supplied by the antenna to the receiver under the reception conditions given above.

# Appendices

---

### 8.1 Linear array factor program

This program was created for use with MATLAB in order to allow the array factor for linear arrays with general spacing and element excitation to be evaluated and plotted; subroutines, S-POLAR and CARPOL are copyright © 1984–94 by Mathworks Inc.

Matlab for Windows V4.2c1  
The Mathworks Inc  
3 Apple Hill Drive  
Natick  
MA 01760–2098  
USA.

MATLAB command window display for array program entitled 'p'

```
>> p
Enter a 1 for true or 0 for false
Please note that all current phases are given relative to the
current into the 1st antenna
Enter the details of the array

Please enter the number of antennas in the array >>4

Is each antenna excited by current of same magnitude? >>0

Is each antenna excited by current of same phase? >>0
```

Is each antenna separated by same distance? >>0

Please enter magnitude of the current to antenna 1 >>1

Does phase of current increase in uniform steps? >>0

Please enter magnitude of current to antenna number:

2

>>1

Please enter phase (in degrees) between antennas numbered:

1

2

>>45

Please enter the separation (in terms of wavelength) between ANTENNA 1 and antenna:

2

>>0.5

Please enter magnitude of current to antenna number:

3

>>1

Please enter phase (in degrees) between antennas numbered:

2

3

>>45

Please enter the separation (in terms of wavelength) between ANTENNA 1 and antenna:

3

>>1.0

Please enter magnitude of current to antenna number:

4

>>1

Please enter phase (in degrees) between antennas numbered:

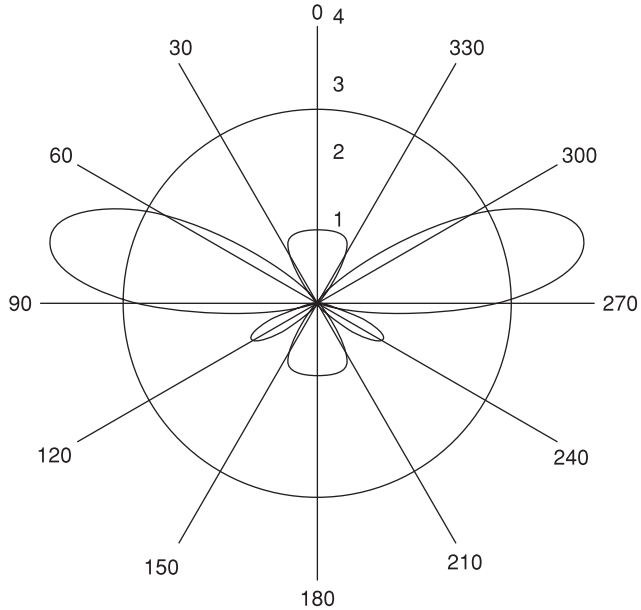
3

4

>>45

Please enter the separation (in terms of wavelength) between ANTENNA 1 and antenna:

4



Output figure for the array program entitled 'P' for a four-antenna array with  $0.5\lambda$  uniform separation, uniform phase shift between each antenna of  $45^\circ$  and uniform excitation current of 1 A

```
>>1.5
```

```
The following instructions are to calculate the beamwidth of the
1st antenna array pattern.
```

```
Please use the mouse to click on the upper left intersection of
the red graphed lines.
```

```
Please use the mouse to click on the lower left intersection of
the red graphed lines.
```

```
Values for the array
```

```
Maximum field =
```

```
3.9999
```

```
Tilt from x-axis =
```

```
15.0697
```

```
Beamwidth in degrees =
```

```
27.2592
```

### Printout of M-file 'P'

```
% This M-file 'P' plots linear antenna array factor for an array
with varying amplitude and phase of excitation current.
```

```
clg
```

```

% Clear all buffers
n = 0;
d1 = 0;
d2 = 0;
d3 = 0;
d4 = 0;
a = 0;
a0 = 0;
phase = 0;
alpha = 0;
Er = 0;
Ereal = 0;
sep = 0;
number = 0;
next = 0;
z = 0;
term = 0;
power = 0;
rho = 0;
r = 0;
ptl = 0;
ptu = 0;

disp('Enter a 1 for true or 0 for false');
disp('Please note that all current phases are given relative to
the current into the 1st antenna');

disp('Enter the details of the array');

n = input('Please enter the number of antennas in the array >>');
d1 = input('Is each antenna excited by current of same
magnitude? >>');
d2 = input('Is each antenna excited by current of same phase? >>');
d3 = input('Is each antenna separated by same distance? >>');

% Response to d1 = input('Is each antenna excited by current of
same magnitude? >>');

if d1 == 1
    a = input('Please enter magnitude of current (a) >>');
    a0 = a;
else
    d1 = 0;
    a0 = input('Please enter magnitude of the current to antenna
1 >>');
end

```

```

% Response to d2 = input('Is each antenna excited by current of
same phase? >>');

if d2 == 1
    alpha = 0;
    phase = 0;
    d4 = 2;
else
    d4 = input('Does phase of current increase in uniform steps?
>>');
    if d4 ==1
        phase = (pi/180)*input('What is the uniform phase
difference in degrees? >>');
    else
        d4 = 0;
    end
end

% Response to d3 = input('Is each antenna separated by same
distance? >>');

if d3 == 1
    sep = input('Please enter uniform separation distance as
ratio of wavelength (z) >>')
else
    d3 = 0;
end

% Set initial value of Er
Er = a0;

% Set variable theta
theta = 0:0.01:2*pi;

% Loop that increments Er by value of Er for each antenna

for i = 1:1:(n-1)
    number = i;
    next = i+1;

    % Enter magnitude of currents to each antenna
    if d1 == 0
        disp('Please enter magnitude of current to antenna number:')
        disp(next)
        a = input('>>');
    end
end

```

```

% Enter phase between antennas
if d4 == 0
    disp('Please enter phase(in degrees) between antennas
    numbered:')
    disp(number)
    disp(next)
    phase = pi/180*(input('>>'));
end;

% Increment value of phase by phase difference
alpha = alpha+phase;

% Calculate distance of antenna from origin if separation
uniform
if d3 == 1
    z=i*sep;
end

% Enter separation between antennas and origin if separation
is not uniform
if d3 == 0
    disp('Please enter the separation (in terms of wavelength)
    between ANTENNA 1 and antenna:')
    disp(next);
    z = input('>>');
end

% Calculate value of Er at this antenna and then increment Er
term = a*exp(-j*alpha)*exp(j*2*pi*z*cos(theta));
Er = Er + term;
end

% Plot absolute value of Er on polar graph
Ereal = abs(Er);
s_polar (theta, Ereal, 'r');

% Find 1/root(2) times max field and draw circle with radius of
this value
power = max (Ereal);
r = power/(sqrt(2));
hold on;
phi = 0:pi/60:2*pi;
rho = r*(ones(size(phi)));
s_polar(phi, rho, 'r');
hold on;

```

```

disp('The following instructions are to calculate the beamwidth
of the 1st antenna array pattern.');
```

Please use the mouse to click on the upper left intersection of the red graphed lines.');

```

[cxeu, cytu] = ginput(1);
[ptu, peu] = carpol(cxeu, cytu);
disp('Please use the mouse to click on the lower left
intersection of the red graphed lines.');
```

[cxel, cytl] = ginput(1);

```

[ptl, pel] = carpol(cxel, cytl);

beamwidth = ptl - ptu;

centre = ptl - (beamwidth/2);

tilt = 180 - centre;

disp('Values for the 1st array')
disp('Maximum field = ');
disp(power);
disp('Tilt from x-axis = ');
disp(tilt);
disp('Beamwidth in degrees = ');
disp(beamwidth);
```

### Printout of 'S\_POLAR' called in M-file 'P'

```

function pol = polar(theta,rho,line_style)
% SECOND_POLAR
% Plot to be used for antenna patterns.
% Note that theta is measured from the z-axis and rotates in a
  clockwise direction.
% SECOND_POLAR(THETA, RHO) makes a plot using polar coordinates
  of
% the angle THETA, in radians, versus the radius RHO.
% SECOND_POLAR(THETA,RHO,S) uses the linestyle specified in
  string S.
% See PLOT for a description of legal linestyles.
%
% See also PLOT, LOGLOG, SEMILOGX, SEMILOGY.

if nargin < 1
  error('Requires 2 or 3 input arguments.')
```

```

elseif nargin == 2
    if isstr(rho)
        line_style = rho;
        rho = theta;
        [mr,nr] = size(rho);
        if mr == 1
            theta = 1:nr;
        else
            th = (1:mr)';
            theta = th(:,ones(1,nr));
        end
    end
else
    line_style = 'auto';
end
elseif nargin == 1
    line_style = 'auto';
    rho = theta;
    [mr,nr] = size(rho);
    if mr == 1
        theta = 1:nr;
    else
        th = (1:mr)';
        theta = th(:,ones(1,nr));
    end
end
if isstr(theta) | isstr(rho)
    error('Input arguments must be numeric.');
```

```

end
if any(size(theta) ~= size(rho))
    error('THETA and RHO must be the same size.');
```

```

end

% get hold state
cax = newplot;
next = lower(get(cax,'NextPlot'));
hold_state = ishold;
% get x-axis text color so grid is in same color
tc = get(cax,'xcolor');
```

```

% Hold on to current Text defaults, reset them to the
% Axes' font attributes so tick marks use them.
fAngle = get(cax, 'DefaultTextFontAngle');
fName = get(cax, 'DefaultTextFontName');
fSize = get(cax, 'DefaultTextFontSize');
fWeight = get(cax, 'DefaultTextFontWeight');
set(cax, 'DefaultTextFontAngle', get(cax, 'FontAngle'), ...
```

```

'DefaultTextFontName', get(cax, 'FontName'), ...
'DefaultTextFontSize', get(cax, 'FontSize'), ...
'DefaultTextFontWeight', get(cax, 'FontWeight')

% only do grids if hold is off
if ~hold_state

% make a radial grid
hold on;
hhh = plot([0 max(theta(:))],[0 max(abs(rho(:)))]);
v = [get(cax,'xlim') get(cax,'ylim')];
ticks = length(get(cax,'ytick'));
delete(hhh);
% check radial limits and ticks
rmin = 0; rmax = v(4); rticks = ticks-1;
if rticks > 5 % see if we can reduce the number
    if rem(rticks,2) == 0
        rticks = rticks/2;
    elseif rem(rticks,3) == 0
        rticks = rticks/3;
    end
end

% define a circle
th = 0:pi/50:2*pi;
xunit = cos(th);
yunit = sin(th);
% now really force points on x/y-axes to lie on them exactly
inds = [1:(length(th)-1)/4:length(th)];
xunits(inds(2:2:4)) = zeros(2,1);
yunits(inds(1:2:5)) = zeros(3,1);

rinc = (rmax-rmin)/rticks;
for i = (rmin+rinc):rinc:rmax
    %plot(xunit*i,yunit*i,'-', 'color',tc,'linewidth',1);
    text(0,i+rinc/20,[' ' num2str(i)], 'verticalalignment',
        'bottom' );
end

% plot spokes
th = (1:6)*2*pi/12;
cst = cos((pi/2)+th); snt = sin((pi/2) + th);
cs = [-cst; cst];
sn = [-snt; snt];
plot(rmax*cs,rmax*sn,'-', 'color',tc,'linewidth',1);

```

```

% annotate spokes in degrees
    rt = 1.1*rmax;
    for i = 1:max(size(th))
        text(rt*cst(i),rt*snt(i),int2str(i*30),'horizontalalignment',
            'center' );
        if i == max(size(th))
            loc = int2str(0);
        else
            loc = int2str(180+i*30);
        end
        text(-rt*cst(i),
            -rt*snt(i),loc,'horizontalalignment','center' );
    end

% set viewto 2-D
    view(0,90);
% set axis limits
    axis(rmax*[-1 1 -1.1 1.1]);
end

% Reset defaults.
set(cax, 'DefaultTextFontAngle', fAngle , ...
        'DefaultTextFontName', fName , ...
        'DefaultTextFontSize', fSize, ...
        'DefaultTextFontWeight', fWeight );

% transform data to Cartesian coordinates.
xx = rho.*cos((pi/2)+theta);
yy = rho.*sin((pi/2)+theta);

% plot data on top of grid
if strcmp(line_style,'auto')
    q = plot(xx,yy);
else
    q = plot(xx,yy,line_style);
end
if nargin > 0
    hpol = q;
end
if ~hold_state
    axis('equal');axis('off');
end

% reset hold state
if ~hold_state, set(cax,'NextPlot','next'); end

```

### Printout of 'CARPOL' called in M-file 'P'

```

function [th,r,z] = carpol(x,y,z)
% CARPOL Transform Cartesian coordinates to polar.
% [TH,R] = CARPOL(X,Y) transforms data stored in Cartesian
% coordinates to polar coordinates. If [M,N] = SIZE(X), then
% Y must also be the same size. TH is returned in radians.
% [TH,R,Z] = CARPOL(X,Y,Z) transforms data stored in Cartesian
% coordinates to cylindrical coordinates. If [M,N] = SIZE(X),
% then
% Y and Z must be the same size.
%
% See also CART2SPH, SPH2CART, POL2CART.

% L. Shure, 4-20-92.
% Copyright (c) 1984-94 by The MathWorks, Inc.

t = (180/pi)* atan2(y,x);
if t<0;
    th = 360+t;
else
    th = t;
end
r = sqrt(x.^2+y.^2);
    
```

## 8.2 Reciprocity in a two-port network

Consider the two-port network shown in Figure A8.1, in which each port terminated in a different impedance,  $Z_{01}$  and  $Z_{02}$ .

In terms of  $S$  parameters (Appendix 8.4), the reciprocity condition is given by [67]

$$Z_0^{-1} \mathbf{S} = \tilde{\mathbf{S}} Z_0^{-1} \quad (\text{A8.1})$$

where  $\sim$  denotes matrix transpose.

Hence

$$\begin{bmatrix} \frac{S_{11}}{Z_{01}} & \frac{S_{12}}{Z_{02}} \\ \frac{S_{21}}{Z_{02}} & \frac{S_{22}}{Z_{02}} \end{bmatrix} = \begin{bmatrix} \frac{S_{11}}{Z_{01}} & \frac{S_{21}}{Z_{02}} \\ \frac{S_{12}}{Z_{01}} & \frac{S_{22}}{Z_{02}} \end{bmatrix} \quad (\text{A8.2})$$

or

$$S_{12} Z_{02} = S_{21} Z_{01} \quad (\text{A8.3})$$

Thus the two-port network is reciprocal not only as normally reported, when  $S_{12}$  and  $S_{21}$  (valid only when  $Z_{01}$  and  $Z_{02}$ ) are equal, but very importantly, especially for antenna

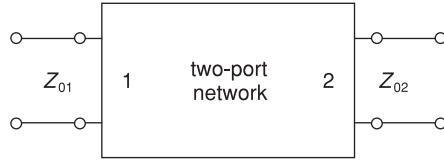


**Figure A8.1** Two-port network with arbitrary terminating impedances

work, when equation (A8.3) in its full form is satisfied. This is important when the antenna is considered as a two-port matching network between a generator or load at one impedance level and free space at  $377 \Omega$  impedance.

**References**

[67] Kerns, D.M. and Beatty, R.W., *Basic Theory of Waveguide Junctions and Introductory Microwave Network Analysis*, Pergamon Press, 1967.

**8.3 Noise-equivalent bandwidth, minimum discernible level and noise temperature measurement**

**Noise-equivalent bandwidth**

The noise-equivalent bandwidth of a system allows a more accurate appraisal of a filter's effect on system noise floor to be made [68]. Consider the filter shown in Figure A8.2. For this filter, the output noise power spectrum is  $G_y(f) = |H(f)|^2 G_x(f)$ , where  $G_x(f)$  is the noise power applied to the input of the filter. At the output of the filter, average noise power  $N$  is equal to

$$N = \int_{-\infty}^{\infty} |H(f)|^2 G_x(f) df \tag{A8.4}$$

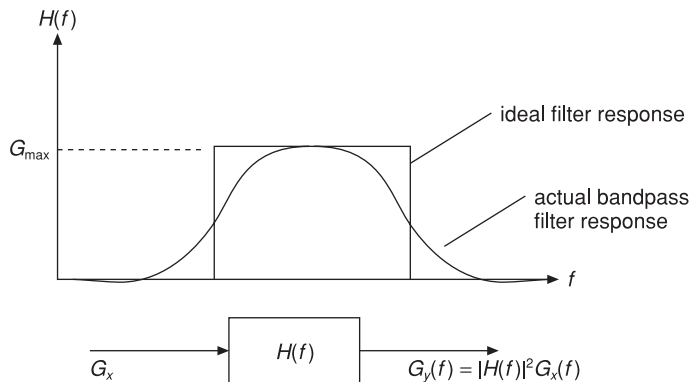


**Figure A8.2** Noise-equivalent bandwidth

For the general case, if  $H(f)$  and  $G_x(f)$  are known then equation (A8.4) can be evaluated. Often white noise (i.e. noise with a flat power spectral density response, equivalent to an impulse in the time domain) is used to test systems. Hence if we model the white noise as a constant,  $k/2$ , over the bandwidth of interest, we can write

$$\text{let } G_x(f) = \frac{k}{2}$$

thus, using equation (A3.1)

$$N = \int_{-\infty}^{\infty} |H(f)|^2 \frac{k}{2} df = k \int_0^{\infty} |H(f)|^2 df \quad (\text{A8.5})$$

Now we can define noise equivalent bandwidth,  $B_n$ , as

$$B_n = \frac{1}{G_{\max} \int_0^{\infty} |H(f)|^2 df} \quad (\text{A8.6})$$

where  $G_{\max} = |H(f)|_{\max}^2$ . For example, calculate the noise-equivalent bandwidth of a single-pole  $RC$  low-pass filter:

$$H(f) = \frac{1}{1 + \omega RC}$$

$$|H(0)|^2 = 1$$

$$\therefore B_n = \frac{1}{1} \int_0^{\infty} \left| \frac{1}{1 + \omega RC} \right|^2 df$$

or

$$B_n = \int_0^{\infty} \frac{df}{[1 + (f/B)]^2} = \frac{\pi}{2} B \text{ radians}$$

Thus if we had used the 3 dB cut-off point,  $B$ , to define the system bandwidth, we would have underestimated the noise level of the system by  $\pi/2$ .

## Minimum discernible signal

The minimum discernible signal (MDS) is defined as the input signal level where the output signal power equals the noise power; it is considered to be the minimum signal that can be detected by a system, i.e. when signal power is at the MDS level the receiver output is 3 dB above its noise level.

By using average thermal noise power,  $kTB$ , together with a 3 dB MDS level expressed in decibels, we can define the noise floor,  $N$ , of the system as

$$N = -174 + 10 \log_{10} B + 3 \text{ dB} + NF \quad (\text{A8.7})$$

where  $NF$  is the system noise figure. Combining the results above with the noise figure formula for a cascaded system (Section 5.3) and the path equation calculation for the

example in Section 5.2 gives the standard method for calculating the carrier-to-noise ratio at the detector input of a receiver given the system parameters, antenna gain, link length, transmitted power level, etc.

### Noise temperature measurement

Noise temperature measurement techniques are based on supplying a known amount of excess noise to the RF input of the device under test and measuring the change in noise output level [68]. If the noise temperature of the device under test is  $T_{RX}$ , and a noise source is available that has a noise temperature  $T_{ON}$  when switched ON and  $T_{OFF}$  when switched OFF, the system noise temperatures are

$$T_{SYS} = T_{RX} + T_{ON} \text{ (noise source on)}$$

and

$$T'_{SYS} = T_{TX} + T_{OFF} \text{ (noise source off)}$$

The noise power from the receiver is proportional to the system noise temperature, so the on/off power ratio  $Y$  is given by

$$Y = (T_{RX} + T_{ON}) / (T_{RX} + T_{OFF})$$

If we know  $T_{ON}$  and  $T_{OFF}$  and can measure  $Y$ , we can calculate  $T_{RX}$ :

$$T_{RX} = (T_{ON} - YT_{OFF}) / (Y - 1)$$

The main problem is to generate RF noise at two different known noise temperatures,  $T_{ON}$  and  $T_{OFF}$ . The simplest but least accurate way is to use the thermal noise from a 50  $\Omega$  resistor at two known physical temperatures. This is called the hot/cold method and is the closest we can get to a fundamental measurement of noise temperature. In practice, electronic noise sources based on zener diodes are used in most laboratories [69].

### References

- [68] Mumford, W.W. and Scheibe, E.H., *Noise Performance Factors in Communication Systems*, Horizon House, 1968.
- [69] Townsend, A.A.R., *Analog Line-of-Sight Radio Links*, Prentice Hall International, 1987.

### 8.4 Scattering parameter matrix

Consider a linear  $N$ -port network with each of its  $N$  ports terminated in different characteristic impedance values  $Z_{01}$ ,  $Z_{02}$ ,  $Z_N$ . The port terminal currents are  $I_1$ ,  $I_2$ ,  $I_N$ , and the terminal voltages are  $V_1$ ,  $V_2$ ,  $V_N$ . The various ratios of  $V$  and  $I$  give the port input and transfer impedances or admittances. An alternative way of viewing the

problem is to define reflected,  $b_i$ , and incident,  $a_i$ , waves at the  $k$ th port. The ratio of  $a_k/b_k$  gives the port input reflection coefficient. These waves can be defined in units of (power)<sup>1/2</sup> as

$$a_k = \frac{V_k^+}{\sqrt{Z_{0k}}} = I_k^+ \sqrt{Z_{0k}} \quad (\text{A8.8})$$

and

$$b_k = \frac{V_k^-}{\sqrt{Z_{0k}}} = I_k^- \sqrt{Z_{0k}} \quad (\text{A8.9})$$

where superscript ‘+’ indicates an incident voltage wave and superscript ‘-’ indicates a reflected voltage wave.

In terms of the concepts of forward and reverse travelling waves developed in Section 6.1, we can write the terminal voltage  $V_k$  as

$$V_k = V_k^+ + V_k^- = \sqrt{Z_{0k}}(a_k + b_k) \quad (\text{A8.10})$$

and terminal current  $I_k$  as

$$I_k = I_k^+ - I_k^- = \frac{1}{\sqrt{Z_{0k}}}(a_k - b_k) \quad (\text{A8.11})$$

Solving equations (A8.8) through (A8.11) for  $a_k$  and  $b_k$  gives

$$a_k = \frac{1}{2} \left( \frac{V_k}{\sqrt{Z_{0k}}} + I_k \sqrt{Z_{0k}} \right) \quad (\text{A8.12})$$

and

$$b_k = \frac{1}{2} \left( \frac{V_k}{\sqrt{Z_{0k}}} - I_k \sqrt{Z_{0k}} \right) \quad (\text{A8.13})$$

With reference to Figure A8.3, we can see that in matrix form, using scattering matrix rotation  $S_{ij}$  that

$$\begin{aligned} b_1 &= S_{11} a_1 + S_{12} a_2 + \dots + S_{1n} a_n \\ b_n &= S_{N1} a_1 + S_{N2} a_2 + \dots + S_{NN} a_n \end{aligned} \quad (\text{A8.14})$$

so that in compact matrix form

$$[\mathbf{b}] = [\mathbf{S}][\mathbf{a}] \quad (\text{A8.15})$$

The elements  $S_{kk}$  represent the situation where all other ports except the  $k$ th port are terminated in their relevant characteristic impedances, so there are no incident or reflected signals from these ports; hence from equation (A8.15) and when port  $kk$  is fed with a generator, then due to residual generator to port mismatch at port  $k$

$$S_{kk} = \frac{b_k}{a_k} \quad (\text{A8.16})$$

Under this condition,  $S_{kk}$  represents the input reflection coefficient at port  $k$ .

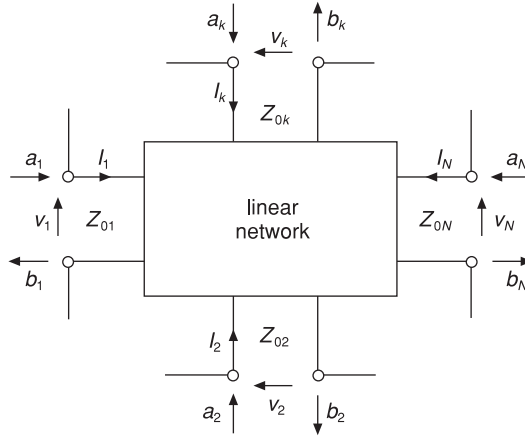


Figure A8.3 N-port linear network definitions

Similarly, the various port-to-port transmission coefficients can be found by connecting a generator to the port of interest and terminating all other ports in suitably matched load impedances e.g.

$$S_{ij} = \frac{b_i}{a_j} \tag{A8.17}$$

It is useful in antenna work to be able to convert *S* parameters to impedance, *Z*, parameters and vice versa. Equations (A8.18) and (A8.19) give the general relationships between two-port *S* parameters and two-port *Z* parameters [70]. Alternatively, after suitable impedance normalisation these transformations can be realised directly by direct plotting of *S* parameters in polar form on to a Smith chart and then reading off the corresponding real and imaginary impedance values.

$$\begin{bmatrix} S_{11} & S_{12} \\ S_{21} & S_{22} \end{bmatrix} = \frac{1}{\left(\frac{Z_{11}}{Z_{01}} + 1\right)\left(\frac{Z_{22}}{Z_{02}} + 1\right) - \frac{Z_{12}Z_{21}}{Z_{01}Z_{02}}} \begin{bmatrix} \left(\frac{Z_{11}}{Z_{01}} - 1\right) \cdot \left(\frac{Z_{22}}{Z_{02}} + 1\right) - \frac{Z_{12}Z_{21}}{Z_{01}Z_{02}} & \left[ 2\sqrt{\frac{Z_{02}}{Z_{01}} \frac{Z_{12}}{Z_{02}}} \right] \\ \left[ 2\sqrt{\frac{Z_{01}}{Z_{02}} \frac{Z_{21}}{Z_{01}}} \right] & \left(\frac{Z_{11}}{Z_{01}} + 1\right) \cdot \left(\frac{Z_{22}}{Z_{02}} - 1\right) - \frac{Z_{12}Z_{21}}{Z_{01}Z_{02}} \end{bmatrix} \tag{A8.18}$$

$$\begin{bmatrix} Z_{11} & Z_{12} \\ Z_{21} & Z_{22} \end{bmatrix} = \frac{1}{(1 - S_{11})(1 - S_{22}) - S_{12}S_{21}} \begin{bmatrix} Z_{01}[(1 + S_{12})(1 - S_{22}) + S_{12}S_{21}] & \left[ 2Z_{01}S_{12}\sqrt{\frac{Z_{02}}{Z_{01}}} \right] \\ \left[ 2Z_{02}S_{21}\sqrt{\frac{Z_{02}}{Z_{01}}} \right] & Z_{02}[(1 - S_{11})(1 + S_{22}) + S_{12}S_{21}] \end{bmatrix} \tag{A8.19}$$

**References**

[70] Kerns, D.M. and Beatty, R.W., *Basic Theory of Waveguide Junctions and Introductory Network Analysis*, Pergamon Press, 1967.

# Bibliography

---

## Books

### Microwave engineering

- Collin, R.E., *Foundations for Microwave Engineering*, 2nd edition, McGraw-Hill International, 1992.
- Edwards, T.C., *Foundations for Microstrip Circuit Design*, John Wiley & Sons, 1981.
- Fusco, V.F., *Microwave Circuits: Analysis and Computer-Aided Design*, Prentice Hall International, 1987.
- Harsany, C., *Principles of Microwave Technology*, Prentice Hall, 1996.
- Liao, S.Y., *Engineering Applications of Electromagnetic Theory*, West Publishing Company, 1988.
- Pennock, S.R. and Shepherd, P.R., *Microwave Engineering, with Wireless Applications*, McGraw-Hill, 1998.
- Pozar, D.M., *Microwave Engineering*, 2nd edition, John Wiley & Sons, 1997.
- Rizzi, P.A., *Microwave Engineering Passive Circuits*, Prentice Hall International, 1988.

### Antenna techniques

- Balanis, A., *Antenna Theory: Analysis and Design*, 2nd edition, John Wiley & Sons, 1996.
- Blake, L.V., *Antennas*, Artech House, 1984.
- Carr, J., *Newnes Antenna Toolkit*, Butterworth Heinemann, 1997.
- Chang, K., *Microwave Ring Circuits and Antennas* (Wiley Series in Microwave and Optical Engineering), John Wiley & Sons, 1996.
- Collin, R.E. and Zucher, F.J., *Antenna Theory*, Parts I, II, McGraw-Hill, 1969.
- Drabowitch, S., Bradford, L. and Papiernik, A., *Modern Antennas (Microwave and RF Technology, Volume 12.0)*, Chapman & Hall, 1997.
- Hall, G.L. (ed.), *The ARRL Antenna Book*, 14th edition, American Radio Relay League, 1982.
- IEEE Std 145-1983, IEEE Standard Definitions of Terms for Antennas, *IEEE Trans on Antennas and Propagation*, Vol. AP-31, No. 6, 1983.

- Johnson, R.C., *Designer Notes for Microwave Antennas*, Artech House, 1991.
- Kidal, P.-S., *Foundations of Antennas, A Unified Approach*, Studentlitteratur, Lund, 2000.
- Kraus, J.D., *Antennas*, 2nd edition, McGraw-Hill, 1988.
- Kumar, A., *Antenna Design with Fiber Optics*, Artech House, 1996.
- Lee, K.F., *Principles of Antenna Theory*, John Wiley & Sons, 1984.
- Monser, G.J., *Antenna Design: A Practical Guide*, McGraw-Hill, 1996.
- Orr, I. and Cowan, S.D., *Simple, Low-Cost Wire Antennas for Radio Amateurs*, Rac Books, 1990.
- Orr, W.I. and Cowan, S.D., *All About Vertical Antennas*, reissue edition, Rac Books, 1997.
- Stutzman, W.L. and Theile, G.A., *Antenna Theory and Design*, 2nd edition, John Wiley & Sons, 1998.
- Terman, F.E. (ed.), *Antennas*, Vols I, II, McGraw-Hill, 1950.

### Antenna measurements

- IEEE Std 149-965, *IEEE Standard Test Procedures for Antennas*, Wiley-Interscience, 1980.
- Slater, D., *Near-field Antenna Measurements*, Artech House, 1991.

### Antenna CAD techniques

- Diaz, L. and Milligan, T., *Antenna Engineering Using Physical Optics, Practical CAD Techniques and Software*, Artech House, 1996.
- Herscovici, *CAD of Aperture-Fed Microstrip Transmission Lines and Antennas*, Artech House, 1998.
- Popovic, B.D., *CAD of Wire Antennas and Related Radiating Structures*, Research Studies Press, 1991.
- Sainati, R.A., *CAD of Microstrip Antennas for Wireless Applications*, Artech House, 1996.

### Electromagnetic theory

- Bhattacharyya, K., *High-Frequency Electromagnetic Techniques; Recent Advances and Applications* (Wiley Series in Microwaves), John Wiley & Sons, 1995.
- Cloude, S.R., *Introduction to Electromagnetic Wave Propagation and Antennas*, Springer Verlag, 1996.
- Jordan, E.C. and Balmain, K.G., *Electromagnetic Waves and Radiating Systems*, 2nd edition, Prentice Hall EE Series, 1968.
- Karmel, P.R., Colef, G.D. and Camisa, R.L., *Introduction to Electromagnetic and Microwave Engineering*, John Wiley & Sons, 1998.
- Paul, C.R. and Nasar, S.A., *Introduction to Electromagnetic Fields*, McGraw-Hill, 1982.
- Popovic, B.D. and Kolundzija, B.M., *Analysis of Metallic Antennas and Scatterers*, IEEE, 1994.
- Qian, Y. and Itoh, T., *FDTD Analysis and Design of Microwave Circuits and Antennas, Software and Applications*, Realize Inc., Tokyo, 1998.
- Ramo, S., Whinnery, J.R. and van Duzer, T., *Fields and Waves in Communication Electronics*, John Wiley and Sons, 1965.
- Salazar-Palma, M., Sarkar, K., *et al.*, *Interactive and Self-Adaptive Finite-Element Electromagnetic Modelling*, 1998.
- Smith, G.S., *An Introduction to Classical Electromagnetic Radiation*, Cambridge University Press, 1997.
- Stratton, J.A., *Electromagnetic Theory*, McGraw-Hill, 1941.

- Stutzman, W.L., *Polarization in Electromagnetic Systems*, Artech House, 1993.
- Volakis, J.L., Chatterjee, K.K. and Leo C., *Finite Element Method for Electromagnetics: Antennas, Microwave Circuits and Scattering Applications*, IEEE Press, 1998.
- Yamashita, E., *Analysis Methods for Electromagnetic Wave Problems*, Artech House, 1997.

## Specialist antenna texts

- Bahl, I.J. and Bhartia, P., *Microstrip Antennas*, Artech House, 1980.
- Bhartia, P., *Millimeter-Wave Microstrip and Printed Circuit Antennas*, Artech House, 1991.
- Burberry, R.A., *VHF and UHF Antennas*, IEEE Electromagnetic Waves Series 35, Peter Peregrinus, 1992.
- Burrows, M.L., *ELF Communications Antennas*, Peter Peregrinus, 1978.
- Fong, L.K. and Wei, C., *Advances in Microstrip and Printed Antennas* (Wiley Series in Microwave and Optical Engineering), John Wiley & Sons, 1997.
- Gupta, K.C. and Benalla, A., *Microstrip Antenna Design*, Artech House, 1988.
- Hansen, R.C., *Phased Array Antennas*, John Wiley & Sons, 1998.
- James, J.R. and Hall, P.S., *Microstrip Antenna Theory and Design*, Peter Peregrinus, 1981.
- Kumar, A. and Hristov, H.D., *Microwave Cavity Antennas*, Artech House, 1989.
- Navarro, J.A. and Chang, K., *Integrated Active Antennas and Spatial Power Combining*, John Wiley & Sons, 1996.
- Olver, A.D., Clarricoats, P.J.B., Kishk, A.A. and Shafai, L., *Microwave Horns and Feeds*, IEEE Electromagnetic Wave Series 39, 1994.
- Pozar, D.M. and Schaubert, D.H. (eds), *Microstrip Antennas, The Analysis and Design of Microstrip Antennas and Arrays*, IEEE Press, 1995.
- Rumsey, V.H., *Frequency Independent Antennas*, Academic Press, 1966.
- Salema, C., Fernandes, C. and Jha, R.K., *Solid Dielectric Horn Antennas*, Artech House, 1998.
- Scott, C., *Modern Methods of Reflector Antenna Analysis and Design*, Artech House, 1990.
- Wood, P.J., *Reflector Antenna Analysis and Design*, Peter Peregrinus, 1980.
- Zurcher, J. and Gardiol, F.E., *Broadband Patch Antennas*, Artech House, 1995.

## Handbooks

- Carr, J.J., *Practical Antenna Handbook*, 3rd edition, McGraw-Hill, 1998.
- Chang, K. (ed.), *Handbook of Microwave and Optical Components*, Vol. I, *Microwave Passive and Antenna Components*, John Wiley & Sons, 1989.
- Fujimoto, K. and James, J.R., *Mobile Antenna Systems Handbook*, Artech House, 1994.
- James, J.R. and Hall, P.S. (eds), *Handbook of Microstrip Antennas*, Vols 1 and 2, Peter Peregrinus, 1989.
- Jasik, H., *Antenna Engineering Handbook*, McGraw-Hill, 1961.
- Johnson, R.C., *Antenna Engineering Handbook*, 3rd edition, McGraw-Hill, 1993.
- Lo, Y.T. and Lee, S.W. (eds), *Antenna Handbook: Theory, Applications and Design*, Van Nostrand Reinhold, 1988.
- Lo, Y.T. and Lee, S.W., *Antenna Handbook*, Van Nostrand Reinhold, 1993.
- MacNamara, M., *Handbook of Antennas for EMC* (Artech House Antenna Library), Artech House, 1995.
- Mailloux, R.J., *Phased Array Antenna Handbook* (Artech House Antenna Library), Artech House, 1994.
- Orr, W.I. and Cowan, S.D., *Beam Antenna Handbook*, Rac Books, 1991.

- Rudge, A.W., Milne, K., Olver, A.D. and Knight, P. (eds), *The Handbook of Antenna Design*, Vols I and II, Peter Peregrinus, 1982.
- Skolnik, I., *Radar Handbook*, 2nd edition, McGraw-Hill, 1989.
- Smith, B.L. and Carpentier, M. (eds), *The Microwave Engineering Handbook*, Vol. II, *Microwave Circuits, Antennas and Propagation*, Chapman & Hall, 1993.

## General reading

- Fourikis, N., *Phased Array-Based Systems and Applications*, John Wiley & Sons, 1997.
- IEEE Antennas and Propagation Magazine*, editor, W.R. Stone, IEEE, 445 Hoes Lane, PO Box 1331, Piscataway, NJ 08855-1331, USA.
- IEEE Transactions on Antennas and Propagation*, publisher IEEE, 445 Hoes Lane, PO Box 1331, Piscataway, NJ 08855-1331, USA.
- Kitsuregawa, T., *Advanced Technology in Satellite Communications Antennas: Electrical and Mechanical Design*, Artech House, 1990.
- Kozakoff, D.J., *Analysis of Radome-Enclosed Antennas*, Artech House, 1997.
- Levy, R., *Structural Engineering of Microwave Antennas: For Electrical, Mechanical and Civil Engineering*, Institute of Electrical and Electronic Engineers, 1996.
- Okamoto, T., *Smart Antenna Systems and Wireless LANs*, Kluwer Academic Publishers, 1998.
- Setian, L., *Practical Communication Antennas with Wireless Applications*, Prentice Hall, 1997.
- Siwiak, K., *Radiowave Propagation and Antennas for Personal Communications*, 2nd edition, Artech House, 1998.
- Toomay, J.C., *Radar Principles for the Non-specialist*, 2nd edition, Scitech Publishing, 1998.

## Software

- Advanced Automated Smith Chart, Version 3.0, software and user's manual, L. Sshwab, Artech House, 1998.
- Awas for Windows: Analysis of Wire Antennas and Scatterers, software and user's manual, A.R. Djordjevic, M.B. Bazar, T.K. Sarkar and R.F. Harrington, Artech House, 1995.
- CAD for Linear and Planar Antenna Array of Various Radiating Elements, software and user's manual, M. Mikavica and A. Nestic, Artech House, 1992.
- CAD of Aperture-fed Microstrip Transmission Lines and Antennas, software and user's manual, N. Herscovici, Artech House, 1996.
- Plot SMITH + <sup>TM</sup>, Applied Wave Research, Artech House, 1997.
- TRANSLIN: Transmission Line Analysis & Design, software and user's manual, P. Delmastro, Artech House, 1999.
- TRAVIS Pro: Transmission Line Visualization, software and user's manual, professional version, R.G. Kaires and B.T. Hickman, Artech House, 1995.
- WIPL: Electromagnetic Modelling of Composite Wire and Plate Structures, software and user's manual, B.M. Kolundzija, J.S. Ognjanovic, T.K. Sarker and R.F. Harrington, Artech House, 1995.

## Video

- Microwave Transmission Lines and their Physical Realizations*, S.L. March, Artech House, 1998.

# Glossary of terms

---

**Ampere's law:** relates magnetic field to current flow and vice versa.

**antenna:** a physical structure that is capable of receiving or transmitting electromagnetic energy over a specified frequency range.

**antenna array:** an assembly of antenna elements designed to enhance directivity.

**aperture distribution:** the field strength profile across the radiating face of an antenna array.

**array factor:** a mathematical relationship that embodies the geometrical distribution of elements in an array.

**attenuator:** a device for reducing signal strength.

**AUT:** antenna under test.

**balun:** a balanced to unbalanced transformer.

**binomial distribution:** an aperture distribution that produces no side lobes.

**broadside array:** an array where the elements are arranged so that their axes lie in parallel and are fed so that the array radiates normal to the array axis.

**co-linear array:** an array where the elements have their axes aligned.

**dipole:** a balanced fed straight-wire antenna.

**directivity:** the focusing ability of an antenna relative to that of an isotropic source.

**distributed element:** a circuit whose size is equivalent to a wavelength at its operating frequency.

**Dolph-Tchebyscheff distribution:** an aperture distribution that produces the narrowest beamwidth for a pre-specified side-lobe level.

**duplexer:** a three-port filter used to isolate receive and transmit signals in a wireless system.

**effective aperture:** the equivalent radiating aperture of an antenna after its efficiency has been taken into account.

**effective length:** the length of a theoretical antenna that has uniform current distribution and equivalent radiation properties to an actual antenna.

**EIRP:** effective isotropic radiated power; it is equal to the product of available transmitter power and transmitter antenna gain.

**electromagnetic radiation:** the process by which accelerated charges deliver energy into free space.

**element pattern:** the radiation pattern for a single radiating element.

**end-fire array:** an array where the elements are fed so that radiation occurs along the array axis.

**far field:** the region far enough from an antenna such that reactive energy is negligible.

**Faraday's law:** relates induced voltage to rate of change to magnetic flux and vice versa.

**Fraunhofer region:** the far field of an antenna or antenna array.

**Free-space wave impedance:** The ratio of the  $E$  field and  $H$  field plane wave components, equal to  $377 \Omega$ .

**Fresnel region:** the near-field region of an antenna or antenna array.

**front-to-back ratio:** the ratio between the radiated field in the end-fire direction to the radiated field in the direction opposite to end fire.

**grating lobes:** undesirable side lobes that occur for array element spacings of greater than one wavelength.

**group pattern:** the product of an element pattern and array factor for an array comprised of identical elements.

**half-power beamwidth:** the angular separation between the directions on each side of the direction of maximum radiation, where the far-field radiated field has fallen by  $-3$  dB.

**Hertzian dipole:** an elementary antenna consisting of an infinitesimally short length of wire.

**Huygen's principle:** each point of a wavefront acts as a secondary source of propagating energy, which in turn creates a new wavefront.

**induced-emf:** the voltage induced in an antenna element due to an incident electric field.

**induction field:** the near-field region of an antenna or an antenna array.

**insertion loss:** the additional attenuation caused by the introduction of a device with loss into a system.

**isotropic source:** a fictitious source of electromagnetic energy that is radiated uniformly in all directions.

**$L$  match:** a matching circuit topology.

**lumped element:** a circuit whose size is small compared with a wavelength at its operating frequency.

**matching:** the technique used to ensure maximum power transfer from one device to another.

**Maxwell's equations:** a set of mathematical equations that when used with suitable boundary conditions defines the macroscopic behaviour of electromagnetic waves.

**monopole:** a vertical antenna fed with respect to a conducting ground plane.

**mutual coupling:** energy leaked from one source and picked up by another in the same array.

**near field:** The region close enough to an antenna or antenna array that considerable reactive energy exists.

**neper:** transmission line loss expressed in natural logarithmic units.

**phase velocity:** the velocity of a phase front of a propagating signal.

**phased array:** an antenna array where a progressive phase shift is introduced along the array in order to steer its far-field radiation pattern.

**PI match:** a matching circuit topology.

**plane wave:** a propagating wave whose wavefront is an equiphase surface.

**polar pattern:** a graph in polar coordinates that shows an antenna or antenna array's radiated electric field intensity as a function of angle.

**polarized wave:** the orientation of the electric field vector of a propagating electromagnetic wave.

**power gain:** the product of directivity and efficiency of a particular antenna.

**Poynting's theorem:** allows instantaneous power per unit area delivered by a electromagnetic wave to be deduced.

**quality factor:** a measure of the resonant behaviour of an antenna or lumped tuned circuit.

**radiation efficiency:** the ratio of radiation resistance to the total losses in an antenna.

**radiation resistance:** a fictitious resistance chosen such that the average power dissipated in it is equal to that dissipated by the electromagnetic energy radiated from the antenna.

**reciprocity:** the property whereby a passive linear antenna exhibits the same terminal characteristics on transmit as on receive.

**reflection coefficient:** a measure of the amount of signal reflected from an antenna or matching circuit terminals.

**return loss:** reflection coefficient expressed in decibels.

**side lobe:** radiation from an antenna that does not lie along its principal radiation direction.

**Smith chart:** a graphical tool used to facilitate impedance-matching problems.

**spherical coordinate system:** coordinate system for uniquely identifying a point located on the surface of a sphere.

**standing wave:** a wave with fixed node and antinode positions.

**TEE match:** a matching circuit topology.

**transverse electromagnetic waves:** electric and magnetic field vectors are orthogonal to the direction of wave propagation.

**VSWR:** voltage standing wave ratio; a measure of how well an antenna is impedance-matched to a receiver or transmitter.



# Index

---

- absorbing material, 117
- AC decoupling, 114
- accelerated charge, 1
- active region equi-angular spiral, 196
- Ampere's law, 20
- anechoic environment, 117
- antenna array
  - binominal, 73
  - broadside, 64–5
  - co-linear, 59, 60–2
  - Dolph-Tchebyscheff, 74–5
  - effect of mutual coupling on gain, 84, 88
  - end-fire, 65–6
  - end-fire with mutual coupling, 85
  - front-to-back ratio, 87
  - group pattern, 63
  - non-uniform current excitation, 72–3
  - pattern nulls, 63, 66
  - pencil beam, 71
  - resultant pattern, 59
  - stacked, 70–2
  - two-element, 59
- antenna definitions
  - aperture, 95–7
  - array, 56
  - array factor, 58, 125
  - axial ratio, 108, 120, 122
  - bandwidth, 37, 76
  - boresight, 7
  - calibrated, 125
  - directivity, 33
  - effective length, half-wave dipole, 53
  - effective length, height, 42, 95
  - external load impedance, 51
  - half-power beamwidth, 9
  - input impedance, 76
  - mutual coupling, 57
  - radiation efficiency, 34, 36
  - reciprocity, transmit/receive, 95
- antenna measurement
  - beamwidth, 117
  - cardinal cuts, 117
  - directivity, 121
  - field strength, 123
  - gain comparison method, 121
  - gain substitution method, 122
  - scaling, 125
  - test range length, 113
- antenna reactance, 13, 80
- antenna types
  - capacitor loaded, 48–9
  - dielectric resonator, 192–3
  - equi-angular spiral, 195–6
  - finite-length dipole, 40–55
  - fractal, 197–8
  - helical, 182–5
  - Hertzian, 5–18
  - horn, 186–7
  - microstrip patch, 172–7
  - planar inverted-F, 190–2

- antenna types (*continued*)
  - reflectarray, 193–5
  - reflector, 177–2
  - travelling-wave, 187–9
  - Yagi, 170–2
- antenna under test, 118
- aperture blocking, 181
- aperture distribution
  - field calculation, 69
  - side lobe response, 69
  - uniform, 68
- array factor program, 201–11
- attenuator
  - network, 136
  - power dissipation, 141
- attenuator pad, 137
- available noise power, 102
- average antenna impedance, 79
- average power flow, 28
  
- backscatter, 100
- balanced feed, 148, 159
- balun matching, 148–51
  - impedance transforming, 150
  - quarter wavelength, 149
  - shielded, 149
  - torodial wire, 150
- bandwidth efficiency trade-off, 167
- beam divergence, 177
- beam-shaping, 181
- bilateral transmission path, 101
- Biot-Savart law, 12
- bow-tie antenna, 198
- broadband antenna, 195
  
- capacitive region, 12
- carrier-to-noise ratio, 214
- cascaded system noise, 106
- cavity coupling, 165
- charge packet, 18
- circular polarisation definitions, 109
- circular polarisation measurement methods
  - circular component, 118
  - linear component, 118–19
  - spinning dipole, 118
- circular polarisation synthesis, 109
- clearance, 114
- coaxial cable, 137, 148
- co-linear array aperture, 63
- compact antenna range, 117
- conductivity, 21, 125
  
- conformal antenna, 172
- conformal surface, 193
- helical antenna conical mode, 182
- conjugate matching, 154, 161
- coordinate system
  - Cartesian, 10
  - spherical, 4
- co-polar radiation, 117
- corporate fed, 193
- Coulomb field, 2
- cross-polarisation radiation, 117
- current
  - charging, 22
  - density, 21, 22
  - director element, 170
  - displacement, 21
  - distribution finite-length dipole, 42–3
  - driven element, 170
  - driving point, 42
  - time delayed, 14
- current distribution
  - constant, 5–8, 47
  - linear, 47
  - sinusoidal, 42, 43
  
- DC biasing, 144
- DC block, 146
- decibel
  - relative to a milliwatt, dBm, 54
  - relative to an isotropic source, 33
- dielectric losses, 129
- diffraction, 116
- dipole
  - half-wave gain, 49
  - Hertzian, 5, 30, 166
  - image over ground plane, 89, 90
  - short, 47
- directivity
  - $N$ -element array, 62
  - microstrip patch antenna, 176
  - stacked array, 71–2
  - uniform aperture distribution, 69
- distance to far-field, 112–13
- duality, 168
- duplexer, 104
  
- effect of current at resonance, 76
- effective
  - aperture, 98
  - isotropic radiated power, EIRP, 99
  - noise temperature, 102

- effective (*continued*)
  - noise temperature of matched attenuator, 103–4
- efficiency factor, 36
- electric field
  - cancellation, 90, 165
  - radial, 4
  - radiated, 15
  - tangential, 5
- electrically large antenna, 177
- electrically short antenna, 37
- electromagnetic compatibility, 125
- electromagnetic radiation production, 1
- electronically steerable array, 67
- E*-plane horn, 186
- end-fire operation, 65–6
- equatorial plane, 89
- excess noise, 214
  
- F antenna, 190
- Fano's limit, 77
- Faraday's law, 20
- far-field, 16, 122
- far-field pattern
  - cuts, azimuth, elevation, 117
  - electronic steering, 67
  - microstrip patch antenna, 176
- field-sensing, 165
- flux density, 21
- focal length, 181
- folded slot antenna, 169
- Fourier integral, 69
- four-wire travelling wave antenna, 189
- fractal, 197
- fractal antenna, 197–8
- Fraunhofer region, 112
- free electrons, 17
- free-space impedance, 14
- free-space link equation, 98–9
- free-space propagation, 20, 25
- free-space wavelength, 6
- frequency-independent antenna, 195
- Fresnel region, 9
- Fresnel zone, 114–15
- Friis noise formulae, 107
- Friis transmission formulae, 99, 122
- front-to-back ratio, 66
  
- gain
  - dipole over ground plane, 91
  - directive gain of an antenna, 33
  - G/T ratio, 107, 127
  - helical antenna, 185
  - maximum theoretical, 38
  - pyramidal horn antenna, 186
  - reflector antenna, 180
  - uniformly illuminated aperture, 72
- geometrical optics, 177
- geosynchronous orbit, 126
- grating lobes, 85
- grazing angle, 116
- ground plane, 90
- guide wavelength, 131
  
- half-power beamwidth
  - full-wave dipole, 45
  - half-wave dipole, 45
  - helical antenna, 185
  - microstrip patch antenna, 176
  - pyramidal horn antenna, 187
  - reflector antenna, 179
- helical antenna
  - angle to first zero, 185
  - axial-mode, 182
  - normal-mode, 182
- hot-cold method, 214
- H-plane horn, 186
- Huygen's principle, 72, 114
  
- illumination tapering, 180
- image cancellation, 90–1
- impedance matching
  - L section, 136, 144
  - microstrip patch, 173, 175
  - PI section, 139, 147
  - stub, 160
  - T section, 139, 145
- impedance transformer
  - half-wavelength, 157
  - quarter-wavelength, 158
- induced-emf method, 79–84
- induction field, 13, 113
- inductive region, 12
- inductive tuning, 190
- input impedance
  - helical, 185
  - microstrip patch, 175
  - Yagi, 172
- insertion gain, 136
- insertion loss, 135
- instantaneous power flow, 28
- inverted antennas, 191

- ionospheric reflection, 189
- isolation, 151
- isotropic radiator, 57
- isotropic source, 8, 31
  
- L antenna, 190
- logarithmic frequencies, 198
- long-distance communications, 189
- lumped element definition, 35, 139
- lumped impedance matching, 136–47
  - LC network, 144
  - reactive matching, 142–7
  - resistive L, 136
  - symmetrical PI, 139
  - symmetrical T, 138
  - T network, 145
  
- Mandelbrot, B., 197
- masthead preamplifier, 144
- matched attenuator noise figure, 104
- MATLAB, 201
- Maxwell's equations, 20–3
- mechanical beam scanning, 182
- microstrip patch antenna feed, 173
- minimum discernable level, 213
- mobile handset, 191, 197
- monopole, 190
- monopole power gain, 90
- multi-path signals, 114
- multiple frequency band operation, 191–2, 197
- mutual coupling, 79–84, 173
  
- near-field definition, 9
- nepers, 132–3, 139, 141
- noise
  - equivalent bandwidth, 102, 212
  - factor, 105
  - figure, 137, 213
  - floor, 213
  - temperature measurement, 214
- non-conducting medium, 22
- non-harmonic frequency, 197
- non-resonant antenna, 187
- N*-port network, 214
  
- obliquity factor, 114, 115
- ohmic resistance, 34, 36
- omnidirectional radiation, 4, 190
- open-area test site, 117
  
- open-circuit termination, 134
- oscillating charge doublet, 9
- overvoltage breakdown, 135
  
- parabolic metal reflector, 177
- parallel plate capacitor, 21
- parasitic reflector, 170
- patch antenna
  - higher-order modes, 173
  - radiation conductance, 175
- pattern multiplication factor, 43–4
- permeability, 21, 125
- permittivity, 125
- phase delay, 57
- phased array, 67, 68
- phasing harness, 158
- planar antenna array, 193
- plane wave propagation, 24–9, 98
- Poincaré sphere, 110
- point-to-point microwave link, 177
- polar pattern
  - definition, 9
  - full-wave dipole, 45
  - half-wave dipole, 45
  - Hertzian dipole, 8
  - reciprocity, transmit/receive, 100–1
- polarisation, 108–12
  - circular, 109
  - diversity, 110
  - ellipse, 108
  - elliptical, 109
  - left hand circular, 109
  - linear, 25, 109
  - right hand circular, 109
  - synthesis of elliptical wave, 111
  - tilt angle, 109, 112
  - un-polarised wave, 110
- power combiners, 151–3
- power gain of an antenna, 32
- power spectral density, 213
- power splitters, 151–3
  - lumped hybrid, 152
  - resistive, 151
  - T junction, 151
  - Wilkinson, 151
- power transfer, 50–1
- Poynting's theorem, 13, 29, 167
- preferential radiation, 56
- preferred resistance values, 140

- printed circuit, 172
- progressive phase lag, 187
- quality factor
  - loaded, 79
  - minimum, 37, 143, 191
  - relationship to antenna bandwidth, 77
  - unloaded, 79
- radar absorber, 117
- radiated power, 31, 34
- radiation resistance
  - definition, 34
  - finite-length dipole, 46
  - half-wave dipole, 46
  - Hertzian dipole, 34
  - monopole, 90
  - short dipole, 48
  - slot, 169
  - small loop, 167
- radiometric methods, 38
- receive antenna equivalent circuit, 51
- reciprocal network, 172
- reciprocity, 80, 211–12
- reference antenna, 33
- reflection coefficient, 134
- reflector antenna feed, 180, 181
- relative bandwidth, 78
- return loss, 134
- rhombic antenna, 189
- right hand screw rule, 30
- S parameters, 118, 211, 214–16
- satellite receiver noise, 107
- secondary radiation, 135, 148
- self-impedance, 79
- short-circuit termination, 134
- side lobes, 46, 113, 180
- Sierpinski monopole, 197
- signal-to-noise ratio, 104, 108
- sky temperature, 104
- slot antenna, 167–70
  - directivity, 169
  - effective aperture, 169
  - reflector backed, 169
- small loop antenna, 165
- Smith, P.H., 129
- Smith chart, 153–61
- spatial feed, 193
- spherical wavefront, 72, 177
- spillover, 181
- squint, 195
- standard reference antenna, 121
- standard gain horn antenna, 187
- standing wave, 133, 135
- solid angle definition, 34
- Stokes parameters, 110
- straight-wire travelling-wave antenna, 187
- stub matching, 156, 157, 159
- surface wave losses, 172, 192
- surveillance receiver, 195
- system link budget, 99
- television reception, 127
- terminating impedance, 134
- thermal noise, 101, 213
- Thevenin's theorem, 81
- time-domain pulse tracking, 18
- time varying current excitation, 13
- transfer admittance, 214
- transfer impedance, 214
- transmission line
  - attenuation per unit length, 131
  - capacitance per unit length, 159
  - characteristic impedance, 129, 132
  - guide wavelength, 131
  - inductance per unit length, 159
  - matched, 129
  - mismatch, 133
  - phase shift per unit length, 131
  - phase velocity, 131
  - power delivered to load, 135
  - propagation constant, 131, 138
  - stub matching, 156, 157
  - uniform, 129
- transverse electromagnetic wave, 24, 109, 112
- tuned circuit, 37
- two-port network, 211
- uniformly illuminated aperture, 180
- unipole, 90
- unit pattern, 61
- unit vector, 12
- vector network analyser, 118
- velocity, 2, 28
- velocity slowing factor, 131
- voltage pulse excitation, 17
- voltage standing wave ratio, VSWR, 133

wave equation, 24, 110  
wave impedance, 6  
wave number, 6  
wavefront, 4  
Wheeler box, 38  
white noise, 101, 213

Yagi, Hidet Sugu, 170  
Yagi-Uda antenna, 170  
  
Z parameters, 216  
zener diode, 214  
zero side lobes, 74



